

**MOLECULAR GENETIC INVESTIGATION OF  
AUTOSOMAL RECESSIVE  
NEURODEVELOPMENTAL DISORDERS**

by

MANJU ANN KURIAN

A thesis submitted to  
The University of Birmingham  
for the degree of  
DOCTOR OF PHILOSOPHY

School of Clinical and Experimental Medicine  
The Medical School  
University of Birmingham  
July 2010

UNIVERSITY OF  
BIRMINGHAM

**University of Birmingham Research Archive**

**e-theses repository**

This unpublished thesis/dissertation is copyright of the author and/or third parties. The intellectual property rights of the author or third parties in respect of this work are as defined by The Copyright Designs and Patents Act 1988 or as modified by any successor legislation.

Any use made of information contained in this thesis/dissertation must be in accordance with that legislation and must be properly acknowledged. Further distribution or reproduction in any format is prohibited without the permission of the copyright holder.

*Men ought to know that from the brain and from the brain only arise our pleasures, joys, laughter, and jests as well as our sorrows, pains, griefs and tears. ... It is the same thing which makes us mad or delirious, inspires us with dread and fear, whether by night or by day, brings us sleeplessness, inopportune mistakes, aimless anxieties, absent-mindedness and acts that are contrary to habit...*

*Hippocrates (Fifth century B.C.)*

## **Abstract**

Development of the human brain occurs in a number of complex pre- and postnatal stages which are governed by both genetic and environmental factors. Aberrant brain development due to inherited defects may result in a wide spectrum of neurological disorders which are commonly encountered in the clinical field of paediatric neurology. In the work for this thesis, I have investigated the molecular basis and defined the clinical features of three autosomal recessive neurological syndromes. I studied a cohort of children with early onset epileptic encephalopathy and, in one family, identified a novel homozygous pathogenic mutation of *PLCB1*. I have also utilised autozygosity mapping techniques to study consanguineous families with a complex motor disorder, infantile parkinsonism-dystonia, and identified loss-of-function mutations in the gene encoding the dopamine transporter (*SLC6A3*). Subsequent acquisition of a cohort of similarly affected children allowed detailed clinical and molecular characterisation of this novel disorder, dopamine transporter deficiency syndrome. Finally I have delineated the clinical and genetic features of *PLA2G6*-associated neurodegeneration. The identification of disease-causing genes contributes greatly to understanding the disease mechanisms underlying such early-onset disorders, and also provides novel insights into normal human neurodevelopment.

***I would like to dedicate this thesis to my husband, David and our beautiful daughter, Imogen. I am forever indebted to you both for your constant love and support which has enabled me to bring this work to completion.***

***Over the years, I have been privileged to work with a number of neurologically impaired children and their families, who have taught me so much, and continue to be a constant source of inspiration. Given the nature of this thesis, no dedication would be complete without a tribute to their courage, patience and perseverance.***

# Acknowledgements

It is with great pleasure that I acknowledge the help and encouragement given to me during this period of research. Firstly, I cannot thank my supervisor Eamonn Maher enough for truly inspiring me, and for all the encouragement and support over the last few years. Thank you also to Paul Gissen for being a fantastic mentor and kindred spirit, and for the many helpful academic discussions.

I am grateful to my laboratory colleagues in the Section of Medical and Molecular Genetics, especially Neil Morgan and Esther Meyer (for excellent laboratory training and also for kindly proof reading this thesis) and to Fatimah Rahman and Louise Tee (for kindly undertaking SNP arrays). Thank you also to the West Midlands Regional Genetic Laboratory for all their practical assistance, including the diagnostic screening of *PLA2G6* for referred patients.

I have had the great pleasure of working with some wonderful clinicians and I would especially like to thank Evangeline Wassmer for her incredible support and clinical input into this research. A thesis of this nature would not have been possible without excellent training in the semiology of movement disorders, and I am indebted to Martin Smith and Hardev Pall for providing this. Many thanks to Mary King for all the support and continuous teaching over the years, and for guiding me in how to become a paediatric neurologist.

I am particularly thankful to my collaborators, who have facilitated this work. Firstly, I would like to especially thank Maarten Reith and his group at NYU who

performed all functional investigations on mutant hDAT (Chapter 4, 5 and Appendix 2) and provided Figure 4-9 (Page 147). Thank you also to the many clinicians and research groups who have sent us samples over the years, especially Birgit Assmann, Terry Sanger, Grace Vassallo, Ingrid Scheffer and the UKISS group. Collaboration with the BPNSU (British Paediatric Neurology Surveillance Unit) also contributed greatly to the acquisition of the infantile spasms cohort. Many thanks to Lesley MacPherson and Katherine Foster for their radiological expertise in analysing the MR/CT imaging of the PLAN cohort. Thank you also to Birgit Assmann for assistance with Figure 4-1 and Table 5-3.

This PhD would not have been possible without generous funding from several organisations: the BCH Research Foundation, BDF NewLife and Action Medical Research.

Special thanks must be given to my Mum for her unfailing love and never-ending support and encouragement in everything that I have wanted to do. I am also grateful to my brother, Matthew for all the help and support. Thank you to my late father for instilling a belief that I could achieve anything I put my mind to. I would hope that, had he been alive today, this work would have made him proud.

# Contents Listings

Title  
Abstract  
Dedication  
Acknowledgements  
Table of Contents  
List of Illustrations  
List of Tables  
Abbreviations

## Table of Contents

<b>1</b>	<b>General Introduction.....</b>	<b>1</b>
<b>1.1</b>	<b>Introduction and overview.....</b>	<b>2</b>
<b>1.2</b>	<b>Normal and abnormal brain development.....</b>	<b>4</b>
1.2.1	Primary neurulation.....	7
1.2.2	Prosencephalic development.....	8
1.2.3	Development of the cerebellum.....	9
1.2.4	Neuronal proliferation.....	9
1.2.5	Neuronal migration.....	10
1.2.6	Organisation.....	11
1.2.7	Myelination.....	13
1.2.8	Summary.....	13
<b>1.3</b>	<b>Paediatric neurology.....</b>	<b>14</b>
<b>1.4</b>	<b>Epilepsy.....</b>	<b>15</b>
1.4.1	Epidemiology.....	15
1.4.2	Definitions.....	15
1.4.3	Classification of epileptic seizures.....	17
1.4.4	Classification of epilepsy syndromes.....	19
1.4.5	Mechanisms of epileptogenesis in the immature brain.....	21
1.4.5.1	Seizure susceptibility factors.....	21
1.4.5.2	The epileptogenic cascade.....	23
1.4.6	Genetics and epilepsy.....	23
1.4.7	Summary.....	25
<b>1.5</b>	<b>Movement disorders and the basal ganglia.....</b>	<b>26</b>
1.5.1	Introduction.....	26
1.5.2	Neuroanatomy of the basal ganglia.....	28
1.5.3	Functional aspects of the basal ganglia.....	29
1.5.3.1	Input connections to the basal ganglia.....	29
1.5.3.2	Output connections from the basal ganglia.....	29
1.5.4	Basal ganglia disease mechanisms in motor disease.....	32
1.5.4.1	The firing rate model.....	33
1.5.4.2	Firing pattern model.....	33
1.5.5	Summary.....	34
<b>1.6</b>	<b>Gene identification.....</b>	<b>35</b>
1.6.1	Why study rare recessive neurological diseases? .....	35
1.6.2	Approaches to gene identification.....	37
1.6.2.1	Functional cloning.....	37
1.6.2.2	Positional cloning.....	38

1.6.3	Haplotypes and genetic markers.....	39
1.6.4	Informativeness of markers.....	40
1.6.5	Maps.....	41
1.6.6	Linkage.....	42
1.6.7	Recombination fraction.....	42
1.6.8	LOD scores and critical values.....	43
1.6.9	Autozygosity mapping.....	45
1.6.9.1	Introduction.....	45
1.6.9.2	Consanguinity and the UK Pakistani population.....	45
1.6.9.3	Principles of autozygosity mapping.....	48
1.6.9.4	Mathematical model for autozygosity mapping.....	49
1.6.9.5	The power of autozygosity mapping.....	50
1.6.9.6	Pitfalls of autozygosity mapping.....	51
1.7	<b>Conclusion.....</b>	<b>53</b>

<b>2</b>	<b>General Methods .....</b>	<b>54</b>
----------	------------------------------	-----------

<b>2.1</b>	<b>Ascertainment of patients and control subjects.....</b>	<b>55</b>
2.1.1	Patient recruitment.....	55
2.1.2	Consent and ethics approval.....	56
2.1.3	Patient assessment and acquisition of blood samples.....	56
2.1.4	DNA from control subjects.....	56
<b>2.2</b>	<b>Materials.....</b>	<b>57</b>
2.2.1	Chemical reagents.....	57
2.2.2	Kits.....	58
<b>2.3</b>	<b>DNA Analysis .....</b>	<b>58</b>
2.3.1	DNA Extraction.....	58
2.3.2	SNP genotyping arrays.....	58
2.3.3	Microsatellite marker genotyping.....	59
2.3.3.1	Primers for PCR .....	59
2.3.3.2	PCR amplification for microsatellite marker genotyping.....	60
2.3.3.3	Analysis of microsatellite marker PCR products.....	61
2.3.4	Gene sequencing.....	61
2.3.4.1	Primers for sequencing candidate genes.....	61
2.3.4.2	PCR amplification for gene sequencing.....	61
2.3.4.3	Agarose gel electrophoresis.....	62
2.3.4.4	PCR product clean-up.....	63
2.3.4.5	Cycle sequencing.....	64
2.3.4.6	Sequencing reaction clean-up preparation.....	64
2.3.4.7	Preparation and analysis of sequencing reactions.....	65
2.3.5	Long range PCR.....	65
<b>2.4</b>	<b>RNA Analysis.....</b>	<b>67</b>
2.4.1	Isolation of total RNA.....	67
2.4.2	Reverse transcription and amplification of RNA (RT-PCR).....	67
2.4.2.1	Reverse transcription.....	67
2.4.2.2	Design of primers for PCR amplification of cDNA.....	68
2.4.2.3	PCR amplification of cDNA.....	68
<b>2.5</b>	<b>Website addresses for internet resources.....</b>	<b>69</b>

<b>3</b>	<b>Early Onset Epileptic Encephalopathy and <i>PLCB1</i>.....</b>	<b>70</b>
----------	---	-----------

<b>3.1</b>	<b>Introduction.....</b>	<b>71</b>
<b>3.2</b>	<b>The spectrum of early onset epileptic encephalopathies.....</b>	<b>72</b>



3.2.1	Ohtahara syndrome (OS) .....	73
3.2.2	Early myoclonic epileptic encephalopathy (EME).....	74
3.2.3	Migrating partial seizures of infancy (MPSI) .....	75
3.2.4	West syndrome (WS) .....	76
3.2.5	Classical Dravet syndrome (DS) .....	79
<b>3.3</b>	<b>Monogenic defects in infantile epileptic encephalopathies.....</b>	<b>81</b>
<b>3.4</b>	<b>Methods.....</b>	<b>85</b>
3.4.1	Clinical case acquisition and assessment.....	85
3.4.1.1	Acquisition of consanguineous family and index case.....	85
3.4.1.2	Clinical assessment.....	85
3.4.1.3	Acquisition of infantile epileptic encephalopathy cohort.....	85
3.4.2	Molecular genetic investigation.....	86
3.4.2.1	Isolation of DNA and cDNA.....	86
3.4.2.2	Genome wide scan.....	86
3.4.2.3	Development of primers.....	86
3.4.2.4	PCR Amplification and sequencing.....	90
<b>3.5</b>	<b>Results.....</b>	<b>91</b>
3.5.1	Clinical assessment of index case and family.....	91
3.5.2	Molecular genetic investigation.....	97
3.5.2.1	Genome-wide scan.....	97
3.5.2.2	Genomic DNA Sequencing of PLCB1.....	98
3.5.2.3	Characterisation of the putative deletion.....	98
3.5.2.4	cDNA sequencing of PLCB1.....	100
3.5.2.5	PLCB1 mutational analysis of other cases.....	103
<b>3.6</b>	<b>Discussion.....</b>	<b>103</b>
<b>3.7</b>	<b>Conclusion.....</b>	<b>109</b>

<b>4</b>	<b>Infantile Parkinsonism-Dystonia and <i>SLC6A3</i>.....</b>	<b>110</b>
----------	---	------------

<b>4.1</b>	<b>Introduction.....</b>	<b>111</b>
4.1.1	The monoamine neurotransmitter biosynthetic pathway.....	111
4.1.2	Clinical features of neurotransmitter disorders.....	114
4.1.3.	Diagnosis of inherited neurotransmitter disorders.....	117
4.1.3.1	Diagnostic lumbar puncture (LP).....	117
4.1.3.2	Blood and urine investigations.....	118
4.1.3.3	Enzyme analysis.....	119
4.1.3.4	Phenylalanine (phe) loading test.....	119
4.1.3.5	Genetic analysis.....	120
4.1.4	Treatment of neurotransmitter disorders.....	122
4.1.5	Other monoamine neurotransmitter disorders.....	123
<b>4.2</b>	<b>Materials and methods.....</b>	<b>124</b>
4.2.1	Clinical assessment.....	124
4.2.1.1	Case acquisition.....	124
4.2.1.2	Clinical phenotyping.....	124
4.2.1.3	CSF neurotransmitter analysis/biochemical investigations.....	124
4.2.2	Molecular genetic investigation.....	125
4.2.2.1	DNA extraction.....	125
4.2.2.2	Genome wide scan.....	125
4.2.2.3	Microsatellite marker analysis of the IPD locus.....	125
4.2.2.4	Multipoint linkage analysis.....	126
4.2.2.5	Gene sequencing.....	128
4.2.3	Functional analysis of mutant DAT proteins.....	130
<b>4.3</b>	<b>Results.....</b>	<b>130</b>

4.3.1	Clinical assessment .....	130
4.3.2	Results of molecular genetic investigation.....	135
4.3.2.1	Genome wide scan.....	135
4.3.2.2	Microsatellite marker analysis.....	135
4.3.2.3	Multipoint linkage analysis.....	139
4.3.2.4	Candidate gene selection and mutational analysis.....	139
<b>4.4</b>	<b>Discussion.....</b>	<b>142</b>
4.4.1	The dopamine transporter.....	142
4.4.2	Functional investigation of mutant hDAT proteins.....	143
<b>4.5</b>	<b>Conclusion.....</b>	<b>148</b>

<b>5</b>	<b>Dopamine Transporter Deficiency Syndrome.....</b>	<b>150</b>
----------	--	------------

<b>5.1</b>	<b>Introduction.....</b>	<b>151</b>
<b>5.2</b>	<b>Methods .....</b>	<b>152</b>
5.2.1	Clinical assessment of DTDS patients.....	152
5.2.1.1	Acquisition of DTDS cases.....	152
5.2.1.2	Clinical phenotyping.....	152
5.2.1.3	Biochemical investigations.....	153
5.2.1.4	Neuroradiology.....	153
5.2.2	Molecular genetic investigation.....	153
5.2.2.1	SLC6A3 mutational analysis.....	153
5.2.2.2	Long range PCR.....	153
5.2.3	Functional and molecular analysis of mutant DAT proteins.....	154
<b>5.3</b>	<b>Results.....</b>	<b>155</b>
5.3.1	Clinical phenotyping of DTDS.....	155
5.3.1.1	Family history.....	155
5.3.1.2	Pregnancy and early neonatal course.....	155
5.3.1.3	Onset of clinical symptoms in infancy.....	156
5.3.1.4	Clinical features of the DTDS movement disorder.....	157
5.3.1.5	Disease course.....	159
5.3.1.6	Response to therapeutic strategies.....	161
5.3.2	CSF neurotransmitter analysis and other investigations.....	164
5.3.3	Neuroradiological findings.....	166
5.3.3.1	Brain MRI and MRS.....	166
5.3.3.2	Nuclear brain imaging.....	167
5.3.4	Molecular genetic investigation.....	169
5.3.4.1	SLC6A3 mutational analysis.....	169
5.3.4.2	Characterisation of the deletion in patient 8.....	176
<b>5.4</b>	<b>Discussion.....</b>	<b>178</b>
5.4.1	Dopamine: anatomical distribution and physiological role.....	178
5.4.2	The structure and physiological function of DAT.....	180
5.4.3	The role of dopamine dysregulation in human diseases.....	182
5.4.4	The role of variants in SLC6A3 in human disease.....	182
5.4.5	Clinical features of DTDS.....	184
5.4.6	Genetic features of DTDS.....	185
5.4.7	Functional analysis of mutant DAT proteins.....	188
5.4.8	Proposed disease mechanisms in DTDS.....	193
5.4.9	DTDS is a dopamine 'transportopathy'.....	197
5.4.10	Differences between DTDS and other related disorders.....	197
5.4.11	DTDS and the SLC6A3 knockout mouse model.....	198
5.4.12	Therapeutic strategies in DTDS.....	199
<b>5.5</b>	<b>Conclusion.....</b>	<b>201</b>

<b>6</b>	<b>PLA2G6-associated neurodegeneration (PLAN).....</b>	<b>202</b>
6.1	<b>Introduction.....</b>	<b>203</b>
6.1.1	Spectrum of NBIA disorders.....	203
6.1.2	Radiological diagnosis of NBIA disorders.....	205
6.2	<b>PKAN.....</b>	<b>207</b>
6.2.1	Clinical syndromes.....	207
6.2.1.1	Typical PKAN.....	207
6.2.1.2	Atypical PKAN.....	208
6.2.1.3	HARP Syndrome.....	209
6.2.2	Radiological features of PKAN.....	209
6.2.3	Neurological investigations in PKAN.....	210
6.2.4	Molecular genetics of PKAN.....	210
6.3	<b>PLAN.....</b>	<b>212</b>
6.3.1	Discovery of a second NBIA locus .....	212
6.3.2	Identification of PLA2G6 mutations in NBIA and INAD.....	213
6.3.3	PLAN is clinically heterogeneous.....	213
6.4	<b>Materials and Methods.....</b>	<b>214</b>
6.4.1	Clinical assessment.....	214
6.4.1.1	Case acquisition.....	214
6.4.1.2	Clinical phenotyping.....	214
6.4.2	Molecular genetic investigation.....	215
6.5	<b>Results.....</b>	<b>216</b>
6.5.1	Clinical phenotype of PLAN.....	216
6.5.1.1	Family history.....	216
6.5.1.2	Presenting clinical symptoms and signs.....	216
6.5.1.3	Disease progression.....	217
6.5.2	Radiological findings.....	220
6.5.3	Results of other investigations.....	226
6.5.3.1	Neurophysiology and histology.....	226
6.5.3.2	Other investigations.....	226
6.5.4	Results of molecular genetic investigation.....	227
6.6	<b>Discussion.....</b>	<b>228</b>
6.6.1	Clinical features of infantile PLAN.....	228
6.6.2	Radiological features of infantile PLAN.....	229
6.6.3	Features on neurological investigation of infantile PLAN.....	230
6.6.4	Other PLAN phenotypes.....	230
6.6.4.1	Childhood onset PLAN.....	231
6.6.4.2	Adult onset PLAN.....	232
6.6.5	Postulated function of <i>PLA2G6</i> .....	236
6.6.6	Genetic features of PLAN.....	237
6.7	<b>Conclusion.....</b>	<b>240</b>
<b>7</b>	<b>References.....</b>	<b>242</b>
<b>8</b>	<b>Appendix.....</b>	<b>272</b>

# List of Illustrations

<b>Figure 1-1</b> <i>Schematic representation of the brain illustrating the possible origins and clinical symptoms of focal seizures.....</i>	18
<b>Figure 1-2</b> <i>Schematic representation of the major input and output connections of the basal ganglia (Adapted from Kandel, 2000b).....</i>	27
<b>Figure 1-3</b> <i>Coronal section of the brain illustrating a schematic representation of the basal ganglia structures.....</i>	28
<b>Figure 1-4</b> <i>Schematic representation of the hyperdirect, direct and indirect pathways of the basal ganglia.....</i>	30
<b>Figure 1.5</b> <i>The principle of autozygosity mapping, in which the specific mutation of a disease gene (indicated by the black arrow) can be passed on from a common ancestor (CA) to offspring and the product of a consanguineous marriage, can result in affected offspring.....</i>	49
<b>Figure 3-1</b> <i>Burst-suppression pattern on EEG .....</i>	74
<b>Figure 3-2</b> <i>EEG of a patient (age 8 months) with infantile spasms. The chaotic, high amplitude spike and slow wave pattern of hypsarrhythmia is evident.....</i>	78
<b>Figure 3-3</b> <i>EEG of patient aged 8 months demonstrating electrodecrement on EEG following the onset of a clinical spasm (indicated by the black arrow).....</i>	78
<b>Figure 3-4</b> <i>Family tree of consanguineous kindred Affected child with epileptic encephalopathy is indicated by black shading (IV:1). Circles indicated females; squares indicate males; diamonds indicate undisclosed gender.....</i>	94
<b>Figure 3-5</b> <i>Schematic representation of the evolution of the index case's clinical course over the first 28 months of his life (prior to his death at 2.9 years) N Normal EEG H Hypsarrhythmic pattern on EEG E Encephalopathic pattern on EEG – diffuse generalised slowing .....</i>	95

**Figure 3-6***EEG recordings of index case (VI:1)***3-6A***Hypsarrhythmia on interictal EEG, age 8.5 months..... 96***3-6B***Non specific excessive generalised slow wave activity on sleep EEG recording, age 13 months..... 96***Figure 3-7***Copy number variant analysis, indicating a homozygous deletion of approximately 0.5Mb at chromosome 20p12.3, in the region of PLCB1..... 97***Figure 3-8***Agarose gel photograph illustrating PCR amplification of exons 1-4 of PLCB1 in the index case and his parents. A hyperladder has been added to lane 1 to aid estimation of PCR product size**M III:7 (Mother of index case)**F III:8 (Father of index case)**A IV:1 (index case)**In III:7 and III:8 all 4 exons were amplifiable. However, in the index case, on repeated attempts, PCR amplification of exons 1, 2 and 3 was not possible. Exon 4 was amplifiable in the index case..... 98***Figure 3-9***Long Range PCR Amplification**A - IV:1 (Index Case)**P - III:8 (Father)**C1-C16 - Control DNA samples**Agarose gel photograph illustrating PCR amplification (using primers FP and RP for long range PCR) of a ~7kb product in both the index case (IV:1) and his father (III:8). PCR amplification was not achieved in control samples (C1-16 shown here)**A hyperladder has been added to lane 1 to aid estimation of PCR product size... 99***Figure 3-10***Definition of the genomic breakpoint of the deletion. The upstream genomic breakpoint was determined to be between 8,034,442 and 8,034,510bp and the downstream genomic breakpoint was determined to be between 8,520,654 and 8,520,722bp. A 68bp sequence which showed 100% sequence homology for both the upstream and intron 3 sequence was identified (highlighted in the yellow box). .... 101***Figure 3-11***Sequencing analysis of genomic and cDNA in the index case's mother (III:7) and father (III:8) for PLCB1 exons 24 and 31. Although there is biallelic expression of SNPs rs2076413 (G/A) and rs2294597 (C/T) in genomic DNA, there is monoallelic expression of these SNPs rs2076413 (A) and rs2294597 (T) in cDNA..... 102***Figure 3-12***Proposed cellular function of PLCB1. The G-protein coupled mACh receptor activates PLCB1 which hydrolyses  $PIP_2$  to DAG and  $IP_3$ . DAG directly activates PKC, whereas  $IP_3$  activates the  $IP_3$ -activated ER-Ca channel. Ca released from*

the ER also activates PKC. PKC phosphorylates the potassium ( $K^+$ ) channel increasing  $K^+$  efflux causing depolarisation (Kurian et al., 2010a)..... 106

#### Figure 4-1

The monoamine metabolism pathway

Metabolic pathway of serotonin and dopamine biosynthesis (solid arrows), catabolism (dotted arrows) and salvage (dashed arrows). The biogenic amines are boxed in orange. Tetrahydrobiopterin ( $BH_4$ ) is the essential cofactor for the rate-limiting enzymes tyrosine hydroxylase (TH) and tryptophan hydroxylase.  $BH_4$  is synthesised de novo via steps 8-11 and recycled via the salvage pathway (steps 12-13).

**GTP** is guanosine triphosphate,  **$H_2NP_3$**  is dihydroneopterin triphosphate, **NEO** is neopterin, **6-PTP** is 6-pyruvoyltetrahydropterin, **SPT** is sepiapterin,  **$BH_4$**  is tetrahydrobiopterin and  **$qBH_2$**  is (quinonoid) dihydrobiopterin, **5-HTP** is 5-hydroxytryptophan, **L-DOPA** is levodihydroxyphenylalanine (levodopa), **OMD** is 3-ortho-methyldopa, **VLA** is vanillyllactic acid, **5-5-HIAA** is 5-hydroxyindoleacetic acid, **HVA** is homovanillic acid.

**1** is tryptophan hydroxylase; **2** is tyrosine hydroxylase (**TH**); **3** is aromatic L-amino acid decarboxylase (**AADC**); **4** is monoamine oxidase (**MAO**); **4a** is monoamine oxidase plus aldehyde dehydrogenase; **5** is catechol-O-methyltransferase (**COMT**); **6** is dopamine  $\beta$ -hydroxylase; **7** phenylethanolamine N-methyltransferase **8** is GTP-cyclohydrolase I (**GTPCH I**); **9** is 6-pyruvoyltetrahydropterin synthase (**PTPS**); **10** is aldose reductase; **11** is sepiapterin reductase (**SR**); **12** is pterin-4 $\alpha$ -carbinolamine dehydratase; **13** is dihydropteridine reductase (**DHPR**)..... 113

#### Figure 4-2

Family trees of consanguineous kindreds. Children affected with IPD are indicated by black shading. Circles indicate females; squares indicate males; diamonds indicate undisclosed gender

**Figure 4-2A** Family A kinship..... 132

**Figure 4-2B** Family B kinship..... 133

#### Figure 4-3

Microsatellite marker linkage analysis on chromosome 5 in Family A

Affected individuals are shaded in black. SLC6A3 gene is located at 5p15.3. Microsatellite markers are positioned according to physical distance (MB). Haplotypes for these markers are shown and the disease associated haplotypes are boxed in blue. The two affected children share a common homozygous haplotype in this region. (N) –Novel microsatellite marker..... 136

#### Figure 4-4

Microsatellite Marker Analysis on chromosome 5 in family B

The affected child is shaded in black. Microsatellite markers are positioned according to physical distance (MB). Haplotypes for these markers are shown and the disease associated haplotypes are boxed in red. Microsatellite markers show evidence of segregation with disease status in this family.(N) –Novel microsatellite marker..... 137

**Figure 4-5**

Localisation of the disease locus on chromosome 5 on 250K SNP array

SNP array data is illustrated on family A: Patient #1 (VII:1), Patient #2 (VII:3) and the unaffected sibling of patient 1 (VII:2)

Dark blue: AA homozygous SNP call

Mid blue: BB homozygous SNP call

Light blue: No call

White: AB Heterozygous call

Patient #1 and #2 display a region of SNP homozygosity from 0 – 2.3MB

The unaffected sibling (VII:2) does not display this common SNP homozygosity and has a heterozygous SNP haplotype in this region.....

138

**Figure 4-6**

SLC6A3 mutations in Family A and Family B.

The alignments of SLC6A3 nucleotides c.1091-c.1116 (Panel A, B and C) and c.1168 -c.1197 (Panel D, E and F) are shown. Panel B illustrates c.1103T>A in Family A. Panel E illustrates c.1184C>T in family B.....

140

**Figure 4-7**

Conservation of the mutated DAT1 residues Leu368 and Pro395.

Five representative vertebrate sequences are aligned. Leucine 368 (Leu368) and Proline (Pro395) are coloured in red. Residues matching the consensus sequence are in grey.....

141

**Figure 4-8**

Expression of the Leu368Gln hDAT and Pro395Leu hDAT in transiently transfected HEK293 cells via immunoblotting analysis

Cells were transiently transfected with WT hDAT, Leu368Gln hDAT, Pro395Leu hDAT, and reagent only. In each respective panel, the same amount of protein was loaded in all lanes. Biotinylated (surface) protein (left panel) and total lysate (right panel) were probed with anti-DAT antibody for detection of the relative expression level of WT and mutant DAT protein. Anti- $\beta$ -actin antibody showed the relative equivalent loading of total protein. There was no  $\beta$ -actin in the surface preparation .....

145

**Figure 4-9**

Two-dimensional representation of dopamine transporter topology based on LeuT structure

Twelve transmembrane domains are shown with helically unwound regions in first and sixth domain; extracellular and intracellular loops include helical portions (e2, e3, e4a, e4b, and i1, 15, respectively). Leu368, subject to missense mutation, is shown in red at the top of transmembrane domain 7, one helix turn under Met371 in blue. Pro395, also subject to missense mutation, is shown in red in the e4b portion of extracellular loop 4, one helix turn above Ala399 in blue. In the three-dimensional structure, sodium ions interact with residues of transmembrane domains 1, 6, and 8, and also 7 .....

147

**Figure 5-1**

MR Brain of patient 9, age 2.2 years

Axial T-1 weighted images demonstrating symmetrical periventricular white matter changes (yellow arrows)..... 166

**Figure 5-2**

Nuclear brain imaging (in age-matched individuals) using single photon emission computed tomography (SPECT) after administration of the dopamine transporter ligand DaTSCAN (Ioflupane, <sup>123</sup>I)

**Figure 5-2A** DaTSCAN imaging in a control subject demonstrating normal distribution of dopamine transporter sites.

**Figure 5-2B** DaTSCAN imaging in a patient with juvenile parkinsonism (age 9.2 years), showing bilateral symmetrical loss of dopamine transporter sites from the lentiform nuclei.

**Figure 5-2C** DaTSCAN imaging in patient 3 (age 10 years) indicating complete loss of dopamine transporter sites in the basal nuclei. This results in high background counts on the image without any activity from the basal nuclei..... 168

**Figure 5-3**

Novel mutations identified in patient 4, 5, 6, 7, 9, 10 and 11..... 171

**Figure 5-3A: Patient 4**

The alignments of SLC6A3 nucleotides c.1153-c.1156 and first 9 nucleotide bases in intron 8 are illustrated

The homozygous splice variant c.1156+5delG is boxed in yellow..... 171

**Figure 5-3B: Patient 5**

The alignments of SLC6A3 nucleotides c.469-c.475 and c.1658-c.1664 are illustrated

The 2 heterozygous missense mutations identified are boxed in yellow..... 171

**Figure 5-3C: Patient 6**

The alignments of SLC6A3 nucleotides c.1028-c.1031 and the first six nucleotide bases of intron 7 are illustrated

The homozygous splice variant c.1031+1G>A is boxed in yellow..... 172

**Figure 5-3D: Patient 7**

The alignments of SLC6A3 nucleotides c.396-c.405 are illustrated

No DNA was available from the child who had died prior to genetic investigation

A heterozygous deletion c.399delG (boxed in yellow) was identified in both parents..... 172

**Figure 5-3E: Patient 9**

The alignments of SLC6A3 nucleotides c.978-c.985, c.1312-c.1318 and

c.1584-c.1589 are illustrated. The 3 heterozygous mutations

(2 missense and one nonsense) identified are boxed in yellow..... 173

**Figure 5-3F: Patient 10**

The alignments of SLC6A3 nucleotide c.667 –c.676 are illustrated

The homozygous missense change 671T>C is boxed in yellow..... 174

**Figure 5-3G: Patient 11**

The alignments of SLC6A3 nucleotides c.1557-c.1567 are illustrated

The homozygous missense change c.1561C>T is boxed in yellow..... 174

**Figure 5-4**

Conservation of the mutated SLC6A3 residues Val158, Leu224, Gly327, Arg521, Pro529, Pro554. Six representative vertebrate sequences are aligned..... 175



### Figure 5-5

Definition of the SLC6A3 deletion in patient 8

**Figure 5-5A** Agarose gel photograph of PCR amplification of introns 10 to 14 of SLC6A3 showing the presence of bands in patient 8 (Lane 5) and their parent (Lane 6) and the absence of bands in normal controls (Lanes 1-4). Lane 7 is a negative control.

**Figure 5-5B** Determination of the DNA sequence of the genomic breakpoint of the deletion. The exons that are present are indicated in red (exon 11 and 14). The deleted exons/introns are represented in grey (exon 12 and 13). The telomeric and centromeric genomic breakpoints were mapped to 1,455,093 – 1,455,095bp (intron 13, shaded in blue) and 1,460,244 - 1,460,246bp (intron 11, shaded in blue). There is a 3 base region of homologous sequence which show 100% homology in both intron 11 and 13 (shaded yellow box).....

177

**Figure 5-6** Protein structure of the dopamine transporter and identified variants to date. Adapted from Giros & Caron (1993).....

187

### Figure 5-7

Expression of wild-type (WT) and mutant hDAT in HEK293 cells via immunoblotting analysis. Cells were transiently transfected with WT, mutant hDAT, or reagent only (mock). The same amount of total lysate protein was loaded in all lanes. Protein was probed with antibody against the C-terminus (top panel) or N-terminal (middle panel) of DAT. Anti- $\beta$ -actin antibody showed the relative equivalent loading of total protein (bottom panel) .....

191

### Figure 5-8

Diagram of a dopaminergic synapse postulating disease mechanisms in DTDS (adapted from Blackstone 2009). The presynaptic neuron, postsynaptic neuron and synaptic cleft are illustrated in the normal and DTDS disease state. Dopamine (indicated by orange circles) may bind presynaptically to  $D_2$  autoreceptors, perisynaptically to DAT and postsynaptically to  $D_1$  and  $D_2$  receptors.  $D_1$  and  $D_2$  receptors are coupled to adenylyl cyclase (A) via G proteins (GP). Dopamine may also be metabolised to HVA by COMT and MAO-B. In DTDS, there is reduced DAT-mediated re-uptake of dopamine into the presynaptic cleft. This results in excess synaptic dopamine, which is converted by COMT to HVA. Excess synaptic dopamine may also overstimulate  $D_2$  autoreceptors which will inhibit the activation of tyrosine hydroxylase, thereby reducing endogenous dopamine production. Prolonged dopamine in the synaptic cleft may also cause some downregulation/desensitisation of postsynaptic  $D_1$  and  $D_2$  receptors thereby altering downstream signalling.....

196

### Figure 6-1

Examples of MR Images of NBIA disorders

6-1A Patient age 5.9 years, classical PKAN. Axial T2-weighted FSE (fast spin echo) sequences showing bilateral eye-of-the-tiger sign with a medial central hyperintense region (yellow arrow) surrounding a region of hypointensity (white arrow) in the globus pallidi

6-1B Patient, age 12 years, childhood PLAN. Axial susceptibility-weighted image showing abnormal low signal in the globus pallidi

6-1C Patient, age 9 years, idiopathic NBIA. Axial T2-weighted gradient echo image showing abnormal low signal in the globus pallidi

6-1D Patient age 12 years, idiopathic NBIA. Axial T2-weighted image (contrast enhanced fast field echo, FFE) showing reduction in T2 signal in the substantia nigra .....	206
<b>Figure 6-2</b>	
Development of neurological features in the PLAN cohort.....	218
<b>Figure 6-3</b>	
MR Imaging of patient 4, age 5.8 years: axial FLAIR (6-3A) and coronal T2-weighted (6-3B) sequences showing cerebellar cortical atrophy and gliosis, with increased CSF spaces around the cerebellum and increased signal on T2 and FLAIR sequences in the residual cortex of the cerebellum.....	220
<b>Figure 6-4</b>	
MR imaging of patient 6, age 13.9 years (6-4A and 6-4B) and patient 4, age 5.9 years (6-4C and 6-4D). Axial T2* gradient sequences (6-4A, 6-4B, 6-4C) and coronal T2-weighted sequence (6-4D) showing marked reduction in T2 signal in the globus pallidi (6-4A,6-4C) and more medially on 6-4C and substantia nigra (6-4B,6-4D). The degree of iron deposition is much more marked in patient 6 (the older child) compared to patient 4 .....	222
<b>Figure 6-5</b>	
MR imaging: Axial T2-weighted sequences in 3 children within the cohort. The abnormal reduced signal in the globus pallidi increases in severity with increasing age.....	223
<b>Figure 6-6</b>	
MR imaging: Sagittal T1-weighted sequence showing thin, elongated and vertical orientation of the splenium (posterior) corpus callosum (long arrow). Note marked atrophy of the vermis of the cerebellum (short arrow)	
Patient 4, age 2.3 years.....	224
<b>Figure 6-7</b>	
Schematic representation of PLA2G6 protein structure (adapted from Balsinde & Balboa 2005, Morgan et al., 2006) and reported PLA2G6 mutations (Morgan et al., 2006, Kurian et al 2008, Gregory et al 2008, Carrilho et al 2008, Paisan Ruiz et al 2009, Sina et al 2009, Wu et al 2009, Crompton et al 2010). The protein consists of 7 ankyrin repeats (green), a proline-rich motif (blue) a glycine rich nucleotide binding site (brown), a lipase motif (red), a putative C-terminus calcium-dependent calmodulin binding site (purple) and three proposed caspase cleavage sites (orange). Numbers indicate amino acids. Missense mutations are indicated above the protein and deletions, duplications, nonsense, and splice site mutations are indicated below the protein. Mutations described in infantile PLAN (black), childhood PLAN (yellow) and adult PLAN (red) are illustrated.....	239

# List of Tables

<b>Table 1-1</b> <i>Major events in development of the human brain (adapted with data from Volpe 2008a; Volpe, 2008b), and some examples of single gene defects causing aberrant brain development.....</i>	<b>5</b>
<b>Table 1-2</b> <i>Molecular determinants of neuronal migration (adapted from Volpe, 2008b).....</i>	<b>11</b>
<b>Table 1-3</b> <i>Classification of the epilepsies (adapted from Berg et al., 2010).....</i>	<b>17</b>
<b>Table 1-4</b> <i>Classification of epilepsy (adapted from Engel, 2006).....</i>	<b>20</b>
<b>Table 1-5</b> <i>Genes associated with the idiopathic epilepsies (adapted from Mulley et al., 2003).....</i>	<b>24</b>
<b>Table 1-6</b> <i>Degrees of consanguinity and its effect on F and R and risk of autosomal recessive disease in offspring (Adapted from Young, 1999).....</i>	<b>46</b>
<b>Table 2-1:</b> <i>Web-based resources.....</i>	<b>69</b>
<b>Table 3-1</b> <i>Clinical features of the infantile epileptic encephalopathies.....</i>	<b>80</b>
<b>Table 3-2</b> <i>Single gene defects associated with infantile and childhood epileptic encephalopathies.....</i>	<b>82</b>
<b>Table 3-3</b> <i>Primers used for genomic PLCB1 sequencing .....</i>	<b>87</b>
<b>Table 3-4</b> <i>Primers used for cDNA PLCB1 sequencing.....</i>	<b>89</b>
<b>Table 3-5</b> <i>Primers used for long range PCR and delineation of the genomic breakpoint.....</i>	<b>89</b>
<b>Table 3-6</b> <i>PLCB1 Transcripts (adapted from Ensembl genome browser).....</i>	<b>105</b>
<b>Table 4-1</b> <i>Clinical features of the monoamine neurotransmitter disorders.....</i>	<b>116</b>

<b>Table 4-2</b>	
<i>Characteristic biochemical profile of the monoamine neurotransmitter disorders.....</i>	<b>121</b>
<b>Table 4-3</b>	
<i>Microsatellite markers used for linkage analysis of the common regions of homozygosity identified in the affected children of family A.....</i>	<b>126</b>
<b>Table 4-4</b>	
<i>Primers used for sequencing of coding regions of SLC6A3 gene.....</i>	<b>129</b>
<b>Table 4-5</b>	
<i>Phenotypic data for children with IPD.....</i>	<b>134</b>
<b>Table 4-6</b>	
<i>Multipoint Linkage analysis for Family A and Family B.....</i>	<b>139</b>
<b>Table 4-7</b>	
<i>Dopamine transport and cocaine analogue binding by Wild-type, Leu368Gln and Pro395Leu hDAT.....</i>	<b>144</b>
<b>Table 5-1</b>	
<i>Primers used for cycle sequencing of deletion-specific amplicon in order to determine the genomic breakpoint of the deletion.....</i>	<b>154</b>
<b>Table 5-2</b>	
<i>Overview of clinical features in DTDS.....</i>	<b>163</b>
<b>Table 5-3</b>	
<i>CSF neurotransmitter findings in the DTDS cohort.....</i>	<b>165</b>
<b>Table 5-4</b>	
<i>SLC6A3 mutations identified in the DTDS cohort.....</i>	<b>170</b>
<b>Table 5-5</b>	
<i>Dopamine transport and cocaine analogue binding by wild-type and mutant hDAT.....</i>	<b>190</b>
<b>Table 6-1</b>	
<i>Age of onset of clinical features for patients in the PLAN cohort.....</i>	<b>219</b>
<b>Table 6-2</b>	
<i>Radiological findings in the cohort.....</i>	<b>225</b>
<b>Table 6-3</b>	
<i>Mutations identified in the cohort.....</i>	<b>227</b>
<b>Table 6-4</b>	
<i>Comparison of the clinical features of PKAN and PLAN.....</i>	<b>234</b>
<b>Table 6-5</b>	
<i>Comparison of the features of PKAN and PLAN on investigation.....</i>	<b>235</b>

## Abbreviations

[ <sup>3</sup> H]CFT	2 beta-carbomethoxy-3- beta-(4-fluorophenyl)-N-[ <sup>3</sup> H]methyltropine)
3-OMD	3-O-methyldopa
5-HIAA	5-hydroxyindoleacetic acid
5-HTP	5 hydroxytryptophan
6-PTP	6-pyruvoyltetrahydropterin
AADC	Aromatic L-amino acid decarboxylase
ACTH	Adrenocorticotrophic hormone
ADHD	Attention deficit hyperactivity disorder
AGS	Aicardi-Goutieres syndrome
AMPA	α-amino-3-hydroxy-5-methyl-isoxazole propionate
AMV	Avian Myeloblastosis Virus
APGAR	Scoring system to evaluate the condition of a newborn
AR	Autosomal recessive
ARX	Aristaless related homeobox
ATP	Adenosine triphosphate
BH <sub>4</sub>	Tetrahydrobiopterin
BLAST	Basic Local Alignment Search Tool
B <sub>max</sub>	Maximal binding
bp	Base pairs
BPNA	British Paediatric Neurology Association
BPNSU	British Paediatric Neurology Surveillance Unit
Ca/Ca <sup>2+</sup>	Calcium
cAMP	Cyclic adenosine monophosphate
CDKL5	Cyclin dependent kinase-like 5
cDNA	Complementary deoxyribonucleic acid
CK	Creatine kinase
Cl <sup>-</sup>	Chloride
cM	CentiMorgan
CNS	Central nervous system
CNV	Copy number variant
COMT	Catechol-O-methyltransferase
CSF	Cerebrospinal fluid
CT	Computerised tomography
C-terminus	Carboxy terminus
CTG	Cardiotocography
D <sub>1</sub>	D <sub>1</sub> dopamine receptor
D <sub>2</sub>	D <sub>2</sub> dopamine receptor
DAG	Diacylglycerol
DAT	Dopamine transporter
DAT1	Gene encoding the dopamine transporter ( <i>SLC6A3</i> )
DaTSCAN	(123)I-FP-CIT ioflupane [(123)I-2beta-carbomethoxy-3beta-(4-iodophenyl)-N-(3-fluoropropyl) nortropine
DBH	Dopamine β-hydroxylase

dbSNP	A comprehensive SNP database
DHPR	Dihydropteridine reductase
DNA	Deoxyribonucleic acid
dNTP	Dideoxynucleotides
DOPAC	3,4-dihydroxyphenylacetic acid
DS	Dravet syndrome
DTDS	Dopamine transporter deficiency syndrome
EDTA	Ethylenediaminetetraacetic acid
EEG	Electroencephalogram
EL	Extracellular loop
EME	Early myoclonic epileptic encephalopathy
EMG	Electromyogram
ER	Endoplasmic reticulum
ERG	Electroretinogram
F	Coefficient of inbreeding
FFE	Fast field Echo
FLAIR	Fluid-attenuated inversion recovery
FSE	Fast spin Echo
G protein	Guanine nucleotide binding protein
GABA	$\gamma$ -aminobutyric acid
GEFS+	Generalized epilepsy with febrile seizures-plus
GPe	Globus pallidus externa
GPi	Globus pallidus interna
GTP	Guanosine triphosphate
GTPCH	GTP-cyclohydrolase
H	Heterozygosity
H <sub>2</sub> NP <sub>3</sub>	Dihydroneopterin triphosphate
H <sub>2</sub> O	Water
hDAT	Human dopamine transporter
HEK-293	Human embryonic kidney 293 cells
HPLC	High pressure liquid chromatography
HVA	Homovanillic acid.
HWE	Hardy Weinberg equilibrium
IBZM	[ <sup>123</sup> I]iodobenzamide
iGluR	Inotropic glutamate receptor
IL	Intracellular loop
ILAE	International League Against Epilepsy
INAD	Infantile neuroaxonal dystrophy
IP <sub>3</sub>	Inositol 1,4,5-trisphosphonate
IPD	Infantile parkinsonism-dystonia
iPLA2-VI	Calcium independent phospholipase A2 group 6 enzyme
K <sup>+</sup>	Potassium
Kb	Kilobases
K <sub>d</sub>	Binding affinity
kDa	KiloDalton
K <sub>i</sub>	Potency of inhibition

L-dopa	Levodihydroxyphenylalanine (levodopa)
LeuT	Bacterial leucine transporter from <i>Aquifex aeolicus</i>
LOD score	Log10 of the odds, $Z(\theta)$ , likelihood odds ratio
LP	Lumbar puncture
LREC	Local research ethics committee
mACh	Muscarinic acetylcholine receptor
MAO	Monoamine oxidase
Mb/MB	Megabase
mGluR	Metabotropic glutamate receptor
MLPA	Multiplex ligation-dependent probe amplification
MPSI	Migrating partial seizures of infancy
MPTP	1-methyl-4-phenyl-1,2,3,6-tetrahydropyridine
MR	Magnetic resonance
MRI	Magnetic resonance imaging
mRNA	Messenger ribonucleic acid
MRS	Magnetic resonance spectroscopy
Na <sup>+</sup>	Sodium
NCAM	Neural cell adhesion molecule
NCBI	National Centre for Biotechnology Information
NCS	Nerve conduction studies
NEO	Neopterin
NHS	National Health Service
NMDA	N-methyl-D-aspartate
N-terminal	Amino-terminus, NH <sub>2</sub> -terminus
OMD	3-ortho-methyldopa
OMIM	Online Mendelian Inheritance in Man
OS	Ohtahara syndrome
PCBD	Pterin-4a-carbinolamine dehydratase
PCR	Polymerase chain reaction
Phe	Phenylalanine
PIC	Polymorphism information content
PIP <sub>2</sub>	Phosphatidylinositol 4,5-bisphosphonate
PKAN	Pantothenate kinase associated neurodegeneration
PKC	Protein kinase C
PLA2G6	Phospholipase A2, group 6
PLAN	PLA2G6-associated neurodegeneration
PLCB1	Phospholipase C Beta 1
PTPS	Pyruvoyltetrahydropterin synthase
qBH <sub>2</sub>	(quinonoid) Dihydrobiopterin
R	Recombinant
RFLP	Restriction Fragment Length Polymorphism
RNA	Ribonucleic acid
ROPD	Rapid onset dystonia parkinsonism
SCN1A	Sodium channel, neuronal type 1, alpha subunit
SLC6A3	Solute carrier family 6 (neurotransmitter transporter, dopamine), member 3
SLE	Systemic lupus erythematosus

SMEI	Severe myoclonic epilepsy of infancy
SNP	Single nucleotide polymorphism
SPECT	Single photon emission computed tomography
SPT	Sepiapterin
SR	Sepiapterin reductase
STXBP1	Syntaxin binding protein 1
TBE	Tris-borate/EDTA
TH	Tyrosine hydroxylase
UCSC	University of California, Santa Cruz
UKISS	United Kingdom Infantile Spasms Study
UNISTS	A comprehensive database of sequence tagged sites (STS)
UTR	Untranslated region
UV	Ultraviolet
VEP	Visual evoked potential
VLA	Vanillylactic acid
VMAT	Vesicular monoamine transporter
WHO	World Health Organisation
WS	West syndrome
WT	Wild type
$\alpha$	alpha, also proportion of affected individuals homozygous by descent
$\beta$	beta
$\gamma$	gamma



# **Chapter 1**

## **General Introduction**

## 1.1 Introduction and overview

*‘The task of neural science is to explain behaviour in terms of the activities of the brain. How does the brain marshal its millions of individual nerve cells to produce behaviour, and how are these cells influenced by the environment...? The last frontier of the biological sciences – their ultimate challenge – is to understand the biological basis of consciousness and the mental processes by which we, perceive, move, think and remember’*

*Eric Kandel (Recipient of the Nobel Prize for Medicine, 2000)*

Molecular biology has provided important insights into human brain function, predominantly by expanding knowledge on how the brain develops, how nerve cells communicate, how different patterns of neural interconnections give rise to a variety of motor acts and human perceptions, and how communication between neurons are modified by human experiences and diseases.

At a molecular level, advances in neural science have been achieved in a number of ways (Kandel *et al.*, 2000a). The characterisation of ion channel structure and function has greatly facilitated the analysis of neurobiological problems. Structural studies have also deepened the understanding of membrane receptors coupled to intracellular secondary messenger systems, and the role of these systems in modulating the physiological responses of nerve cells.

With the possible exception of trauma, it is quite possible that every disease affecting the human nervous system has some inherited component, ranging from monogenic inheritance to genetic susceptibility. Advances in molecular biology, (such as the Human Genome Project and whole genome sequencing) have certainly facilitated the identification of genes contributing to specific

neurological disorders. Characterisation of genes encoding ion channels, membrane proteins/receptors, growth factors, transcriptional regulatory factors and cell/substrate adhesion molecules have transformed the study of neuroscience from a descriptive discipline into a mechanistic one. Indeed, the molecular mechanisms underlying the assembly of functional neuronal circuitry (including the specification of cell fate, cell migration, axonal growth, target recognition and synapse formation) are increasingly understood. The ability to develop genetically modified organisms (such as zebrafish, mice and primates) has additionally allowed us to elucidate how single gene defects may cause neurological abnormalities at both a gross phenotypic and cellular/molecular level. Such animal models have also greatly contributed to understanding the pathogenic mechanisms underlying human neurological diseases.

For the work described in this thesis, I have utilised my skills as a paediatric neurologist to accurately phenotype and categorise children with complex neurological disorders. I have subsequently undertaken molecular genetic investigation in order to identify disease-causing genes and define the clinical spectrum of such genetic disorders. I will describe one epilepsy syndrome (*PLCB1*-infantile epileptic encephalopathy) and two predominantly extrapyramidal syndromes affecting the basal ganglia (dopamine transporter deficiency syndrome and *PLA2G6*-associated neurodegeneration). Understanding the molecular and cellular mechanisms underlying the pathophysiology of these neurological syndromes will enhance the knowledge of brain development and neural function, and can also facilitate the future development of novel therapeutic strategies.

In this introductory chapter, I will briefly describe the salient features of normal and abnormal brain development (and the wide variety of associated monogenic neurological diseases). I will also summarise the evolution of paediatric neurology as a distinct clinical specialty, and provide an overview of the breadth of neurological disorders encountered in this field, with a focus on epilepsy and movement disorders (relating directly to diseases investigated in this thesis). The general principles of gene mapping will also be discussed.

## ***1.2 Normal and abnormal brain development***

Monogenic defects may affect the developing brain at any stage of pre- and postnatal neural development, leading to a wide spectrum of neurological disorders. The major stages of normal brain development and some examples of genetic defects causing aberrant brain development are summarised in Table 1-1. Each developmental phase is also briefly discussed below (Volpe, 2008a; Volpe, 2008b).

**Table 1-1**

**Major events in development of the human brain (adapted with data from Volpe 2008a; Volpe, 2008b), and some examples of single gene defects causing aberrant brain development**

Developmental Phase	Single gene defects	References
Primary neurulation (Peak time 3-4 weeks gestation)		
Craniorachischisis totalis	A variety of neural tube defects may be caused by:- Variants in genes <i>MTHFR</i> , <i>MTRR</i> , <i>MTHFD1</i> <i>VANGL1</i> , <i>VANGL2</i> <i>COL18A1</i> (Knobloch syndrome) <i>MKS1</i> , <i>RPGRIP1L</i> (Meckel syndrome)	Greene <i>et al.</i> , 2009 Lei <i>et al.</i> , 2010; Kibar <i>et al.</i> , 2007, 2009 Sertie <i>et al.</i> , 2000 Kyttala <i>et al.</i> , 2006; Delous <i>et al.</i> , 2007
Anencephaly		
Myeloschisis		
Encephalocoele		
Myelomeningocoele		
Prosencephalic development (Peak time 2-3 months gestation)		
Atelencephaly	<i>SIX3</i>	Wallis <i>et al.</i> , 1999
Holoprosencephaly	<i>SIX3</i> , <i>SHH</i> , <i>TGIF</i> , <i>ZIC2</i> <i>PTCH1</i> , <i>TGDF1</i> , <i>FAST1</i> , <i>GLI2</i>	Wallis and Muenke, 2000
Agenesis of the corpus callosum	Many syndromes e.g. <i>ARX</i> (XLAG), <i>L1CAM</i> (CRASH)	Paul <i>et al.</i> , 2007
Septo-optic dysplasia	<i>HESX1</i>	Thomas <i>et al.</i> , 2001
Development of the cerebellum (Peak time 2-3 months gestation) Many diseases, examples including:-		
Dandy Walker malformation	<i>ZIC1</i> , <i>ZIC4</i>	Grinberg <i>et al.</i> , 2004
Joubert syndrome	<i>NPHP1</i> , <i>CEP290</i> , <i>AHI1</i> , <i>TMEM67</i>	Parisi <i>et al.</i> , 2008
Neuronal proliferation (Peak time 2-4 months gestation)		
Primary microcephaly	<i>MCPH1</i> , <i>CDK5RAP2</i> , <i>ASPM</i> , <i>CENPJ</i> , <i>STIL</i>	Thornton <i>et al.</i> , 2009
Macrocephaly	<i>PTEN</i> , <i>VG5Q</i> , <i>NSD1</i> , <i>FMR1</i> ,	Williams <i>et al.</i> , 2008
Neurocutaneous syndromes	<i>NF1</i>	Williams <i>et al.</i> , 2008

<b>Neuronal migration (Peak time 3-5 months gestation)</b>		
Schizencephaly	<i>EMX2</i>	Brunelli <i>et al.</i> , 1996
Lissencephaly	Type I: <i>PAFAH1B1, RELN, TUBA1A, VLDLR, DCX, ARX</i> Type II: <i>POMT1, POMT2, FKRP, LARGE</i>	Spalice <i>et al.</i> , 2009 Vajsaar <i>et al.</i> , 2006
Pachygyria	<i>TUBA1A</i>	Poirier <i>et al.</i> , 2007
Band heterotopias	<i>PAFAH1B1, FLNA, ARFGEF2</i>	Spalice <i>et al.</i> , 2009
Polymicrogyria	<i>SRPX2, PAX6, TBR2, KIAA1279, RAB3GAP1, COL18A1</i>	Spalice <i>et al.</i> , 2009
Focal cerebrocortical dysgenesis	?Variants of <i>TSC1</i>	Spalice <i>et al.</i> , 2009
<b>Organisation (Peak time 5 months gestation-postnatal) Spectrum of disorders including:-</b>		
Mental retardation (with/ without seizures)	Many, including <i>ARX</i> <i>ARHGEF6, OPHN1, PAK3</i>	Bienvenu <i>et al.</i> , 2002 Chechacz and Gleeson 2003
Rett syndrome	<i>MECP2</i>	Amir <i>et al.</i> , 1999
Angelmans syndrome	<i>UBE3A</i>	Kishino <i>et al.</i> , 1997
<b>Myelination (Peak time Birth-several years postnatal) Disorders of dysmyelination include:-</b>		
Perlizaesus-Merzbacher disease	<i>PLP1</i>	Hodes <i>et al.</i> , 1993
Perlizaesus-Merzbacher like disease	<i>GJC2</i>	Bugiani <i>et al.</i> , 2006
Krabbe's disease	<i>GALC</i>	Sakai <i>et al.</i> , 1994
Metachromatic leukodystrophy	<i>ARSA</i>	Polten <i>et al.</i> , 1991
Canavan disease	<i>ASPA</i>	Kaul <i>et al.</i> , 1993
Alexander disease	<i>GFAP</i>	Brenner <i>et al.</i> , 2001
Vanishing white matter disease	<i>EIF2B1, EIF2B2, EIF2B3, EIF2B, EIF3B5</i>	Van der Knaap <i>et al.</i> , 2002
Megalencephalic leukoencephalopathy with subcortical cysts	<i>MLC1</i>	Ilja Boor <i>et al.</i> , 2006

### 1.2.1 Primary neurulation

Primary neurulation refers to the formation of the neural tube at week 3-4 of gestation (Volpe, 2008a). The nervous system originates from the dorsal aspect of the embryo as a plate of tissue differentiating from the central ectoderm. The underlying notochord and chordal mesoderm induce formation of the neural plate (~ day 18). The chordal mesoderm then induces dorsal invagination of the lateral margins of the neural plate, thus forming the neural tube, which gives rise to the central nervous system (CNS). At a molecular level, surface glycoproteins, cell-cell recognition and adhesive interactions with the extracellular matrix are believed to play an important role in adhesion of the neural folds. The action of specific regional patterning genes (bone morphogenetic proteins and sonic hedgehog) homeobox genes, surface receptors and transcription factors is also contributory. Animal studies have recently demonstrated an essential role for the planar cell polarity pathway in mediating a morphogenetic process called convergent extension during neural tube formation (Kibar *et al.*, 2007). During neural tube closure, neural crest cells form and give rise to dorsal root ganglia, sensory ganglia of the cranial nerves, autonomic ganglia, Schwann cells and cells of the pia and arachnoid. Interaction of the neural tube with the surrounding mesoderm gives rise to the dura and axial skeleton (skull and vertebrae).

Disturbance of primary neurulation is associated with a number of brain malformations (Table 1-1). The underlying aetiology is often complex and multifactorial. Environmental components (such as folate deficiency and teratogens such as thalidomide and anti-epileptic agents) may play a role.

Single gene defects (Table 1-1) and chromosomal abnormalities (such as chromosomal trisomies and duplications) are also reported (Volpe, 2008a).

### **1.2.2 Prosencephalic development**

Prosencephalic development begins at 5-6 of gestation and occurs in three sequential stages which result in formation of much of the face and forebrain (Volpe, 2008a):-

- a. Prosencephalic formation (week 5-6) from the rostral end of the neural tube.
- b. Prosencephalic cleavage (week 5-6) involves horizontal cleavage (forming the paired optic vesicles, olfactory bulbs and tracts), transverse cleavage (to separate the telencephalon from the diencephalon) and sagittal cleavage (to form the paired cerebral hemispheres, lateral ventricles and basal ganglia from the telencephalon).
- c. Midline prosencephalic development (month 2-3), with formation of the commissural, chiasmatic and hypothalamic plates. These structures form the corpus callosum/septum pellucidum, optic nerve chiasm and hypothalamus respectively.

Forebrain development is governed by dorsoventral patterning molecular pathways, including the sonic hedgehog signalling pathway and the nodal pathway. Aberrant prosencephalic development may arise from a number of genetic defects (Table 1-1).



### **1.2.3 Development of the cerebellum**

Development of the cerebellum will be discussed in this section as the critical embryonic time period is in parallel with prosencephalic development. The primordia of the cerebellar hemispheres appear in week 5 as bilateral thickenings of the dorsal surface of the rhombencephalon (Ten Donkelaar and Lammens, 2009). By continued growth of this region, the primitive vermis and cerebellar hemispheres become apparent. Progenitor cells in the subependymal germinative zones of the rhombic lip generate neurons that migrate radially (to form the dentate nucleus, other nuclei and the Purkinje cells) and migrate tangentially over the surface of the cerebellum to produce the external granule cell layer. Cells from this external granular layer will then migrate inward through the Purkinje cells and form the internal granule cells of the mature cerebellum.

Inherited cerebellar malformations are diverse and extensive and include disorders of the vermis (such as Joubert syndrome, Table 1-1) as well as those primarily involving the cerebellar hemispheres (such as lissencephalies with cerebellar hypoplasia, congenital muscular dystrophies and metabolic disorders).

### **1.2.4 Neuronal proliferation**

Major proliferative events occur between 2-4 months of gestation (Volpe, 2008b). All neuronal glia are derived from the ventricular and subventricular zones, present in the subependymal location at every level of the developing nervous system. Phase 1 (between 2-4 months) is concerned with the

generation of radial glia and neuronal proliferation. Phase 2 (from 5 months gestation to ~11 months after birth) is associated primarily with glial proliferation. The proliferative events (involving the radial glial cells as neuronal progenitor cells) are modulated by several key signalling pathways involving the Notch receptor, the ErbB receptor (through the ligand neuregulin) and the fibroblast growth factor receptor (Ever and Gaiano, 2005). Other critical molecular determinants include beta-catenin, a protein that functions in the decision of progenitors to proliferate or differentiate (Chenn and Walsh, 2002). Radial glial cells are progenitors for many neuronal cell types (cortical neurons, astrocytes, oligodendrocytes and neural stem cells) and also guide for neuronal migration. Genetic disorders of neuronal proliferation include the primary microcephaly syndromes as well as disorders of macrocephaly and neurocutaneous syndromes (Table 1-1).

### **1.2.5 Neuronal migration**

Neuronal migration refers to the process by which millions of nerve cells move from their sites of origin in the ventricular and subventricular zones to other loci within the CNS (Valiente and Marín, 2010). The peak time period is from 3-5 months gestation. Within the cerebrum, radial migration results in formation of the projection neurons of the cortex. Tangential migration form GABA ( $\gamma$ -aminobutyric acid)-expressing interneurons of the cerebral cortex. Radial glial cells guide this process of migration. There are a number of key molecular determinants of neuronal migration, summarised in Table 1-2.

A wide variety of neuronal migration disorders are caused by single gene defects including schizencephaly, lissencephaly, pachygyria, polymicrogyria, heterotopias and focal cerebrocortical dysgenesis (Table 1-1). In the more severe disorders of neuronal migration, seizures may be a prominent early clinical feature.

**Table 1-2**  
***Molecular determinants of neuronal migration (adapted from Volpe, 2008b)***

Preplate neurons and extracellular matrix	Fibronectin
	Chondroitin
	Heparan sulphate
	Fukutin proteoglycans
	GABA receptors
	Integrins
	Laminin
	Reelin
Radial Glia	Erb B <sub>4</sub> receptors
	Brain lipid binding protein (BLBP)
Migrating Neurons	Notch receptors
	Neuregulin
	Astrotactin
	Doublecortin
	Platelet activating factor acetylhydrolase subunit 1
	Filamin 1
	Cyclin dependent kinase 5
	Neural cell adhesion molecule (NCAM)
	N-methyl-D-aspartate (NMDA receptors)
	Calcium channels
	GABA receptors

### 1.2.6 Organisation

Organisational events occur from about 5 months gestation to several years into postnatal life. During organisation, there is establishment and differentiation of the subplate neurons (SPN) (Kanold and Luhmann, 2010). These SPNs function as the site of synaptic contact for 'waiting' thalamocortical and corticocortical afferents before formation of the cortical plate. SPNs provide a functional link between 'waiting afferents' and cortical targets, have a role in

axonal guidance into the cerebral cortex for ascending afferents and are also involved in cerebral cortical organisation and synaptic development. The next phases of organisation involve lamination (attainment of proper alignment, orientation and layering of cortical neurons), elaboration of dendritic and axonal ramifications and synaptogenesis. The factors that stimulate synaptic formation initially include activity-independent events (molecular mechanisms involved in targeting), followed by activity-dependent events (Klintsova and Greenough, 1999). Modulation of ion channels (especially calcium-permeable channels by neurotransmitters such as glutamate) and modulation of cell surface receptors (by a variety of ligands) play an important role in this process. Selective apoptosis (programmed cell death) of neuronal process and synapses then occurs, mediated by the action of specific genes and their transcription factors (Bergeron and Yuan, 1998). During this phase of brain development, glial proliferation and differentiation result in the formation of astrocytes, oligodendrocytes and microglia (Volpe, 2008b).

Disorders resulting from abnormal neural organisation are less well understood. A primary disturbance of neural organisation is thought to be involved in a number of disorders resulting from monogenic defects (Table 1-1) and other aetiologies. Diseases include mental retardation with/without seizures, Rett syndrome, Down syndrome, Fragile X syndrome, Angelmans syndrome and Duchenne muscular dystrophy. Disrupted organisation may also contribute to the pathophysiology of brain abnormalities observed in prematurity and perinatal injury.

### 1.2.7 Myelination

Myelination is a process by which axons develop a surrounding myelin membrane, creating an insulating layer that promotes fast conduction of nerve impulses (Thaxton and Bhat, 2009). The time period for myelination is long, beginning in the 2<sup>nd</sup> trimester of pregnancy and continuing into adult life. The fastest changes in myelination occur with the first 8 postnatal months. Myelination is nearly completed by 2 years of age. Initial proliferation and differentiation of oligodendroglial cells is followed by elaboration of the cell membrane to form the myelin sheath. Myelination is determined at a molecular level by a variety of growth factors, hormones cytokines, surface receptors and secreted ligands (Thaxton and Bhat, 2009).

Aberrant myelination is seen in a wide variety of neurological disorders including demyelinating disorders (such as multiple sclerosis) and white matter diseases of dysmyelination. Examples of monogenic leukodystrophies include Perlizaeus-Merzbacher disease, Canavan disease, Alexander disease, metachromatic leukodystrophy and Krabbe's disease (Table 1-1).

### 1.2.8 Summary

As illustrated in Chapter 1.2, genetic defects impacting on brain development account for a variety of early-onset neurodevelopmental disorders. These conditions are associated with a wide spectrum of neurological symptoms and signs. From a practical perspective, the diagnosis and management of children affected with such disorders involves clinicians with an expertise in paediatric neurology.

### **1.3 Paediatric neurology**

*‘Without patients, knowledge is only knowledge’* Takasha Shiihara (2009)

More than 100 years ago, long before paediatric neurology was established as a distinct clinical specialty, physicians from many different disciplines contributed to the evolution of this field (Millichap and Millichap, 2009). The biographies of most of these founders of paediatric neurology are included in books by Ashwal (1990) and Aird (1994). Obstetricians also contributed to this field by recognising the causal role of birth difficulties and prematurity in neonatal asphyxia and cerebral palsy (Little, 1862). Among the earliest contributors, Sigmund Freud, the psychiatrist, directed a clinic for such children with cerebral palsy and published on the definition and nature of this disorder in 1897. Bernard Sachs, a neuropsychiatrist, wrote a landmark textbook of paediatric neurology in 1895, and also further contributed to the classification of cerebral palsy in 1926. In the 1930s, Ford, a neurologist, is remembered for his classic book, *Diseases of the Nervous System in Infancy, Childhood and Adolescence* which, in context, was an incredible achievement, written almost quarter of a century before the formal evolution of the clinical specialty. In the 1950s, several academics and clinicians developed specialty clinics for children with neurological disorders and wrote extensively on childhood epilepsy, cerebral palsy, and meningitis. In the 1960s paediatric neurology was recognised as a distinct subspecialty within the field of neurology.

The field of paediatric neurology has rapidly expanded over the last 50 years. In the UK, there are ~90 consultant paediatric neurologists [British Paediatric

Neurology Association (BPNA) secretariat, personal communication, 2010]. Paediatric neurology involves the care of children and adolescents with acute, recurrent and chronic disorders of the nervous system. Clinical fields include neonatal neurology, cerebral palsy, neurometabolic disorders, neurocutaneous syndromes, epilepsy, disorders of balance and movement, grey and white matter diseases, brain injury, tumours, vascular diseases, neuromuscular disorders and neurological impairment in systemic diseases. In Chapter 1.4 and 1.5, I will focus on the features of two specific areas of paediatric neurology pertaining to the disease described in this thesis: (i) epilepsy and (ii) movement disorders associated with basal ganglia dysfunction.

## **1.4 Epilepsy**

### **1.4.1 Epidemiology**

Epilepsy is one of the oldest conditions known to mankind and it is still the most common neurological disorder – at any given time it is estimated that 50 million people worldwide have a diagnosis of epilepsy (WHO, 2001b). The worldwide prevalence is estimated at 2.7—17.6 per 1000, with the highest incidence in infancy/early childhood and old age (Banerjee *et al.*, 2009).

### **1.4.2 Definitions**

**The epilepsies:** a group of neurological disorders characterised by recurrent epileptic seizures which are unprovoked by any immediate identified cause (ILAE, 1993).

**Epileptic seizure:** a transient occurrence of signs and/or symptoms due to abnormal excessive or synchronous neuronal activity in the brain. (Fisher *et al.* 2005).

**Electroencephalogram (EEG):** a graphical record of the electrical activity of the brain (usually taken from surface scalp electrodes) produced by an electroencephalograph. EEG recordings may be ictal (when electrical activity during a seizure event is captured on EEG) or interictal (EEG recording undertaken between seizures). The EEG may be helpful towards diagnosing epilepsy or an epilepsy syndrome and may also give a crude insight into overall brain function. A sleep EEG recording may also be useful for the diagnosis of certain epilepsy syndromes (El Shakankiry, 2010).

**Epilepsy syndrome:** an electroclinical syndrome characterised by clinical features, signs, and symptoms that together define a distinctive, recognizable clinical disorder. These often become the focus of treatment trials as well as of genetic, neuropsychological, and neuroimaging investigations. These are distinctive disorders identifiable on the basis of a typical age of onset, specific EEG characteristics, seizure types, and often other features which, when taken together, permit a specific diagnosis. The diagnosis in turn often has implications for treatment, management, and prognosis (Berg *et al.*, 2010).

**Epileptic encephalopathy:** a group of conditions where the epileptic activity itself may contribute to severe cognitive and behavioural impairments above and beyond what might be expected from the underlying pathology alone and



that these can worsen over time. These impairments may be global or more selective and they may occur along a spectrum of severity (Berg *et al.*, 2010).

### 1.4.3 Classification of epileptic seizures

Seizures are mainly classified as either generalised or focal events (Berg *et al.*, 2010), as summarised in Table 1-3.

**Table 1-3**  
**Classification of the epilepsies (adapted from Berg *et al.*, 2010)**

<b>Generalised</b>	Tonic-clonic (in any combination)
	Absence: Typical Atypical
	Absence with special features: Myoclonic absence Eyelid myoclonia
	Myoclonic Myoclonic-tonic Myoclonic-atonic
	Clonic
	Tonic
	Atonic
<b>Focal</b>	
<b>Unknown</b>	Epileptic spasms

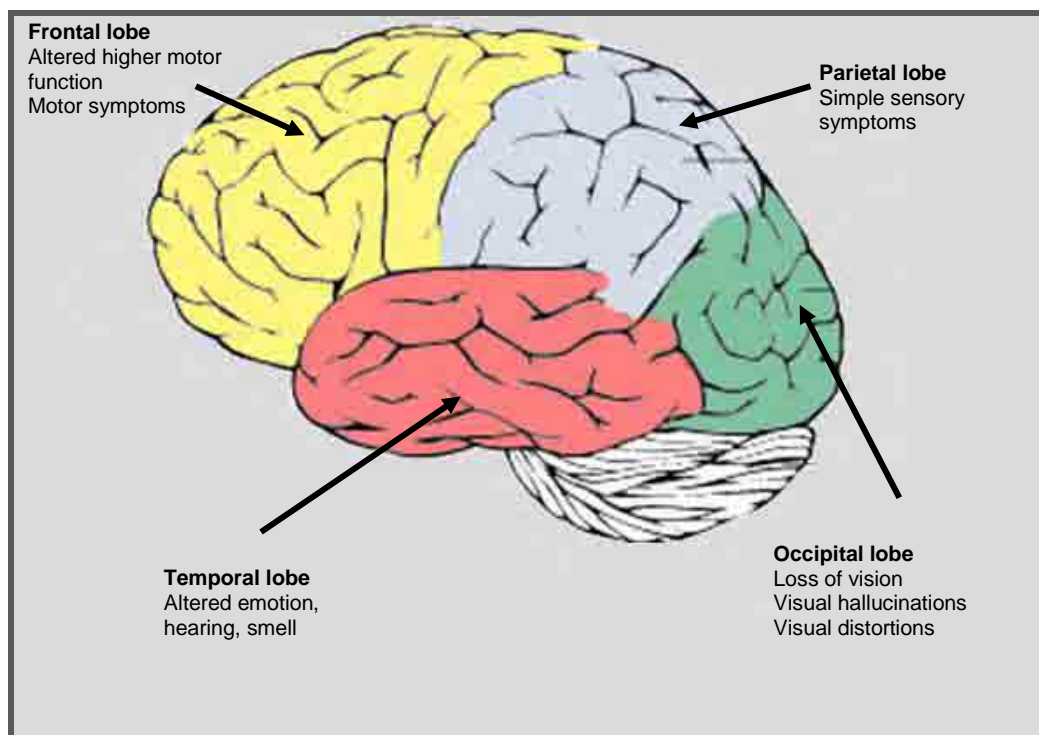
**Generalised epileptic seizures** are conceptualized as originating at some point within, and rapidly engaging, bilaterally distributed networks. Such bilateral networks can include cortical and subcortical structures, but do not necessarily involve the entire cortex.

**Focal epileptic seizures** are conceptualized as originating within networks limited to one hemisphere. They may be discretely localized or more widely distributed. Focal seizures may originate in subcortical structures. For each seizure type, ictal onset is consistent from one seizure to another, with preferential propagation patterns that can involve the contralateral hemisphere. In some cases, however, there is more than one network, and more than one

seizure type, but each individual seizure type has a consistent site of onset. Focal seizures may be described and classified by whether they are (i) motor or sensory events or (ii) according to the region of the brain from which they originate (Figure 1-1), or (iii) whether they are accompanied by impairment of consciousness (Berg *et al.*, 2010).

**Figure 1-1**

*Schematic representation of the brain illustrating the possible origins and clinical symptoms of focal seizures*



### 1.4.4 Classification of epilepsy syndromes

A pragmatic classification of the various epilepsy disorders was proposed by the Task Force on Classification and Terminology (Engel, 2006) according to level of specificity and within those designations, by age where meaningful. An overview of epilepsy syndromes is given in Table 1-4. The specific epileptic encephalopathy syndromes occurring in children under <1 year of age are discussed in more detail in Chapter 3 (Table 1-4, boxed in red). No reference to aetiology is made in this classification system and indeed the same aetiology may give rise to a number of electroclinical syndromes (see Chapter 3). The classification is thus helpful for the diagnosis of age-dependent electroclinical syndromes and although it may direct further diagnostic investigations and management strategies, it is not an *aetiological* classification system reflecting the underlying basis of disease.

**Table 1-4**  
**Classification of epilepsy (adapted from Engel, 2006)**

Neonatal period (< 4 weeks)	Benign familial neonatal epilepsy (BFNE)
	<b>Early myoclonic encephalopathy (EME)</b>
	<b>Ohtahara syndrome</b>
Infancy (<1 year)	<b>Epilepsy of infancy with migrating focal seizures</b>
	<b>West syndrome</b>
	Myoclonic epilepsy in infancy (MEI)
	Benign infantile epilepsy
	Benign familial infantile epilepsy
	<b>Dravet syndrome</b>
	Myoclonic encephalopathy in non-progressive disorders
Childhood (1-12 years)	Febrile seizures plus (FS+) (can start in infancy)
	Panayiotopoulos syndrome
	Epilepsy with myoclonic atonic (previously astatic) seizures
	Benign epilepsy with centrotemporal spikes (BECTS)
	Autosomal-dominant nocturnal frontal lobe epilepsy (ADNFLE)
	Late onset childhood occipital epilepsy (Gastaut type)
	Epilepsy with myoclonic absences
	Lennox-Gastaut syndrome
	Epileptic encephalopathy with CSWS
	Landau-Kleffner syndrome (LKS)
	Childhood absence epilepsy (CAE)
Adolescence–Adult (>12 years)	Juvenile absence epilepsy (JAE)
	Juvenile myoclonic epilepsy (JME)
	Epilepsy with generalized tonic–clonic seizures alone
	Progressive myoclonus epilepsies (PME)
	Autosomal dominant epilepsy with auditory features (ADEAF)
	Other familial temporal lobe epilepsies
Less specific age relationship	Familial focal epilepsy with variable foci (childhood to adult)
	Reflex epilepsies
Distinctive constellations	Mesial temporal lobe epilepsy with hippocampal sclerosis
	Rasmussen syndrome
	Gelastic seizures with hypothalamic hamartoma
	Hemiconvulsion–hemiplegia–epilepsy
	Epilepsies that do not fit into any of these diagnostic categories can be distinguished first on the basis of the presence or absence of a known structural or metabolic condition (presumed cause) and then on the basis of the primary mode of seizure onset (generalized vs. focal)
Structural-metabolic epilepsies	Malformations of cortical development
	Neurocutaneous syndromes
	Tumour
	Infection
	Trauma
	Angioma
	Perinatal insults
	Stroke
	Etc.
Conditions with epileptic seizures traditionally not given a diagnosis of epilepsy	Benign neonatal seizures (BNS)
	Febrile seizures (FS)
Epilepsies of unknown cause	

### **1.4.5 Mechanisms of epileptogenesis in the immature brain**

Epileptogenesis is defined as the process whereby a neuronal network develops recurrent epileptic seizures *de novo* or following an insult, and is also the process whereby seizures become more severe and frequent in chronic epilepsy (Rakhade and Jensen, 2009). Animal models of epilepsy and human tissue studies suggest that epileptogenesis involves a cascade of molecular, cellular and neuronal network alterations.

#### **1.4.5.1 Seizure susceptibility factors**

A number of factors regulating neuronal excitability have been implicated in the increased seizure susceptibility of the immature brain (Rakhade and Jensen, 2009).

##### (i) Enhanced excitation of the immature brain

During synaptogenesis and brain development, excitation predominates over inhibition within neuronal networks of the cerebral cortex and limbic structures in the neonatal period and during the first few years of life (Sanchez and Jensen, 2001). Excitatory ion channels and transporters are expressed at levels that promote excitation, whereas inhibition is relatively underdeveloped compared with later life.

Glutamate is the predominant excitatory amino acid neurotransmitter in neurons. Glutamate receptors (GluRs) are developmentally regulated in neurons and glia (Silverstein and Jensen, 2007). Ionotropic GluRs (iGluRs) are ligand-gated ion channels that permit the flux of sodium, potassium and calcium ions to varying degrees, depending on their subunit make-up (Lau and Zukin,

2007). The main iGluR subtypes are *N*-methyl-D-aspartate receptors (NMDARs),  $\alpha$ -amino-3-hydroxy-5-methyl-4-isoxazole propionate receptors (AMPA) and kainate receptors. The characteristic patterns of NMDAR and AMPAR subunit expression in the developing brain lead to increased calcium influx and extended current decay times (Lau & Zukin, 2007, Kumar *et al.*, 2002) which enhance excitability. This excitability is implicated in rapid physiological synaptogenesis that occurs during brain development, but also lowers the threshold for seizures in the immature brain.

Glutamate also activates metabotropic GluRs (mGluRs), the G-protein-coupled receptors that mediate slow synaptic responses (Nakanishi, 1994). Compared with the iGluRs, less information is available regarding developmental regulation of mGluRs. Results from a study in rodents, however, showed that mGluR1 expression might peak in the first postnatal week, whereas mGluR2, mGluR3 and mGluR5 levels mature by the second postnatal week (Avallone *et al.*, 2006). Agonists of group I mGluRs exert proconvulsant effects, suggesting that elevated levels of receptors from this group might have a role in early excitability.

#### (ii) Diminished GABAergic inhibition in early life

While the major inhibitory neurotransmitter  $\gamma$ -aminobutyric acid (GABA) is inhibitory and hyperpolarizing in the mature brain, it may be excitatory and depolarizing in the immature brain (Loturco *et al.*, 1995). GABA release can activate GABA<sub>A</sub> receptors (GABA<sub>A</sub>Rs), which are ligand-gated chloride channels. In immature neurons, the intracellular chloride concentration is higher than the extracellular concentration, so GABA<sub>A</sub>R activation leads to an efflux of

such ions, thereby depolarizing the cell. This depolarizing effect is largely attributable to differences in expression of the chloride transporters in the immature brain (Dzhala *et al.*, 2005).

#### (iii) Excitability and ion channels

Like ligand-gated receptors, voltage-gated ion channels affect neuronal excitability, and their expression is developmentally regulated. Mutations in genes coding for voltage-gated potassium, calcium and sodium channels are linked to early onset epilepsy disorders (see Chapter 1.4.6).

#### **1.4.5.2 The epileptogenic cascade**

It is postulated that epileptogenesis occurs via a number of major stages known as the 'epileptogenesis cascade' (Rakhade and Jensen, 2009). Early acute changes include rapid alterations in ion channel activity, post-translational changes to existing proteins (for example, neurotransmitter receptors) and activation of immediate early genes (including *Fos*, *Jun*, *Egr1*, *Egr4*, *Homer1*, *Nurr77*, and *Arc*, Herdegen and Leah, 1998). The subacute period of hours to weeks can include processes such as activation of transcription, neuronal death and inflammation. Chronic changes that occur over weeks to months include anatomical alterations such as neurogenesis, mossy fibre sprouting, network reorganization, and gliosis.

#### **1.4.6 Genetics and epilepsy**

Since antiquity, it has been recognised that many types of epilepsy have an inherited component, as demonstrated by numerous twin studies, family aggregation studies and multiplex family studies (Helbig *et al.*, 2008). Epilepsies

associated with a heritable component may be classified as either idiopathic epilepsies (absence of neurological deficits, intellectual disability, or brain lesions with no known/suspected external cause and suspected to have a genetic component) or symptomatic epilepsies (mainly secondary to neurodevelopmental defects). The symptomatic epilepsies of genetic origin are associated with a wide variety of neurodevelopmental genetic defects, including those causing defects in primary neurulation, prosencephalic development, neuronal proliferation, neuronal migration, organisation and myelination (as discussed in Chapter 1.2 and Table 1-1). In contrast, the idiopathic epilepsies are mainly associated with genetic defects of ion channels, the so-called 'channelopathies' (Mulley *et al.*, 2003). The genes associated with idiopathic epilepsy syndromes are summarised in Table 1-5.

**Table 1-5**  
**Genes associated with the idiopathic epilepsies**  
**(adapted from Mulley *et al.*, 2003)**

Epilepsy syndrome	Gene	Reference
Benign familial neonatal seizures	KCNQ2 KCNQ3	Biervert <i>et al.</i> , 1998 Singh <i>et al.</i> , 1998 Dedek <i>et al.</i> , 2001 Charlier <i>et al.</i> , 1998
Benign familial neonatal-infantile seizures	SCN2A	Heron <i>et al.</i> , 2002
Generalised epilepsy, febrile seizures plus (Severe myoclonic epilepsy of infancy)	SCN1A SCN1B SCN2A	Escayg <i>et al.</i> , 2000 (Claes <i>et al.</i> , 2001) Wallace <i>et al.</i> , 1998 Sugawara <i>et al.</i> , 2001
Autosomal dominant nocturnal frontal lobe epilepsy	CHRNA4 CHRNA2 GABRG2	Steinlein <i>et al.</i> , 1995 De Fusco <i>et al.</i> , 2000 Baulac <i>et al.</i> , 2001
Autosomal dominant juvenile myoclonic epilepsy	GABRA1	Cossette <i>et al.</i> , 2002
Autosomal dominant partial epilepsy with auditory features	LG1	Kalachikov <i>et al.</i> , 2002
Childhood absence epilepsy	GABRG2	Wallace <i>et al.</i> , 2001



Mutations of voltage-gated potassium channels interfere with the normal hyperpolarizing potassium ion current and promote repetitive action potential firing (Castaldo *et al.*, 2002). Voltage-gated sodium channel abnormalities have also been implicated in a number of epilepsy syndromes (Table 1-5). To date, more than 300 mutations in *SCN1A* have been identified. Gain-of-function mutations are a primary cause of generalized epilepsy with febrile seizures-plus (GEFS+). Lossin *et al.* (2002) analysed the functional effects of three *SCN1A* mutations. The mutant forms affected channel inactivation leading to a persistent inward sodium current, suggesting the likely basis for in-vivo hyperexcitability. In contrast, most cases of severe myoclonic epilepsy of infancy (SMEI) result from loss-of-function *SCN1A* mutations and studies using mouse models suggest that there is selective loss of sodium ion currents and reduced excitability of GABAergic inhibitory interneurons, which leads to hyperexcitability, epilepsy and ataxia. (Escayg and Goldin, 2010).

### 1.4.7 Summary

From Chapter 1.2 and 1.4 it is evident that epilepsy may arise in association with a number of genetic defects. In Chapter 3, I will describe a patient with an infantile epileptic encephalopathy associated with a novel deletion of the gene *PLCB1*. *PLCB1* is postulated to disrupt muscarinic acetylcholine receptor signalling, thereby affecting normal inhibitory neuronal circuitry and increasing seizure susceptibility.

## **1.5 Movement disorders and the basal ganglia**

### **1.5.1 Introduction**

Clinical observations first suggested the involvement of the basal ganglia in the control of movement and pathophysiology of movement disorders (Kandel *et al.*, 2000b). Post-mortem brain examinations of patients with Parkinson disease, Huntington's chorea and hemiballismus revealed pathological changes in these subcortical nuclei. This led to the conclusion that dysfunction of the basal ganglia could result in both hyperkinetic and hypokinetic movement disorders.

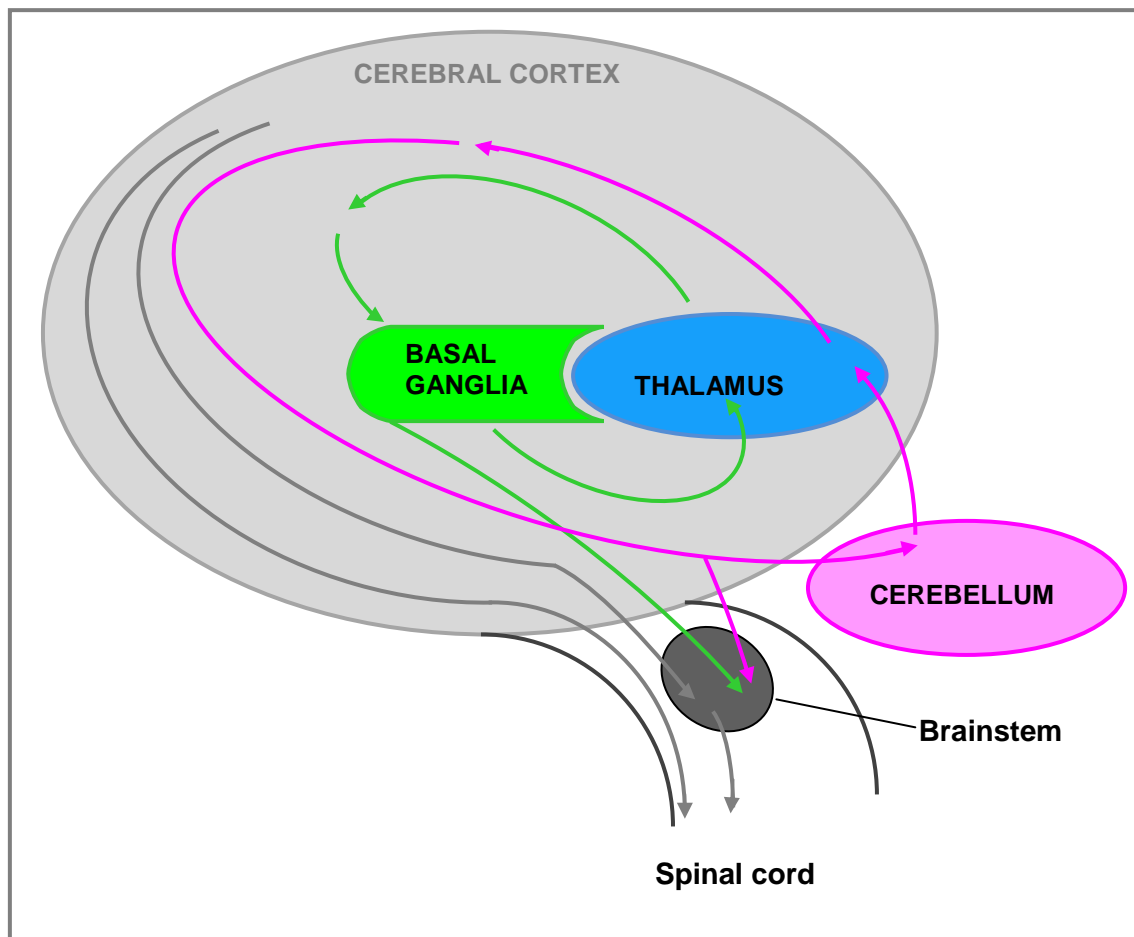
Within the field of paediatric neurology, a number of movement disorders are encountered, in which the origin of disease is believed to be within the basal ganglia. Such diseases may clinically manifest as abnormal involuntary hyperkinetic disorders (including chorea, athetosis, ballismus, dystonia, myoclonus, tics and tremor) and also as hypokinetic phenotypes (such as bradykinesia in parkinsonism). Normal motor function may be significantly affected. The underlying causal factors of basal ganglia-related disorders are diverse, and include genetic defects, neurotransmitter imbalance, infection, post-infective phenomena and metabolic diseases, as well as a plethora of unexplained conditions.

In clinical practice, the generic term 'extrapyramidal disorders' is commonly used to describe this group of disorders. In this context, 'extrapyramidal' refers to the concept that the dysfunctional system predominantly originates outside the pyramidal tract. This term, although didactically useful, is actually not wholly accurate. Indeed the pyramidal and extrapyramidal components interact and

share common pathways for the control of voluntary movement. The motor actions of the basal ganglia are mediated in large part through the supplementary, premotor and motor cortices via the pyramidal system. Indeed, complex interrelationships between the basal ganglia, cerebellum, thalamus and cerebral cortex (Figure 1-2) render the classification of 'basal ganglia disease', although perhaps clinically useful, somewhat arbitrary.

**Figure 1-2**

*Schematic representation of the major input and output connections of the basal ganglia (Adapted from Kandel, 2000b)*

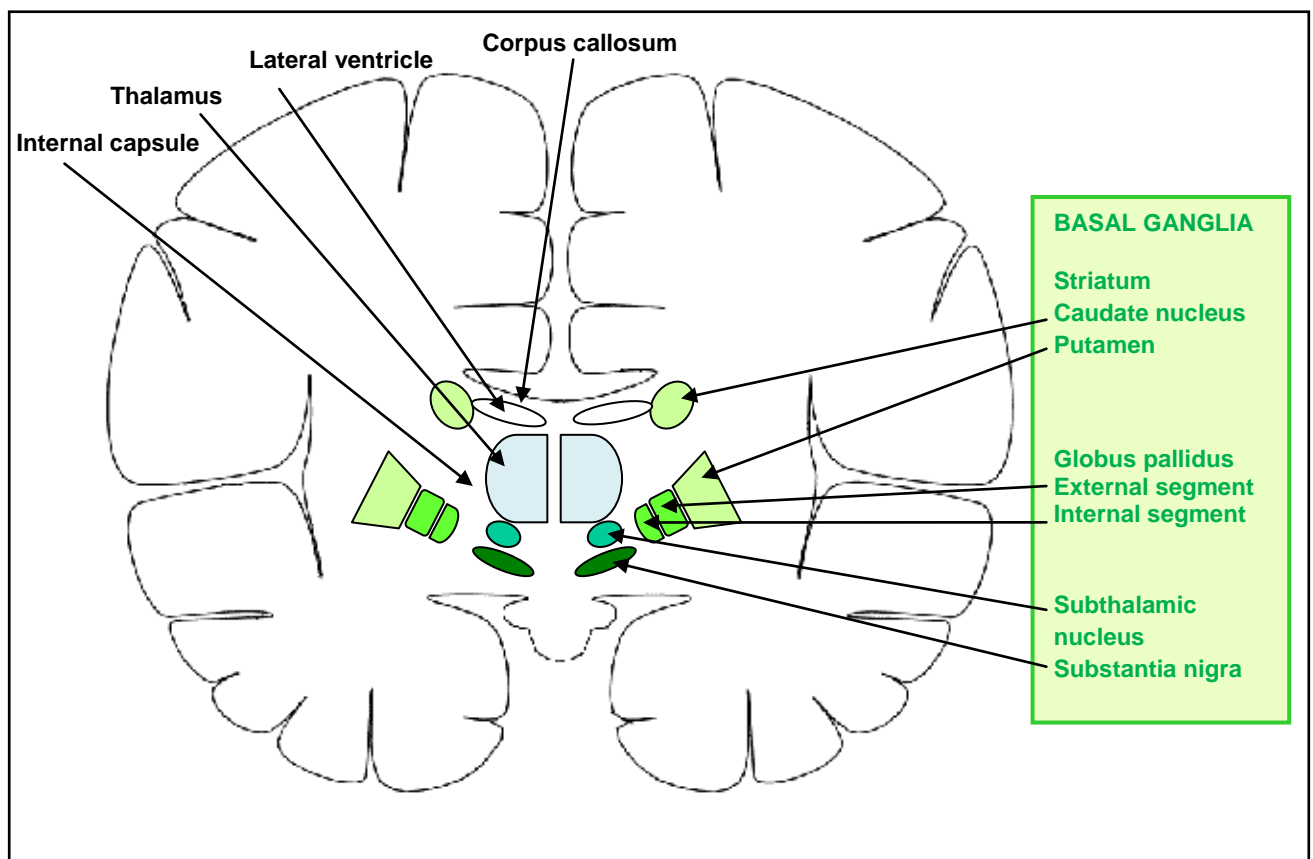


### 1.5.2 Neuroanatomy of the basal ganglia

The basal ganglia consist of several interconnected subcortical nuclei with major projections to the cerebral cortex, thalamus and certain brainstem nuclei. They receive major input from the cerebral cortex and thalamus and send their output back to the cortex (via the thalamus) and to the brainstem (Figure 1-2). The four principal nuclei of the basal ganglia (illustrated in Figure 1-3) are (i) the striatum - caudate nucleus and putamen, separated by the internal capsule and ventral striatum which includes the nucleus accumbens (ii) the globus pallidus - internal segment, GPi, and external segment, GPe (iii) the substantia nigra pars reticulara and pars compacta and (iv) subthalamic nuclei.

**Figure 1-3**

*Coronal section of the brain illustrating a schematic representation of the basal ganglia structures*



### 1.5.3 Functional aspects of the basal ganglia

Connections of the basal ganglia may be summarised as follows:-

#### 1.5.3.1 Input connections to the basal ganglia

The major input to the basal ganglia is from excitatory glutaminergic projections from the cortex to the striatum. The striatum also receives excitatory projections from the thalamus, dopaminergic projections from the midbrain and serotonergic input from the raphe nuclei (Kandel, 2000b).

The subthalamic nuclei receive direct cortical inputs, so is therefore considered another input station of the basal ganglia, in addition to the striatum. This 'hyperdirect' pathway (Figure 1-4) conveys strong excitatory signals from the cortex to the globus pallidus with faster conduction velocity than the striatal pathways.

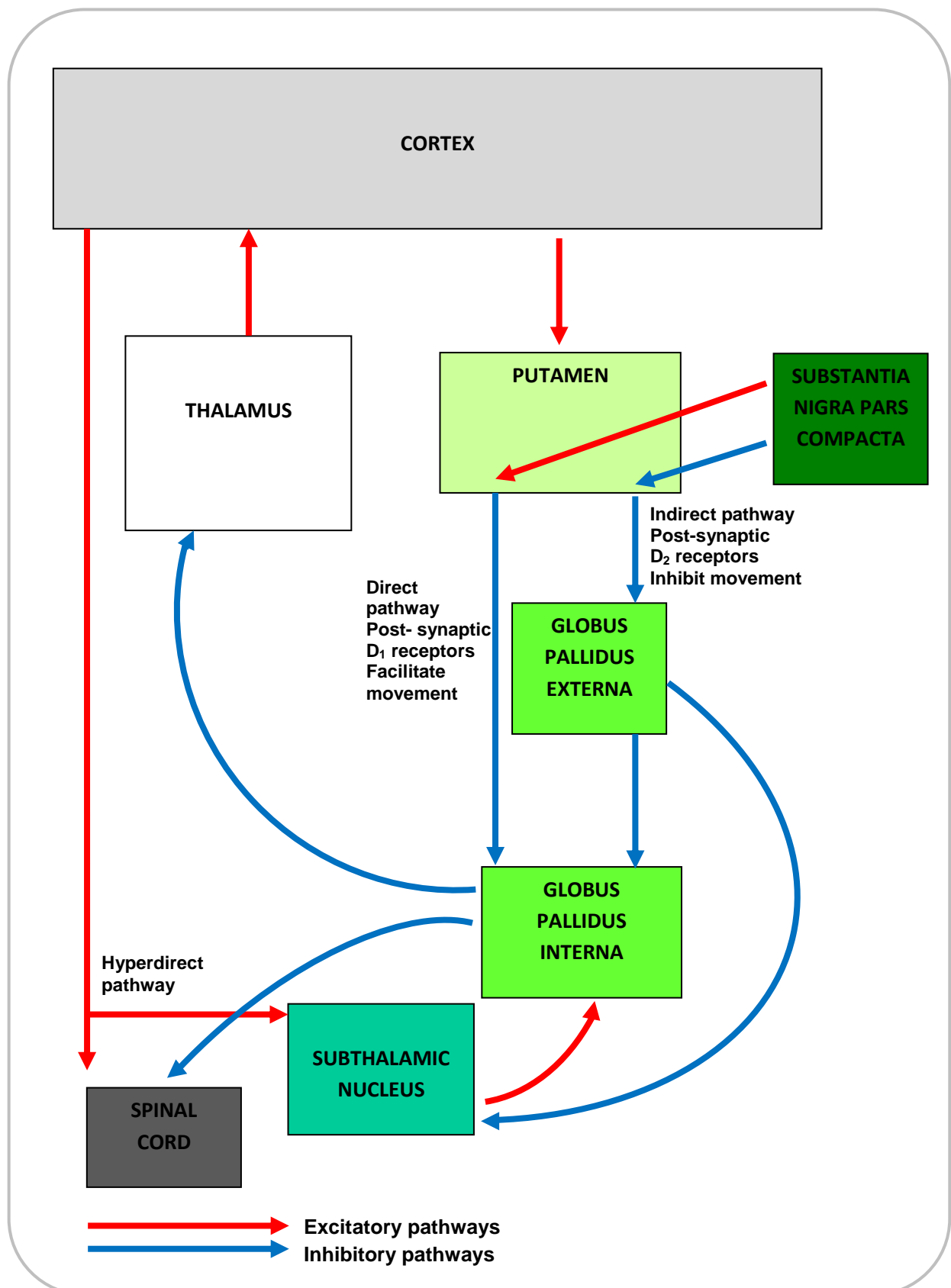
#### 1.5.3.2 Output connections from the basal ganglia

The two major basal ganglia output pathways are from the internal segment of the globus pallidus and from the substantia nigra. This inhibitory output is modulated by the *direct* and *indirect* pathway (Alexander and Crutcher, 1990; Nambu, 2008), which run from the striatum to the output nuclei (Figure 1-4).

Dopaminergic projections from the substantia nigra pars compacta differentially modulate the activity of striatal projection neurons in the direct and indirect pathways. Dopamine excites striatal neurons in the direct pathway through dopamine D<sub>1</sub> receptors while it inhibits striatal neurons in the indirect pathway through dopamine D<sub>2</sub> receptors.

**Figure 1-4**

*Schematic representation of the hyperdirect, direct and indirect pathways of the basal ganglia*



The direct pathway arises from GABAergic striatal neurons containing substance P and dynorphin. When the direct pathway is activated by phasic excitatory inputs (Figure 1-4), the tonically active neurons in the pallidum are suppressed, thus allowing the cortex to be activated. The direct pathway thus provides positive feedback in the circuit between the basal ganglia and thalamus by disinhibiting the thalamus and increasing thalamocortical activity, thereby facilitating movement.

The indirect pathway arises from GABAergic striatal neurons containing enkephalin and neurotensin. In contrast to direct pathway, the indirect pathway increases inhibition of the thalamus as can be seen by considering the polarity of the connections between the striatum and the external pallidal segment, between the external segment and the subthalamic nucleus and between the subthalamic nucleus and the internal pallidal segment (Figure 1-4). The indirect pathway thus provides negative feedback in the circuit between the basal ganglia and the thalamus by inhibiting thalamocortical neurons and thereby inhibiting movement.

This direct/indirect pathway model of basal ganglia circuitry is widely accepted. However it is most certainly oversimplified and interconnections of the cortico-basal ganglia loop are in reality much more complex (Nambu, 2008). Nevertheless, this basic model does still provide a decent insight into the functions of the basal ganglia (Nambu, 2008). In simple terms, disinhibition via the direct pathway releases a selected motor program. Signals through the hyperdirect and indirect pathways make clear the initiation and termination of a selected motor program. In addition to a temporal aspect, the enhancement by

differential inputs through the hyperdirect, direct, and indirect pathways may work spatially as well. Signals through the hyperdirect and indirect pathways activate the pallidum and substantia nigra neurons extensively, thereby inhibiting large areas of the thalamus. Signals through the direct pathway, however, disinhibit thalamic neurons centrally. However the hyperdirect and indirect pathways inhibit thalamic neurons in the more extensive surrounding area, which are involved in other competing motor programs. Thus the hyperdirect, direct, and indirect pathways ensure that only the selected motor program is executed at the selected time, and other competing motor programs are cancelled. The oculomotor, prefrontal, and limbic loops seem to control the activity of corresponding cortical areas in a similar manner to the motor loop.

There is also evidence implicating basal ganglia circuits in non-motor function, such as cognition, attention, learning (especially motor learning), potentiation of behaviour-guiding rules and mood (Salinas *et al.*, 2000). These circuits originate in the prefrontal and limbic regions of the cortex and engage with specific areas of the striatum, pallidum and substantia nigra (Kandel, 2000b). The neurotransmitters serotonin and dopamine are thought to play an important role in these non-motor functions.

#### **1.5.4 Basal ganglia disease mechanisms in motor disease**

From Chapter 1.5.2 and 1.5.3, it can be postulated that movement disorders of the basal ganglia may be associated with structural or biochemical disruption of the basal ganglia pathways. Two disease models are proposed and although they provide some useful insights, the mechanisms of disease are far from fully



elucidated. These theories may explain some, but not all, of the clinical semiology observed in these disorders (Nambu, 2008):-

#### **1.5.4.1 The firing rate model**

It has been proposed that activity imbalance between the direct and indirect pathways may affect the mean firing rate of the output nuclei of the basal ganglia, thereby inducing hypokinetic or hyperkinetic disorders (De Long, 1990).

In states of dopamine depletion, such as Parkinson's disease (Obeso *et al.*, 2008) a decrease in tonic excitation of the *direct* pathway and increase in tonic inhibition in the *indirect* pathway result in overall increased activity in globus pallidus interna/substantia nigra pars reticulara. The ensuing inhibition of thalamic and cortical neurons results in hypokinesia/akinesia. On the other hand, in hyperkinetic disorders, excessive inhibition in the GPi through the *hyperdirect*, *direct*, and *indirect* pathways may induce uncontrollable disinhibition in the thalamus and cortex, leading to involuntary movements. Electrophysiological studies using 1-methyl-4-phenyl-1,2,3,6-tetrahydropyridine (MPTP)-induced parkinsonian monkeys have failed to corroborate this postulated increase in GPi activity (Wichmann, 1999). In contrast, decreased GPi activity has been reported in hyperkinetic animal models (such as the *DYT1* mouse model) which supports this firing rate model (Chiken *et al.*, 2008).

#### **1.5.4.2 Firing pattern model**

In both affected patients and animal models of movement disorders disturbed information processing is a postulated disease mechanism, as oscillatory and/or synchronised activity is observed (Bergmann *et al.*, 1998). The measured

frequency bands include the frequency of resting tremor (4–9 Hz) and the beta band (10–30 Hz) (Brown, 2007). The significance beta band oscillation is not entirely clear, but it may be associated with akinesia. Indeed, treatment for akinesia (with drugs/ stereotaxic surgery) has been shown to suppress this beta band oscillation. However, in the course of MPTP treatment of primates, the appearance of parkinsonian motor symptoms precedes that of oscillatory activity which does not support the firing pattern model (Leblois *et al.*, 2007).

### 1.5.5 Summary

In Chapter 1.5, I have outlined the anatomical and functional aspects of the basal ganglia and its postulated role in disease. Disorders of the basal ganglia may thus arise from a wide variety of causes. These include hypoxic-ischaemic events involving the basal ganglia, tumours, infection, CNS autoimmune diseases, post-infectious disorders, neurodegeneration with brain iron accumulation, inborn errors of metabolism, genetic syndromes and disorders of neurotransmitter imbalance. In Chapters 4 and 5, I will describe identification of a novel gene (*SLC6A3*) postulated to disrupt dopamine regulation in the basal ganglia, thereby resulting in a complex (primarily extrapyramidal) infantile-onset movement disorder. In Chapter 6, the clinical and genetic delineation of children with an infantile-onset disorder of brain iron accumulation in the basal ganglia will be described (*PLA2G6*-associated neurodegeneration).

## **1.6 Gene identification**

### **1.6.1 Why study rare recessive neurological diseases?**

The research described in this thesis has primarily focused on the mapping and identification of genes causing rare autosomal recessive neurological disorders. As described in the previous sections of this chapter, the molecular mechanisms accounting for a great number of neurological disorders remain yet to be elucidated. Although it may be argued that the time and effort spent in the study of such rare diseases greatly exceeds their relative contribution to improving the morbidity of the general population, often such studies will have implications for more common diseases and disease susceptibility.

This is exemplified by the glucocerebrosidase gene *GBA*. While loss of function of both alleles causes the relatively rare autosomal recessive syndrome Type 1 Gaucher's disease, its heterozygous loss of function has been shown to increase the risk of developing Parkinson's disease more than five-fold (Lees *et al.*, 2009).

Another example is Aicardi-Goutieres syndrome (AGS), a (mainly) autosomal recessive encephalopathy. In its most classical form, the clinical phenotype is considered to be the Mendelian mimic of *in utero* congenital viral infection (Crow and Livingston, 2008). In AGS, altered alpha interferon function is a major pathological feature, which is also seen in systemic lupus erythematosus (SLE). Interestingly (i) some children with AGS develop early onset SLE, (ii) heterozygous mutations in *AGS1 (TREX1)* cause a cutaneous form of SLE and (iii) pathogenic mutations in *TREX1* are the single most common monogenic

cause of SLE (Crow and Rehwinkel, 2009). In AGS, endogenous nucleic acids accumulate and are sensed as 'non-self', leading to an interferon-mediated immune response. By defining the precise mechanisms involved in this disorder, future targeted interruption of specific stages of the molecular pathway may lead to the development of novel therapeutic strategies. Identification of genes causing rare recessive neurological disorders may, as illustrated here, provide novel insights into normal biology, disease pathophysiology, disease susceptibility and potential therapeutic targets.

The impact of gene identification for a family must also not be underestimated. In my clinical experience as a paediatric neurologist, parents of children with complex neurological disorders are almost invariably keen to pursue investigations in order to determine an underlying diagnosis. This may often require invasive neurological tests, such as a lumbar puncture (LP) and tissue biopsy. Identification of disease-causing gene mutations will allow accurate diagnosis for an affected patient. This can often give parents 'closure' and will negate the need for further diagnostic investigations. It will also facilitate genetic counselling, carrier testing and prenatal diagnosis for other at-risk family members.

## 1.6.2 Approaches to gene identification

There are essentially two approaches that can be used to identify a disease-causing gene. Firstly suitable candidate genes may be selected, independent of chromosomal location (functional cloning). Secondly, a chromosomal region may be pinpointed and candidate genes within the region are subsequently selected (positional cloning) (Wicking and Williamson, 1991). In practical terms, the most efficient and effective way to identify genes is by utilising both strategies, the *positional-candidate approach* (Deloukas *et al.*, 1998).

### 1.6.2.1 Functional cloning

Functional cloning requires a detailed knowledge of a particular disease phenotype and the biological defect causing it. A classical example of functional cloning was in the identification of mutations in the gene coding for phenylalanine hydroxylase (*PAH*) which causes phenylketonuria (DiLella *et al.*, 1987). Prior to genetic mapping, this was the main approach for the identification of disease causing genes.

The approach is still being today, for example when there are potentially suitable candidate genes for a specific disorder. For example, the genetic investigation of patients with attention deficit hyperactivity disorder (ADHD) has involved extensive screening of genes affecting the catecholaminergic and serotonergic pathways (Faraone and Mick, 2010). Once gene identification has linked a specific phenotype to a particular biological pathway, this approach of functional cloning allows selection of further candidate genes from the same pathway that may cause identical or related conditions. This is exemplified by

the identification of *RAB3GAP2* mutations in Martsolf syndrome (Aligianis *et al.*, 2006) following the identification of *RAB3GAP1* mutations in Micro syndrome (Aligianis *et al.*, 2005).

Functional cloning has been greatly aided by analysis of mouse mutants which have been generated by systematic mutagenesis programs. Completion of the mouse genome project has aided this approach (Waterston *et al.*, 2002). As discussed in Chapter 3, human-mouse homologies may be particularly valuable, as mutations in specific genes may often cause similar phenotypes.

#### **1.6.2.2. Positional cloning**

Positional cloning aims to define a chromosomal segment within which a disease-causing gene is located. The Human Genome Project (Venter *et al.*, 2001) has greatly facilitated this approach to gene identification, by providing physical and genetic maps enabling one to locate markers and genes within a specific chromosomal region. The resources provided by public databases such as 'NCBI', 'Ensembl' and 'UCSC Genome Bioinformatics site' include detailed information about numerous polymorphic markers spread throughout the genome, genetic maps based on these markers, a physical map based on latest genomic sequence information, a rapidly expanding map of expressed sequences and information management and search tools. Direct mapping of Mendelian disorders is achieved by linkage analysis which allows the localisation of a gene to a chromosomal region (or locus). Once the disease locus is established, then candidate genes may be selected for screening, based on information about the gene function, tissue expression pattern and homologies to other genes or animal models.

### 1.6.3 Haplotypes and genetic markers

A **haplotype** is a set of closely linked alleles (either genes or DNA polymorphisms) which are inherited as a unit. The word originates from 'haploid genotype'. Haplotypes are used extensively in genetic mapping and population studies. The original haplotypes were constructed on the basis of blood groups (Morton, 1955). Progress in genetic mapping has been greatly aided by the development of more widespread polymorphic markers such as Restriction Fragment Length Polymorphisms (RFLPs), microsatellite markers (Weber and May, 1989) and single nucleotide polymorphisms. In this thesis, I have utilised microsatellite markers and single nucleotide polymorphisms (SNPs) as markers in genetic mapping.

**Microsatellite markers** (or short tandem repeat polymorphisms) are multiple repeats of 2, 3 or 4 bases. They are extremely polymorphic, may be analysed by polymerase chain reaction (PCR) and are present approximately every 30,000 bases in the genomic sequence (Stallings *et al.*, 1991). Many successful mapping projects have been achieved by the use of microsatellites to conduct genome-wide scans (for example, Aligianis *et al.*, 2005).

**SNPs** are now much more widely used in genetic mapping studies in the study of complex multifactorial diseases, diseases with Mendelian inheritance and copy number variants (CNVs). The first SNP array for genome wide scan was produced by Affymetrix GeneChip® 10K Xba Array containing 11,555 SNP markers (Affymetrix Inc, Santa Clara, CA). Since 2004, several successful mapping projects have been accomplished using this 10K array (for example

Gissen *et al.*, 2004). SNPs are biallelic so they are almost invariably less polymorphic (and thus less informative) than microsatellite markers. However, the great advantage is that the density of SNPs in the human genome allows the researcher to obtain higher resolution mapping information. Currently, the Affymetrix® Genome-Wide Human SNP Array 6.0 contains more than 906,600 SNPs and more than 946,000 probes for the detection of copy number variation. Recent advances in SNP genotyping have also facilitated the construction of a detailed human haplotype map of over 3.1 million SNPs (International HapMap consortium 2007).

#### 1.6.4 Informativeness of markers

For a marker to be useful in linkage analysis of inherited disorders, its state needs to be known for at least one parent (who is a heterozygote). Heterozygosity of the marker in the study population is a measure of its informativity. Heterozygosity ( $H$ ) is calculated by the following equation:

$$H = 1 - \sum_i p_i^2$$

where  $p_i$  is the population frequency of the  $i$ th allele (Ott, 1991). In consanguineous populations, the members of the kindred are more likely to be homozygous for markers by descent and  $H$  is therefore reduced and is  $(1-F)H$ , where  $F$  is the inbreeding coefficient.

The term polymorphism information content (PIC) is also used for the assessment of marker informativity. PIC defines the probability that one could identify which allele of a given parent was transmitted to a given offspring, the



other parent being genotyped as well (Botstein *et al.*, 1980). This is equal to the marker heterozygosity, less the frequency for which the other parent is heterozygous for the same marker alleles:

$$PIC = 1 - \sum_{i=1}^{n-1} p_i^2 - \sum_{i=1}^{n-1} \sum_{j=i+1}^n 2p_i^2 p_j^2$$

### 1.6.5 Maps

A number of genetic and physical maps of the genome have been developed, and these maps are fundamental tools for mapping and gene identification. Genetic maps were developed by tracing the inheritance of phenotypes and/or polymorphic markers through successive generations. Polymorphic loci are positioned relative to one another on the basis of the frequency at which they recombine during meiosis. The unit of distance is the centiMorgan (cM) and 1cM denoted a 1% chance of recombination.

Examples of genetic maps that have been constructed over the last two decades include the Généthron map (a microsatellite marker-based linkage map, Weissenbach *et al.*, 1992; Dib *et al.*, 1996) and the Marshfield map. The Marshfield map was based on the genotyping of around 8,000 microsatellite markers in eight large, three generation families from the Centre d'Etude du Polymorphisme Human (CEPH) collection containing 188 meioses (Broman *et al.*, 1998). More recent maps include those generated by deCODE Genetics in Iceland, with substantially improved resolution of up to five times the resolution of previous maps (Kong *et al.*, 2002). This map was based on the genotyping of 5,136 microsatellite markers, in 146 nuclear families containing 1,257 meioses.

The construction of these genetic maps and intermediate physical maps has significantly contributed to sequencing the entire human genome in the Human Genome Project (Venter *et al.*, 2001). In the human genome, 1cM corresponds, on average, to roughly a physical map distance of 1Mb, although the relationship varies across the genome.

### 1.6.6 Linkage

In 1911, Morgan reported that meiotic recombination events were less likely to occur between two loci that are close together on a chromosome than between two loci which are widely separated or on different chromosomes (Morgan, 1911). Linkage between two markers is defined as occurring when recombination events occur less than 50% of the time, with a resultant recombination fraction of  $<0.5$  (Ott, 1999). This indicates that the loci are on the same chromosome and close to each other.

### 1.6.7 Recombination fraction

The recombination fraction ( $\theta$ ) represents the proportion of offspring who are recombinant (R) (as opposed to non recombinant, NR) between two given loci.

It is calculated as follows:

$$\theta = \frac{R}{(R + NR)}$$

When two loci are syntenic (physical, co-localised), there is a much greater chance that they will co-segregate if they are close together, resulting in a lower recombination fraction. If two loci coincide,  $\theta$  is 0. When they are further apart, there is a higher chance of crossover and  $\theta$  increases. The maximum value for  $\theta$  is 0.5, which signifies that the two loci are not linked. The distance

between two markers on a genetic map is expressed as  $\theta$  and measured in cM. One cM denotes a 1% of recombination and, as previously discussed in Chapter 1.6.5, roughly corresponds to a physical distance of 1Mb. The relationship between physical distance and genetic distance is however non-linear, and it appears that certain chromosomal regions are particularly prone to recombination (recombination 'hot-spots'), for example, between regions of homologous repetitive sequence. Recombination events are relatively more common in telomeric regions, and less common near the centromere. They are also more common in females.

### 1.6.8 LOD scores and critical values

Linkage analysis essentially determines whether  $\theta$  observed between two markers significantly differs from 0.5.

When phase is known, (alleles for both markers can be unequivocally assigned),  $\theta$  can be calculated by counting up all the recombinations. Where parental phase and genotypes are not known for the studied meiosis, this is not possible. Thus, likelihood ratio testing has been employed for human linkage analysis (Ott, 1999). The probability of linkage is calculated as the LOD score,  $Z(\theta)$  (Morton, 1955). The LOD score is the logarithm of the odds that the pedigree is linked ( $H_1$ ) as opposed to being unlinked ( $H_0$ ) and is expressed as follows:

$$Z(\theta) = \log_{10} \left[ \frac{L(H_1)}{L(H_0)} \right] = \log_{10} \left[ \frac{L(\theta)}{L(\theta=0.5)} \right]$$

For each pedigree, the LOD score is calculated at a range of  $\theta$  values. The most likely recombination fraction is the value at which the LOD score is highest. In a set of families, the overall probability is the product of the probabilities in each family, therefore LOD scores (being logarithms) can be added up across families (see Chapter 4).

In 1955, Morton proposed criteria for linkage that are still in use today. Linkage is accepted when  $Z_{max} > 3$  for autosomal loci (or  $Z_{max} > 2$  for X-linked loci) and linkage is rejected when  $Z_{max} < -2$ . These values correspond to significance levels not exceeding 0.001 ( $Z_{max} > 3$ ), and 0.01 ( $Z_{max} > 2$ ). Because of the prior probability of a chance linkage between two traits, the p-value associated with a LOD score of 3.0 is approximately 0.04 (i.e. consistent with a false-positive rate of 1 in 25).

In order to obtain statistical proof of linkage of a disease locus to a particular marker locus, it is necessary to calculate a LOD score by using two-point or multipoint linkage analysis. Two-point linkage analysis is used to establish whether there is linkage between one marker locus and one disease locus. It is often seen as a rough or 'coarse' indication of the location of the disease locus. Multipoint linkage analysis is essentially an extension of two-point analysis in which, instead of finding the recombination fraction between a single marker and a disease locus, the disease locus is mapped against several markers simultaneously. In contrast to two-point linkage analysis multipoint linkage therefore extracts more information from the genotyping data and can give an indication of the likely position of the disease locus relative to the markers.

Generally multipoint linkage gives higher LOD-scores than those achieved with two-point analysis.

## **1.6.9 Autozygosity mapping**

### **1.6.9.1 Introduction**

In 1953, Smith recognised that searching for homozygous regions by descent in consanguineous families offered a powerful strategy for mapping autosomal recessive disorders. Almost 35 years later, advances in molecular techniques (such as the development of genetic maps) allowed Lander and Botstein (1987) to reintroduce this concept and formulate a technique called 'homozygosity mapping' for the mapping of autosomal recessive disorders in consanguineous kindreds. As a locus can be homozygous by virtue of parental descent from a common ancestor, and thus autozygous, this methodology is also termed autozygosity mapping (Mueller and Bishop, 1993). One of the first disorders to be mapped this way was alkaptonuria (Pollak *et al.*, 1993) and over the last 17 years a multitude of disorders have been successfully mapped this way (examples of such mapping in neurological diseases include publications by Aligianis *et al.*, 2005, Morgan *et al.*, 2006, Bockenhauer *et al.*, 2009).

### **1.6.9.2 Consanguinity and the UK Pakistani population**

Successful autozygosity mapping relies on the identification of consanguineous kindreds in which there are multiple affected children with an identical disorder. Consanguinity is defined as a union between couples who are related as second cousins or closer, equivalent to a coefficient of inbreeding (F) in their offspring of  $\geq 0.156$ . A 2<sup>nd</sup> cousin couple share 1/32 of their autosomal genes.

Their children have identical gene copies at 1/64 of all loci.  $F$  thus relates to a child of a consanguineous relationship and indicates the probability that the child will be homozygous for a specific gene/marker (at a specific locus) derived from a common ancestor. The coefficient of relationship ( $R$ ) relates to a consanguineous couple and represents the proportion of genes that they would expect to share by descent from a common ancestor (Table 1-6).

**Table 1-6**

***Degrees of consanguinity and its effect on  $F$  and  $R$  and risk of autosomal recessive disease in offspring (Adapted from Young, 1999)***

Parental relationship	$R$	$F$	Autosomal recessive disease risk in progeny
Siblings	1/2	1/4	1/8
Half siblings	1/4	1/8	1/16
Uncle-niece/aunt-nephew	1/4	1/8	1/16
Double 1 <sup>st</sup> cousins	1/4	1/8	1/16
1 <sup>st</sup> cousins	1/8	1/16	1/32
Double 2 <sup>nd</sup> cousins	1/16	1/32	1/64
2 <sup>nd</sup> cousins	1/32	1/64	1/128

Consanguineous marriages are common practice in a number of communities worldwide. In Arab populations the most common type of consanguineous marriage occurs between first cousins who are children of two brothers, whereas in the Indian subcontinent uncle-niece marriages are the most commonly encountered form of consanguineous relationship. Although the potential genetic risks are recognised within these communities, this risk is often outweighed by the perceived social advantages of greater family and marital stability. A consanguineous marriage is believed to strengthen family ties and avoid health or financial uncertainties that arise through marriage to a spouse external to the family or community. Economic reasons are also considered important in consanguineous marriages. In countries where dowry payments

are usual, these costs are minimised or completely removed (Bittles, 2001; Modell and Darr, 2002). Within certain communities, consanguineous couples will often marry and have children earlier, and may have increased family sizes, further increasing the likelihood of expression of a recessive disorder.

At the population level, the effect of customary consanguineous marriage depends on the frequency and nature of all recessive diseases in the population and on the population structure. Documented effects include increased infant mortality, congenital malformations, learning difficulties, blindness, hearing difficulties and metabolic disorders. A meta-analysis of 38 studies (mainly from developing countries) showed an average increase of infant mortality by 4.4% amongst offspring of first cousins compared with unrelated controls (Bittles and Neel, 1994). It is however important to remember that disorders that lead to death in countries with poor medical resources may otherwise be successfully treated in developed countries.

In unrelated parents, the prevalence of serious congenital abnormalities and genetic disorders is 2 - 2.5% (Congenital Anomalies Register) and around 4% in some longer term studies. These risks are doubled for children from 1<sup>st</sup> cousin relationships. A Birmingham study (Bundey and Alam, 1993) found 0.4% of the North European couples to be related, whereas among British Pakistanis, 69% of couples were related and 57% were first cousins. Amongst the British Pakistani children the birth prevalence of all congenital and genetic disorders was 7.9%, almost double that of Northern European children (4.3%). The prevalence of (definite, probable or possible) recessive disorders was 3.0–3.3%

in the British Pakistani children, ~10 times higher than in the North European children (0.28%).

Because of the complex social aspects involved, the clinical approach has to be to offer improved access to genetic counselling, rather than to discourage consanguinity, which can often be a fundamental part of tradition in these communities. This includes carrier testing for at-risk couples (sometimes even prior to marriage and having children) as well as prenatal diagnosis. Prenatal diagnosis by chorionic villus sampling in the first trimester for severe disorders (such as thalassaemia) is becoming increasingly acceptable to such communities (Darr and Modell, 1988).

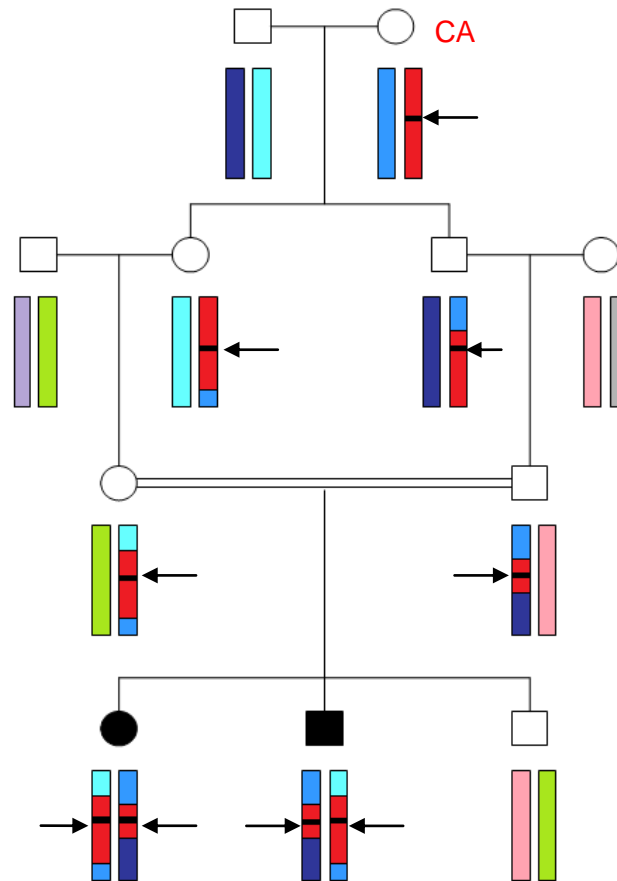
#### **1.6.9.3 Principles of autozygosity mapping**

Figure 1-5 illustrates the family tree of a hypothetical consanguineous family in which two children are affected with an autosomal recessive condition. The disease allele has been passed down through successive generations from the common ancestor (CA). The affected children have thus inherited both copies of this disease allele from their parents, and are thus homozygous-by-descent for this gene. In addition, the chromosomal segment surrounding the gene is also homozygous (shaded in red). Recombination events during meiosis lead to a reduction in the size of the autozygous (red) chromosomal segment over successive generations. Disease loci in consanguineous kindreds are thus normally (but not always) located in such homozygous regions of the genome. These homozygous regions can thus be identified using genome-wide SNP arrays and microsatellite markers. Once homozygous regions are identified, the region of interest can be examined for candidate genes for sequencing.



**Figure 1.5**

*The principle of autozygosity mapping, in which the specific mutation of a disease gene (indicated by the black arrow) can be passed on from a common ancestor (CA) to offspring and the product of a consanguineous marriage, can result in affected offspring*



#### 1.6.9.4 Mathematical model for autozygosity mapping

The mathematical model of homozygosity mapping was formalised by Lander and Botstein (1987). For a child from a consanguineous union, the probability of being homozygous-by-descent  $F_q$  is equal to the disease allele frequency ( $q$ ) multiplied by  $F$  (the coefficient of inbreeding), assuming that the disease is in Hardy Weinberg equilibrium (HWE). The probability that the child is not homozygous as there has been random meeting of 2 alleles is:

$$(1-F)q^2$$

If the disease gene is in HWE in the population, then the proportion of affected individuals homozygous by descent ( $\alpha$ ) is:

$$\alpha = \frac{Fq}{Fq + (1-F)q^2}$$

If  $q$  is small, then it is more likely that  $\alpha \sim 1$ . This equation thus demonstrates the validity of the assumption that for a rare recessive disorder, the disease gene will lie within a homozygous region. On the converse, parents of children with recessive disorders are more likely to be related.

#### 1.6.9.5 The power of autozygosity mapping

A LOD score can be constructed on the basis of  $\alpha$  and  $F$ . The region around a disease gene will be homozygous by descent with a probability  $\alpha$ , while unlinked region will have a probability of homozygosity by descent of  $F$ . Thus the ratio of  $\alpha:F$  is the odds in favour of linkage (assuming that the genotyping is fully informative. In a 1<sup>st</sup> cousin union ( $F=1/16$ ) with a region that is definitely homozygous by descent, there is an odds ratio of 16:1 in favour of linkage, i.e. a LOD score of 1.204. Through detecting common regions of homozygosity in 3 separate 1<sup>st</sup> cousin unions (all with one child affected with a common phenotype), a significant LOD score of 3.61 would be obtained (providing markers are informative and  $\alpha \sim 1$ ).

Using more distally related families for mapping will increase the power to detect linkage. An affected child of 2<sup>nd</sup> cousin parents could derive a maximum LOD score of 2.41. This concept is illustrated in Chapter 4, where linkage to a

disease locus (and a significant LOD score of  $>5$ ) was established using 2 separate families (with a total of only 3 affected children).

#### **1.6.9.6 Pitfalls of autozygosity mapping**

It is important to note that autozygosity mapping has a number of pitfalls which need to be carefully considered when embarking on mapping studies.

The majority of these recessively inherited diseases are rare and it can be often very difficult to ascertain a sufficient number of patients with the same/ related phenotypes to embark on autozygosity mapping studies. Another problem is that in many parts of the world family sizes tend to be smaller, often no more than three to four children, making it unusual for there to be more than two affected siblings within a sibship (Mueller and Bishop, 1993). As discussed in Chapters 3-6 of this thesis, a potential solution to this problem is by setting up collaborative projects and pooling clinical resources.

Investigating rare diseases within isolated communities also has other problems. A number of families will harbour a 'private mutation' for an inherited disorder. In such cases it may prove difficult to find other families (even with similar phenotypes) who have mutations in the same gene. Proof of pathogenesis can thus be very difficult in these isolated cases.

Rarely, autosomal recessive disease in consanguineous kindreds may be caused by compound heterozygous mutations. In such cases, the disease locus may not be within a region of homozygosity, and thus will not be detected when performing a genome-wide scan for homozygous regions. This is evident in Karak syndrome. In the original report of this syndrome, described by Mubaidin *et al.*, (2003), the

two affected boys were born to first cousin parents from an inbred Jordanian family. The family structure was suggestive of autosomal recessive (or X-linked) inheritance. However, phenotypic similarity with other patients with mutations in *PLA2G6* prompted screening of this gene, and compound heterozygous *PLA2G6* mutations were identified in both boys (Morgan *et al.*, 2006). Microsatellite marker analysis of the region on chromosome 22 revealed that both boys shared a common heterozygous haplotype that was different to their parents. Thus, in this family, if mapping studies had been undertaken, the disease locus would have been missed as it was not contained within a homozygous region in the affected individuals.

Miano *et al.*, (2000) found that allelic heterogeneity may occur even within single consanguineous kindred, which results in loss of homozygosity in flanking markers and failure to detect linkage with a false-negative result. In their cited example, the true locus for enhanced S-cone syndrome was missed as one of the four affected individuals from one kindred was found to be a compound heterozygote for the disorder. The other three were homozygous for one of these detected mutations. Miano *et al.*, also reported that autozygosity can be detected in families that are unrelated to the disease, an explanation being that “hidden” consanguinity in pedigree founders may add to the likelihood of detection of such regions. Another pitfall is in underestimating the extent of inbreeding which can potentially inflate the LOD scores, increasing the chance of a false-positive linkage.

Locus heterogeneity describes the situation where the same clinical phenotype can result from mutations at any one of several genetic loci. Autosomal recessive

diseases can be extremely heterogeneous, as has been shown for autosomal recessive microcephaly in the Pakistani community (Woods *et al.*, 2005). Before undertaking linkage analysis for a particular genetic disease, it is important to investigate whether any previous data has already mapped any disease loci, or at least suggested genetic heterogeneity. Ideally, if possible, linkage studies should be performed in one large consanguineous family with multiple affected individuals (for example, Morgan *et al.*, 2006), as this can be much more powerful than using several different families with one or two affected individuals. Once linkage is established in the large family, other smaller consanguineous families can be investigated for linkage to the same region. Such approaches are not always possible, but if they are, they can overcome this problem of locus heterogeneity.

## **1.7 Conclusion**

In this chapter, I have given a broad overview of inherited neurological disorders and methods by which disease-causing genes may be identified. From my perspective as a paediatric neurologist, it is striking that, for the majority of these neurological disorders, there is no curative treatment and therapeutic strategies to date are generally supportive or palliative. One hopes that future advances in molecular biology and identification of further single gene disorders will not only help elucidate pathophysiological processes (thereby enhancing understanding of normal physiology and disease mechanisms), but also facilitate the development of therapeutic targets for future possibly curative treatments for neurological diseases. Promising work in such treatment of inherited neurological disorders is already underway (Kinali *et al.*, 2009; Zeng *et al.*, 2010).

## **Chapter 2**

### **General Methods**

This chapter describes the general procedures used widely in this thesis. Specific methodologies pertaining to individual chapters are contained therein.

## ***2.1 Ascertainment of patients and control subjects***

### **2.1.1 Patient recruitment**

In this thesis, molecular genetic investigations were undertaken in consanguineous kindreds containing children affected with undiagnosed, early-onset, complex neurological disorders. The families originated from a variety of ethnic backgrounds (Pakistani, North Indian, Bangladeshi and mixed European descent). For each neurological condition, a cohort of patients (with a similar clinical phenotype) from non-consanguineous families was also established. Autozygosity mapping strategies were utilised to establish disease loci and identify novel disease-causing genes in consanguineous families. Sequencing of these genes was subsequently undertaken in the relevant cohort of sporadic cases in order to establish mutation frequency.

Consanguineous families and sporadic cases with the following neurological conditions were recruited:-

- Infantile spasms (West syndrome)
- Infantile parkinsonism-dystonia (dopamine transporter deficiency syndrome)
- *PLA2G6*-associated neurodegeneration (PLAN)

Patients were recruited through the NAMR (National Autozygosity Mapping Resource) from:-

- UK NHS (National Health Service) regional genetics services
- UK NHS tertiary paediatric neurology departments
- The British Paediatric Neurology Association Surveillance Unit (BPNSU)
- Worldwide collaboration with internationally-based paediatric neurologists

### **2.1.2 Consent and ethics approval**

Informed consent was obtained from all participants and the study was approved by the LREC (Local Research Ethics Committee). All clinical research adhered to principles outlined by the Declaration of Helsinki.

### **2.1.3 Patient assessment and acquisition of blood samples**

For most UK-based families, I performed a detailed clinical assessment including a full medical history and systemic/neurological examination. Blood samples were taken from all affected individuals, both parents and any unaffected siblings. For families based outside the UK, clinical data was acquired by liaising with the referring clinician. Questionnaires were used to gather clinical data and extensive video footage of affected children was analysed for accurate neurological phenotyping. For such internationally acquired cases, the referring clinician sent either DNA or fresh blood samples (in EDTA tubes) for DNA and RNA extraction by the West Midlands Regional Genetics Laboratory.

### **2.1.4 DNA from control subjects**

Control DNA samples were kindly donated by the West Midlands Regional Genetics Laboratory for assessing population frequencies of identified genomic



variants. The surnames of the families were used to select which control panel they fitted into, after which they were anonymised.

## **2.2 Materials**

### **2.2.1 Chemical reagents**

Acetamide	Sigma
Agarose	Bioline
2X Biomix™ Red	Bioline
dNTPs (diluted from 100mM to a working stock of 2mM)	Bioline
EDTA (ethylenediaminetetraacetic acid)	Sigma
ExoSAP-IT®	USB Corporation, USA
Ethanol	Fisher Scientific
Ethidium bromide	Sigma
GC rich solution of FastStart Taq DNA Polymerase Kit	Roche
Genescan-500 LIZ Size Standard	Applied biosystems
Hi-Di Formamide	Applied biosystems
Hyperladder™ I (Separation range 200 – 10000bp)	Bioline
Hyperladder™ VI (Separation range 10090 – 48000bp)	Bioline
MicroCLEAN®	Web Scientific
Primers	Sigma
10X TBE Electrophoresis Buffer (diluted to 1X)	Geneflow
Water (distilled-RNase/DNase free, dH <sub>2</sub> O)	Invitrogen

### 2.2.2 Kits

Affymetrix Genome-Wide 250K SNP Array	Affymetrix Ltd
BigDye Terminator Cycle Sequencing Kit version 3.1	Applied biosystems
BigDye 5X Sequencing Buffer (25nM Tris pH 8.7, 4mM MgCl <sub>2</sub> )	Applied biosystems
PCR Extender System (5 Prime for Long Range PCR)	Flowgen Bioscience
Puregene Genomic DNA Purification Kit	Gentra systems
QIAquick Gel Extraction kit	Qiagen
Reverse transcription system A3500	Promega

## 2.3 DNA analysis

### 2.3.1 DNA extraction

DNA extraction was kindly performed either by the West Midlands Regional Genetics Laboratory or by referring genetic centres. DNA was extracted from blood using the Puregene Genomic DNA Purification kit according to the manufacturer's instructions. Extracted genomic samples were then quantified by spectrophotometry (by measurement of A260:A280 ratios).

### 2.3.2 SNP genotyping arrays

In order to identify regions of common homozygosity and/or genomic copy number variants, a genome-wide scan using the Affymetrix 250K Sty SNP array was undertaken in affected children and their unaffected siblings. This microarray technology allows the simultaneous genotyping of a subject's DNA for 238,304 SNPs. SNP genotyping was kindly performed by a research

laboratory technician, according to the manufacturer's instructions (Affymetrix GeneChip Human Mapping 250K Assay Manual). In brief, genomic DNA (250ng) was digested with Sty I restriction enzymes (New England Biolabs) and ligated to Sty I adaptors using T4 DNA Ligase (New England Biolabs). Three PCR reactions were set up for each sample with primer 002 (Affymetrix) and Titanium DNA Amplification Kit (Clontech). The PCR products were run on a 1.5% agarose gel, and ranged in size from 200-1100bp. The PCR products were cleaned up using a DNA Amplification clean-up kit (Clontech). The amplified DNA was then fragmented (to create products of <200bp), then labelled and hybridized to the Sty1 250K SNP chip (Affymetrix). Washing and staining of the arrays was then performed by a fluidics station. The chips were subsequently scanned using a gene-chip scanner (Affymetrix GeneChip Scanner 3000; Affymetrix) via GCOS 1.3 software. Data analysis was then undertaken (using GTYPE 4.1 software) to derive SNP genotypes, marker order and linear chromosomal location. Subsequent copy number analysis was performed using the Copy Number Analysis Tool (CNAT) 4.0.1.

### **2.3.3 Microsatellite marker genotyping**

#### **2.3.3.1 Primers for PCR**

The details of all microsatellite markers (and their UNISTS identification number) used for genotyping and fine mapping are tabulated in the relevant chapters. Forward and reverse primer sequences for known microsatellite markers were obtained from each marker's entry on the UNISTS database. Di- tri- and tetra-nucleotide markers with high heterozygosity scores were selected

using NCBI UNISTS and Ensembl genome browsers. Fluorescent dyes (FAM-blue, HEX-yellow, TET-green) were added to the 5' end of the forward primer. Novel microsatellite markers were also designed and utilised for genotyping. The specific genomic region of interest was displayed on the UCSC genome browser and all microsatellites within this region were viewed. A tandem sequence of greater than 20 di- tri- or tetra-nucleotide repeats was chosen from this DNA contig and primer sequences were designed in the flanking genomic sequence using the Primer3 package. The region containing the tandem repeat, forward primer and reverse primer were all checked on NCBI BLAST (Basic Local Alignment Search Tool) to ensure primer specificity to the region around the novel microsatellite.

### **2.3.3.2 PCR amplification for microsatellite marker genotyping**

PCR amplification was performed in 10µl reactions as follows:-

- 1.0µl genomic DNA (20ng/µl)
- 5.0µl Biomix™ Red 2X
- 3.6µl dH<sub>2</sub>O
- 0.2µl (2.0pmol) forward primer (tagged with fluorescent dye)
- 0.2µl (2.0pmol) reverse primer

Biomix™ Red is a premixed, pre-optimised 2X solution designed for high throughput PCR applications. It contains an ultra-stable *Taq* DNA polymerase and an inert red dye, permitting easy visualisation and direct gel loading.

After an initial denaturation at 95°C for 5 min, a standard PCR protocol was followed: 30 cycles of 95°C for 30s, annealing at 55°C for 30s and extension at

72°C for 30s, followed by a final extension step at 72°C for 5 min. Each set of PCR reactions included a negative control (in which dH<sub>2</sub>O was added instead of DNA) to check for contamination.

#### **2.3.3.3 Analysis of microsatellite marker PCR products**

Markers run on the ABI 3730 DNA Analyzer were initially diluted 1:15 with dH<sub>2</sub>O. 1µl of the diluted PCR product was added to 10µl Hi-Di Formamide and 0.04µl Genescan-500 LIZ size standard. PCR product sizes were determined using Genemapper v4.0 software (Applied Biosystems).

### **2.3.4 Gene sequencing**

#### **2.3.4.1 Primers for sequencing candidate genes**

The DNA template for each gene sequenced in this thesis was downloaded from the Ensembl database. All transcripts for each gene were examined to ensure that primers were designed to cover all coding exons. Intronic primers flanking the coding sequence were designed for PCR amplification using ExonPrimer and Primer3.

#### **2.3.4.2 PCR amplification for gene sequencing**

Standard conditions for PCR amplification were used. PCR amplification was performed in 25µl reactions as follows:-

- 5.0µl genomic DNA (20ng/µl)
- 12.5µl Biomix<sup>TM</sup> Red 2X
- 6.5µl dH<sub>2</sub>O
- 0.5µl (5.0pmol) forward primer

- 0.5µl (5.0pmol) reverse primer

For GC-rich fragments, PCR amplification was performed in 25µl reactions:-

- 5.0µl genomic DNA (20ng/µl)
- 12.5µl Biomix™ Red 2X
- 5µl GC rich solution
- 1.5µl dH<sub>2</sub>O
- 0.5µl (5.0pmol) forward primer
- 0.5µl (5.0pmol) reverse primer

PCR conditions were an initial denaturation of 95°C for 5 min followed by 30 cycles of 45s denaturation at 95°C, 45s annealing at 50-65°C (temperature optimised specifically for each amplification reaction) and 1 min extension at 72°C. This was followed by a final extension step at 72°C for 5 min. Each set of PCR reactions included a negative control (in which dH<sub>2</sub>O was added instead of DNA) to check for contamination.

#### **2.3.4.3 Agarose gel electrophoresis**

PCR products were checked on 1.5% horizontal agarose gels to separate the PCR products and to ensure that the PCR reaction had worked without contamination. The agarose gels were made by melting agarose with 1X TBE in a domestic 600W microwave oven, then cooling the mixture before adding ethidium bromide (0.5µg/ml final concentration) and casting the gel in a gel casting tray. The PCR products were loaded directly. Loading buffer was not required with the use of Biomix™ Red as the mix is of sufficient density to sink to the bottom of each well in the gel. A DNA sizing ladder (Hyperladder I) was

added to lane 1 to check for correct PCR product size. Separation of DNA was achieved by electrophoresis at 60-140V for 30-120 min (depending on the gel size and PCR product size). The bands were visualised using Ethidium Bromide and a UV transilluminator (254nm wavelength).

#### **2.3.4.4 PCR product clean-up**

The PCR product was cleaned up (to remove unwanted dNTPs and primer) by one of three methods. The Exo-SAP-IT® PCR product clean up kit was used to purify PCR products. ExoSAP contains Exonuclease I and Shrimp Alkaline Phosphatase. 2.5µl of PCR product was mixed with 2µl of ExoSAP-IT and incubated at 37°C for 15 min. Subsequent inactivation of enzymes was achieved by incubation at 80°C for 15 min. PCR products were also cleaned up using MicroCLEAN. 2.5µl MicroCLEAN was added to 2.5µl of PCR product, incubated at room temperature for 5 min and then centrifuged at 4000rpm at 20°C for 40 min. The supernatant was removed by briefly spinning the plate upside down at 500rpm at 20° for 30s. The pellet was left to air-dry and then reconstituted with 4.5µl dH<sub>2</sub>O. In cases where PCR products were not clean and multiple bands were visible on gel electrophoresis, gel extraction of specific bands was performed. The PCR product was run on a 2% agarose gel. The fragment of interest was excised from the gel using a sterile scalpel, using a UV transilluminator for visualisation. Purification of gel-extracted products was then undertaken using the QIAquick™ Gel Extraction kit (Qiagen). Approximately 3 volumes of Buffer QG was added to 1 volume of gel (approximately 450µl) and incubated at 55°C until the agarose gel dissolved. Then one gel volume of isopropanol was added. The tube contents were then added to a Qiaquick spin

column and centrifuged for 1 minute. The flow-through was discarded and a further 500µl of Buffer QG was added and centrifuged for 1 min. The flow-through was again discarded and 750µl of PE buffer was added to the column and centrifuged again for 1 min. The flow-through was discarded and the column centrifuged again to remove residual PE buffer. The Qiaquick column was then placed into a clean 1.5ml microfuge tube and the DNA bound to the column was eluted by the addition of 20µl dH<sub>2</sub>O and centrifuging for a further min.

#### **2.3.4.5 Cycle sequencing**

The purified PCR product was then sequenced in both forward and reverse directions using relevant primers. Each 10µl reaction was set up as follows:-

- 4.5µl purified PCR product
- 0.5µl BigDye Reaction Mix
- 2.0µl 5X Sequencing buffer
- 1.0µl dH<sub>2</sub>O
- 2.0µl forward or reverse primer (4pmol)

The cycling conditions were 96°C for 3 min followed by 30 cycles of 96°C (30s), 50°C (15s) and 60°C (4 min).

#### **2.3.4.6 Sequencing reaction clean-up preparation**

Sequencing reactions were cleaned up to remove any incorporated dye terminators. The EDTA method of precipitation was used. To the 10µl sequencing reaction, 1µl EDTA (250nM) was added and mixed before adding 30µl of absolute ethanol. This was incubated for 5-10 min at room temperature



and then centrifuged for 20 min at 2000rpm (20°C). The supernatant was removed by briefly spinning the plate upside down to a maximum of 400rpm. 90µl of 70% ethanol was then added, mixed and the plate centrifuged again for a further 10 min at 2000rpm (20°C). The supernatant was discarded by inverting the plate and spinning to 400rpm. The pellet was left to air dry.

#### **2.3.4.7 Preparation and analysis of sequencing reactions**

Pellets were resuspended in 10µl Hi-Di Formamide and then denatured for 5 minutes before snap-chilling on ice. Sequencing reactions were run on the ABI 3730 DNA Analyzer. Analysed sequences were then downloaded using 'Chromas' software, printed and assessed manually for mutations.

#### **2.3.5 Long range PCR**

For determination of the genomic breakpoint of putative intragenic deletions, long range PCR techniques were utilised, using the PCR extender system. A forward primer (FP) and reverse primer (RP) were designed outside the margins of the putative deletion. Primers were designed manually by identification of a 25-30 nucleotide base sequence comprising of approximately 50% G and/or C nucleotide bases. Primer specificity was checked on NCBI BLAST. Each 50µl long range PCR amplification reaction was set up using 2 mastermixes as follows:-

*Mastermix 1 (10µl):*

- 8.0µl genomic DNA (20ng/µl)
- 1.0µl (10pmol) of forward primer (FP)
- 1.0µl (10pmol) of reverse primer (RP)

*MasterMix 2 (40µl):*

- 32.1µl dH<sub>2</sub>O
- 5.0µl 10X tuning buffer
- 2.5µl dNTP
- 0.4µl PCR extender

40 µl of mastermix 2 was added to mastermix 1 and the solution was mixed very gently by pipetting up and down.

The plate was placed directly onto the Tetrad preheated to 93°C. PCR conditions were an initial denaturation at 93°C for 5 min followed by 35 cycles of denaturation at 93°C (45s), annealing at 60°C (45s) and extension at 68°C for X min. The extension time for each cycle (X) was determined by, and equivalent to the approximate predicted size of the PCR product in kb. For example, if a PCR amplicon of 8kb was expected, the extension time for each cycle of 8 minutes was used. The long range PCR was completed with a final extension at 68°C for 5min. Subsequent PCR gel electrophoresis and PCR product clean-up was undertaken exactly as described in 2.3.4.3 and 2.3.4.4. For the sequencing reaction, a series of forward/reverse primers were again manually designed at 300-400bp intervals from the original FP/RP. Each sequential primer was utilised for cycle sequencing of the original PCR amplicon in order to determine the exact genomic location of the deletion breakpoint. Subsequent sequencing reaction clean-up and preparation/analysis of sequencing reactions was as described in 2.3.4.5-2.3.4.7.

## **2.4 RNA analysis**

### **2.4.1 Isolation of total RNA**

Total RNA was extracted from fresh blood samples by the West Midlands Regional Genetics Laboratory. Leucocytes were lysed and total RNA recovered in 60ul RNase free water using QIAamp spin columns (QIAamp RNA Blood Mini Kit) without a DNase treatment step. RNA integrity was checked on 2% agarose gels.

### **2.4.2 Reverse transcription and amplification of RNA (RT-PCR)**

#### **2.4.2.1 Reverse transcription**

All samples were reverse transcribed in duplicate and a negative control (which contained no RNA) was included. The Promega reverse transcription system A3500 was used. For each sample a mastermix of 18µl was made with the following reagents:-

- 1.0µl (500ng) random primers
- 0.75µl (15 units) of Avian Myeloblastosis Virus (AMV) reverse transcriptase
- 2.0µl (1/10 volume) of 10X reverse transcriptase buffer
- 0.5µl (20 units) of RNase inhibitor
- 4.0µl (5mM MgCl<sub>2</sub>)
- 2.0µl (1mM) dNTPs
- 7.75µl dH<sub>2</sub>O

2µl (approximately 200-300ng) of total RNA was added to this mastermix to give a final volume of 20µl. An equivalent volume of dH<sub>2</sub>O was added to an

additional tube (instead of RNA) which acted as a control for DNA contamination of the RNA.

The mixture was then reverse transcribed at 42°C for 30 min, followed by 94°C for 2 min to inactivate the reverse transcriptase. The cDNA was then stored at -20°C or used immediately for PCR.

#### **2.4.2.2 Design of primers for PCR amplification of cDNA**

All mRNA transcript variants for a particular gene were verified using both NCBI Nucleotide and a thorough literature search on PubMed. For each mRNA transcript variant, the cDNA sequence was downloaded from Ensembl and primers were designed (using ExonPrimer and Primer3) for amplification and subsequent sequencing of the relevant cDNA sequence.

#### **2.4.2.3 PCR amplification of cDNA**

The PCR was carried out in 25µl reactions. A mastermix was made for each sample as follows:-

- 12.5µl Biomix™ Red 2X
- 10.5µl dH<sub>2</sub>O
- 0.5µl (5pmol) forward primer
- 0.5µl (5pmol) reverse primer

This 24µl pre-mix was added to fresh 0.2ml Eppendorf tubes. 1µl of the cDNA were then added, gently mixed and 40 cycles of PCR performed.

PCR conditions were an initial denaturation at 94°C for 2 min, followed by 40 cycles of 94°C for 10s, annealing at 60°C for 30s and extension at 72°C for 1

min, followed by a final extension step at 72°C for 5 min. The PCR products were then prepared for sequencing as described in Chapter 2.3.4.3–2.3.4.7.

## 2.5 Website addresses for internet resources

A number of websites were utilised for various aspects of experimental design and data analysis (Table 2-1).

**Table 2-1**  
**Web-based resources**

Affymetrix	<a href="http://www.affymetrix.com/estore/">http://www.affymetrix.com/estore/</a>
BLAST	<a href="http://blast.ncbi.nlm.nih.gov/Blast.cgi">http://blast.ncbi.nlm.nih.gov/Blast.cgi</a>
ClustalW2	<a href="http://www.ebi.ac.uk/Tools/clustalw2/index.html">http://www.ebi.ac.uk/Tools/clustalw2/index.html</a>
dbSNP	<a href="http://www.ncbi.nlm.nih.gov/projects/SNP/">http://www.ncbi.nlm.nih.gov/projects/SNP/</a>
Ensembl	<a href="http://www.ensembl.org">www.ensembl.org</a>
ExonPrimer	<a href="http://ihg2.helmholtz-muenchen.de/ihg/ExonPrimer.html">http://ihg2.helmholtz-muenchen.de/ihg/ExonPrimer.html</a>
Berkeley Drosophila Genome Project	<a href="http://www.fruitfly.org/seq_tools/splice.html">http://www.fruitfly.org/seq_tools/splice.html</a>
Gene cards	<a href="http://www.genecards.org/">http://www.genecards.org/</a>
NCBI	<a href="http://www.ncbi.nlm.nih.gov/">http://www.ncbi.nlm.nih.gov/</a>
NCBI Nucleotide	<a href="http://www.ncbi.nlm.nih.gov/sites/nuccore">http://www.ncbi.nlm.nih.gov/sites/nuccore</a>
OMIM	<a href="http://www.ncbi.nlm.nih.gov/sites/entrez?db=OMIM&amp;itool=toolbar">http://www.ncbi.nlm.nih.gov/sites/entrez?db=OMIM&amp;itool=toolbar</a>
Primer3	<a href="http://frodo.wi.mit.edu/primer3/">http://frodo.wi.mit.edu/primer3/</a>
PubMed	<a href="http://www.ncbi.nlm.nih.gov/pubmed/">http://www.ncbi.nlm.nih.gov/pubmed/</a>
Superlink Online	<a href="http://bioinfo.cs.technion.ac.il/superlink-online/">http://bioinfo.cs.technion.ac.il/superlink-online/</a>
The GDB Human Genome database	<a href="http://www.gdb.org/">www.gdb.org/</a>
UCSC	<a href="http://genome.ucsc.edu/">http://genome.ucsc.edu/</a>
UNISTS	<a href="http://www.ncbi.nlm.nih.gov/unists/">http://www.ncbi.nlm.nih.gov/unists/</a>

## **Chapter 3**

### **Early Onset Epileptic Encephalopathy and *PLCB1***

### **3.1 Introduction**

The early onset epileptic encephalopathies are characterised by drug resistant seizures, psychomotor retardation, and, in the majority of cases, a poor neurological outcome. It is postulated that the infantile brain may be particularly susceptible to epileptic encephalopathy because the active and dynamic processes of synaptogenesis, apoptosis and progressive myelination occur in an environment of relative neuronal excitation (Ben-Ari *et al.*, 1997; Vallano, 1998; Simeone *et al.*, 2004). If a sustained diffuse epileptic encephalopathy occurs in the midst of this reorganisation, developmental milestones of brain maturation may not be achieved. Aberrant synaptogenesis and apoptosis may cause the brain to become inappropriately 'hardwired', thus increasing susceptibility to excitation (Rice and Barone, 2000; Velisek and Moshe, 2001; Kalinichenko and Matveeve, 2008; Zupanc, 2009). The result is a severe, early onset epileptic encephalopathy with chronic seizures and concomitant cognitive and motor impairment.

The epileptic encephalopathies of infancy and childhood are often associated with a wide spectrum of aetiologies (including structural abnormalities and inborn errors of metabolism) and identified genetic defects account for a number of cases. In many children the underlying cause is not elucidated, and it is likely that a significant proportion of these cases have a currently undetermined genetic basis. In order to further investigate these disorders, I performed molecular genetic investigations in a consanguineous family with an affected child who presented with seizures in early infancy (and subsequently

developed infantile spasms) and identified a pathogenic deletion of *PLCB1* (MIM \*607120) (Kurian *et al.*, 2010a)

### ***3.2 The spectrum of early onset epileptic encephalopathies***

The early onset epileptic encephalopathies are characterised by the onset of refractory seizures in infancy or early childhood (Zupanc, 2009). They are commonly associated with neurodevelopmental delay or regression and a poor prognosis. They may be clinically classified as epilepsy syndromes, according to specific electro-clinical criteria as follows:-

- *Preferential age of onset at a specific developmental period (age-dependency)*
- *Clinical presentation, seizure semiology and disease evolution*
- *EEG findings*

The epileptic encephalopathy syndromes of infancy and childhood include a wide variety of heterogeneous disorders including Ohtahara syndrome (early infantile epileptic encephalopathy), early myoclonic epileptic encephalopathy, migrating partial seizures of infancy, West syndrome (infantile spasms), Lennox-Gastaut Syndrome, Dravet syndrome, Doose syndrome (myoclonic astatic epilepsy) and other progressive myoclonic epilepsies. Approximately 50% children with an early onset epileptic encephalopathy do not entirely match the electro-clinical criteria of a particular syndrome (Scheffer, personal communication, 2010). The salient features of the major epileptic encephalopathies subtypes that present in infancy (with typical disease onset <1 year of age) are summarised in Table 3-1, and described in detail in the following sections.



### 3.2.1 Ohtahara syndrome (OS)

Ohtahara *et al.* first described the features of this early infantile epileptic encephalopathy in 1976. The majority of cases present either in the neonatal period or in early infancy (Yamatogi and Ohtahara, 2002).

The main seizure pattern is tonic spasms (which may occur in clusters), but other seizure types are also observed (focal and generalised tonic-clonic seizures). Affected children experience a high number of seizures usually ranging from 100-300 single episodes or between 10-20 seizure clusters per day (Aicardi and Ohtahara, 2002).

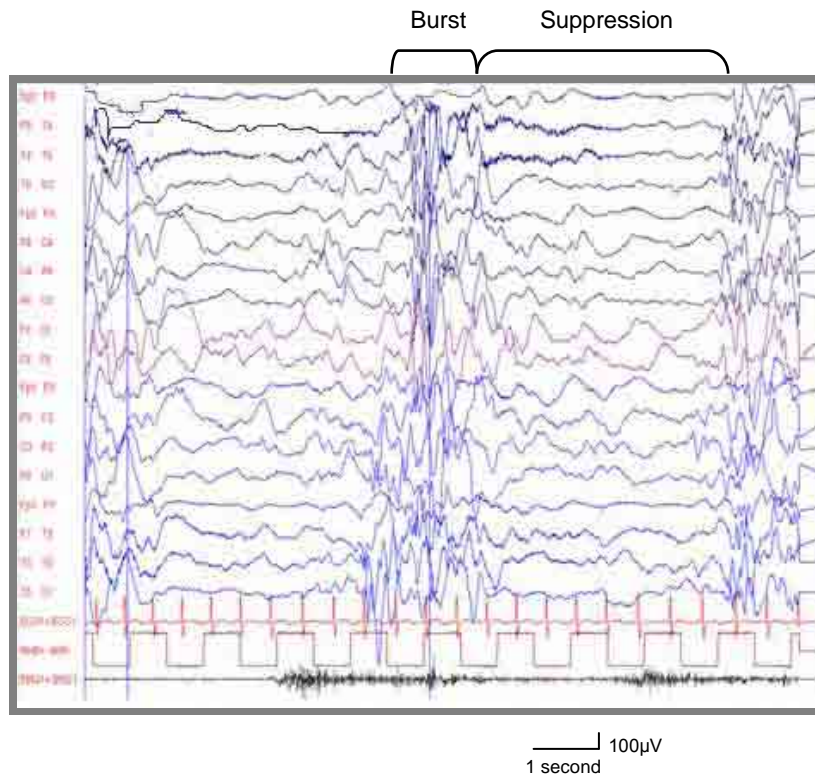
The most specific interictal EEG feature burst-suppression, characterised by high voltage bursts alternating with almost flat suppression phases at an approximately regular rate (Figure 3-1). This specific EEG pattern is important in the diagnosis of OS (Ohtahara *et al.*, 1992; Aicardi and Ohtahara, 2002).

The aetiology of OS is heterogeneous but the syndrome is most commonly associated with structural brain abnormalities such as brain malformations and cortical dysplasias (Yamatogi and Ohtahara, 2002). Recently, mutations in *STXBP1* have been identified in patients with OS (Saitsu *et al.*, 2008, Chapter 3.3).

The prognosis for infants with OS is poor (Yamatogi and Ohtahara, 1981; Ohtahara *et al.*, 1987). Affected children develop drug resistant seizures. During infancy, the EEG pattern changes from burst-suppression to either a hypsarrhythmic or diffuse encephalopathic pattern (Ohtahara and Yamatogi,

1990). Children develop severe psychomotor retardation and are at increased risk of mortality in infancy (Yamatogi and Ohtahara, 2002).

**Figure 3-1**  
*Burst-suppression pattern on EEG*



### 3.2.2 Early myoclonic epileptic encephalopathy (EME)

EME is another epileptic encephalopathy with onset in early infancy usually before 3 months of age (Aicardi and Goutieres, 1978; Dalla Bernardina *et al.*, 1983). Although this syndrome is distinct from OS, both these early infantile encephalopathies share some common features. It is clinically characterised by fragmentary myoclonic jerks or violent myoclonic spasms (Lombroso, 1990). Over time, children also develop focal seizures and tonic events (Aicardi, 1992). Typical interictal EEG demonstrates an invariant burst-suppression pattern similar to OS (Figure 3-1). This pattern is increasingly distinct during deep sleep

and can persist in early childhood. On ictal recordings, each generalized myoclonic jerk is typically associated with a generalized or fragmentary burst of polyspike, spike, and slow wave discharges. In the majority of EME cases, an underlying aetiology is not determined. EME is rarely associated with brain malformations (Guerinni *et al.*, 2003). In a subset of patients, EME may be associated with an inborn error of metabolism such as non-ketotic hyperglycaemia, methylmalonic acidaemia, propionic acidaemia, Menke's disease and pyridoxine dependency. (Ohtahara and Yamatogi, 2003) A therapeutic trial of pyridoxal-5-phosphate and/or folinic acid is thus very important in this group of patients. Like OS, EME may be refractory to antiepileptic medication. The majority of affected children either die within the first 2 years of life or survive with severe neurodevelopmental delay.

### **3.2.3 Migrating partial seizures of infancy (MPSI)**

MPSI was first reported in 1995 (Coppola *et al.*, 1995) and to date approximately 50 worldwide cases have been reported (Coppola, 2009). Seizure onset is usually within the first 6 months of life and semiology is characterised by continuous migrating polymorphous focal seizures (often with secondary generalisation and autonomic features (Coppola, 2009). Multifocal ictal EEG changes are usually characteristic of MPSI. The aetiology is unknown. Mutational screening of *KCNQ2*, *KCNQ3*, *SCN1A*, *SCN2A*, and *CLCN2* genes failed to detect significant results (Coppola *et al.*, 2006). Children with MPSI usually have a poor prognosis, with drug resistant seizures, severe psychomotor retardation and increased risk of mortality.

### 3.2.4 West syndrome (WS)

The clinical features of WS were first reported by Dr West in a letter to the *Lancet* in 1841, describing the semiology of seizures in his own 4 months old son (West, 1841). His account, to this day, is a clinically relevant description of this epileptic encephalopathy:

*“...slight bobbing of the head forward...” which, over time, “...increased in frequency, and at length became so frequent and powerful, as to cause a complete heaving of the head forward toward his knees, and then immediately relaxing into the upright position, something similar to the attacks of emprosthotonus: these bowings and relaxings would be repeated alternately at intervals of a few seconds, and repeated from 10 to 20 or more times at each attack, which attack would not continue more than 2 or 3 minutes; he sometimes has two, three, or more attacks in the day...”*

WS is the most common of all the early onset epileptic encephalopathies, with an average incidence of approximately 0.31 per 1,000 live births (range 0.05 to 0.60 per 1,000 live births) (Frost and Hrachovy, 2003). WS has a typical age of onset between 4 and 8 months of age, and the majority of cases (94%) present before one year of age. Clinical spasms may be flexor, extensor or mixed in nature (Lux and Osborne, 2004a). Spasms are more sustained than myoclonic jerks but do not last as long as a tonic seizure. Brief head nods may be an early subtle presenting feature. Atypical events such as autonomic features and focal events may also occur. The onset of spasms is very often accompanied by neurodevelopmental regression.

The most common EEG pattern is hypsarrhythmia (Figure 3-2) which is a chaotic high voltage pattern of slow waves interspersed at random with asynchronous spikes and sharp waves (Hrachovy and Frost, 2003). An ictal

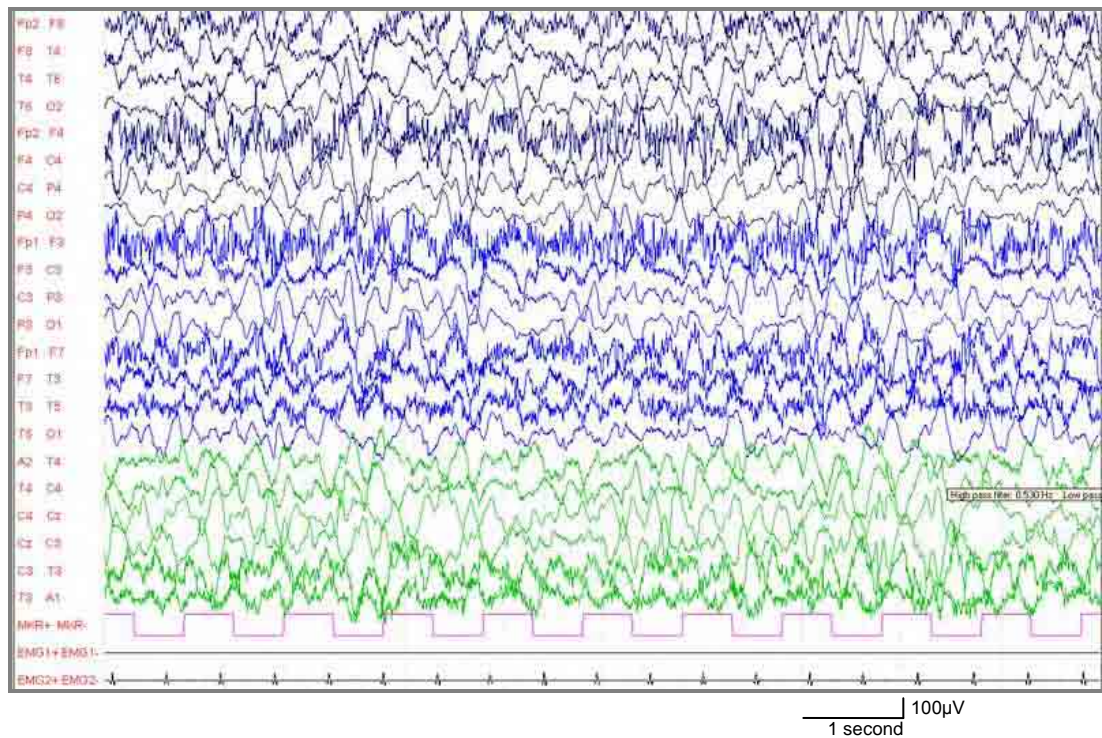
event during an EEG may be associated with an attenuation of voltage known as generalised electrodecrement (Figure 3-3).

A wide variety of aetiologies are associated with WS (Zupanc, 2009), including brain malformations, cortical dysplasias, hypoxic-ischaemic injury, trauma, inborn errors of metabolism, meningitis/encephalitis, chromosomal abnormalities, tuberose sclerosis and other single gene defects (see Chapter 3.3). The multiple aetiologies strongly suggest that WS is the final, common clinical pathway for a diffuse central nervous system abnormality occurring at a specific age-dependent time during brain maturation.

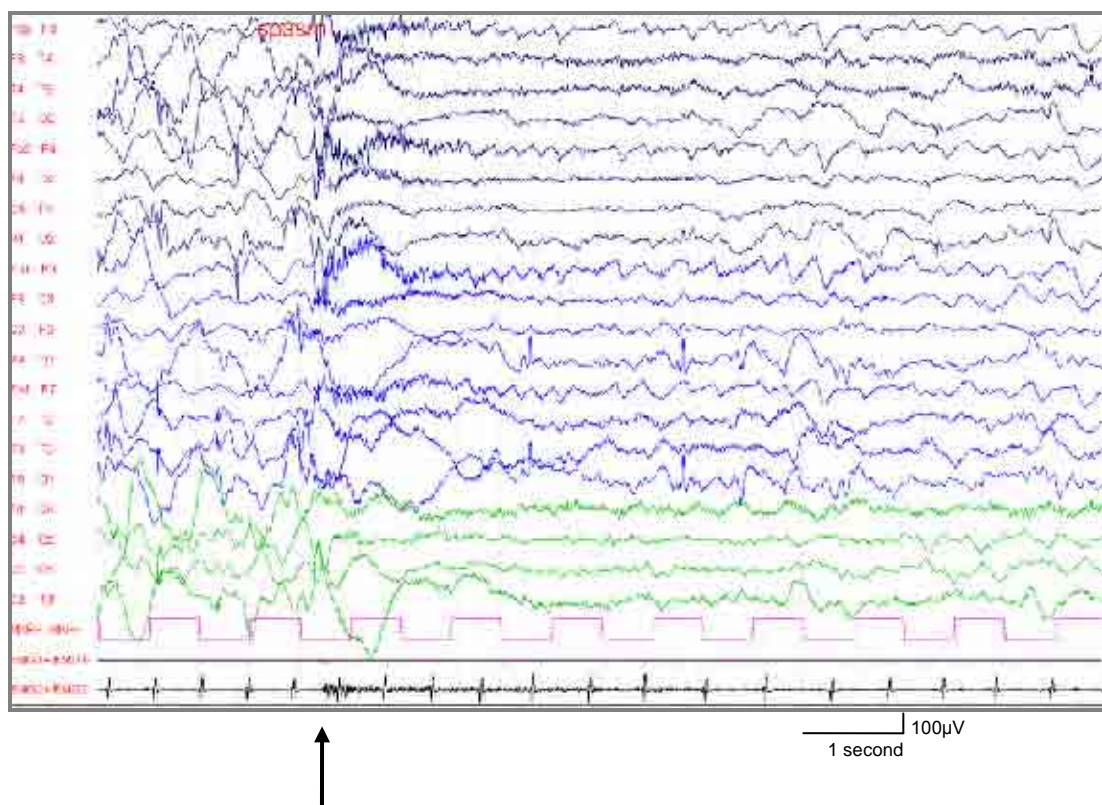
Frost and Hrachovy (2003) reviewed 67 studies regarding outcome in infantile spasms. The average mortality rate was 12% and only 16% had normal development. Approximately one half of patients continued to have seizures at follow-up. Over time, 17% of patients developed Lennox-Gastaut syndrome, an epileptic encephalopathy of childhood characterised by drug-resistant epilepsy, multiple seizure types (especially tonic or atonic seizures), a characteristic EEG (with generalized slow spike and slow wave discharges at 1.5-2 Hz) and poor neurodevelopmental outcome (Zupanc, 2009). Neurologic deficits were present in 44% of patients, and 61% had abnormal EEG findings. Certain factors were predictive of good outcomes. The most favourable prognostic factor was classification into the 'cryptogenic' category (normal prior development, absence of causative factors, normal brain imaging studies). Absence of other seizure types and sustained response to therapy (without relapse) are also considered to be favourable prognostic factors.

**Figure 3-2**

EEG of a patient (age 8 months) with infantile spasms. The chaotic, high amplitude spike and slow wave pattern of hypsarrhythmia is evident

**Figure 3-3**

EEG of patient aged 8 months demonstrating electrodecrement on EEG following the onset of a clinical spasm (indicated by the black arrow)





### 3.2.5 Classical Dravet syndrome (DS)

Charlotte Dravet (1978) first reported a group of children with seizures onset in infancy, early normal development and a devastating course with ongoing seizures and cognitive decline. Classical DS is characterised by the onset of recurrent (often prolonged) episodes of hemiclonic/generalised status epilepticus in previously normal children, from approximately 6 months of age (Dravet *et al.*, 2005). This is followed by the evolution of other seizure types (myoclonic, complex partial, absence and atonic seizures) in early childhood. Seizures are refractory to most anti-epileptic medications and may even be exacerbated by certain agents (carbamazepine and lamotrigine) (Guerrini *et al.*, 1998). The developmental trajectory of DS is classically normal in infancy and then plateaus thereafter. Regression may also be evident, often in the context of multiple episodes of status epilepticus. Over time, ataxia and pyramidal signs may also evolve. The EEG is usually normal in the first two years of life, after which generalized spike wave activity (with photosensitivity) may develop. Multifocal discharges are also frequent. Brain MRI is usually normal although non-specific changes such as mild atrophy may be seen. In the majority of cases, intellectual disability and a seizure disorder persist into adulthood. (Jansen *et al.*, 2006). Following the seminal finding that *de novo* mutations of *SCN1A* underlie Dravet syndrome (see Chapter 3.3), many studies have confirmed high mutation frequency rates, with 70–80% cases having *SCN1A* mutations (Claes *et al.*, 2003), including many alleged cases of ‘vaccine encephalopathy’ (Berkovic *et al.*, 2006).

**Table 3-1**  
**Clinical features of the infantile epileptic encephalopathies**

Syndrome	Ohtahara syndrome (OS)	Early myoclonic epileptic encephalopathy (EME)	Migratory partial seizures of infancy (MPSI)	West syndrome (WS)	Dravet syndrome (DS)
Typical age of clinical presentation	<1 month	<3 months	<6 months	<12 months (average 4-8 months)	<12 months (average 6 months)
Predominant seizure type at presentation	Tonic	Myoclonic	Focal	Flexor/extensor spasms	Hemiclonic Generalised tonic colic
Typical EEG at presentation	Suppression-burst	Suppression-burst	Multifocal abnormalities	Hypsarrhythmia Ictal electrodecrement Suppression-burst in sleep	Normal
Commonly associated aetiologies	Brain malformations Including cortical dysplasias	Inborn errors of metabolism	Unknown	Brain malformations Hypoxic-ischaemic injury Trauma Inborn errors of metabolism Meningitis/ encephalitis, Chromosomal abnormalities Tuberose sclerosis	Episodes triggered by fever
Single gene defects identified or implicated	<i>STXBP1</i>	<i>SLC25A22</i>	None	<i>ARX</i> <i>CDKL5</i> <i>STXBP1</i> <i>MAGI2</i>	<i>SCN1A</i>



### ***3.3 Monogenic defects in infantile epileptic encephalopathies***

As described in 3.2, the infantile epileptic encephalopathies are associated with a diverse spectrum of aetiologies. Single gene defects have been identified in some patients with infantile epilepsy syndromes. In OMIM, the monogenic infantile epileptic encephalopathies are classified as follows:-

- Early infantile epileptic encephalopathy type 1 (*ARX*, MIM #308350)
- Early infantile epileptic encephalopathy type 2 (*CDKL5*, MIM #300672)
- Early infantile epileptic encephalopathy type 3 (*SLC25A22*, MIM #609304)
- Early infantile epileptic encephalopathy type 4 (*STXBP1*, MIM #612614)
- Severe myoclonic epilepsy of infancy (*SCN1A*, MIM #607208)

The salient features of these genes and their proposed role in the pathogenesis of these epilepsy syndromes are summarised in Table 3-2. Mutations of such disease-causing genes are proposed to cause infantile epileptic encephalopathy through a wide variety of underlying disease mechanisms, including defective interneuron function ('interneuronopathies'), synaptic vesicle dysfunction, disrupted transport of excitatory/inhibitory neurotransmitters and ion channel defects (Table 3-2).

**Table 3-2****Single gene defects associated with infantile and childhood epileptic encephalopathies**

Gene	MIM Inheritance	Proposed physiological of protein	References	Epilepsy Syndrome	Postulated disease mechanism	References
ARX	*300382 X-linked	ARX interacts via its homeodomain with IPO13, a mediator of nuclear import.	Shoubridge <i>et al.</i> , 2007	WS	Interneuron specific loss, especially calbindin expressing interneurons, resulting in an overall increase in excitation. Functional impairment of GABAergic interneurons in the basal ganglia is thought to play an important role.	Stromme <i>et al.</i> , 2002 Marsh <i>et al.</i> , 2009 Friocourt and Parnavelas, 2010
CDKL5	*300203 X-linked	Kinase involved in autophosphorylation and phosphorylation of other proteins such as MECP2. MECP2 may recruit CDKL5 to a DNA binding complex that contains a functional substrate of the kinase.	Mari <i>et al.</i> , 2005 Lin <i>et al.</i> , 2005	WS in 'Rett' like patients	Mutations may either disrupt CDKL5 phosphorylation role (required for its entrance into the nucleus) or cause protein mislocalisation in the cytoplasm (a portion of the COOH-terminal domain is responsible for a stable residency in this nuclear compartment probably through protein-protein interactions).	Kalscheuer <i>et al.</i> , 2003 Weaving <i>et al.</i> , 2004 Bertani <i>et al.</i> , 2006
SLC25A22	*609302 Autosomal recessive	SLC25A22 is prominently expressed in the brain cortex, hippocampus and pontine nuclei. It catalyses co-transport of L-glutamate with H <sup>+</sup> or its exchange with OH <sup>-</sup>	Fiermont <i>et al.</i> , 2002 Molinari <i>et al.</i> , 2005	EME (Described in one family)	Defective patient fibroblast glutamate oxidation Defective [ <sup>14</sup> C]glutamate uniport and [ <sup>14</sup> C]glutamate/glutamate exchange by mutant protein in reconstituted proteoliposomes	Molinari <i>et al.</i> , 2005
STXBP1	*602926 Autosomal dominant	Regulation of synaptic vesicle release, in part, by binding to syntaxin 1A and the SNARE complex	Dulubova <i>et al.</i> , 2007 Toonen and Verhage 2007	OS WS	Impaired STXBP1 mutant protein binding to syntaxin leading to defective vesicle release Mutant STXBP1 protein much more thermolabile than wild type protein	Saitsu <i>et al.</i> , 2008
SCN1A	*182389 Autosomal dominant	SCN1A forms the glycosylated alpha subunit of the voltage-sensitive sodium channel, essential for the generation and propagation of action potentials in the brain	Isom <i>et al.</i> , 2002	DS	Reduced sodium currents in GABAergic inhibitory interneurons resulting from heterozygous SCN1A mutations may cause the hyperexcitability that leads to epilepsy in patients with SMEI	Claes <i>et al.</i> , 2001 Yu <i>et al.</i> , 2006

Although many of these genes were initially identified in the context of early onset epileptic encephalopathy syndromes, over time, extensive mutational analysis of other epileptic disorders has revealed that they are also associated with other epileptic syndromes and neurodevelopmental phenotypes. *ARX* mutations have been identified in at least ten well-defined clinical entities (Shoubridge *et al.*, 2010), including Ohtahara, Partington and Proud syndromes, X-linked infantile spasms, X-linked lissencephaly with ambiguous genitalia, X-linked myoclonic epilepsy and non-syndromic intellectual disability. Mutations in *SCN1A* have now been documented in a spectrum of epilepsy syndromes, ranging from the relatively benign generalized epilepsy with febrile seizures plus [GEFS(+)] to Dravet syndrome and also in rare cases of familial migraine (Gambardella *et al.*, 2009). *De novo STXBP1* mutations have been identified in patients with mental retardation and non-syndromic epilepsy (Hamdan *et al.*, 2009) and more recently in patients presenting initially with WS (Scheffer, personal communication, 2010). This phenotypic pleiotropy is evidence that defects in such genes may contribute not only to epileptogenesis, but also to aberrant brain development.

Other genes have been implicated in specific conditions in which infantile epileptic encephalopathy may be a feature of the syndrome. On chromosome 7q11.23-q21.1, interstitial deletions involving *MAGI2* (MIM \*606382) have been detected in patients with a severe form of Williams-Beuren syndrome (MIM #194050) associated with WS (Marshall *et al.*, 2008). *MAGI2* encodes a synaptic scaffolding protein that interacts with Stargazin, a protein also associated with epilepsy in the stargazer mouse (Deng *et al.*, 2006). More

recently mutations in *PNKP* (MIM \*605610), causing DNA repair defects, have been identified in patients with a novel syndrome 'MCSZ', characterised by microcephaly, early onset intractable seizures and developmental delay (Shen *et al.*, 2010). Defects in *SPTAN1* (MIM \*182180) encoding alpha-II spectrin have been identified in individuals with features of WS associated with severe cerebral hypomyelination, spastic quadriplegia, and developmental delay. It is postulated that the pathological aggregation of alpha/beta spectrin heterodimers and abnormal axon initial segment integrity resulting from *SPTAN1* mutations are involved in the pathogenesis of infantile epilepsy (Saitou *et al.*, 2010). In 2009, mutations in *PCDH19* were originally detected in patients with X-linked epilepsy and mental retardation limited to females (Dibbens *et al.*, 2009). More recently, *PCDH19* mutations have also been identified in (mainly female) patients with early onset epileptic encephalopathy and an *SCN1A*-negative Dravet's phenotype (Depienne *et al.*, 2009, Marini *et al.*, 2010). The unusual disease expression pattern in females (and mosaic males) implies that cellular interference may be an important pathogenic mechanism (Dibbens *et al.*, 2009, Depienne *et al.*, 2009)

Despite these genetic advances, there are a significant proportion of patients with infantile epileptic encephalopathy of undetermined aetiology (Scheffer, personal communication, 2010). In WS, an underlying cause cannot be identified ~43% patients (Lux *et al.*, 2004b). It is likely that a number of these patients will have an underlying monogenic aetiology. In order to further investigate these disorders, molecular genetic investigation was undertaken in a consanguineous family using autozygosity mapping strategies.

## **3.4 Methods**

### **3.4.1 Clinical case acquisition and assessment**

#### **3.4.1.1 Acquisition of consanguineous family and index case**

A national surveillance study was set up in collaboration with the BPNSU (British Paediatric Neurology Surveillance Unit) in order to identify all UK cases of infantile epileptic encephalopathy of undetermined aetiology. The index case and family studied in this chapter was one of the families acquired through this reporting service.

#### **3.4.1.2 Clinical assessment**

For accurate phenotyping, the index case was clinically assessed independently by two paediatric neurologists. The medical notes were examined for details of disease evolution and the results of neurological investigations.

#### **3.4.1.3 Acquisition of infantile epileptic encephalopathy cohort**

In order to screen identified genes for mutation frequency, DNA from patients was ascertained through the BPNSU (as outlined above), the UKISS (United Kingdom Infantile Spasms Study) group, and from a cohort of patients from the Epilepsy Research Centre, Melbourne, Australia. All patients had an undetermined infantile epileptic encephalopathy (and no structural brain abnormality) and the majority developed WS. For all patients, written informed consent was provided and study approval was obtained from local ethics committees.

## 3.4.2 Molecular genetic investigation

### 3.4.2.1 Isolation of DNA and cDNA

DNA was extracted from peripheral lymphocytes using standard techniques (Chapter 2.3.1). cDNA was obtained by reverse transcription of RNA as described in Chapter 2.4.1 and 2.4.2.1.

### 3.4.2.2 Genome wide scan

Array studies and copy number variant analysis was undertaken (by Fatimah Rahman) in the index case using the Affymetrix 250K SNP microarray (Affymetrix UK Ltd) as described in Chapter 2.3.2.

### 3.4.2.3 Development of primers

All annotations and physical positions are recorded as in NCBI Genome 37.1 build. The DNA template of *PLCB1* was taken from Ensembl genome browser chromosome 20p12.3, NC\_000020.10 (8,112,824–8,949,003bp). Based on all Ensembl coding transcript variants of this gene, primer pairs for exon-specific PCR amplification of the genomic exons (and flanking exon-intron boundaries) were designed either manually or using Primer3 software (Table 3-3). Primer pairs for amplification of cDNA fragments of *PLCB1* transcripts were manually designed (Table 3-4). In order to define the deletion breakpoint, a forward primer upstream of exon 1 (FP) and a reverse primer in intron 3 (RP) were manually designed (Table 3-5) for long range PCR amplification. Sequential forward primers (A-G) were then designed for sequencing this amplicon to determine the exact deletion breakpoint DNA sequence (Table 3-5).

**Table 3-3 Primers used for genomic PLCB1sequencing**

TRANSCRIPT NUMBER								Primer Sequence	Annealing Temp (°C)	PCR Product Size (bp)
001	003	004	005	007	008	201	202			
1F	1F	1F	1F					CTCAACCCGGAGTGACGCCTTG	60	200
1R	1R	1R	1R					CTTTGGCAGATGCCAACCTG		
2F	2F	2F	2F					AAAATGCCATGTCTAATTTCTTTG	58	328
2R	2R	2R	2R					AAGATCTGTGAAATGGATGTTCTTC		
3F	3F	3F	3F					GAGGAAAGAAATATCCCAACTGC	58	346
3R	3R	3R	3R					AAAGTGTTCAGGGCATACTGGC		
4F	4F	4F	4F				1F	TTGAAGTTATGCTATCACGTTGG	58	291
4R	4R	4R	4R				1R	AAAATTCAGTCTTTTGACAGGC		
5F	5F	5F	5F				2F	GCCAAAGCTAAAAGCATGTGTC	55	220
5R	5R	5R	5R				2R	TCACAAAGGAGAAAGGAACTG		
6F	6F	6F	6F				3F	AAATGTACAAAGGCATGGGC	60	245
6R	6R	6R	6R				3R	GGCTGCTGGAGAAACAAAAC		
7F	7F	7F	7F				4F	TGGCATCATCTGTTAGTGCTG	58	272
7R	7R	7R	7R				4R	TCATGGAAGCTCTTAATTTCTCTC		
8F							5F	GGTGGGTACACAAGAAAGAA	58	289
8R							5R	CCACCATATTCTCAATGCC		
	8F	8F	8F					AAACAGGGGAGGGAGGAAGC	62	240
	8R	8R	8R					CCAAGTCCTGCTCTAGCCAC		
	9F	9F	9F					CACAGTGTTTTTCAGGGCAAG	58	391
	9R	9R	9R					TGGTGTTCCCTAACTCCCAGC		
	10F	10F	10F					AAAAGAGGCGACTTGACACC	58	265
	10R	10R	10R					AGGTTGGTGAAATTTGGTGAG		
	11F	11F	11F					ACCACGGTCATCCTTGCTTC	58	293
	11R	11R	11R					TTTCTACCTTAGGAGGCTTTAACC		
	12F	12F	12F					TCAGGCCATTTCGATACAATTC	58	274
	12R	12R	12R					TGATAAACAATTACTCAGTATGCCC		
	13F	13F	13F					TTCAGGTTCTTTGGATAAGCC	58	209
	13R	13R	13R					TTTCCCTCAACCTCATTTCATC		
	14F	14F	14F					AGGGGATCTGAAAGAGGGAG	58	297
	14R	14R	14R					CCCAGAGCAGCAATTCTTAAAC		
	15F	15F	15F					CAAATGCTGTAAGCTAAATGTTG	58	190
	15R	15R	15R					AGACCCAGGAGAGTACAGGG		
	16F	16F	16F					TGAATCATGTTGTCATTTTCCTG	58	261

	16R	16R	16R				TCTTTGGTCCCATTACTCCG		
	17F	17F	17F				TGAGGATTATTTGCCCTCAAC	58	322
	17R	17R	17R				GGCTATATACTTAAGCCATTTTATGC		
	18F	18F	18F				CCAAATGGAGAAAGATGGAAG	58	310
	18R	18R	18R				CTGGCAATTTTCTCTCCCC		
	19F	19F	19F			1F	CAAAAGTGGACTGGGATCAAC	58	324
	19R	19R	19R			1R	AAGCCACTTCTTTATGCAATG		
	20F	20F	20F	1F		2F	TTGCTGAAGAGCATTGTGG	58	406
	20R	20R	20R	1R		2R	GAATGGCTTTCAAAAGGTAATTG		
	21F	21F	21F	2F		3F	GAAAAAGAAAGCTAGTCCTGATTG	58	337
	21R	21R	21R	2R		3R	AACTAAATCTCATCGCCCTTG		
	22F	22F	22F	3F		4F	CATGCTTTCATCACATAGATGC	58	292
	22R	22R	22R	3R		4R	GCTTTGTTTGGTTCAGTTTCC		
	23F	23F	23F	4F		5F	ATGAATGCATGGACTGATGG	58	316
	23R	23R	23R	4R		5R	TGCTATTCTTCTCCCAAGG		
				5F		6F	CCTTAAGGGAAAGGCTGGCTC	58	305
				5R		6R	CCAGGAGAATGGCGTGAACC		
	24F	24F	24F				GCCTTGTTGGTTTAGGAAGG	58	265
	24R	24R	24R				TGGCACTAATGAACTGGAGG		
	25F	25F	25F				AAAGAGATTAGATTCAAGGCC	58	227
	25R	25R	25R				CCTCTCCTCTAAATACTTCCACTG		
	26F	26F	26F				TTTCCATCTGGATGTTACAGC	58	381
	26R	26R	26R				TCTTGCCATGGTACAGGTCC		
	27F	27F	27F				TTCCCTCCACCTTGTTATGG	58	302
	27R	27R	27R				ATCCAAAGTTTCTCTATAAGGGAG		
	28-29F	28-29F	28-29F				TGGGAAGGAAGCTCTGTTTG	58	435
	28-29R	28-29R	28-29R				CACGAAGGAGTCTTTGACTGG		
	30F	30F	30F				GCAACAGAGCGAAACCTTG	58	359
	30R	30R	30R				ACCCTGTGAAACAGCTCTGC		
	31F	31F	31F		1F		TGAAAAGCTTTCGGTATTTTCTG	58	247
	31R	31R	31R		1R		ATGTAAACCAGGAAGGTTTTACTC		
					2F		GGGTAGACAGGTTACATACAG	58	300
					2R		GGCACAACGTTTTTAAGCCATGAAG		
	32F						GAGTTTCTATGGGAGTGGG	60	393
	32R						CTCGGGAAGATGGTCTGGG		
		32F	32F				CAAATAATTGGAACACCAGATG	58	235
		32R	32R				CCTTCTCTCAAAAGCGACCC		



**Table 3-4**  
**Primers used for cDNA *PLCB1* sequencing**

ENSEMBL <i>PLCB1</i> TRANSCRIPT			PRIMER SEQUENCE	Annealing Temperature (°C)	PCR product size (bp)
003	004	005			
1F	1F	1F	ACGGTCCCCAGTCCCTG	62	565
1R	1R	1R	GAATACGCCCTTCTGGAGTG		
2F	2F	2F	CAGTTTGGCAACAAACCTGC	64	569
2R	2R	2R	AGTGAGAAAGGGGCTGAGAC		
3F	3F	3F	GACAAATATCAGTGGATGGGTTC	62	576
3R	3R	3R	TTTTGCCGCTTCCTTCTG		
4F	4F	4F	GATGCCCTTCTCATGGAGC	60	572
4R	4R	4R	AGTGCCACCATCTGACAACC		
5F	5F	5F	CAAAATGCAGCTTAGCAGG	60	571
5R	5R	5R	TGGTTCCTTTCATTCCCTTAGAC		
6F	6F	6F	TGGCCTGTTTGAGAATAGCAG	60	576
6R	6R	6R	CCAGGTCTTTCATTTCTTTGTAGTG		
7F	7F	7F	GCTCCAGGTTCTGTAAAGGC	60	633
7R	7R	7R	CTCCTCTTCCATCTGACTTTTG		
8F	8F	8F	AAGTTGACGGATGTGCGCAG		
8R			AGAGTCCGATGACGCTGG	60	586
	8R	8R	CTTTTCCAGGGTCTGAGGAC	60	575

**Table 3-5**  
**Primers used for long range PCR and delineation of the genomic breakpoint**

PRIMER	PHYSICAL LOCATION (bp)	PRIMER SEQUENCE
UPSTREAM FORWARD PRIMER (FP)	8 029271	GAGCTTATCTTCGGGGATAGCTACTC
INTRON 3 REVERSE PRIMER (RP)	8 522598	GATGGTGAAGGTGTTGGTGCTGCAAGGG
UPSTREAM FORWARD PRIMER A	8 030637	GCCCAGGTTTTCTTTCCAGGG
UPSTREAM FORWARD PRIMER B	8 031845	GCATATATTGAACCAGCCTTG
UPSTREAM FORWARD PRIMER C	8 032258	GCTTTCGGAGAGTGTATGTGTGCGAGG
UPSTREAM FORWARD PRIMER D	8 032438	GTCTTGCTAGCGGTTTATC
UPSTREAM FORWARD PRIMER E	8 033042	CTATTAGGTCTGCTTGGTG
UPSTREAM FORWARD PRIMER F	8 033663	CAGCTGGTACCAGTTG
UPSTREAM FORWARD PRIMER G	8 034292	CCATTGCTGATACCCTTTC

#### 3.4.2.4 PCR amplification and sequencing

Investigation of *PLCB1* was undertaken. PCR amplification and sequencing of genomic DNA (as described in Chapter 2.3.4.2–2.3.4.7) was performed in the index case, his family and also in 60 patients from the infantile epileptic encephalopathy cohort. Sequencing of *PLCB1* cDNA (using methodology described in 2.4.2.3) from the parents of the index case was also performed.

Long range PCR techniques (as described in Chapter 2.3.5) were utilised to characterise the genomic breakpoints of the putative deletion in the index case and his family. Once the PCR reaction was set up, the plate was placed directly onto the Tetrad preheated to 93°C. PCR conditions were an initial denaturation at 93°C for 5 min followed by 35 cycles of denaturation at 93°C (45s), annealing at 60°C (45s) and extension at 68°C for 8 min (the estimated predicted size of the PCR product was 7-8kb). The long range PCR was completed with a final extension at 68°C for 5min. Subsequent PCR gel electrophoresis and PCR product clean-up was undertaken exactly as described in 2.3.4.3 and 2.3.4.4. Each sequential forward primer (FP and Primer A-G) was utilised for cycle sequencing of the original PCR amplicon in order to determine the exact genomic location of the deletion breakpoint. Subsequent sequencing reaction clean-up and preparation/analysis of sequencing reactions was as described in 2.3.4.5 -2.3.4.7.

## **3.5 Results**

### **3.5.1 Clinical assessment of index case and family**

A male infant presented in early infancy with seizures. He was the first child of consanguineous (first cousin) healthy parents from Bangladesh (Figure 3-4). His younger brother (currently 16 months old) was fit and well. There was no family history of epilepsy or other progressive neurological disorders. Initially the pregnancy followed a normal course with no history of abnormal fetal movements. However, during the third trimester there were concerns regarding moderate intrauterine growth retardation. Labour was induced at 38 weeks gestation and he was born by normal vaginal delivery. Birth weight was 2.44 kg (2<sup>nd</sup> centile) and head circumference was 32 cm (0.4<sup>th</sup> centile). His early neonatal course was uneventful.

The infant's clinical course is summarised in Figure 3-5. Seizures heralded disease onset at 10 weeks of age. Focal seizures were characterised by eye rolling, lip smacking, drooling and peri-oral cyanosis followed by tonic stiffening and flexion of arms and legs. Each seizure was short, lasting between 5 and 20 seconds. Sometimes clusters of 10-20 seizures would occur several times in a 24 hour period. On clinical examination, he had mild axial hypotonia and his head circumference was on the 0.4<sup>th</sup> centile, but otherwise detailed neurological examination revealed no abnormalities. At 10 weeks, neurodevelopmental assessment was age-appropriate. At this stage, awake and sleep EEG was normal for age. Clinical seizures were not observed during the EEG recording. Phenobarbitone therapy was subsequently instigated. He had no further

seizures till 6 months of age. At this stage, the recurrence of seizures (which were identical in semiology to the previous seizures) was managed by a further increment of the phenobarbitone dosage. He was seizure-free again for a further 2 months.

At 8 months, he developed the clinical and EEG features of WS. Clinical spasms were characterised by sudden symmetrical whole body flexion. Episodes lasted 1-2 seconds, followed by a pause for 5-10 seconds, then followed by a further spasm. Over a 24 hour period, he had 2-5 such clusters of spasms (each lasting 10-60 minutes). The onset of spasms was associated with regression in all areas of development. Hypsarrhythmia was evident on EEG (Figure 3-6A) which persisted despite two weeks of vigabatrin therapy. Cessation of spasms was subsequently achieved by a course of prednisolone therapy.

At 10 months, he developed seizures of different semiology. Seizure onset was heralded by an arrest of activity followed by staring, irregular breathing and bilateral peri-oral twitching. Over the next 2 years, he developed recurrent tonic and generalised tonic-clonic seizures. By 13 months, the EEG showed features of a diffuse encephalopathic process characterised by generalised slowing (Figure 3-6B). Sustained seizure control was not achieved despite the use of multiple anti-epileptic agents (Figure 3-5). The parents declined a trial of ACTH therapy.

His head circumference continued to track along the 0.4<sup>th</sup> centile (body weight, 2<sup>nd</sup> centile). Following the onset of clinical spasms at 8 months, there was

progressive developmental regression. By 2.5 years, he was functioning at the 0-3 month level, such that he could not lift his head when prone or roll over. Visual fixing and following was inconsistent. Over time, he developed severe head lag, axial hypotonia and a spastic quadriparesis.

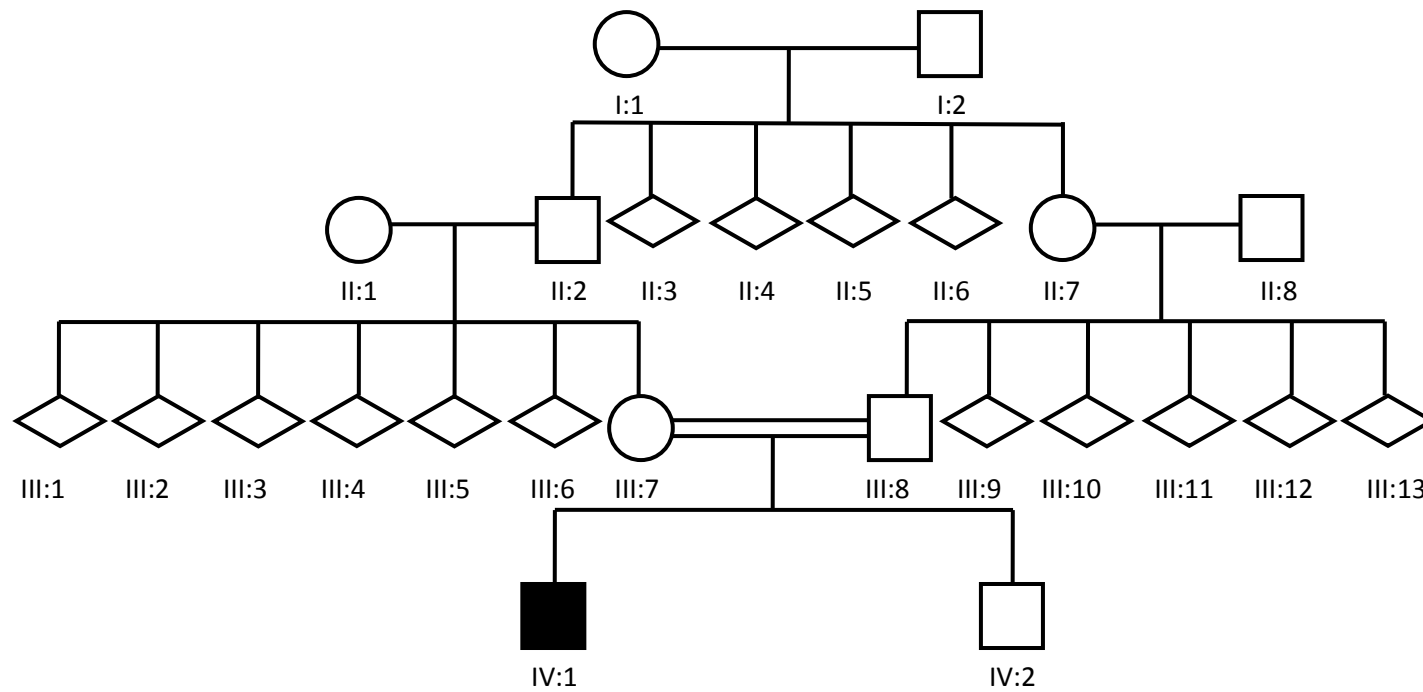
MRI brain scans (at age 5 and 13 months) were normal but no further imaging studies were undertaken during the course of his life. Visual evoked responses (VEP) and electroretinogram (ERG) at age 6 months were normal. Wood's light examination and extensive neurometabolic investigations were also normal.

At 2.9 years of age, he developed adenovirus pneumonitis (confirmed by blood PCR analysis) followed by a secondary bacterial respiratory infection. He required ventilator support (with high frequency oscillation and nitric oxide therapy) for progressive respiratory difficulties. He failed to clinically respond to antiviral drugs, multiple antibiotic agents, inotropic support and a trial of steroids. He died secondary to cardiorespiratory failure. Post mortem examination of the brain was not performed.

**Figure 3-4**

*Family tree of consanguineous kindred*

*Affected child with epileptic encephalopathy is indicated by black shading (IV:1). Circles indicated females; squares indicate males; diamonds indicate undisclosed gender*



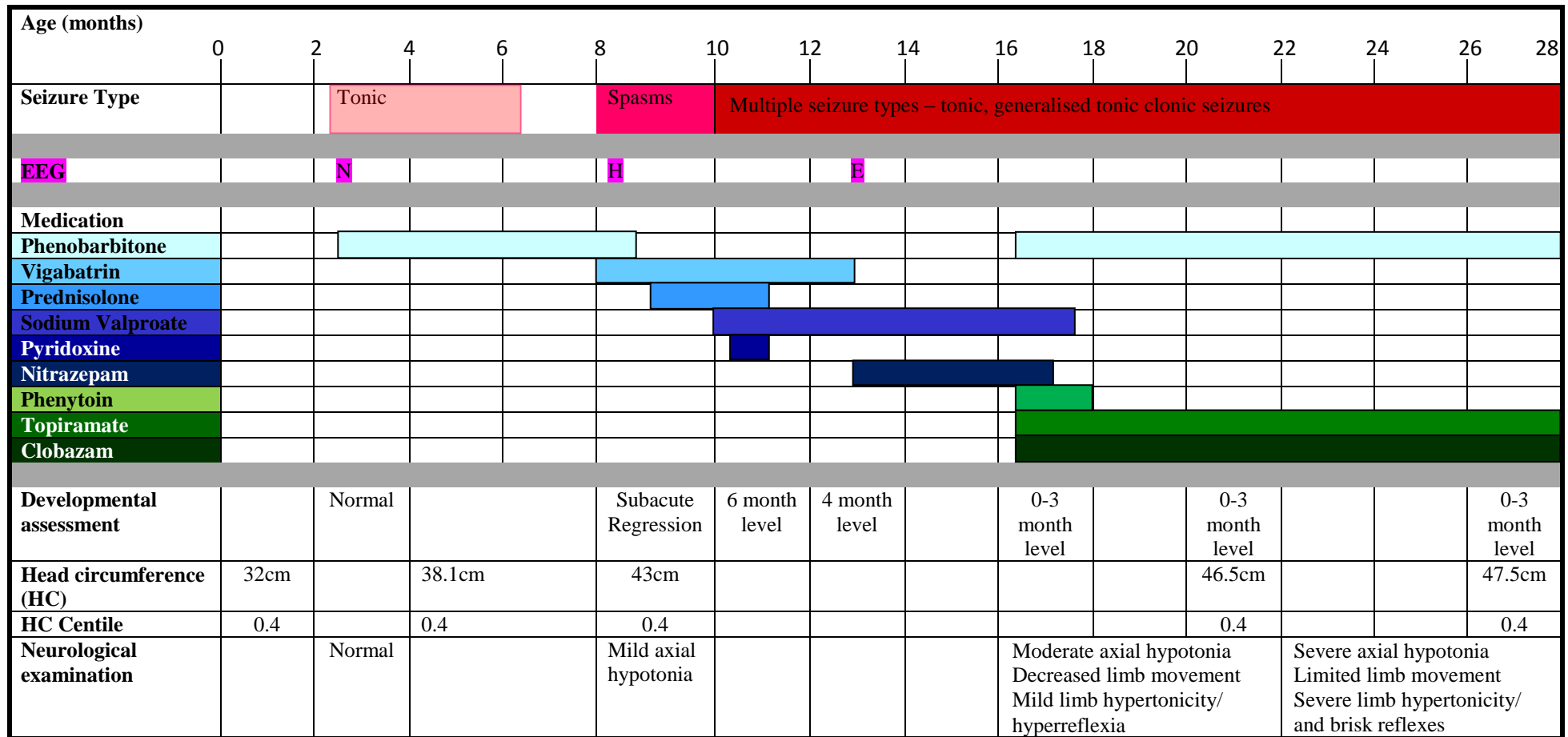
**Figure 3-5**

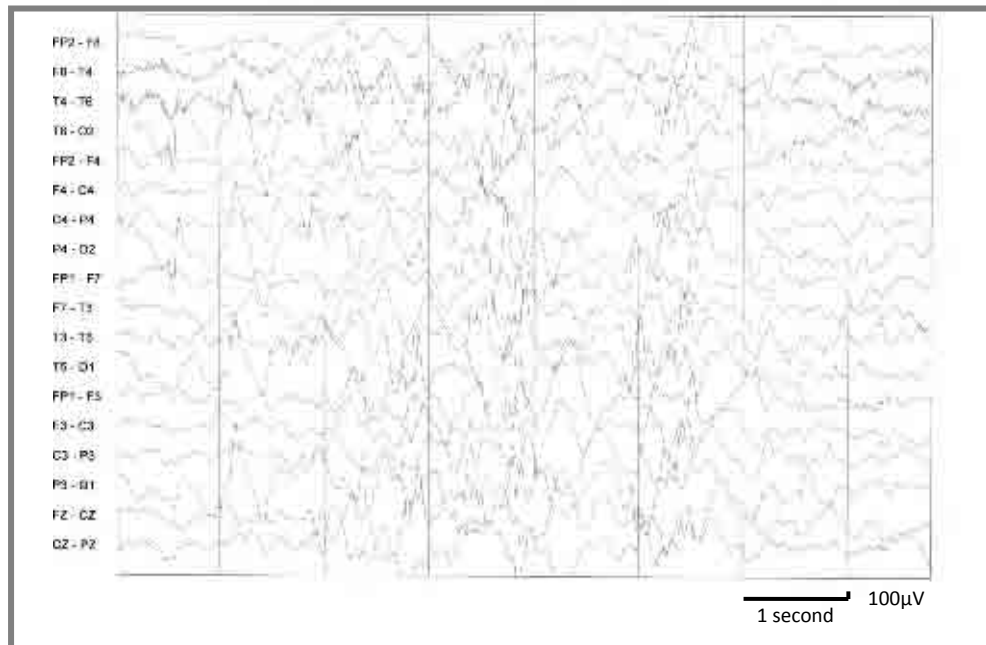
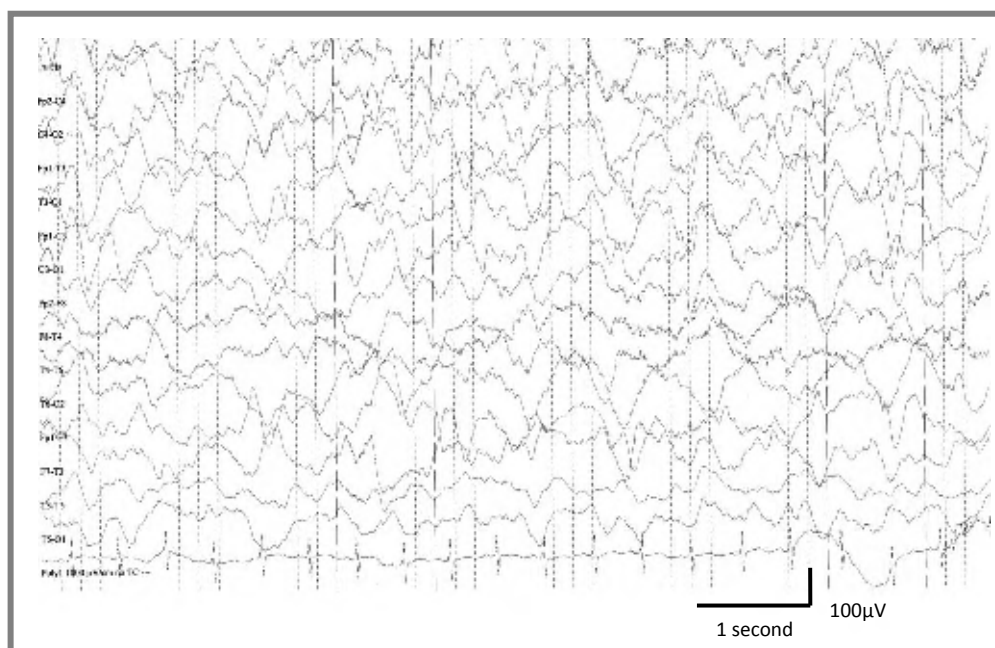
Schematic representation of the evolution of the index case's clinical course over the first 28 months of his life (prior to his death at 2.9 years)

N Normal EEG

H Hypsarrhythmic pattern on EEG

E Encephalopathic pattern on EEG – diffuse generalised slowing



**Figure 3-6***EEG recordings of index case (VI:1)***3-6A***Hypsarrhythmia on interictal EEG, age 8.5 months***3-6B***Non specific excessive generalised slow wave activity on sleep EEG recording, age 13 months*



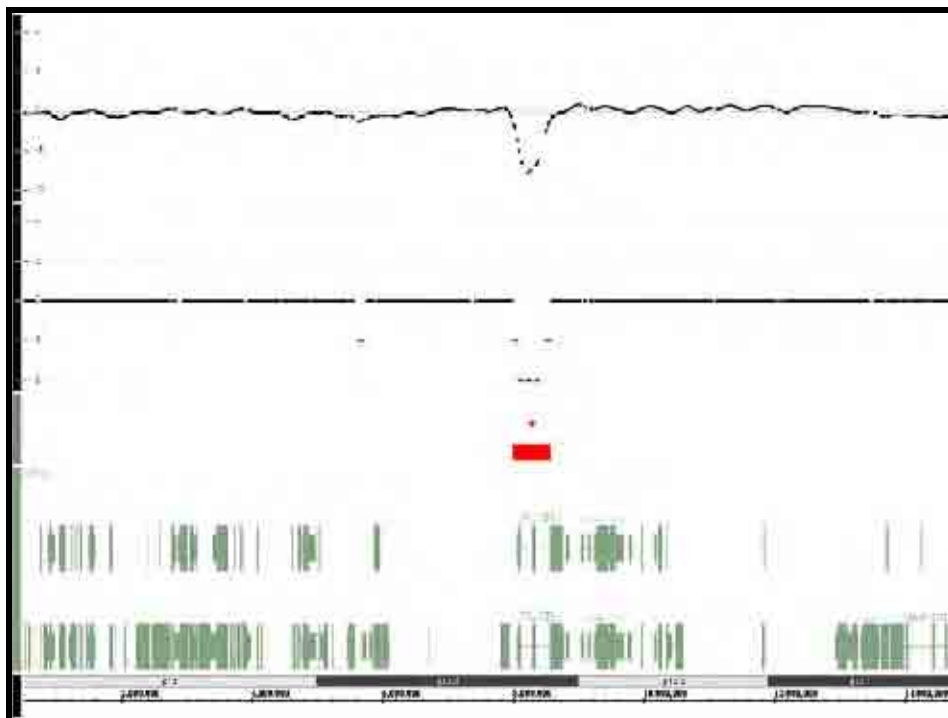
## 3.5.2 Molecular genetic investigation

### 3.5.2.1 Genome-wide scan

Using the Affymetrix 250K SNP, whole genome array studies were undertaken in the index case IV:1. On detailed analysis, a 0.5Mb region containing 23 sequential absent SNP calls was identified between SNP rs6118078 (8,048,714bp) and rs6086520 (8,507,651bp). This 0.5Mb region (from ~8.04Mb to 8.50Mb) was located within an extended region of homozygosity on chromosome 20 (with SNP homozygosity evident from 5.26Mb to 10.26Mb). Subsequent copy number analysis for this region indicated a homozygous deletion on chromosome 20 involving the *PLCB1* gene and no other coding genes (Figure 3-7).

**Figure 3-7**

*Copy number variant analysis, indicating a homozygous deletion of approximately 0.5Mb at chromosome 20p12.3, in the region of *PLCB1**



### 3.5.2.2 Genomic DNA sequencing of *PLCB1*

For the index case, specific PCR primers flanking *PLCB1* exons 1, 2 and 3 (predicted to be contained within the deletion) failed to amplify on repeated attempts (Figure 3-8) but all other *PLCB1* coding exons were amplified and sequencing demonstrated no abnormality.

#### **Figure 3-8**

*Agarose gel photograph illustrating PCR amplification of exons 1-4 of *PLCB1* in the index case and his parents. A hyperladder has been added to lane 1 to aid estimation of PCR product size*

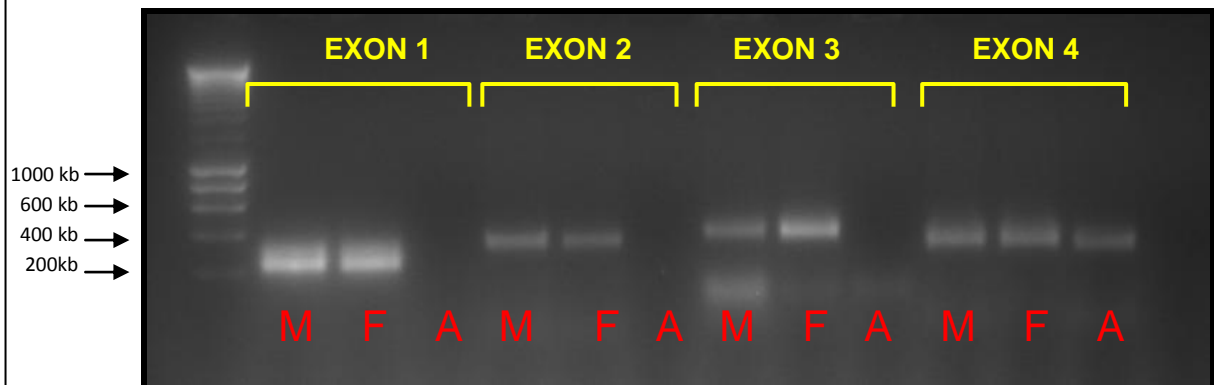
*M III:7 (Mother of index case)*

*F III:8 (Father of index case)*

*A IV:1 (index case)*

*In III:7 and III:8 all 4 exons were amplifiable. However, in the index case, on repeated attempts, PCR amplification of exons 1, 2 and 3 was not possible.*

*Exon 4 was amplifiable in the index case*



### 3.5.2.3 Characterisation of the putative deletion

Repeated failed attempts at PCR amplification of *PLCB1* exons 1, 2, and 3 was further evidence of a possible homozygous deletion in the index case. Long range PCR techniques were employed to characterise the putative deletion.

Using the primers FP and RP, an amplicon of approximately 7kb (Figure 3-9) was obtained in the index case (IV:1). Both parents were also positive for the deletion-specific PCR amplicon. To exclude the possibility that the deletion was a polymorphic variant, 660 ethnically matched control chromosomes were analysed for the presence of the deletion-specific PCR product and did not identify any chromosomes carrying the deletion (Figure 3-9).

### **Figure 3-9**

#### *Long Range PCR Amplification*

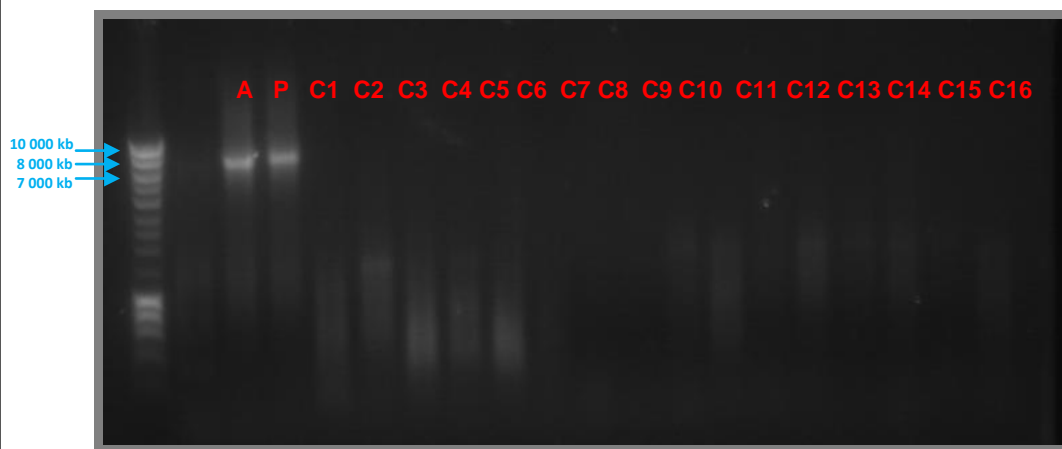
*A - IV:1 (Index Case)*

*P - III:8 (Father)*

*C1-C16 - Control DNA samples*

*Agarose gel photograph illustrating PCR amplification (using primers FP and RP for long range PCR) of a ~7kb product in both the index case (IV:1) and his father (III:8). PCR amplification was not achieved in control samples (C1-16 shown here)*

*A hyperladder has been added to lane 1 to aid estimation of PCR product size*



Sequencing of this PCR fragment (in IV:1, III:7 and III:8) using serial forward primers A-G (Table 3-5) allowed the genomic deletion to be characterised (Figure 3-10). The telomeric and centromeric genomic breakpoints were mapped to 8,034,442-8,034,510bp and 8,520,654-8,520,722bp respectively.

The precise location of the breakpoint could not be further defined as there was a 68bp sequence which showed 100% sequence homology for both the upstream and intron 3 sequence (Figure 3-10) defining a 486kb deletion. Using NCBI BLAST, I determined that the deletion occurred within a region of 96% sequence homology between the upstream sequence (8,029,511 and 8,035,562bp) and intron 3 sequence (8,575,746 and 8,581,771bp). Using genome browsers, I identified a heterozygous deletion with similar breakpoints (8,002,182-8,595,665bp) which was detected in 1/540 HapMap chromosomes. The homozygous deletion has not been reported as a copy number variant.

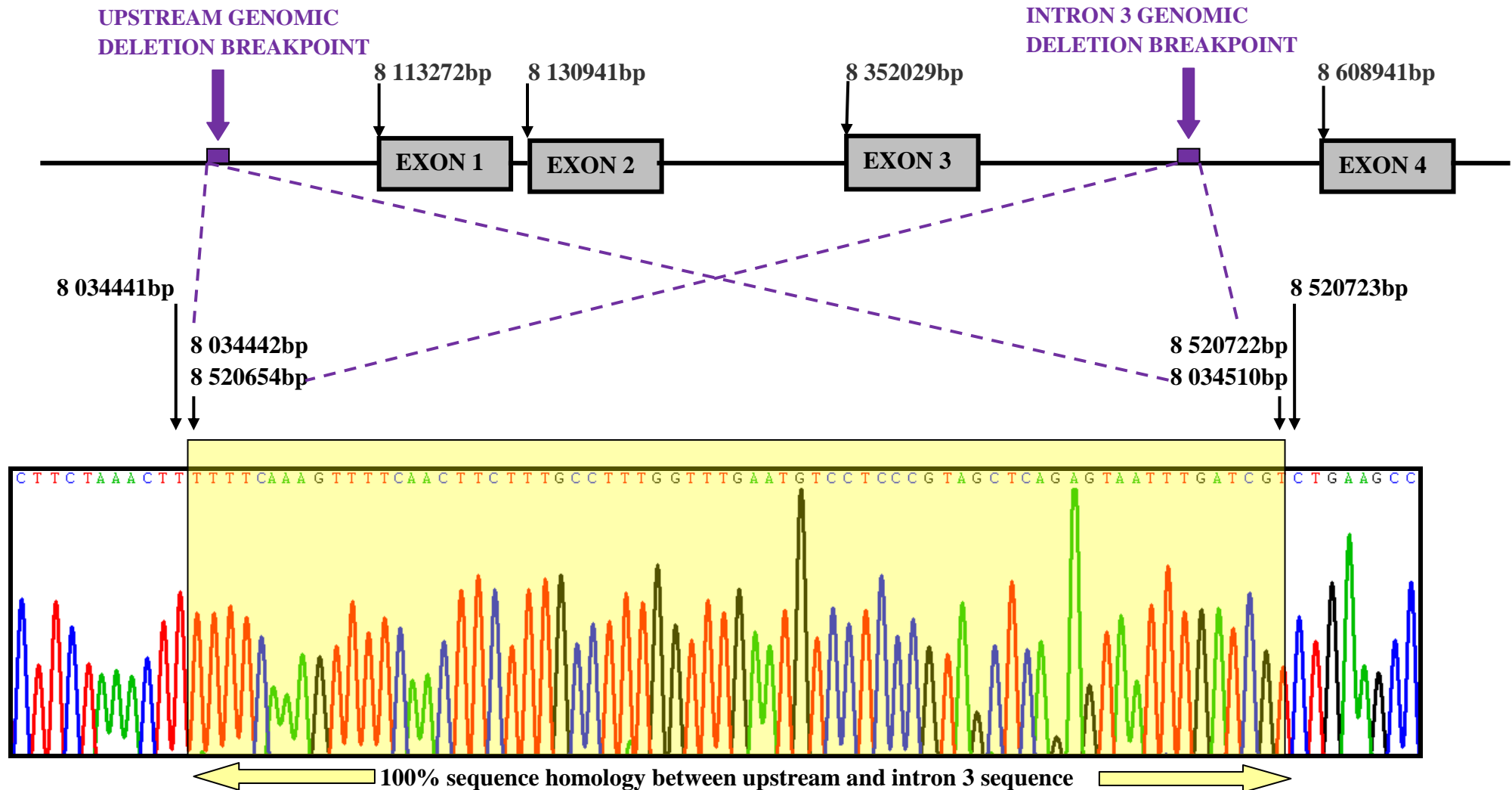
([http://www.sanger.ac.uk/humgen/cnv/data/cnv\\_data/display/](http://www.sanger.ac.uk/humgen/cnv/data/cnv_data/display/), [http://genome.ucsc.edu/cgi-bin/hgc?hgsid=162444873&o=8002181&t=8595665&g=ct\\_WGTPCNV\\_s\\_617&i=.%2Ftrash%2Fct%2Fct\\_genome\\_773f\\_8dfd30.bed+819](http://genome.ucsc.edu/cgi-bin/hgc?hgsid=162444873&o=8002181&t=8595665&g=ct_WGTPCNV_s_617&i=.%2Ftrash%2Fct%2Fct_genome_773f_8dfd30.bed+819)).

#### **3.5.2.4 cDNA sequencing of *PLCB1***

To confirm that the homozygous 0.5Mb deletion produced loss of *PLCB1* expression, *PLCB1* was sequenced in parental cDNA and genomic DNA samples. This revealed two heterozygous SNPs in parental genomic DNA (rs2076413 and rs2294597) but only monoallelic *PLCB1* expression in parental cDNA (Figure 3-11). The expressed allele was the non-deleted allele that had not been inherited by the affected child. These results were consistent with loss of *PLCB1* expression from the deleted allele.

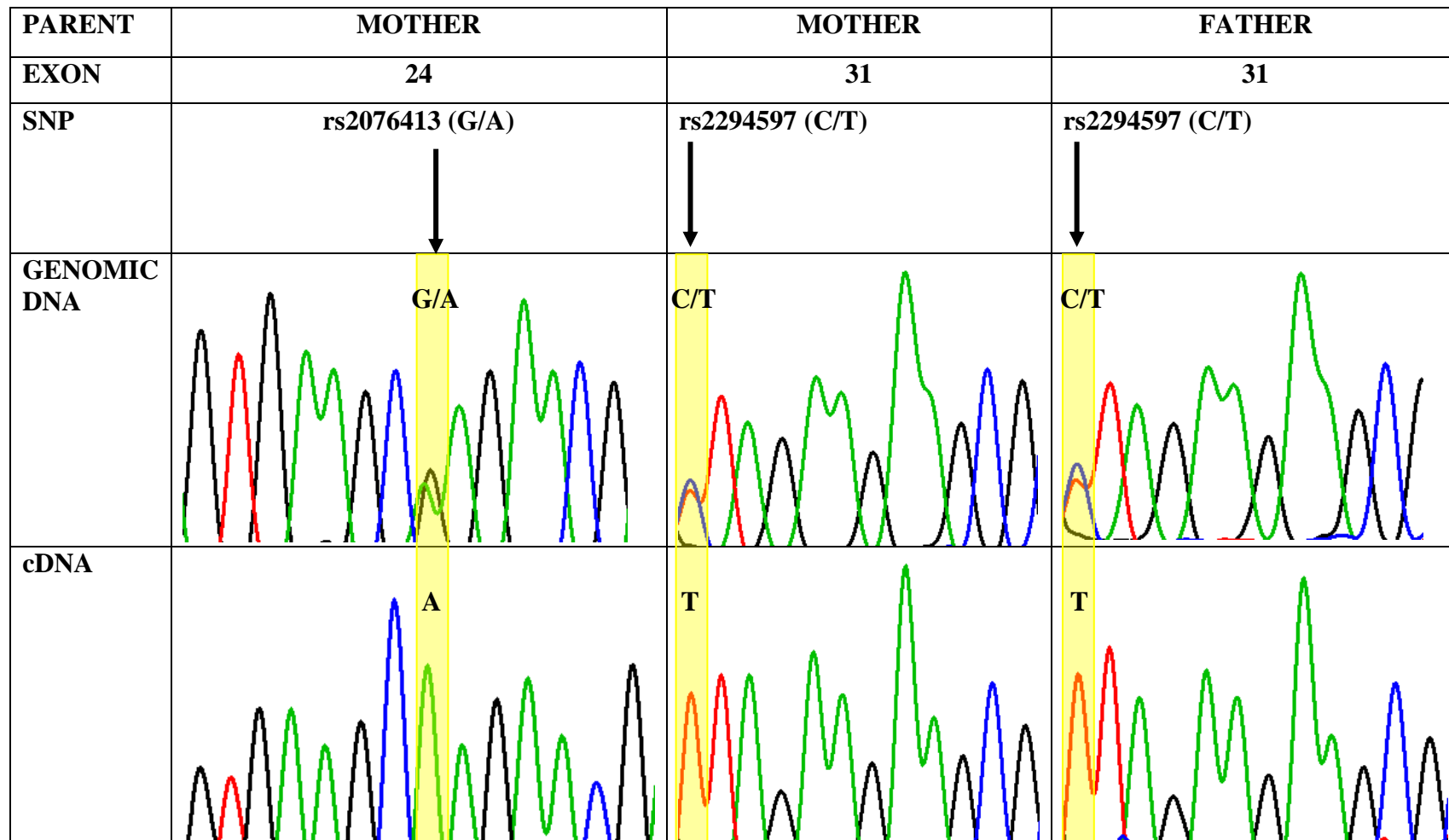
**Figure 3-10**

Definition of the genomic breakpoint of the deletion. The upstream genomic breakpoint was determined to be between 8,034,442 and 8,034,510bp and the downstream genomic breakpoint was determined to be between 8,520,654 and 8,520,722bp. A 68bp sequence which showed 100% sequence homology for both the upstream and intron 3 sequence was identified (highlighted in the yellow box).



**Figure 3-11**

Sequencing analysis of genomic and cDNA in the index case's mother (III:7) and father (III:8) for *PLCB1* exons 24 and 31. Although there is biallelic expression of SNPs rs2076413 (G/A) and rs2294597 (C/T) in genomic DNA, there is monoallelic expression of these SNPs rs2076413 (A) and rs2294597 (T) in cDNA.



### 3.5.2.5 *PLCB1* mutational analysis of other cases

In order to establish the frequency of *PLCB1* mutations, *PLCB1* sequencing and mutational analysis was undertaken in 60 cases (8 familial and 52 sporadic cases) from the acquired cohort. No pathogenic mutations were identified in any cases and none of the samples were positive for the deletion-specific PCR products.

## 3.6 Discussion

In this chapter, I have reported the novel association of infantile epileptic encephalopathy with the first homozygous loss-of-function *PLCB1* mutation described in humans. This infant developed an intractable seizure disorder in early infancy, which subsequently progressed to WS. Over time he continued to have features of a severe epileptic encephalopathy with marked developmental regression and eventual death in early childhood. This identified *PLCB1* deletion shows appropriate familial segregation with disease status, and is absent in an extensive analysis of ethnically-matched control chromosomes.

The homozygous deletion in this patient results in loss of the predicted *PLCB1* promoter sequence (Peruzzi *et al.*, 2002) and the first three coding exons of the gene. No other coding genes are affected by the 0.5Mb deletion. Analysis of parental genomic and cDNA for expressed SNPs in exons 24 and 31 demonstrated that the deleted allele is associated with complete loss of expression of *PLCB1* (although *PLCB1* transcripts are alternatively spliced, the promoter deletion was associated with silencing of *PLCB1* expression in all transcripts). The genomic deletion is likely to have originated from an abnormal

recombination event between two highly homologous repetitive sequences located upstream of exon 1 and in intron 3. It may be that this region on chromosome 20 is particularly susceptible to recombination events. Indeed, similar somatic (heterozygous) rearrangements of this chromosome band 20p12 occur in a number of solid tumours (Peng *et al.*, 2002; Hu *et al.*, 2003; Gordon *et al.*, 2003) and monoallelic interstitial deletions of *PLCB1* have been detected in a cohort of patients who show rapid progression of myelodysplastic syndrome to acute myeloid leukaemia (Lo Vasco *et al.*, 2004).

As outlined in Chapter 3.2, accurate diagnosis and subsequent clinical management of the epileptic encephalopathies is established by careful clinical assessment of seizure semiology, disease evolution and findings on EEG. Identification of causative gene mutations can be helpful in refining the diagnosis but is only possible in some cases. However, defining genetic defects such as *PLCB1* can provide valuable insights into the pathophysiological mechanisms underlying this group of disorders.

*PLCB1* is a member of group of phosphoinositide-specific phospholipase C- $\beta$  enzymes which couple with guanine-nucleotide-binding G proteins to mediate a wide variety of extracellular signals transduced across the cell membrane. There are four known isoenzymes ( $\beta 1$ - $\beta 4$ ). *PLCB1* maps to chromosome 20p12.3 (Peruzzi *et al.*, 2000) at 8,112,824-8,949,003bp and encodes several transcripts ranging in size from 288bp (30 amino acids) to 6729bp (1216 amino acids) (Table 3-6).



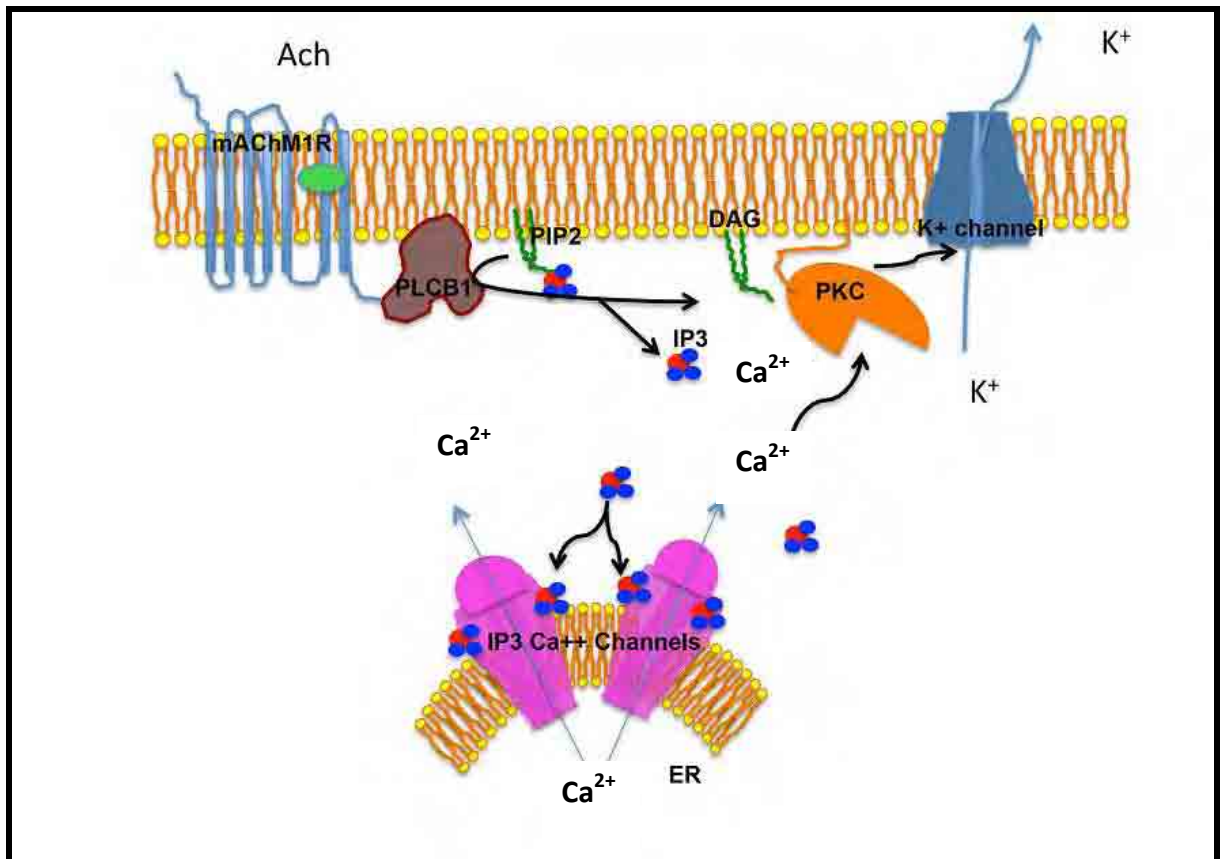
**Table 3-6**  
***PLCB1* Transcripts (adapted from Ensembl genome browser)**

Name	Transcript ID	Length (bp)	Protein ID	Length (amino acids)
PLCB1-001	ENST00000404098	697	ENSP00000384001	232
PLCB1-003	ENST00000338037	6729	ENSP00000338185	1216
PLCB1-004	ENST00000378637	3854	ENSP00000367904	1173
PLCB1-005	ENST00000378641	7295	ENSP00000367908	1173
PLCB1-007	ENST00000439627	707	ENSP00000391162	196
PLCB1-008	ENST00000437439	288	ENSP00000389911	30
PLCB1-201	ENST00000338061	1856	ENSP00000338402	223
PLCB1-202	ENST00000441163	460	ENSP00000396398	152
PLCB1-001	ENST00000404098	697	ENSP00000384001	232

PLCB1 is a post-synaptic receptor activated, G-protein coupled phosphodiesterase, which catalyses the generation of inositol 1,4,5-trisphosphonate (IP<sub>3</sub>) and diacylglycerol (DAG) from phosphatidylinositol 4,5-bisphosphonate (PIP<sub>2</sub>). In turn DAG activates the phosphorylating enzyme protein kinase C (PKC). IP<sub>3</sub> regulates the release of calcium (Ca) from the endoplasmic reticulum (ER) (Figure 3-12) (De Camilli *et al.*, 1996; Hannan *et al.*, 2001). IP<sub>3</sub>, PIP<sub>2</sub> and DAG all have direct effects on vesicular trafficking within the cell (Fisher *et al.*, 1992; Fabbri *et al.*, 1994; De Camilli *et al.*, 1996). PLCB1 thus plays a key role in the intracellular transduction of a large number of extracellular signals (involving neurotransmitters and hormones) thus modulating diverse developmental and functional aspects of the mammalian central nervous system.

**Figure 3-12**

*Proposed cellular function of PLCB1. The G-protein coupled mACh receptor activates PLCB1 which hydrolyses  $PIP_2$  to DAG and  $IP_3$ . DAG directly activates PKC, whereas  $IP_3$  activates the  $IP_3$ -activated ER- $Ca^{2+}$  channel.  $Ca^{2+}$  released from the ER also activates PKC. PKC phosphorylates the potassium ( $K^+$ ) channel increasing  $K^+$  efflux causing depolarisation (Kurian et al., 2010a)*



The consequences of bi-allelic loss of *PLCB1* are evident from a specific *Plcb1* homozygous knockout mouse model (Kim et al., 1997) which presents with an epileptic phenotype. Kim et al., demonstrated that while mice heterozygous for the generated *Plcb1* null mutation were normal and fertile, the homozygote *Plcb1*<sup>-/-</sup> mice displayed retarded growth and low viability after birth. Most mice died suddenly, starting from week three after birth. The death of these mice was preceded by status epilepticus or intractable intermittent seizures. The seizures

were generalised in nature, either tonic events, or generalised tonic-clonic episodes. Histochemical analysis of the *Plcb1*<sup>-/-</sup> hippocampus after spontaneous seizure revealed selective loss of somatostatin-containing interneurons in the hilus (Kim *et al.*, 1997). There is evidence that hilar interneurons containing somatostatin are selectively lost by electrical stimulation of adjacent granule cells of the hippocampus, thus indicating that seizures in *Plcb1*<sup>-/-</sup> are evoked through hippocampal hyperexcitability. *PLCB1* deficiency selectively impairs muscarinic acetylcholine receptor (mACh) signalling (Figure 3-12; Kim *et al.*, 1997) in the hippocampus as well as the temporal cortex and cerebellum. It may thus disrupt normal inhibitory neuronal circuitry, thus lowering the brain's threshold for seizures.

As described in Chapter 3.2, developmental arrest and poor neurological outcome are seen almost universally in infantile epileptic encephalopathies. The exact pathogenic mechanisms for this cognitive decline remain controversial and are yet to be fully elucidated. Although the seizure disorder may itself significantly contribute to the psychomotor difficulties (Dulac *et al.*, 1996), the underlying aetiology may also contribute to the neurodevelopmental outcome. For example (as discussed in Chapter 3.3), defects in genes such as *ARX* cause epilepsy, but may also result in brain malformations and mental retardation.

Studies in mice raise the possibility that loss of *PLCB1* function may also have neurodevelopmental implications independent of (and which may precede the onset of) the seizure disorder (Hannan *et al.*, 2001; Böhm *et al.*, 2002; Spires *et*

*al.*, 2005, McOmish *et al.*, 2008; Koh *et al.*, 2008). *Plcb1*<sup>-/-</sup> mice display a dramatic reduction in group 1 mGluR-stimulated phosphoinositide hydrolysis during cortical barrel formation, resulting in significant disruption of the cytoarchitectural differentiation of barrels in the mouse somatosensory cortex (Hannan *et al.*, 2001). It has also been reported that the ability of muscarinic receptors to induce the inward aftercurrent underlying the slow afterdepolarization is also markedly reduced in a *Plcb1*<sup>-/-</sup> knockout mouse. Accordingly, this phenomenon has been hypothesized to allow for the transient storage of memory traces in neuronal networks (Yan *et al.*, 2009). *Plcb1*<sup>-/-</sup> mice also show absence of long-term depression in the visual cortex (Choi *et al.*, 2005). This data suggests that PLCB1 activation via mGluR5 receptors is critical for the co-ordinated development, differentiation and plasticity of the cortex. In addition to increasing susceptibility to epileptogenesis, loss of PLCB1 function may thus also have independent neurodevelopmental consequences.

Sequencing of *PLCB1* in a further 60 infants with epileptic encephalopathy/WS did not reveal any pathogenic mutations. *PLCB1* mutations are thus rare and likely to account for <5% of such cases (95% CI for 1/61 = 0-4.8%), consistent with genetic heterogeneity in this disorder. It is however important to note that the index case had final MR brain imaging at 13 months of age. The evolution of focal seizures in this patient could potentially herald the development of a radiologically discernible focal brain abnormality that may have only been evident on later scans, following completion of brain myelination after 2 years of age. In the future, mutational screening of *PLCB1* should thus be considered in

all children with early onset epileptic encephalopathy, including those with focal brain abnormalities.

### **3.7 Conclusion**

In this chapter I have described *PLCB1*-associated epileptic encephalopathy in a male infant originating from a consanguineous family. Identification of this homozygous *PLCB1* deletion (inherited in an autosomal recessive manner) has facilitated appropriate genetic counselling and the possibility of future prenatal diagnosis for this family. Although only a single case has been identified, future mutational analysis of further cases of infantile epileptic encephalopathy may identify more *PLCB1* cases, allowing enhanced phenotypic delineation of this disorder. The identification of a human model of *PLCB1* inactivation has also implicated a novel disease pathway (and further potential candidate genes) which can be explored in the future to elucidate the molecular basis of other unresolved epileptic encephalopathies.

## **Chapter 4**

### **Infantile Parkinsonism-Dystonia and *SLC6A3***

## **4.1 Introduction**

The inherited neurotransmitter disorders represent an expanding group of neurometabolic syndromes caused by abnormalities of neurotransmitter synthesis, breakdown and transport (Pearl *et al.*, 2005). This group of diseases include disorders of monoamine, glycine, pyridoxine and GABA metabolism. Patients present with a wide variety of symptoms determined by the type and severity of the disorder. The monoamine neurotransmitter disorders may manifest with neurological features of global developmental delay, pyramidal and extrapyramidal motor deficits, epilepsy and autonomic dysfunction. Infantile parkinsonism-dystonia (IPD) is a monoamine neurotransmitter disorder characterised predominantly by a complex movement phenotype (Assmann *et al.*, 2004). In this chapter, the preliminary clinical investigation and molecular characterisation of IPD will be described (Kurian *et al.*, 2009). Two consanguineous families with IPD were investigated. The disease locus was mapped to chromosome 5p15.3 and different germline *SLC6A3* mutations were identified in both kindreds. Functional studies (undertaken by collaborators) revealed that both mutations led to a reduction in the level of mature dopamine transporter.

### **4.1.1 The monoamine neurotransmitter biosynthetic pathway**

Enzyme defects of the monoamine biosynthetic pathway can result in human neurotransmitter diseases. The monoamine neurotransmitters include the catecholamines (dopamine, norepinephrine and epinephrine) and serotonin. The key synthesis, degradation and salvage pathways are illustrated in Figure

4-1 (Assmann *et al.*, 2003). Tetrahydrobiopterin (BH<sub>4</sub>) is a necessary cofactor for both tryptophan hydroxylase and tyrosine hydroxylase (Longo, 2009). BH<sub>4</sub> is synthesized in three steps from guanine triphosphate. When tetrahydrobiopterin acts as a cofactor for these hydroxylases, it is converted to pterin-4a-carbinolamine and subsequently 'salvaged' back into tetrahydrobiopterin by a 2-step process involving pterin-4a-carbinolamine dehydratase and dihydropteridine reductase. Tryptophan is converted to 5-hydroxytryptophan by tryptophan hydroxylase. Tyrosine is converted to L-dopa by tyrosine hydroxylase. Aromatic L-amino acid decarboxylase then catalyses the conversion of 5-hydroxytryptophan to serotonin and L-dopa to dopamine. Serotonin and dopamine are broken down through similar pathways, which involve monoamine oxidase-A and -B. In addition, dopamine is converted into norepinephrine by dopamine beta-hydroxylase.

**Figure 4-1** The monoamine metabolism pathway

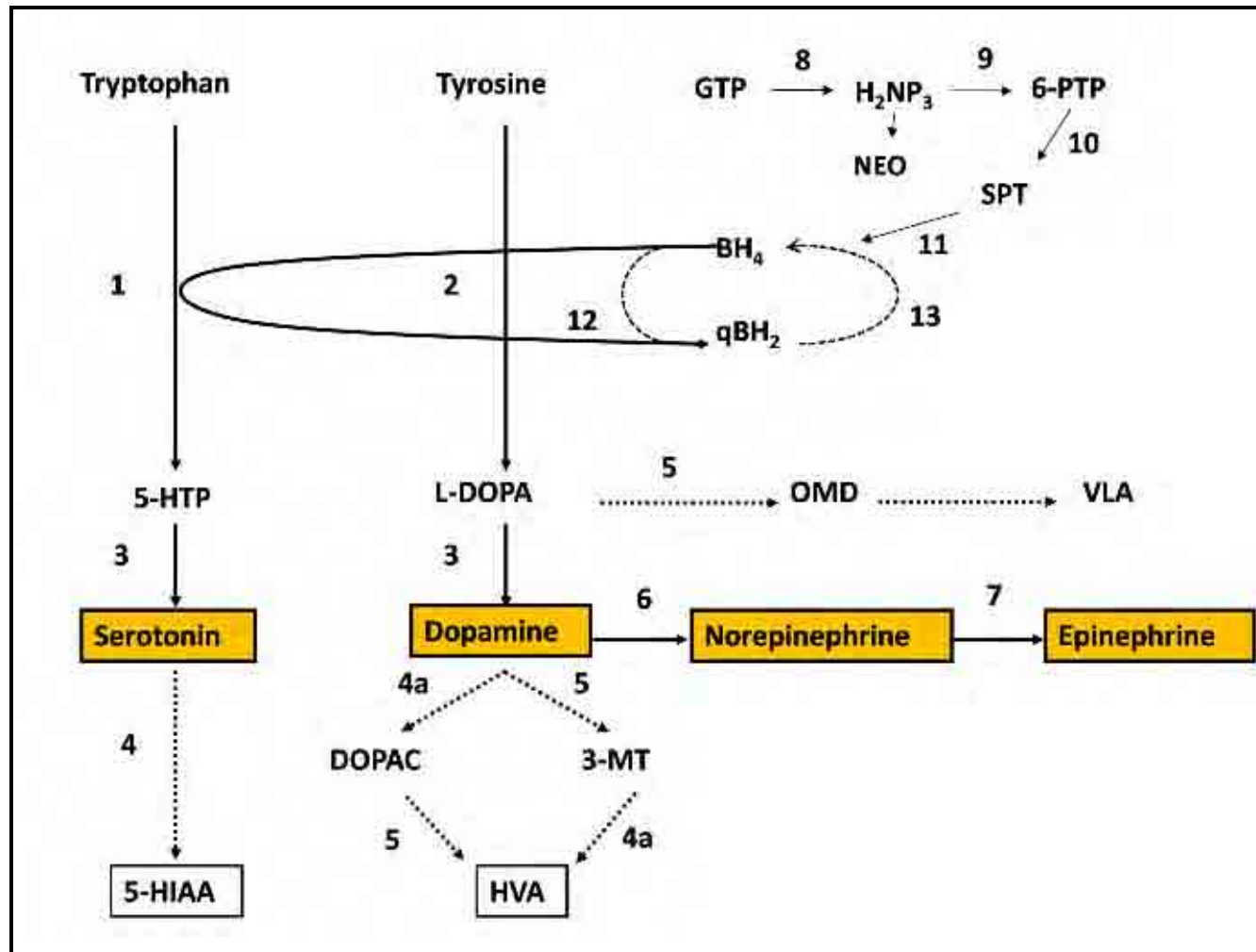
Metabolic pathway of serotonin and dopamine biosynthesis (solid arrows), catabolism (dotted arrows) and salvage (dashed arrows). The biogenic amines are boxed in orange. Tetrahydrobiopterin (BH<sub>4</sub>) is the essential cofactor for the rate-limiting enzymes tyrosine hydroxylase (TH) and tryptophan hydroxylase. BH<sub>4</sub> is synthesised *de novo* via steps 8-11 and recycled via the salvage pathway (steps 12-13).

**GTP** is guanosine triphosphate, **H<sub>2</sub>NP<sub>3</sub>** is dihydroneopterin triphosphate, **NEO** is neopterin, **6-PTP** is 6-pyruvoyltetrahydropterin, **SPT** is sepiapterin, **BH<sub>4</sub>** is tetrahydrobiopterin and **qBH<sub>2</sub>** is (quinonoid) dihydrobiopterin, **5-HTP** is 5-hydroxytryptophan, **L-DOPA** is levodihydroxyphenylalanine (levodopa), **OMD** is 3-ortho-methyldopa, **VLA** is vanillylactic acid, **5-HIAA** is 5-hydroxyindoleacetic acid, **HVA** is homovanillic acid.

**1** is tryptophan hydroxylase; **2** is tyrosine hydroxylase (**TH**); **3** is aromatic L-amino acid decarboxylase (**AADC**); **4** is monoamine oxidase (**MAO**); **4a** is monoamine oxidase plus aldehyde dehydrogenase; **5** is catechol-O-methyltransferase (**COMT**); **6** is dopamine β-hydroxylase; **7** phenylethanolamine N-methyltransferase **8** is GTP-cyclohydrolase I (**GTPCH I**); **9** is 6-pyruvoyltetrahydropterin synthase (**PTPS**); **10** is aldose reductase; **11** is sepiapterin reductase (**SR**); **12** is pterin-4α-carbinolamine dehydratase; **13** is dihydropteridine reductase (**DHPR**)



**Figure 4-1 The monoamine metabolism pathway**  
 Metabolic pathway of serotonin and dopamine biosynthesis  
 (Adapted from Kurian et al., 2010b)



### 4.1.2. Clinical features of neurotransmitter disorders

Inherited defects of the monoamine biosynthetic pathway can result in a number of neurotransmitter disorders in humans (Pearl *et al.*, 2006; Pearl *et al.*, 2007; Longo, 2009). The key clinical features of monoamine neurotransmitter disorders are summarised in Table 4-1.

Hoffmann and colleagues (1998) have attempted to separate the clinical consequences of dopamine and serotonin deficiency. Defects in the metabolism of dopamine show relatively distinct phenotypes. Extrapyrmidal movement features are prominent, especially parkinsonism-dystonia, dystonia and chorea (Assmann *et al.*, 2003). The spectrum of extrapyramidal symptoms is wide, ranging from intermittent focal dystonia (such as in autosomal dominant GTP cyclohydrolase deficiency, Segawa, 2009) to severe, often lethal infantile encephalopathies (such as Type B tyrosine hydroxylase deficiency, Willemsen *et al.*, 2010).

Dopamine deficiency is also associated with other clinical symptoms (Grattan-Smith *et al.*, 2002) including oculogyric crises, meiosis, ptosis, hypersalivation and myoclonic epilepsy. Nonspecific symptoms are also attributable to dopamine deficiency, and include epileptic encephalopathy, progressive mental retardation, microcephaly, swallowing difficulties, limb hypertonia, truncal hypotonia and pyramidal tract dysfunction. The manifestations of serotonin deficiency are less well described but include temperature instability and sweating. Behavioural difficulties and hypotension are seen in neurotransmitter

disorders of monoamine degradation (Brunner *et al.*, 1993; Robertson *et al.*, 1991).

The early onset neurotransmitter disorders display phenotypic similarity to other movement disorders of infantile/childhood onset such as cerebral palsy. The complex motor features seen in these neurotransmitter disorders can mimic spastic diplegia as well as dyskinetic, spastic or mixed cerebral palsy phenotypes. Clinical recognition and appropriate investigation is thus imperative to prevent misdiagnosis and/or diagnostic delay of these disorders (Assmann *et al.*, 2003; Willemsen *et al.*, 2010).

**Table 4-1**  
**Clinical features of the monoamine neurotransmitter disorders**

	MIM	Gene	Inheritance	Summary of common clinical features
<b>Disorders of BH4 synthesis</b>				
Autosomal dominant guanine triphosphate cyclohydrolase (GTPCH) deficiency	#128230	<i>GCH1</i>	AD	Focal limb dystonia (action and postural), torticollis, scoliosis, pes cavus Gait abnormalities including ataxia Tremor
Autosomal recessive GTPCH deficiency	#233910	<i>GCH1</i>	AR	Clinical features evident in these 4 disorders include:- Microcephaly Global developmental delay Irritability, poor feeding, swallowing difficulties and failure to thrive Seizures Extrapyramidal features - dystonia, choreoathetosis, parkinsonism, tremor, oculogyric crises Truncal hypotonia, pyramidal tract features, spasticity Autonomic features Hyperthermia, sweating, hypersalivation, sleep disturbance Intracerebral calcification specifically seen in DHPR deficiency
Pyruvoyl-tetrahydropterin synthase (PTPS) deficiency	#261640	<i>PTS</i>	AR	
Sepiapterin reductase (SPR) deficiency	#612716	<i>SPR</i>	AR/AD	
Dihydropteridine reductase (DHPR) deficiency	#261630	<i>QDPR</i>	AR	
Pterin-4a-carbinolamine dehydratase (PCBD) deficiency	#264070	<i>PCBD</i>	AR	Mild phenotype with transient hyperphenylalaninaemia– may have no neurological symptoms If symptomatic, usually transient neonatal gross motor delay, abnormal tone or tremor
<b>Disorders of Monoamine Synthesis</b>				
Tyrosine hydroxylase (TH) deficiency	#605407	<i>TH</i>	AR	Global developmental delay Type A: infantile hypokinetic-rigid syndrome with dystonia Type B: complex encephalopathy with neonatal onset
Aromatic L-amino acid decarboxylase (AADC) deficiency	#608643	<i>DDC</i>	AR	Developmental delay, Irritability, poor feeding, gastro-oesophageal reflux, constipation, diarrhoea Dystonia, choreoathetosis, decreased voluntary movement Hypertonia, hyperreflexia Ocular features – ptosis, meiosis and oculogyric crises Autonomic features , hypotension, sweating , temperature instability and hyperthermia
<b>Disorders of Monoamine Degradation</b>				
Monoamine oxidase (MAO) deficiency	+309850	<i>MAOA</i> <i>MAOB</i>	X-linked	Monoamine oxidase A deficiency – mental retardation and aggressive behaviour Monoamine oxidase B deficiency - associated with Norrie disease
Dopamine beta-hydroxylase (DBH) deficiency	#223360	<i>DBH</i>	AR	Hypoglycaemia and hyperthermia, ptosis, delayed eye opening in neonates Hypotension (and hypotensive seizures) Impaired/retrograde ejaculation and nocturia

### 4.1.3. Diagnosis of inherited neurotransmitter disorders

When a neurotransmitter disorder is suspected, diagnosis is established on the basis of clinical history and examination together with biochemical investigations, enzyme analysis and mutation analysis of the causative gene (Marin Valencia *et al.*, 2008). A stepwise approach to diagnostic investigations is generally undertaken as follows:-

#### 4.1.3.1 Diagnostic lumbar puncture (LP)

Measurement of lumbar cerebrospinal fluid (CSF) neurotransmitters can aid diagnosis of a neurotransmitter disorder. The amine neurotransmitter metabolites HVA and 5-HIAA can be measured. These are the stable degradation products of dopamine and serotonin respectively and thus provide insight into the turnover of these biogenic amines in the mesolimbic and mesostriatal areas of the brain (Garelis *et al.*, 1974; McConell *et al.*, 1994; Marin-Valencia *et al.*, 2008). Individual pterin species can also be measured. The specific pattern of these neurotransmitter metabolites can thus be indicative of a particular neurotransmitter disorder (Table 4-2) thereby aiding diagnosis.

CSF neurotransmitter analysis is undertaken in collaboration with a specialist neurometabolic laboratory. High pressure liquid chromatography (HPLC) with electrochemical detection and reversed phase column is the most common method chosen to analyse HVA and other monoamine metabolites. These procedures are sensitive and specific in diagnosing such inborn errors of metabolism with rapid reproducible results (Mena *et al.*, 1994). Such laboratories have strict protocols regarding specimen collection and

interpretation, as this standardised approach is essential for reliable results (Bräutigam *et al.*, 2002, Pearl *et al.*, 2005). The rostro-caudal gradient of neurotransmitter metabolites and BH<sub>4</sub> necessitates that the same fraction of CSF must be used for each metabolite analysis (with reference ranges established by the same technique). Samples need to be snap frozen in liquid nitrogen or dry ice, as BH<sub>4</sub> in CSF is labile. Red blood cells in the CSF lead to rapid oxidation of neurotransmitter metabolites and blood-contaminated samples must be centrifuged immediately, with clear CSF transferred to new tubes prior to freezing. CSF samples must be stored at -80°C until analysis. It is important to specify the time of day when the CSF is taken, because diurnal variation can affect metabolite levels. Metabolites are interpreted with reference to age-matched control data. The concentrations of metabolites decrease rapidly within the first few months of life and then continue to decrease, at a slower rate into adulthood (Hyland *et al.*, 1993). It has been proposed that high HVA and 5-HIAA levels in infancy are required to regulate the metabolic pathway during mitosis, neurogenesis, migration and network formation of dopamine neurons.

#### **4.1.3.2 Blood and urine investigations**

As well as CSF investigations, analysis of pterin and biogenic amine metabolites in blood and urine can also aid diagnosis (Table 4-2). As dopamine suppresses the release of prolactin, the level of serum prolactin can sometimes be a useful as a marker of dopamine depletion. In some children with dopamine-deficient states, hyperprolactinaemia may be observed which may even manifest as galactorrhoea prior to the onset of neurological symptoms

(Yeung *et al.*, 2006). Although prolactin measurements can be helpful, it is neither highly specific nor sensitive for dopamine deficiency. Indeed patients with profound dopamine deficiency have had normal serum prolactin while patients with normal dopamine turnover have been reported to have increased prolactin levels (as additional confounding factors, such as the stress/anxiety during blood sampling can alter prolactin levels). Serum prolactin levels should thus be interpreted in clinical context. Serum creatine kinase (CK) levels may also be measured and are particularly useful in aiding the diagnosis of rhabdomyolysis during status dystonicus.

#### **4.1.3.3 Enzyme analysis**

For many neurotransmitter disorders, a biochemical diagnosis can be confirmed by direct measurement of the residual enzyme activity in tissue samples, blood cells or cultured fibroblasts (Table 4-2).

#### **4.1.3.4 Phenylalanine (phe) loading test**

In disorders of bipterin metabolism without hyperphenylalaninaemia (autosomal dominant GTPCH deficiency and sepiapterin reductase deficiency), the diagnostic workup may be aided by a bedside investigation known as the oral phe loading test (Table 4-2, Bandmann *et al.*, 2003). Elevated serum phenylalanine: tyrosine ratios following an oral phe load are diagnostic of a defect in BH<sub>4</sub> metabolism. Measurements are usually taken at 1, 2, 4, and 6 hours, but a single measurement 4 hours post ingestion may be sufficient for diagnosis. Normalisation of serum tyrosine levels after a phe load following

antecedent BH<sub>4</sub> supplementation indicates a defect in BH<sub>4</sub> supplementation rather than phenylalanine hydroxylase activity.

#### **4.1.3.5 Genetic analysis**

Mutational analysis of the specific causative gene (Table 4-1) is also undertaken. In some neurotransmitter disorders, such as tyrosine hydroxylase deficiency, there is a high rate of mutation detection (Willemsen *et al.*, 2010). However in other disorders, such as autosomal dominant GTPCH deficiency, genetic analysis may only yield positive results in approximately 50-60% of patients with true GTPCH deficiency (Tassin *et al.*, 2000). Although comprehensive screening of *GCH1* by conventional and quantitative PCR analysis can further increase the diagnostic yield (Hagenah *et al.*, 2005), it is possible that such patients may harbour mutations which are within the promoter region, deeply intronic or have heterozygous deletions/duplications which have not been detected by direct sequencing. It is important to interpret the results of genetic investigation in the context of the presenting clinical phenotype and biochemical investigations.



**Table 4-2**  
**Characteristic biochemical profile of the monoamine neurotransmitter disorders**

	CSF HVA	CSF 5-HIAA	CSF BH4	CSF BH2	Urine (CSF) Biopterin	Urine (CSF) Neopterin	Serum Phe levels	Other investigations helpful for diagnosis
<b>BH<sub>4</sub> synthesis</b>								
AD GTPCH deficiency	N/↓	N/↓	↓	N	N (↓)	N (↓)	N	Transient hyperphenylalaninaemia on phe loading test Reduced GTPCH enzyme activity
AR GTPCH deficiency	↓	↓	↓	N	↓	↓	↑	Reduced GTPCH enzyme activity
PTPS deficiency	↓	↓	↓	↓	↓(↓)	↑(↑)	↑	Decreased or absent PTPS enzyme activity
SPR deficiency	↓	↓	↓/N	↑	N (↑)	N	N	Increased CSF sepiapterin Transient hyperphenylalaninaemia on phe loading test SPR deficiency on enzyme analysis
DHPR deficiency	↓	↓	↓/N	↑	↓	N	↑	Decreased or absent DHPR enzyme activity
PCBD deficiency	N	N	N	N	↓	N	↑	
<b>Monoamine Synthesis</b>								
TH deficiency	↓	N	N	N	N	N	N	Decreased activity of tyrosine hydroxylase enzyme
AADC deficiency	↓	↓	N	N	N	N	N	Increased CSF urine and plasma L-dopa, 5-hydroxytryptophan and 3-O-methyldopa Decreased plasma catecholamines Decreased AADC enzyme activity
<b>Monoamine Degradation</b>								
MAO deficiency	N	N	N	N	N	N	N	Measurement of urine neurotransmitters and metabolites
DBH deficiency	N/↑	N	N	N	N	N	N	Undetectable norepinephrine/epinephrine and high dopamine in plasma/urine/CSF High plasma dihydroxyphenylacetic acid (DOPAC) Undetectable DBH protein in plasma, CSF, or sympathetic fibres. Undetectable plasma DBH enzyme activity

#### 4.1.4 Treatment of neurotransmitter disorders

Accurate recognition and diagnosis of neurotransmitter disorders has important therapeutic implications as a number of these diseases can be effectively treated (Pearl *et al.*, 2006). In general terms, treatment is aimed at, where appropriate, normalising blood phenylalanine, restoring brain neurotransmitter levels and correcting the deficiency of other chemicals. In conditions associated with hyperphenylalaninaemia, a dietary phenylalanine restriction will normalise levels as in patients with classic phenylketonuria. However in most cases, BH<sub>4</sub> supplementation alone can improve phenylalanine hydroxylase activity in the liver and normalise phenylalanine levels (Longo, 2009). In certain patients with DHPR deficiency, who are resistant to BH<sub>4</sub> therapy, dietary restriction and supplementation with neurotransmitter precursors is needed. As DHPR is important in maintaining folate in its active (tetrahydro) form (Smith *et al.*, 1985), patients with DHPR deficiency may develop cerebral folate deficiency. Therapy with folinic acid has been effective in improving neurological outcome in some of these patients. In conditions of dopamine/serotonin deficiency, a clinical response and improvement or even normalisation of brain neurotransmitters can be obtained with the administration of neurotransmitter precursors (levodopa/carbidopa, 5-hydroxytryptophan) or inhibitors of their degradation (such as the monoamine oxidase inhibitor, selegiline). Therapy with such agents is initiated at low doses and the dose is gradually increased as needed to minimise dyskinesias and other side effects. In some disorders, treatment can lead to complete resolution of symptoms, as illustrated by many patients with autosomal dominant GTPCH deficiency who display a dramatic and

sustained response to relatively low doses of levodopa (L-dopa) (Gordon, 2008).

#### **4.1.5 Other monoamine neurotransmitter disorders**

Advances in biochemical and molecular techniques have greatly increased our current knowledge, understanding and diagnosis of neurotransmitter disorders. Recently, neurotransmitter abnormalities have been described as a secondary phenomenon in a number of neurometabolic diseases (García-Cazorla *et al.*, 2007; García-Cazorla *et al.*, 2008) such as mitochondrial disorders, Reye syndrome, succinic semialdehyde dehydrogenase deficiency, phenylketonuria, Lesch-Nyhan disease and disturbances of folate metabolism (5-methyl tetrahydrofolate deficiency). Abnormalities in HVA levels have also been reported in non-metabolic disease such as hydrocephalus (Gopal *et al.*, 2008), opsiclonus-myoclonus syndrome (Pranzatelli *et al.*, 1995), epilepsy (Shaywitz *et al.*, 1975; Devinsky *et al.*, 1992), infantile spasms (Ito *et al.*, 1980), attention deficit hyperactivity disorder (Gillberg and Svennerholm, 1987), younger cases of Rett syndrome (Nielsen *et al.*, 1992) and children with perinatal asphyxia (Blennow *et al.*, 1995, Serrano *et al.*, 2007).

There also remains a number of neurotransmitter diseases (of likely genetic aetiology) in which the underlying molecular basis is not resolved. Examples of such inherited neurotransmitter disorders include some types of dopa non-responsive dystonia associated with selective reduction of serotonin turnover (Assmann *et al.*, 2002) and infantile parkinsonism-dystonia (IPD) with elevated dopamine metabolites on CSF investigation (Assmann *et al.*, 2004).

In order to define the molecular basis of IPD, I undertook molecular genetic investigations in two consanguineous families using an autozygosity mapping strategy (Kurian *et al.*, 2009).

## **4.2 Materials and methods**

### **4.2.1 Clinical assessment**

#### **4.2.1.1 Case acquisition**

Three affected children with IPD from two unrelated consanguineous families were ascertained through collaborators from the British Paediatric Neurology Association. Family A was of Pakistani origin and family B was of mixed European descent. Informed consent was obtained from all participants and the study was approved by local research ethics committees.

#### **4.2.1.2 Clinical phenotyping**

All three children with IPD were clinically assessed by myself and also independently by another paediatric neurologist. Extensive video footage of the children was examined in order to accurately categorise the observed movement disorder. Patient medical case notes were analysed to establish the clinical history, pattern of disease evolution and response to medication.

#### **4.2.1.3 CSF neurotransmitter analysis/biochemical investigations**

LP for CSF neurotransmitter analysis was performed in all three patients. The results of other biochemical investigations including urine catecholamine metabolite analysis and serum prolactin were also ascertained from the medical notes.

## **4.2.2 Molecular Genetic Investigation**

General molecular genetic techniques were carried out as described in Chapter 2. In this chapter, all annotations and physical positions are recorded as in NCBI Genome 36.3 build.

### **4.2.2.1 DNA Extraction**

DNA was extracted from peripheral lymphocytes using standard techniques.

### **4.2.2.2 Genome wide scan**

In order to identify common regions of shared homozygosity in affected individuals of family A, a genome wide scan using the Affymetrix 250K SNP microarray was initially undertaken. DNA was amplified and hybridized to the Affymetrix 250K SNP chips, as per the manufacturer's instructions. SNP array studies were kindly undertaken by Louise Tee.

### **4.2.2.3 Microsatellite marker analysis of the IPD locus**

All significant regions of common homozygosity identified on genome-wide scan were further investigated for linkage using polymorphic microsatellite markers (<http://www.ncbi.nlm.nih.gov/sites/entrez?db=unists>) (Table 4-3). After PCR amplification of genomic DNA samples, amplified fragments were genotyped using an ABI 3730 Genetic Analyser and analyzed with GeneMapper© software. Scored genotypes were assembled as haplotypes and analysed for evidence of linkage.

**Table 4-3**

***Microsatellite markers used for linkage analysis of the common regions of homozygosity identified in the affected children of family A***

Marker	Start Position (bp)	End Position (bp)	Approximate Size (bp)	UNISTS reference
D5S2488	180431	180657	227-245	28850
D5S1981	1 207429	1 207692	224-268	33655
D5S2005	1 395107	1 395278	169-187	32955
D5S678	1 418810	1 418928	123	64831
D5S1.92	1 925437	1 925876	105-121	Novel marker
D5S1970	2 497996	2 498117	112-128	39892
D5S417	3 174219	3 174442	214	78601
D7S817	32 102921	32 403079	155-177	80302
D7S2211	33 602237	33 602 615	383-384	45359
D7S2758	33 611477	33 611617	138-141	12956
D7S678	43 247692	43 247865	166-180	71858
D7S2436	44 686503	44 686764	222-270	73367
D7S519	46 082558	46 082813	255-268	7883
D7S2561	47 359975	47 360192	212-228	48440
D9S1817	33 849625	33 849887	209-237	14086
D9S1791	36 383383	36 383557	168-190	56137
D9S1874	37 212295	37 212493	167-203	56570
D9S2148	38 285718	38 285887	148-172	64272
D9S273	71 729255	71 729401	199-217	14074
D9S301	72 992540	72 992774	209-237	17012
D14S1280	25 725631	25 725926	289-301	4601
D14S275	25 766620	25 766814	194-205	62366
D14S608	27 919195	27 919400	188-224	60255
D14S70	33 528945	33 529156	212	23745
D14S599	33 723548	33 723631	84-99	3467

#### 4.2.2.4 Multipoint linkage analysis

Multipoint linkage analysis was undertaken combining data from both families and LOD scores were calculated using the SUPERLINK website. To perform multipoint linkage analysis, a pedigree file was prepared containing the genotyping data from both pedigrees studied, for all markers studied (Appendix

1). All 4 markers within the common region of linkage were used for analysis, except the novel marker D5S1.92 for which there was no Marshfield genetic map position available for data analysis. Data sets for both families were created in one pedigree file and the two pedigrees were separated by the headings Pedigree: A (family A) and Pedigree: B (family B). The format for every horizontal line (where each line represents one individual) of the pedigree file consisted of 13 columns as follows:-

- (1) The individual's ID, where each individual is given a unique numerical ID
- (2) The individual's father's ID (0 if unknown)
- (3) The individual's mother's ID (0 if unknown)
- (4) Gender (1 for male, 2 for female)
- (5) Affection status (0 if affected status unknown, 1 for unaffected, 2 for affected)
- (6) – (13) 8 allele markers for the 4 microsatellite markers analysed. For each marker, each allele was labelled as an integer starting with 1 (for the lowest numerical allele call) upwards

Using the SUPERLINK program, analysis was undertaken as follows:-

- The option 'Simplified input format' was chosen
- The number of markers in the simplified input file was inserted (4)
- The disease mutant gene frequency was inserted (0.001)
- The mode of inheritance was chosen (Autosomal recessive)
- The disease penetrance was added (0.99)

Using UNISTS, the Marshfield genetic map position (in cM) for each microsatellite marker was established as below

D5S2488 0.00cM

D5S1981 1.72cM

D5S2005 1.72cM

D5S678 1.72cM

The distances (cM) between the 4 markers were inputted: 1.72, 0.0, 0.0

- A list of sequential marker names was given (D5S2488, D5S1981, D5S2005, D5S678)
- The allele frequencies were assumed to be distributed in a uniform fashion
- The data was then submitted for analysis

#### **4.2.2.5 Gene Sequencing**

Following linkage analysis, mutation analysis of the candidate gene *SLC6A3* was undertaken as described in Chapter 2.3.4 Primer pairs for exon-specific PCR amplification of the 14 translated exons of the *SLC6A3* (ENST00000270349) gene were designed (Table 4-4).



**Table 4-4****Primers used for sequencing of coding regions of *SLC6A3* gene**

Exon	Primer Pairs (5' – 3')	PCR Product Size (bp)	Annealing Temperature (°C)
2	TGGCTGAAGACCAAGAGGG	427	58
	CTCGTTTCCGTACGTGCC		
3	CTCCACGAGGAGAGATGG	263	58
	TTGAAAGCTCCAGCGTCAC		
4	GTTGCTGATGGTGGCTCTG	374	58
	GTGTCCAACCAAGGGGCTAC		
5	CAGTTCCAGGTGGGTTGAC	279	58
	GTGCACCTCCTGTCCAGC		
6	CAGTGTCTGCTCCACCAAG	266	58
	AATGCATATGGAAACCTGGG		
7	AGGGTGCTCAGGTCCTTTG	243	58
	TTCTGGAAGTCAGCGACC		
8	CCCCTTCCCCAGACACAG	315	58
	TCTCCTTCCTCTTTCACAAGG		
9	CAGGATGGGCGGGAGAG	227	62
	GGGTGGAAGGAACCCAAC		
10	TGACAAGTAGGTCTTGGCCC	264	62
	CGTGCCACGTGCTAAGG		
11	GTGTGCACAGTGAATCCC	272	58
	GAAAGGTGTTTCCTCACGG		
12	GAGTCAGCGAGGACCCC	284	62
	CACAGTGACAACCCACATGC		
13	CCTGCTTTGTCCTGGCAC	289	58
	CACGGAGCCTTTCTGGTG		
14	GCAGTGTGAGTCAGTGGTGG	181	58
	CTGAGCTTGGGATCATTCTG		
15	TCAGCTGCTCTTAAATGGGG	146	58
	GGTTTGTTTCGTGTCTCTCCC		

### **4.2.3 Functional analysis of mutant DAT proteins**

All functional investigations were kindly undertaken by collaborators in Professor Reith's group, Department of Psychiatry and Pharmacology, Millhauser Laboratories, New York University School of Medicine, New York, USA. Methodology is described in Appendix 2.

## **4.3 Results**

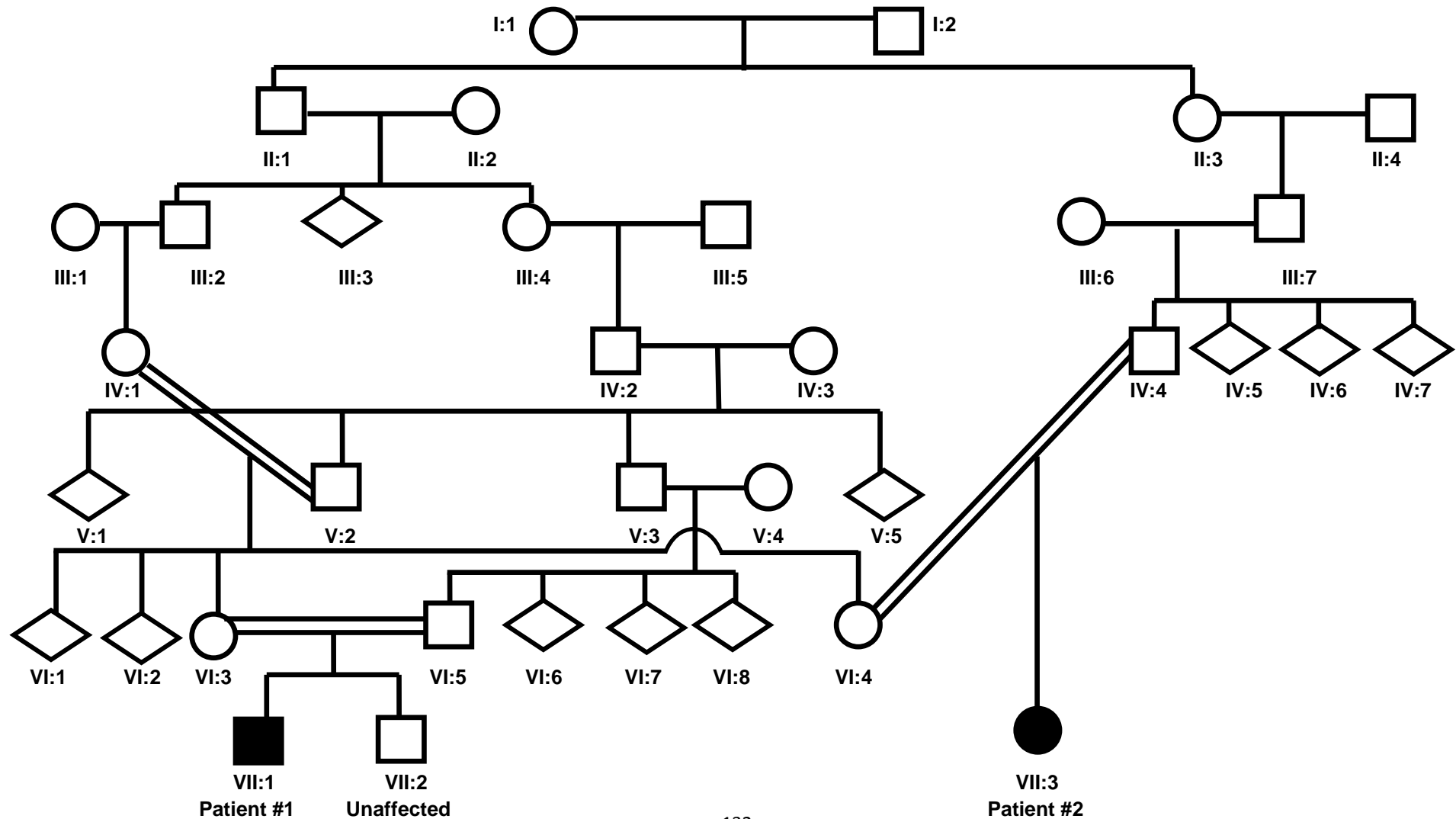
### **4.3.1 Clinical assessment**

Family A, an extended consanguineous kindred of Pakistani origin (Figure 4-2A) had 2 affected children with IPD (Patient #1 and #2) who were first cousins. Family 2 (Figure 4-2B) was of mixed European descent with one affected child (Patient #3). The diagnosis of IPD was based on characteristic clinical features and CSF neurotransmitter studies (Table 4-5). In brief, following a normal pregnancy and birth, all children had neonatal irritability and feeding difficulties. Parkinsonian symptoms heralded disease onset in early infancy and were rapidly followed by the development of pyramidal tract features and dystonia. All patients were initially misdiagnosed with cerebral palsy. On examination at ages 6-12 months, all patients had features of parkinsonism, dystonia and pyramidal tract signs with evidence of global developmental delay. CSF biogenic amine metabolite studies in affected patients revealed markedly elevated concentrations of HVA (with normal 5-HIAA levels). MRI brain did not reveal structural abnormalities in any of the patients. In light of their severe motor disability, neuropsychiatric assessment to determine whether the children had

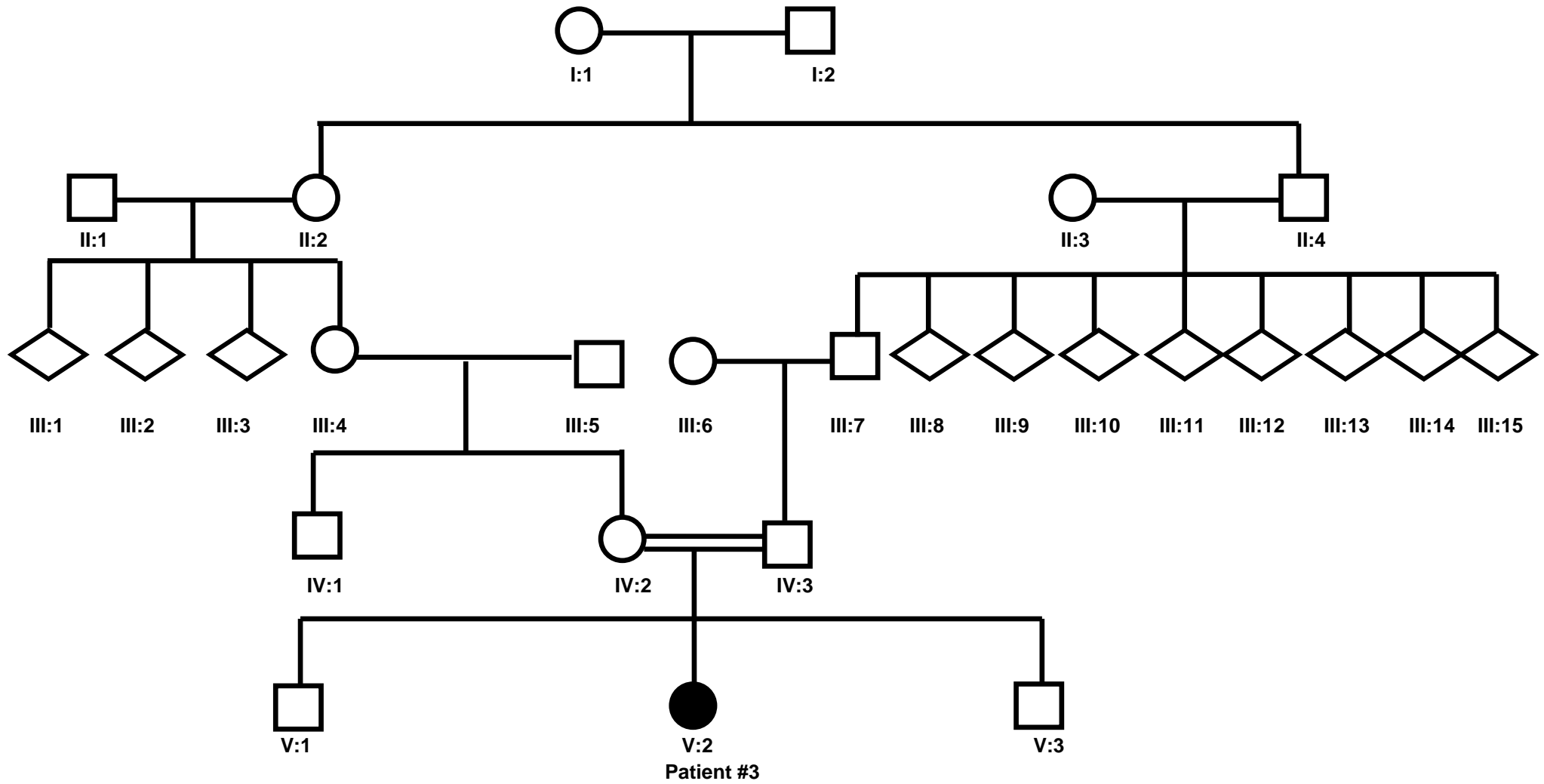
any evidence of cognitive impairment could not be undertaken. All patients showed a poor clinical response to multiple therapeutic agents. CSF HVA levels did not normalise after L-dopa or tetraabenazine therapy. Insertion of a deep brain stimulator device in Patient #3 resulted in some transient improvement of dystonia and rigidity. All children showed a progressive disease course with worsening symptoms of parkinsonism, dystonia and hypertonicity. None of the affected children had evidence of psychiatric or behavioural/conduct disorders. Detailed neurological examination of all the children's parents (aged 21 to 37 years) and siblings (age 1 to 9 years) revealed no neurological abnormalities. Additionally, none of the unaffected family members (including siblings, obligate carrier parents, parental siblings and grandparents) were known to have a neurological, neuropsychiatric or age-related movement disorder.

**Figure 4-2** Family trees of consanguineous kindreds. Children affected with IPD are indicated by black shading. Circles indicate females; squares indicate males; diamonds indicate undisclosed gender

**Figure 4-2A** Family A kinship



**Figure 4-2B**  
*Family B kinship*



**Table 4-5**  
**Phenotypic data for children with IPD**

	Patient #1 Family A	Patient #2 Family A	Patient #3 Family B
<b>Age of child (years) at assessment</b>	3.9	2.5	10.7
<b>Ethnic Origin</b>	Pakistani	Pakistani	Caucasian European
<b>Parental consanguinity</b>	Parents - 1 <sup>st</sup> cousins	Father and maternal grandmother - 1 <sup>st</sup> cousins	Parents 2 <sup>nd</sup> cousins
<b>Family History</b>	Nil	Nil	Nil
<b>Pregnancy and Birth</b>	Normal	Normal	Well controlled gestational diabetes
<b>Early course in infancy</b>	Irritable Feeding Difficulties	Irritable Feeding Difficulties	Irritable Feeding Difficulties
<b>Onset of Symptoms (months)</b>			
Parkinsonism	4	4	5
Dystonia	4	6	5
Pyramidal tract signs	4	6	5
Eye movement disorder	-	-	48
<b>Features on clinical examination</b>			
Generalised bradykinesia	++	++	++
Reduced facial expression	++	++	+
Rigidity	++	++	++
Dystonia	++	++	++
Pyramidal tract signs in limbs	++	++	+
Axial hypotonia/head lag	+	+	++
Global developmental delay	++	++	++
<b>Eye examination</b>			
Saccade initiation failure	-	-	+
Ocular flutter	-	-	++
<b>Investigations</b>			
<b>CSF</b>			
HVA concentration <sup>A</sup>	1873	1704	1135
5-HIAA concentration <sup>B</sup>	141	250	91
HVA:5-HIAA ratio <sup>C</sup>	13.2	6.8	12.5
<b>Urine (Reference Range)</b>			
HVA:Creatine ratio <sup>D</sup>	22	27	ND
<b>Serum</b>			
Prolactin <sup>E</sup>	150	915	688
<b>Clinical Course</b>			
Response to medication*	Nil	Nil	Nil
Response to deep brain stimulator	NA	NA	Some improvement
Progression of symptoms	+	+	+

- Absent

+ Present

++ Present and severe

NA Not applicable

ND Not determined

A Reference range 154 – 867 nmol/L

B Reference range 89 – 367 nmol/L

C Reference range 1.0 – 3.7

D Reference range 2-15µmol/mmol creatinine

E Reference range 93 – 630 mIU/L

\*Therapeutic agents including levodopa, carbidopa, tetraabenazine, diazepam, carbamazepine, baclofen, 5-hydroxytryptophan and trihexyphenidyl

## 4.3.2 Results of molecular genetic investigation

### 4.3.2.1 Genome wide scan

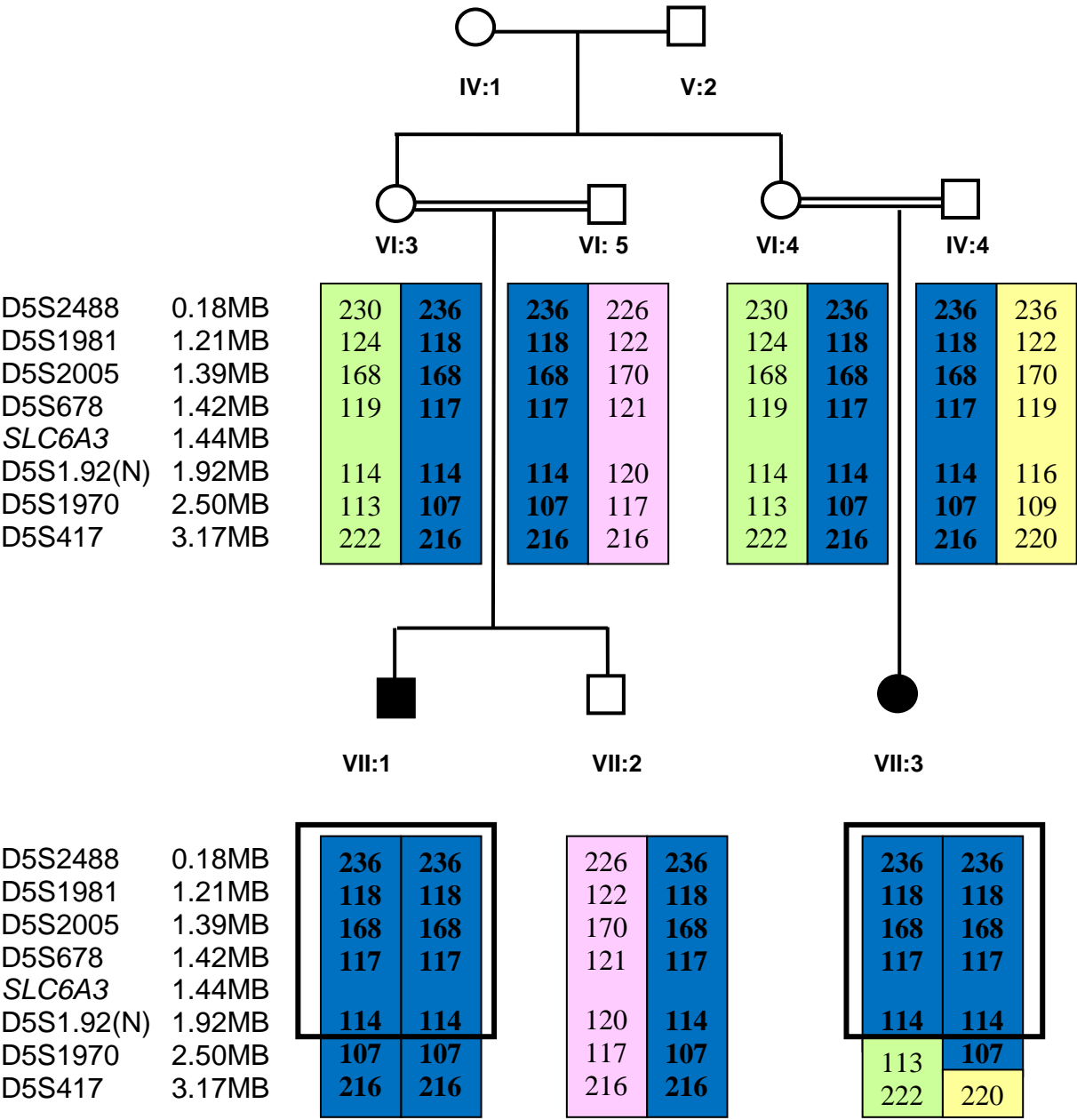
Genome-wide SNP genotyping (with the Affymetrix 250K SNP microarray) was performed in individuals VII:1 (Patient #1), VII:2 (unaffected sibling of Patient #1) and VII:3 (Patient #2) from Family A. In the 2 affected cousins, five possible regions of extended homozygosity (>2Mb) were detected on chromosomes 5 (2.3Mb), 7 (one region of 2Mb and one of 6Mb), 9 (41Mb) and 14 (9Mb).

### 4.3.2.2 Microsatellite marker analysis

These four regions were then further analysed using polymorphic microsatellite markers mapping to these regions of interest (Table 4-3). Linkage to the candidate regions on chromosome 7, 9 and 14 was excluded by segregation of the microsatellite marker alleles (Appendix 3). Genotyping of the family with microsatellite markers within the interval on chromosome 5 revealed an identical homozygous haplotype in the 2 affected children (which was different to that of the unaffected sibling and parents), consistent with possible linkage to this region (Figure 4-3). Subsequent microsatellite marker analysis of family 2 was also consistent with linkage to this region (Figure 4-4). The SNP data for chromosome 5 was further analysed, and showed that Patient #1 and #2 shared a common homozygous haplotype of 201 SNPs from 1 to 2,373,003bp (thereby defining the margins of the homozygous region) whilst the unaffected sibling of patient #1 demonstrated SNP heterozygosity in this region (Figure 4-5).

**Figure 4-3**  
Microsatellite marker linkage analysis on chromosome 5 in Family A

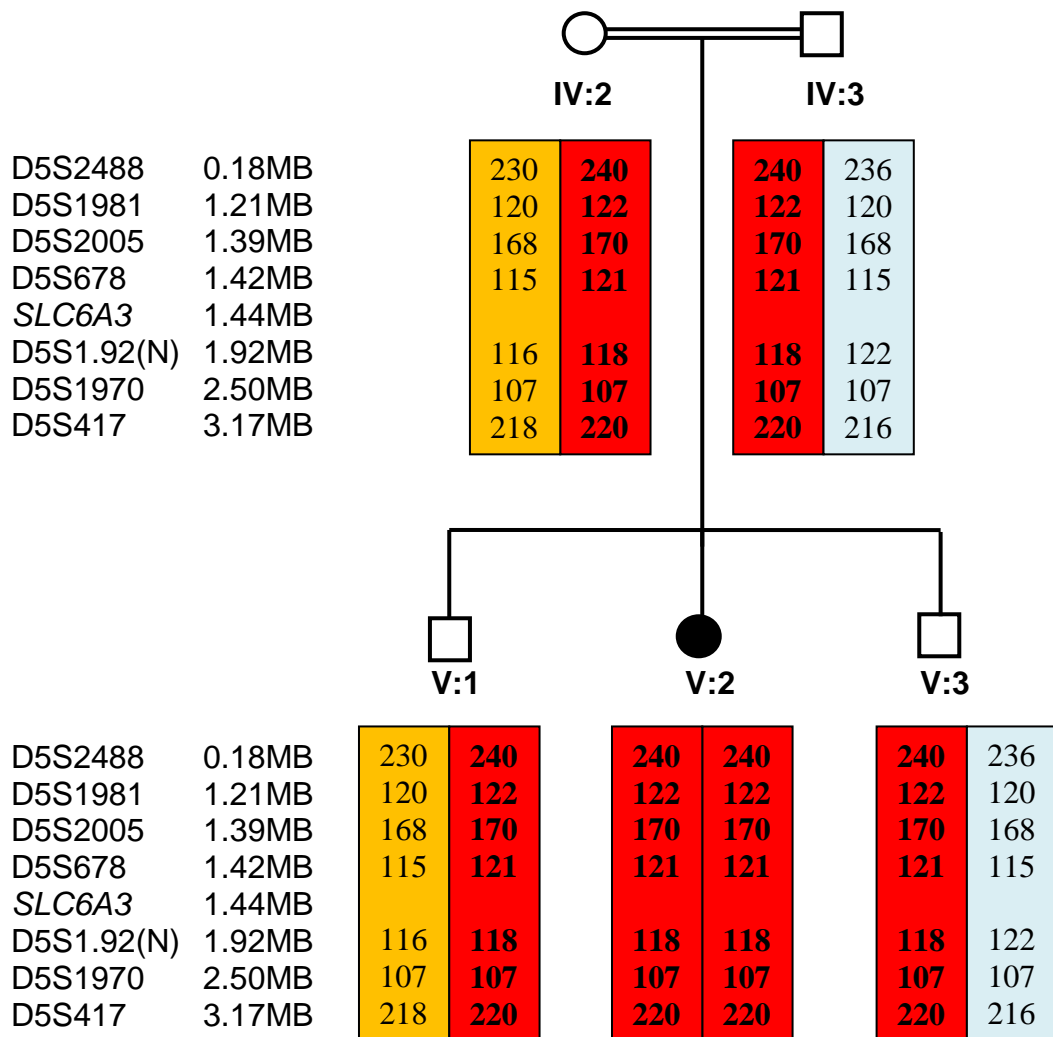
Affected individuals are shaded in black. SLC6A3 gene is located at 5p15.3. Microsatellite markers are positioned according to physical distance (MB). Haplotypes for these markers are shown and the disease associated haplotypes are boxed in blue. The two affected children share a common homozygous haplotype in this region (N) –Novel microsatellite marker





**Figure 4-4****Microsatellite Marker Analysis on chromosome 5 in family B**

The affected child is shaded in black. Microsatellite markers are positioned according to physical distance (MB). Haplotypes for these markers are shown and the disease associated haplotypes are boxed in red. Microsatellite markers show evidence of segregation with disease status in this family.  
(N) – Novel microsatellite marker



**Figure 4-5**

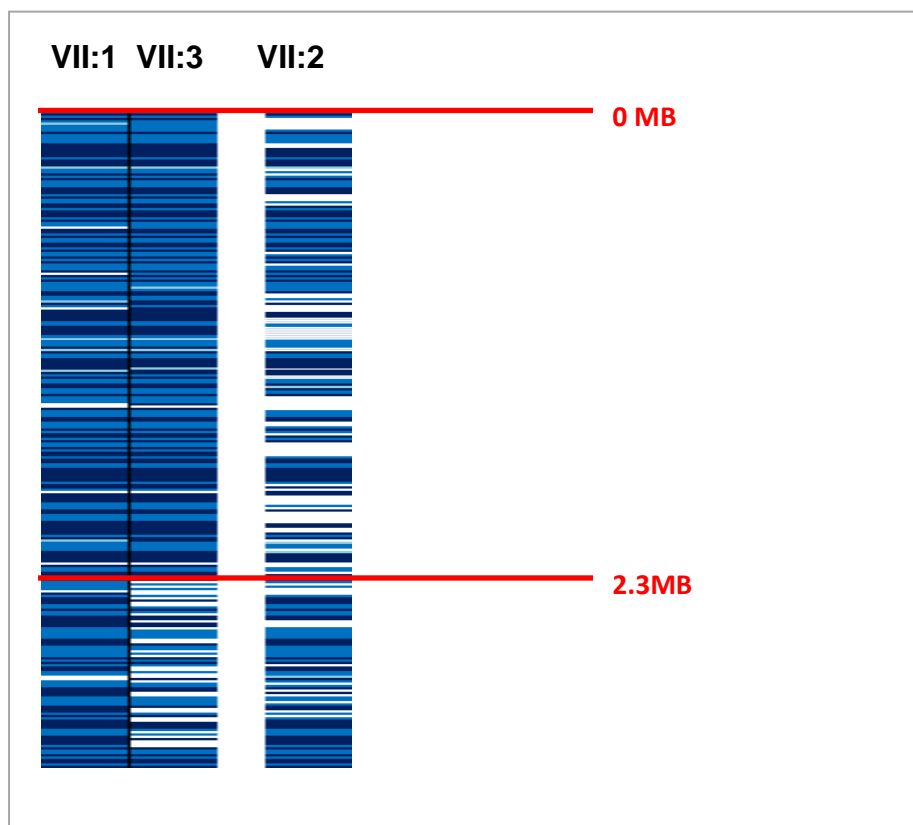
*Localisation of the disease locus on chromosome 5 on 250K SNP array*

*SNP array data is illustrated on family A: Patient #1 (VII:1), Patient #2 (VII:3) and the unaffected sibling of Patient #1 (VII:2)*

- Dark blue: AA homozygous SNP call*
- Mid blue: BB homozygous SNP call*
- Light blue: No call*
- White: AB Heterozygous call*

*Patient #1 and #2 display a region of SNP homozygosity from 0–2.3MB*

*The unaffected sibling (VII:2) does not display this common SNP homozygosity and has a heterozygous SNP haplotype in this region*



#### 4.3.2.3 Multipoint linkage analysis

Results from the multipoint linkage analysis were obtained from the SUPERLINK website (Appendix 1, Table 4-6). A maximum combined LOD-score of 5.28 was obtained.

**Table 4-6**  
**Multipoint linkage analysis for Family A and Family B**

Marker position from marker D5S2488 (cM)	0.0	1.72
<b>Pedigree A (Family A)</b>		
Ln (Likelihood)	-36.4603	3.4589
LOD-Score	-36.4041	3.4833
<b>Pedigree B (Family B)</b>		
Ln (Likelihood)	-27.7487	1.7902
LOD-Score	-27.7270	1.7996
<b>Both pedigrees A and B combined</b>		
Ln (Likelihood)	-64.2090	5.2491
LOD-Score	-64.1311	5.2829

#### 4.3.2.4 Candidate gene selection and mutational analysis

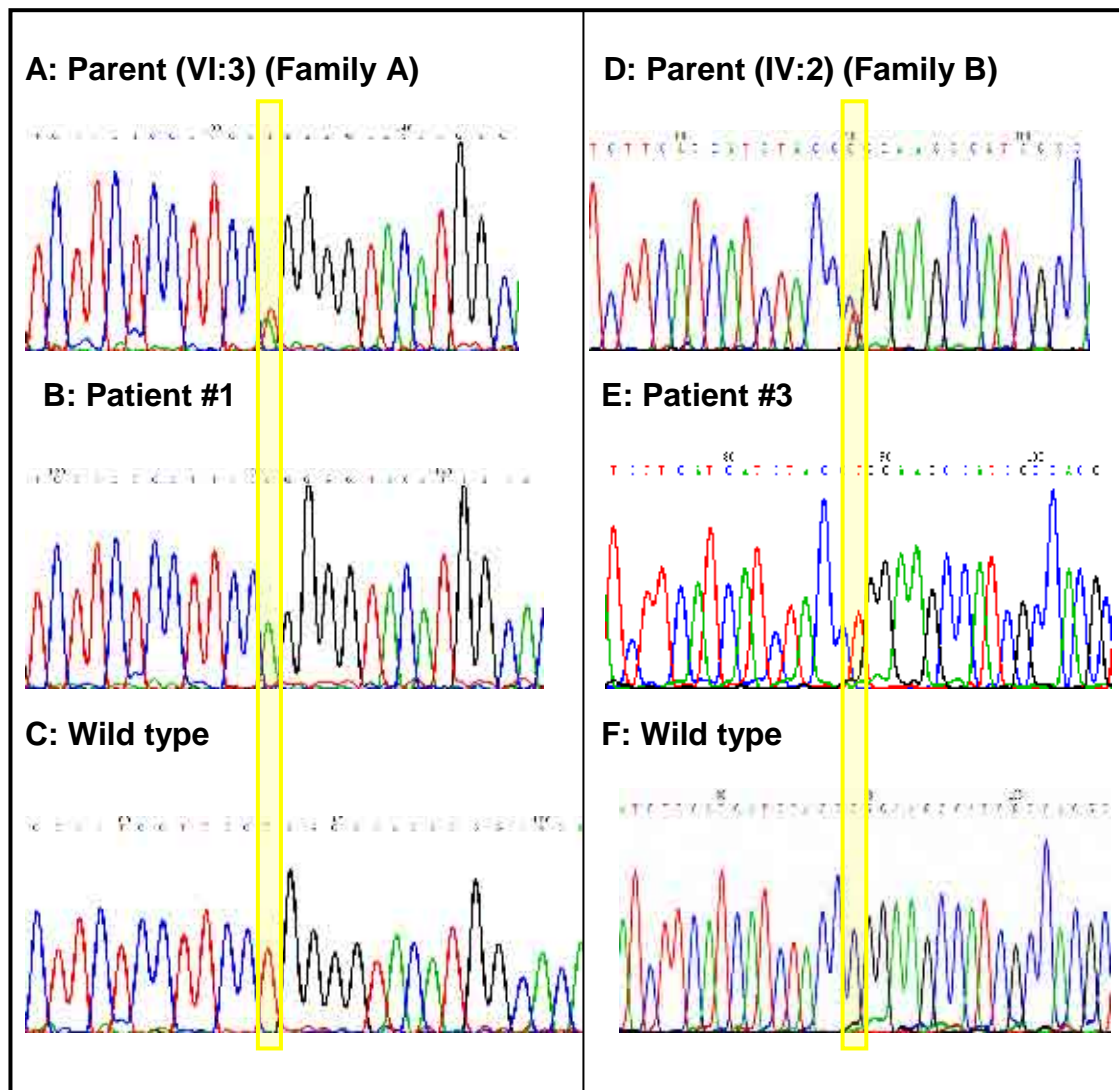
Having established the region on chromosome 5 as the likely IPD locus, the 39 genes within the region were examined for a candidate IPD gene. *SLC6A3* (located at chromosome 5, 1,445,909–1,498,538bp) encoding a dopamine transporter (*DAT1*) was selected as a potential candidate and subsequent mutation analysis of *SLC6A3* was initiated. A homozygous putative missense mutation c.1103T>A, p.Leu368Gln (Figure 4-6) was detected in exon 8 in Patients #1 and #2. *SLC6A3* mutation testing subsequently performed in Family B and a homozygous variant in exon 9, c.1184C>T (p.Pro395Leu), was detected in Patient #3 (Figure 4-6). Both mutations segregated with IPD disease status in the families and neither mutation was detected in an extensive analysis of ethnically-matched control chromosomes (544 Asian and 438

Caucasian control alleles respectively). Sequence alignment showed Leu368 and Pro395 to be highly conserved throughout species (Figure 4-7).

**Figure 4-6**

*SLC6A3 mutations in Family A and Family B*

The alignments of *SLC6A3* nucleotides c.1091-c.1116 (Panel A, B and C) and c.1168 -c.1197 (Panel D, E and F) are shown. Panel B illustrates c.1103T>A in Family A. Panel E illustrates c.1184C>T in family B



**Figure 4-7**

*Conservation of the mutated DAT1 residues Leu368 and Pro395*

*Five representative vertebrate sequences are aligned. Leucine 368 (Leu368) and Proline (Pro395) are coloured in red. Residues matching the consensus sequence are in grey.*

		Leu368		Pro395		
		↓		↓		
Human	DAIV	TTSINSLTSFSSGFVVFSFL	GYMAQKHSVPIGDVAKDGPGLIFIIY	PEAIATLPLS	404	
Dog	DAVI	TTSVNSLTSFSSGFVVFSFL	GYMAQKHSVPIGDVAKDGPGLIFIIY	PEALATLPLS	401	
Mouse	DAII	TTSINSLTSFSSGFVVFSFL	GYMAQKHNVPIRDVAT	DGPGLIFIIY	PEAIATLPLS 403	
Rat	DAII	TTSINSLTSFSSGFVVFSFL	GYMAQKHNVPIRDVAT	DGPGLIFIIY	PEAIATLPLS 403	
Zebrafish	DAII	TSSINSLTSFFS	GFVIFSFL	GYMSQKHNV	ALDKVATDGPGLVFIIY	PEAIATLPGS 413

## 4.4 Discussion

As discussed in the introduction of this chapter, inherited neurotransmitter disorders of infantile onset are usually associated with reduced CSF dopamine metabolites due to enzyme defects of the biogenic amine synthetic pathway (Table 4-2). Unlike these neurotransmitter disorders, IPD is characterised by paradoxically *raised* dopamine metabolites in CSF, and is thus a distinct neurotransmitter disorder associated with unique clinical, biochemical and genetic features.

In this chapter, I have described the clinical phenotype of three patients with IPD, delineated the IPD disease locus and identified loss-of-function mutations of *SLC6A3* in all three patients.

### 4.4.1 The dopamine transporter (DAT)

*SLC6A3* (MIM \*126455) encodes the dopamine transporter and is exclusively expressed in dopaminergic neurons with significantly higher levels of DAT expression in cells of the substantia nigra pars compacta, pars lateralis and ventral tegmental area (Storch *et al.*, 2004). DAT mediates the active reuptake of extraneuronal dopamine and is a principal regulator of the amplitude and duration of dopaminergic action. Dopamine is transported inwardly against its concentration gradient using the driving force of the sodium gradient across the plasma membrane. The transport process of dopamine uptake involves translocation of dopamine, as well as two sodium and one chloride ion across the cell membrane (McElvain *et al.*, 1992). The Na<sup>+</sup>/K<sup>+</sup> pump thus has a crucial

role in generating the electrochemical gradient across the cell membrane. The role of dopamine and its transporter is discussed in more detail in Chapter 5.

#### 4.4.2 Functional investigation of mutant hDAT proteins

All functional investigations were undertaken and analysed by collaborators from Professor Reith's group, Department of Psychiatry and Pharmacology, Millhauser Laboratories, New York University School of Medicine, New York, USA. To determine the effects of the p.Leu368Gln and p.Pro395Leu mutations, mutant hDAT proteins were transiently expressed in HEK-293 cells and their transport activity was compared with that of wild-type hDAT (Table 4-7) (Chen *et al.*, 2004a; Chen and Reith, 2007; Zhou *et al.*, 2007). In experiments carried out in parallel, wild type showed normal transport activity, whereas Leu368Gln and Pro395Leu were devoid of uptake activity. The binding affinity of the cocaine analogue [<sup>3</sup>H]CFT was near-normal in the mutants (30–36nM compared with 16nM in wild type, Table 4-7). In contrast, the potency of dopamine in inhibiting cocaine analogue binding was greatly reduced in Leu368Gln ( $K_i$  increased by an order of magnitude), whereas the potency of dopamine in Pro395Leu was close to that of wild type (Zhou *et al.*, 2007). Thus, both mutations are loss-of-function mutations with respect to the capability of DAT to translocate dopamine, in conjunction with a loss of apparent binding affinity of dopamine in the case of one of the mutations. Maximal binding of [<sup>3</sup>H]CFT to cells, primarily representing surface binding (Chen *et al.*, 2004a), indicated appreciable expression of DAT in both mutants, although Leu368Gln showed a reduction that was statistically significant (Table 4-7).

**Table 4-7**  
**Dopamine transport and cocaine analogue binding by Wild-type, Leu368Gln and Pro395Leu hDAT**

	Wild type	Leu368Gln	Pro395Leu
<b>[<sup>3</sup>H]Dopamine uptake</b> K <sub>m</sub> (μM) V <sub>max</sub> (pmol/min/mg prot.)	0.249 ± 0.029 1.19 ± 0.20	N/A <sup>A</sup> 0 <sup>A</sup>	N/A <sup>A</sup> 0 <sup>A</sup>
<b>[<sup>3</sup>H]CFT binding</b> K <sub>d</sub> (nM) B <sub>max</sub> (pmol/mg prot.)	15.9 ± 1.9 2.14 ± 0.65	35.6 ± 8.2 0.384 ± 0.110 <sup>B</sup>	30.2 ± 6.5 0.962 ± 0.144
<b>Inhibition of [<sup>3</sup>H]CFT binding by dopamine K<sub>i</sub> (μM)</b>	6.58 ± 0.53	52.9 ± 1.7 <sup>B</sup>	3.35 ± 0.65

A No transport activity detectable above non-specific uptake

B *P* < 0.05 (compared with wild type, one-way ANOVA followed by Dunnett multiple comparisons)

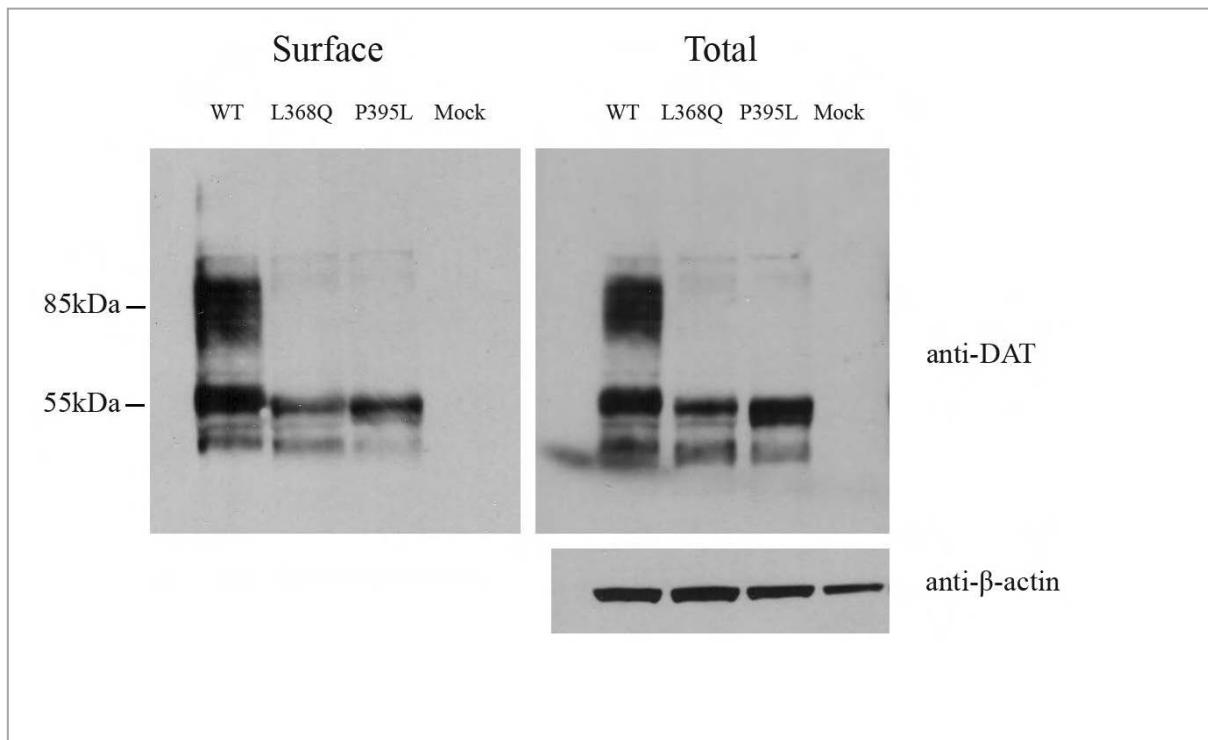
To investigate whether the observed reductions in dopamine transport were related to disordered production, localisation or function of the mutant proteins, immunoblotting was performed. Analysis of whole cell lysates demonstrated equivalent levels of immature (55 kDa) DAT for wild-type and Pro395Leu but there was some reduction for Leu368Gln (total protein loading - as judged by β-actin - was equivalent for wild-type, Leu368Gln and Pro395Leu hDAT). However both mutant proteins demonstrated a profound reduction in mature (85 kDa) DAT compared to wild type DAT. Analysis of surface (biotinylated DAT) showed a similar pattern (Figure 4-8).



**Figure 4-8**

*Expression of the Leu368Gln hDAT and Pro395Leu hDAT in transiently transfected HEK293 cells via immunoblotting analysis*

Cells were transiently transfected with WT hDAT, Leu368Gln hDAT, Pro395Leu hDAT, and reagent only. In each respective panel, the same amount of protein was loaded in all lanes. Biotinylated (surface) protein (left panel) and total lysate (right panel) were probed with anti-DAT antibody for detection of the relative expression level of WT and mutant DAT protein. Anti- $\beta$ -actin antibody showed the relative equivalent loading of total protein. There was no  $\beta$ -actin in the surface preparation



Based on the crystal structure of the bacterial transporter analogue LeuT (Yamashite *et al.*, 2005) the primary substrate site and the sodium binding sites in DAT can be modelled deep in the protein interior where unwinding of the transmembrane helices 1 and 6 allows extensive interactions between protein residues in transmembrane domains 1, 3, 6, 7, and 8 and substrate or sodium (Beuming *et al.*, 2006). A secondary substrate site has been proposed to be located towards the outside of the transporter (Shi *et al.*, 2008) in an

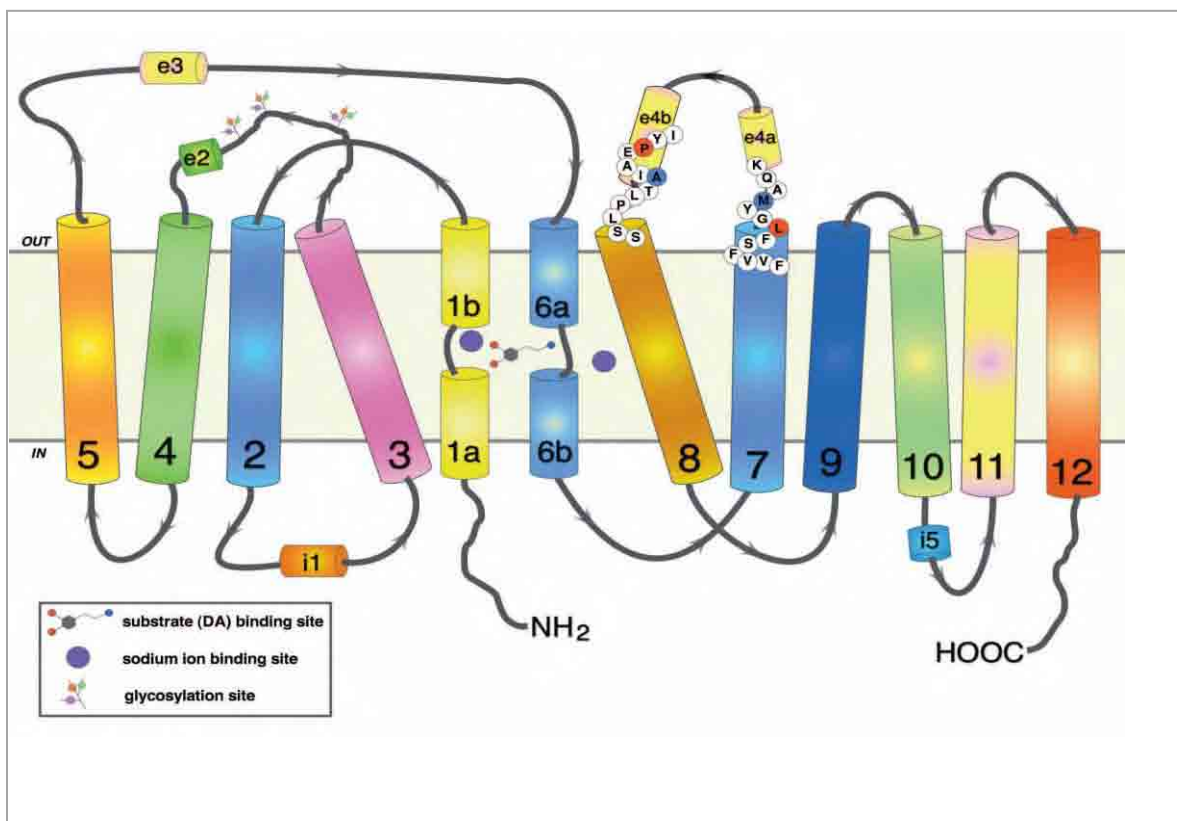
extracellular vestibule where tricyclic antidepressants also bind in LeuT (Zhou *et al.*, 2007; Singh *et al.*, 2007) above the extracellular gate, which, in turn, lies between the two substrate sites.

Among the positions of these two IPD-associated missense mutations reported, Leu368 in hDAT is in transmembrane domain 7 towards the exterior, many helix turns above the residue (Asn353) that presumably interacts with sodium (Figure 4-9). Leu368 is one helix turn under Met371, and is conformationally sensitive to dopamine transport (Norregaard *et al.*, 2003). The position of the second missense mutation, Pro395, is in one of the two helical portions of extracellular loop 4, EL4b, the one closer to transmembrane 8. Pro395 lies just one helix turn above Ala399, a residue that, like Met371, points outward the entire transporter structure and thus is easily accessible to solvent bathing the outside of the protein (Norregaard *et al.*, 2003). Interaction between a sulfhydryl reagent in such solvent and the 399 position is not blocked in the presence of dopamine, whereas that at 371 is highly sensitive to dopamine, i.e., by dopamine causing conformational changes burying the residue away from solvent exposure. In consonance, the missense mutation of Pro395 (above 399) has no impact on dopamine binding affinity, whereas the missense mutation of Leu368 (under 371) appears to interfere with conformational changes occurring with dopamine binding such that dopamine's apparent affinity is strongly reduced. Hence, despite the different impact of the two missense mutations on dopamine binding affinity, the location of the mutations and the mutations and their effect to completely impair transport of dopamine suggested that both mutations might interfere with conformational changes required during transport.

**Figure 4-9**

*Two-dimensional representation of dopamine transporter topology based on LeuT structure*

Twelve transmembrane domains are shown with helically unwound regions in first and sixth domain; extracellular and intracellular loops include helical portions (e2, e3, e4a, e4b, and i1, i5, respectively). Leu368, subject to missense mutation, is shown in red at the top of transmembrane domain 7, one helix turn under Met371 in blue. Pro395, also subject to missense mutation, is shown in red in the e4b portion of extracellular loop 4, one helix turn above Ala399 in blue. In the three-dimensional structure, sodium ions interact with residues of transmembrane domains 1, 6, and 8, and also 7



In this chapter it has also been shown that the marked reduction in mature (glycosylated) 85 kDa DAT expression appears to be a major contributor to reduced dopamine transport. It has previously been demonstrated that immature non-glycosylated (55 kDa) DAT does not transport dopamine as

efficiently as mature 85 kDa DAT (Li *et al.*, 2004). Hence the reduction in mature DAT will undoubtedly impair dopamine transport.

## **4.5 Conclusion**

In this chapter, I have delineated the clinical features of a distinct neurotransmitter disorder and in all 3 patients, identified homozygous loss-of-function mutations in the dopamine transporter gene, *SLC6A3*. Molecular characterisation has provided novel insights into this complex movement disorder. Although the condition appears to be rare, the children described in this chapter were initially diagnosed with cerebral palsy. Following gene identification, I instigated an extensive international search for further similar cases, in order to establish the frequency of *SLC6A3* mutations. A cohort of children with biochemical markers suggestive of this novel syndrome was thus acquired and investigated, in order to further characterise the clinical, biochemical and genetic features of this disorder (see Chapter 5).

Elucidation of the genetic basis of this disorder is of clinical benefit to patients and families. Identification of pathogenic mutations can confirm the clinical and biochemical diagnosis and can also contribute to accurate genetic counselling and prenatal diagnosis. Molecular characterisation of this syndrome may also provide a basis for the future development of effective therapeutic strategies. In these three patients, therapeutic approaches have not biochemically normalised HVA levels or clinically improved patient symptomatology. None of these patients demonstrated a clinical response to L-dopa. L-dopa therapy may be beneficial in some infantile neurotransmitter syndromes (see Chapter 4.1.4),

where exogenous administration can compensate for the reduction in endogenous dopamine production. The lack of clinical response to L-dopa in these three patients is not wholly surprising given that their mutations are predicted to result in complete absence of dopamine transporter activity. Complete loss of transporter function is likely to disrupt the fundamental role of DAT in controlling the amplitude and duration of dopaminergic transmission and it may be that L-dopa supplementation cannot compensate for complete loss of this physiological process. The moderate therapeutic success of deep brain stimulation (DBS) in Patient #3 may be attributable to the hypothesised role of such targeted neuronal high frequency stimulation in the modulation of dopamine, glutamate and GABA neurotransmitter systems within the basal ganglia (McIntyre *et al.*, 2004). It is possible that such selective neuronal activation and suppression as well as changes in network synchrony could potentially alleviate parkinsonian/dystonic symptoms in DAT-associated movement disorders. Elucidation of the molecular basis of this disorder has facilitated a trial of novel therapeutic strategies in some of the affected children. This is discussed in more detail in Chapter 5.

## **Chapter 5**

# **Dopamine Transporter Deficiency Syndrome**

## 5.1 Introduction

Accurate recognition of inherited disorders is important in preventing morbidity from misdiagnosis/diagnostic delay and in facilitating 'personalised medicine'. Advances in molecular diagnosis can lead to the recognition of novel genetic phenotypes that can provide critical insights into pathophysiological disease mechanisms.

In Chapter 4, I described the identification of pathogenic mutations of *SLC6A3* in three patients with IPD (Kurian *et al.*, 2009). Following gene identification, I acquired a cohort of children with a biochemical profile compatible with this novel syndrome. In Chapter 5, I will describe the phenotypic features of these patients, results of *SLC6A3* sequencing and data from functional analysis of mutant human DAT. The physiological role of dopamine and its transporter (DAT) and postulated disease mechanisms in this disorder will also be discussed (Kurian *et al.*, 2010b).

As it is often common practice to name inherited diseases after the underlying pathogenic defect, I have renamed this novel disorder as dopamine transporter deficiency syndrome (DTDS) to reflect the underlying disease mechanism and encompass the wide spectrum of clinical phenotypes seen in this disorder (which extends beyond the clinical features of infantile parkinsonism-dystonia).

DTDS is thus a newly recognised, autosomal recessive disorder related to impairment of dopamine transporter function. Delineation of the clinical, biochemical and genetic features will facilitate early diagnosis and trials of therapeutic agents based on an understanding of the pathophysiology. In

addition careful characterisation of such patients with DTDS should provide novel insights into the multiple and complex role of dopamine homeostasis in the human brain.

## **5.2 Methods**

### **5.2.1 Clinical assessment of DTDS patients**

#### **5.2.1.1 Acquisition of DTDS cases**

Eleven children with DTDS were identified. A brief overview of the clinical phenotype of Patients 1-3 was reported previously in Chapter 4 in association with the initial identification of *SLC6A3* mutations in 2009 (Kurian *et al.*, 2009) and the clinical and biochemical features of patients 4-6 have also been briefly reported in 2004 (Assmann *et al.*, 2004). The 11 subjects were ascertained from paediatric neurologists specialising in movement disorders and biochemical laboratories performing paediatric CSF neurotransmitter analysis (Institute of Child Health, London, UK; Medical Neurogenetics, Atlanta, USA; University Children's Hospital, Heidelberg, Germany).

#### **5.2.1.2 Clinical phenotyping**

All children were clinically assessed by a paediatric neurologist. I assessed all living UK cases (3 patients) and extensive video footage of all cases was examined independently by 3 paediatric neurologists (myself, Dr Birgit Assmann, Germany and Dr Terry Sanger, USA) to accurately categorise the observed movement disorder (with consensus agreement on disparities).



Medical case notes were reviewed to establish the clinical history, pattern of disease evolution, results of investigations and response to medication.

#### **5.2.1.3 Biochemical investigations**

An LP for CSF neurotransmitter analysis was performed in all patients as described in Chapter 4.1.3.1. HVA and 5-HIAA levels were measured. Other investigations included urine catecholamine metabolite analysis, serum prolactin and serum CK.

#### **5.2.1.4 Neuroradiology**

Neuroradiological studies, including magnetic resonance imaging (MRI), magnetic resonance spectroscopy (MRS) and nuclear brain imaging were also evaluated.

### **5.2.2 Molecular genetic investigation**

All annotations and physical positions are recorded as in NCBI Genome 36.3 build

#### **5.2.2.1 *SLC6A3* mutational analysis**

DNA extraction was performed as described in Chapter 2.3.1. *SLC6A3* mutation analysis was performed by direct sequencing as previously described (Chapter 2.3.4) using primer pairs for exon-specific PCR amplification of the 14 translated exons of the *SLC6A3* gene (Table 4-4).

#### **5.2.2.2 Long range PCR**

In patient 8, long range PCR techniques (Chapter 2.3.5) were utilised to characterize a putative deletion. Primers 11F and 14R (Table 4-4) were used to

produce the deletion-specific amplicon. Conditions consisted of an initial denaturation step at 93 °C for 5 min followed by 35 cycles of 45s denaturation at 93 °C, 45s annealing at 60°C and 8 min extension at 68°C with a final extension at 68 °C for 5 min. The PCR products were then checked, cleaned up and prepared for sequencing as described in Chapter 2.3.4.3-2.3.4.7. In order to determine the exact genomic deletion breakpoint DNA sequence, specific primers (Table 5-1) were utilized for cycle sequencing of the deletion-specific amplicon. These reverse primers were designed sequentially 300-400 bases apart from 14R.

**Table 5-1**

***Primers used for cycle sequencing of deletion-specific amplicon in order to determine the genomic breakpoint of the deletion***

Primer	Location (Bp)	Primer Sequence
DAT_13.1R	1,454,057 – 1,454,176	CCACCACTGACTCACACTGC
DAT_13.2R	1,454,401 – 1,454,419	CCTGGAGATGGCTCTTGAG
DAT_13.3R	1,454,710 – 1,454,728	CACTTGACCTGGCTCAGC
DAT_13.4R	1,454,940 – 1,454,961	CATCAGCTTTCCTGGGGCCATG
DAT_13.5R	1,455,276 – 1,455,295	GGAGTGTCTTGTCTCTTCC
DAT_13.6R	1,455,556 – 1,455,575	CAAACACTTGGACACGAATG
DAT_13.7R	1,455,790 – 1,455,808	CACACACACAGTGTTGTGG

### 5.2.3 Functional and molecular analysis of mutant DAT proteins

All functional investigations were kindly undertaken again by collaborators in Professor Reith's group, Department of Psychiatry and Pharmacology, Millhauser Laboratories, New York University School of Medicine, New York, USA. Methodology used in functional investigation is described in Appendix 2.

## **5.3 Results**

### **5.3.1 Clinical phenotyping of DTDS**

The detailed clinical phenotype and pattern of disease evolution in 11 children with DTDS (2 boys and 9 girls) from 10 distinct families is described. The salient clinical features of DTDS are summarised in Table 5-2. 7 children are alive (age range 1.9-11.4 years) and 4 children have died (age of death 9-16 years). Prior to neurological investigation and DAT mutational analysis, most children (7/11) in the cohort were initially misdiagnosed with cerebral palsy.

#### **5.3.1.1 Family history**

Patient 1 and 2 are 1st cousins from a consanguineous Pakistani kindred (family A in Chapter 4) and Patient 6 is of Turkish origin. The remaining eight children are of mixed European descent. Parental consanguinity was evident in 7 families. In 5 cases (patients 1, 3, 6, 10 and 11), parents were 1st or 2nd cousins and in 2 cases (patients 2 and 7), parents were more distally related. In all cases, there was no family history of Parkinson's disease, movement disorders or neuropsychiatric disease. The mother of patient 11 suffered from a severe migraine disorder associated with aura.

#### **5.3.1.2. Pregnancy and early neonatal course**

All children were born following a normal pregnancy, except patient 6, in whom a marked reduction in foetal movements was reported from 35 weeks gestation. All children were born following an uneventful delivery, except patient 8, who was delivered by emergency lower segment caesarean section after an abnormal cardiotocography (CTG) trace suggested foetal distress. At birth, she

initially had low APGAR scores (3-9-9 at 3-5-10 minutes) but responded to a period of bag and mask ventilation followed by nursing in an incubator with ambient oxygen for five days. Neonatal irritability and early feeding difficulties were evident in 6/11 children.

### **5.3.1.3 Onset of clinical symptoms in infancy**

All children presented with neurological symptoms in early infancy (median 2.5 months (range 0.5–7 months). The children were not dysmorphic and there was no evidence of congenital microcephaly (although patient 1 and 2 developed acquired microcephaly within the first year of life). Five children presented with a movement phenotype with prominent hyperkinesia. In another four children, the predominant presenting neurological features were hypokinetic and parkinsonian in nature. Patient 3 and 4 had features of both a hypokinetic and dystonic movement disorder on initial clinical presentation. Presenting parkinsonian features included bradykinesia (6/11), rigidity (4/11), and tremor (3/11). A wide spectrum of dyskinetic phenotypes were seen on presentation: Six children presented with generalised dystonia with frequent protracted exacerbations characterised by severe distress and continuous crying associated with opisthotonus (4/11), oculogyric crises (1/11) and a raised CK in some cases. High amplitude choreiform movements (2/11) and orolingual dyskinesia (5/11) were also observed. Axial hypotonia was evident in 7/11 children presentation. Concerns regarding early developmental progress were raised in 6/11 children.

#### **5.3.1.4 Clinical features of the DTDS movement disorder**

All children in the cohort developed a complex movement disorder characterised by a number of features:-

##### (a) Infantile hyperkinesia

An early hyperkinetic movement disorder (associated with restlessness and irritability) was seen in six patients (Table 5-2). Two patients presented with florid dyskinesia characterised by repetitive generalised involuntary choreiform movements of variable amplitude. A further four patients developed choreiform movements (predominantly repetitive involuntary cycling movements of the lower limbs) within a year of presentation (Table 5-2). In the older patients, the hyperkinetic phenotype diminished gradually during childhood.

##### (b) Orolingual dyskinesia

Orolingual dyskinesia (thrusting choreiform movements of tongue associated with repetitive involuntary opening and closing of the mouth) was evident in six children.

##### (c) Dystonia

Dystonia was a universal feature. In six children it was present at symptom onset and the five other children developed it within one year of clinical presentation (time range 1-10 months). Generalised action and postural dystonia, with no diurnal variation, was evident in all children. All children had oromandibular dystonia with jaw opening. Striatal toe (hyperextension of the great toe) was evident in eight children and five had prominent upper limb dystonia, characterised by dystonic posturing of the arms and hand fisting.

Seven children had recurrent episodic dystonic crises which were often misinterpreted as epileptic events. These episodes were a multiple daily (often nocturnal) occurrence in some children, but in others were infrequent, occurring only once every few months. In some cases, hospitalisation was required for the medical management of such episodes. They often occurred in association with oculogyric crises, irritability, hyperthermia and/or temperature instability and diaphoresis and some children were associated with a rise in CK. In patient 9, severe rhabdomyolysis and deranged liver function tests were also observed during such episodes.

(d) Parkinsonian features

Parkinsonian features eventually became evident in all children with DTDS. Generalised moderate to severe bradykinesia was a common early feature of DTDS (10/11 cases). Six children had slowing of voluntary movement from disease onset and a further four children developed this feature 1–30 months after initial presentation. Generalised rigidity was also seen in the majority (10/11) of children, as a presenting clinical feature in four children and developing in the remaining six cases within one year of symptom onset. Cogwheeling rigidity was also evident in some patients. Over time, all gradually developed hypomimia, 2–18 months after initial clinical presentation (mean age of onset, 7 months). A coarse predominantly distal tremor was present in eight children (three at disease onset and five developed tremor 2–36 months after presentation).

(e) Pyramidal tract features

Although the co-existence of dystonia and rigidity complicated the assessment of resting tone, none of the children had pyramidal tract features at presentation but eight subsequently developed pyramidal signs, including sustained ankle clonus, increased adductor tone and increased 4 limb tone when asleep (Table 5-2). To date 3 young children have no signs of pyramidal tract abnormality (patient 8, 10, and 11, all <5 years of age).

(f) Axial hypotonia

Axial hypotonia, characterised by head lag and truncal hypotonia, was present from the onset in seven cases and developed within one year of clinical presentation in the rest.

(g) Eye movement disorder

Eight children manifested a characteristic eye movement disorder (three at presentation and five, 4-44 months after initial presentation). All these children had ocular flutter (confirmed on electronystagmography in two patients), 7/8 had saccade initiation failure and slow saccadic eye movements. Eyelid myoclonus was described in two patients. Oculogyric crises commonly occurred in two children, and were particularly prevalent during a dystonic storm.

**5.3.1.5 Disease course**

(a) Motor development

All children had severe gross motor delay, failing to achieve motor milestones. Although most children had a limited degree of head control in infancy, none were ever able to voluntarily lift their head when prone, roll over or sit without

support. In early infancy, some children were able to grasp objects but grasping was often bradykinetic and superimposed by dystonia. This skill was lost over time, and eventually children were able to only hold objects placed in palm of hand for brief periods. All children displayed marked progression of motor symptoms and the movement disorder became markedly hypokinetic. Progressive dystonia resulted in severe fixed postural dystonia, particularly affecting the upper limbs. Parkinsonian symptoms also became progressively worse, resulting in akinesia, severe rigidity, marked facial hypomimia and prominent tremor.

*(b) Cognitive development*

No children with DTDS were able to speak, but despite the absence of expressive language (attributed mainly to their motor deficit), parents and clinicians reported that children had good receptive language and situational understanding. Children could often follow simple commands, follow conversations and smile responsively to interaction or humour. With the assistance of speech and language therapists, many children developed methods of non-verbal communication, for example, the use of head and eye pointing techniques. All children had urine and faecal incontinence and required extensive support for feeding and dressing. Despite the severe motor impairment, cognitive skills appeared to be affected to a lesser degree. Formal neuropsychology assessment was not possible in the majority of children due to the degree of physical disability. In patient 3, a formal neurocognitive assessment was undertaken at 11.3 years. On assessment she effectively used a communication book comprising four pictures for judgements via eye gaze.



She also demonstrated good working memory in response to verbal questions and prompted when given alternatives or choices. She was able to effectively mobilise via the use of head switches on her electric wheelchair. Following the introduction of ropinirole therapy, she showed improved motor function and facial expression, further enhancing her communication. She exhibited good social awareness and empathy as demonstrated by her enjoyment of watching the news or age-appropriate films and her ability to identify distressing situations when these are embedded within a complex narrative. She demonstrated accurate recognition of familiar information. She attended sessions in mainstream school and successfully used a Tobii device (a communication aid using eye gaze). Similar devices have also been used to aid learning in other DTDS children.

#### (c) Secondary medical complications and life expectancy

All children with DTDS developed gastro-oesophageal reflux and constipation. Orolingual dyskinesia and generalised bulbar dysfunction resulted in excessive drooling, choking and feeding difficulties and failure to thrive was observed in all patients. Sleeping difficulties, orthopaedic complications and frequent pneumonias were also prevalent in this cohort. Four children have died (median age of death 14.6 years, range 9-16 years) due to respiratory complications (aspiration pneumonia, chest infection) and secondary cardiac failure.

#### **5.3.1.6 Response to therapeutic strategies**

Multiple therapeutic strategies (dopamine agonists, dopamine antagonists, anticholinergics and GABAergic agents and surgical strategies) have been

attempted in the cohort but most were either ineffective or provided only a limited temporary clinical response.

Nine children had a trial of Sinemet (L-dopa with a peripheral dopa decarboxylase inhibitor). A definitive clinical response was observed in two patients. In Patient 9, treatment with L-dopa improved upper limb motor function, facial expression and abolished the episodic crises (of severe dystonia, rhabdomyolysis, excessive sweating and hyperthermia). Four weeks after commencing L-dopa therapy, Patient 11 was noted to be more cheerful, with improved fine motor skills and more voluntary purposeful movement than on previous assessment. A significant reduction in her spontaneous sweating episodes was also reported.

Following genetic diagnosis and proposition of a likely disease mechanism, direct dopamine agonists were tried with some success. Two children continue on ropinirole therapy. Since the instigation of ropinirole at age 10.5 years in patient 3, there has been a reduction in parkinsonian features with increased facial expression, an improved feeding pattern and a mild reduction in bradykinesia of her hands. In patient 9, the introduction of ropinirole (at age 5 years) has led to a sustained improvement in hand function, reduced tremor and reduction of the frequency and severity of dystonic crises.

**Table 5-2: Overview of clinical features in DTDS**

Patient	Current Age (Years)	Neonatal irritability/feeding difficulties	Age at clinical presentation (months)	Early motor features present at disease onset				Early motor features evolving before 3 years of age						Motor features > 3 years				Eye movement disorder	Bulbar dysfunction	Misdiagnosis with cerebral palsy
1	5.7	Y	0.75	P			A	P		DY	A	PT	MD	P	DY	PT	MD	N	Y	Y
2	4.2	Y	3	P			A	P		DY	A	PT	MD	P	DY	PT	MD	N	Y	Y
3	11.4	Y	5	P		DY	A	P	DK	DY	A	PT	MD	P	DY	PT	MD	Y	Y	Y
4	DIED	Y	4	P		DY	A	P	DK	DY	A	PT	MD	P	DY	PT	MD	Y	Y	N
5	DIED	N	4	P			A	P	DK	DY	A	PT	MD	P	DY	PT	MD	Y	Y	Y
6	DIED	N	2.5	P				P	DK	DY	A	PT	MD	P	DY	PT	MD	Y	Y	N
7	DIED	N	1.5		DK	DY		P	DK	DY	A		MD	P	DY	PT	MD	Y	Y	Y
8	2	Y	0.5			DY		P		DY	A		MD	-	-	-	MD	Y	Y	Y
9	6	N	3			DY	A	P		DY	A	PT	MD	P	DY	PT	MD	Y	Y	Y
10	1.9	N	7		DK		A	H	DK	DY	A		MD	-	-	-	MD	Y	Y	N
11	4.3	Y	0.5			DY		P		DY	A		MD	P	DY		MD	N	Y	N

P	Parkinsonian hypokinetic features (bradykinesia, rigidity, tremor, hypomimia)	-	Patient age <3 Years
H	Hypomimia only	Y	Yes
DK	Dyskinesia (chorea, restlessness)	N	No
DY	Dystonia		
MD	Motor developmental delay in gross motor skills		
A	Axial hypotonia		
PT	Pyramidal tract features		

### 5.3.2 CSF neurotransmitter analysis and other investigations

The results of CSF neurotransmitter analysis are given in Table 5-3. Biogenic amine metabolite analysis revealed the universal finding of increased levels of the dopamine metabolite HVA and a normal concentration of the serotonin metabolite 5-HIAA (using age related laboratory-specific reference ranges) (Hyland *et al.*, 1993; Bräutigam *et al.*, 1998). As a consequence, all children had a raised CSF HVA: 5-HIAA ratio (range in DTDS, 5.0-13.2, normal range approximately 1.3-4.0), thus reflecting an overflow of dopamine metabolites in the CSF in the presence of normal serotonin metabolites. Urine HVA excretion was moderately elevated in 6/7 children investigated (range in DTDS 22-47, normal range 2-15  $\mu\text{mol}$  HVA/mmol creatine). Pterin levels (neopterin, 7, 8-dihydrobiopterin, and tetrahydrobiopterin) were consistently normal in all children in the cohort, except in patient 8 who had a mild reduction in neopterin and tetrahydrobiopterin.

Serum prolactin was elevated in patient 2 and 3 but found to be consistently normal on repeated testing in other children (Patient 1, 4, 7, 8 and 9). Elevated serum CK activity was evident in 6/11 children (242–1773 IU/L, normal range 24-173 IU/L). Five of these children also had further elevation of CK during dystonic crises.

**Table 5-3**  
**CSF neurotransmitter findings in the DTDS cohort**

Patient number	Age at LP (years)	CSF HVA		CSF 5-HIAA		CSF HVA:5-HIAA Ratio <sup>B</sup>
		Concentration nmol/L	Reference Range <sup>A</sup> nmol/L	Concentration nmol/L	Reference Range <sup>A</sup> nmol/L	
1	3.5	1873	154-867	141	89-367	13.2
2	1.3	1704	154-867	250	89-367	6.8
3	2.5	1135	154-867	91	89-367	12.5
4	3.7	2046	384-769	169	110-265	12.1
	4.0	1914	384-769	165	110-265	11.6
	8.9	1099	285-560	131	101-237	8.4
5	5.0	1633	154-867	143	89-367	11.4
6	3.0	1810	154-867	149	89-367	12.1
7	7.5	1043	346-716	158	100-245	6.6
	8.3	814	339-668	143	109-214	5.7
8	0.5	2048	310-1100	238	150-800	8.6
	0.75	1114	403-919	225	170-412	5.0
9	1.5	2280	294-1115	176	129-520	12.9
	2.5	1345	233-928	176	74-345	7.7
10	0.8	3000	295-932	285	114-336	10.5
11	4.2	1600	233-928	145	74-345	11.0

**A** Age-related HVA and 5-HIAA reference ranges were established by each laboratory according to laboratory-specific sampling protocols

**B** The HVA /5-HIAA ratio is stable throughout the cranio-caudal gradient and does not change significantly with age.

Published data suggests that the normal range (above 4 months of age) is approximately 1.3–4.0 (Hyland et al., 1993; Brautigam et al., 1998; Brautigam et al., 2002)

### 5.3.3 Neuroradiological findings

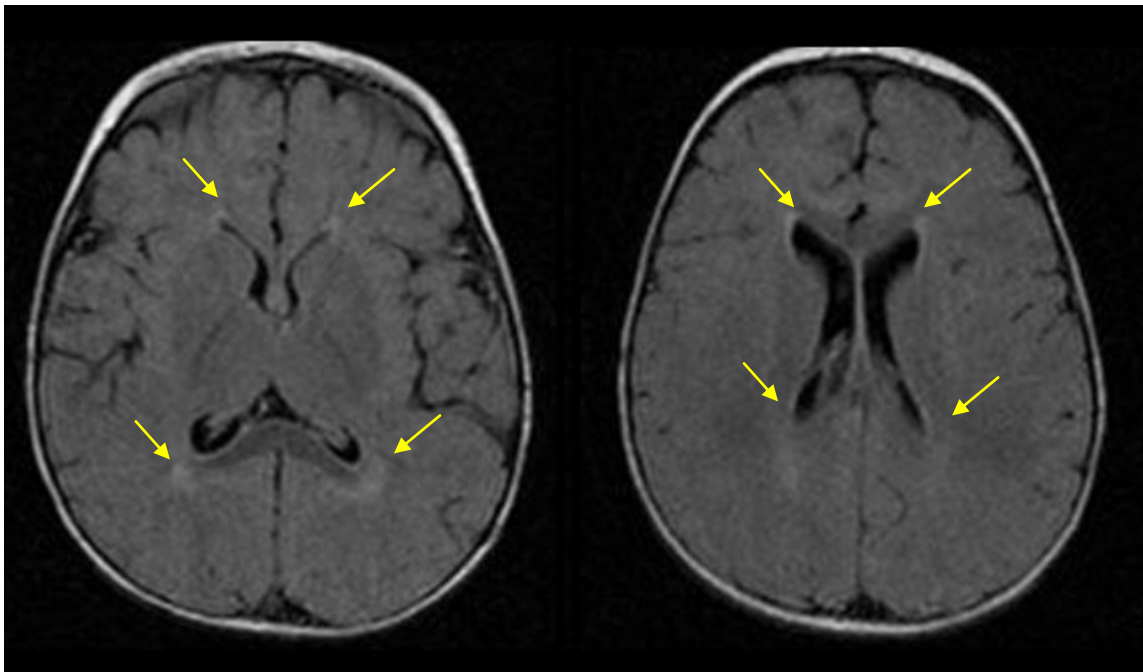
#### 5.3.3.1 Brain MRI and MRS

All children had an MRI brain scan. No structural defects were present and no signal abnormalities were evident in the basal ganglia. 8/11 of the children in the DTDS cohort had evidence of subtle neuroradiological abnormalities (prominence of the external frontotemporal subarachnoid spaces and mild delay in myelination). Patient 9 had evidence of a white matter abnormality similar to periventricular leukomalacia (Figure 5-1).

**Figure 5-1**

*MR Brain of patient 9, age 2.2 years*

*Axial T-1 weighted images demonstrating symmetrical periventricular white matter changes (yellow arrows)*



### 5.3.3.2 Nuclear brain imaging

Nuclear brain imaging using single photon emission computed tomography (SPECT) was performed in two children. Following genetic diagnosis, SPECT brain imaging was undertaken in patient 3 after administration of the dopamine transporter ligand, DaTSCAN<sup>TM</sup> (GE Healthcare), a solution of ioflupane [(123)I-2beta-carbomethoxy-3beta-(4-iodophenyl)-N-(3-fluoropropyl) nortropane, (123)I-FP-CIT, 123I ]. The DaTSCAN imaging showed complete loss of dopamine transporter activity in the basal nuclei (Figure 5-2). Prior to genetic confirmation of DTDS, patient 4 had SPECT brain imaging with the ligand [123I]iodobenzamide (IBZM). The ratio of dopamine 2 receptor density in the striatum compared with the frontal cortex was reduced (1.21, adult reference range 1.5–1.55).

**Figure 5-2**

Nuclear brain imaging (in age-matched individuals) using single photon emission computed tomography (SPECT) after administration of the dopamine transporter ligand DaTSCAN (loflupane,  $^{123}\text{I}$ )

**Figure 5-2A** DaTSCAN imaging in a control subject demonstrating normal distribution of dopamine transporter sites.

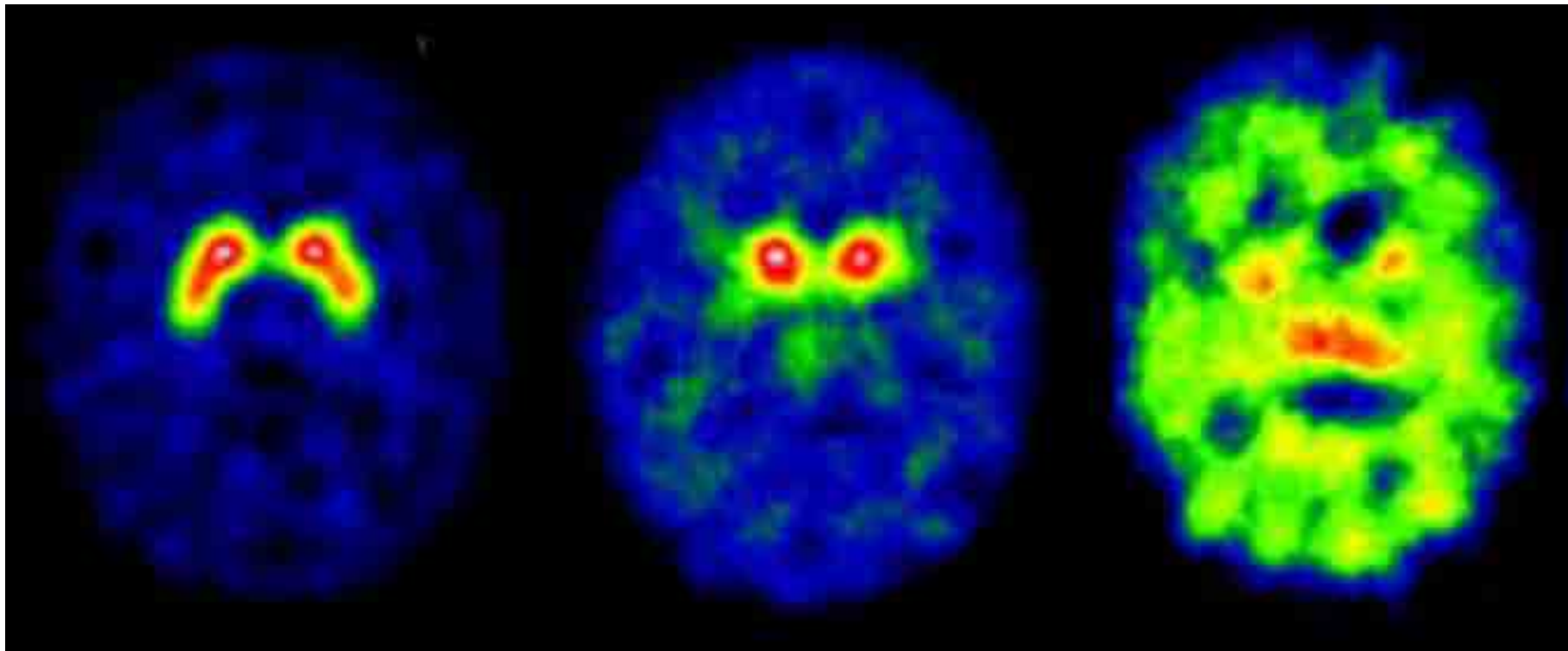
**Figure 5-2B** DaTSCAN imaging in a patient with juvenile parkinsonism (age 9.2 years), showing bilateral symmetrical loss of dopamine transporter sites from the lentiform nuclei.

**Figure 5-2C** DaTSCAN imaging in patient 3 (age 10 years) indicating complete loss of dopamine transporter sites in the basal nuclei. This results in high background counts on the image without any activity from the basal nuclei.

**5-2A**

**5-2B**

**5-2C**





### 5.3.4 Molecular genetic investigation

#### 5.3.4.1 *SLC6A3* mutational analysis

*SLC6A3* gene mutations were identified in all eleven cases (Table 5-4). Mutations identified in cases 1-3 have previously been reported in Chapter 4. Nine novel *SLC6A3* mutations were detected in patients 4-11 (Figure 5-3). Overall, nine patients (seven with consanguineous parents) had homozygous mutations and two children (Patient 5 and 9, born to unrelated parents) had compound heterozygous mutations. Three *SLC6A3* variants were detected in patient 9 who inherited p.Gly327Arg and p.Gln439X from her mother and p.Pro529Leu from her father (Figure 5-3E).

Overall, 14 missense mutations, 4 splice site variants, 4 deletions and 1 nonsense mutation were identified. All mutations segregated appropriately with DTDS disease status in each family. None of the identified mutations were reported as polymorphisms in genomic databases and none were identified in an extensive analysis of 300-400 ethnically matched control chromosomes. Sequence alignment for the novel missense mutations showed Val158, Gly327, Arg521, Pro529 and Pro554 to be highly conserved throughout vertebrate species and Leu224 to be highly conserved throughout mammalian species (Figure 5-4).

**Table 5-4**  
**SLC6A3 mutations identified in the DTDS cohort**

Patient	Ethnicity	Parents Related	Mutation(s)	State	Effect on protein product	Reference where mutation reported
1	Pakistani	Yes	c.1103T>A	Homozygous	p.Leu368Gln	Kurian <i>et al.</i> , 2009
2	Pakistani	Yes	c.1103T>A	Homozygous	p.Leu368Gln	Kurian <i>et al.</i> , 2009
3	Mixed European Descent	Yes	c.1184C>T	Homozygous	p.Pro395Leu	Kurian <i>et al.</i> , 2009
4	Mixed European Descent	No	c.1156+5delG	Homozygous	Unknown	Novel mutation
5	Mixed European Descent	No	c.472G>T c.1661C>T	Compound Heterozygous	p.Val158Phe p.Pro554Leu	Novel mutations
6	Turkish	Yes	c.1031+1G>A	Homozygous	Unknown	Novel mutation
7	Mixed European Descent	Yes	c.399delG	Homozygous	p.Ile134SerFsX5	Novel mutation
8	Mixed European Descent	No	c.1499_1767del	Homozygous	p.Gly500GlufsX13	Novel mutation
9	Mixed European Descent	No	c.979G>A c.1315C>T c.1586C>T	Compound Heterozygous (3 variants)	p.Gly327Arg p.Gln439X p.Pro529Leu	Novel mutations
10	Mixed European Descent	Yes	c.671T>C	Homozygous	p.Leu224Pro	Novel mutation
11	Mixed European Descent	Yes	c.1561C>T	Homozygous	p.Arg521Trp	Novel mutation

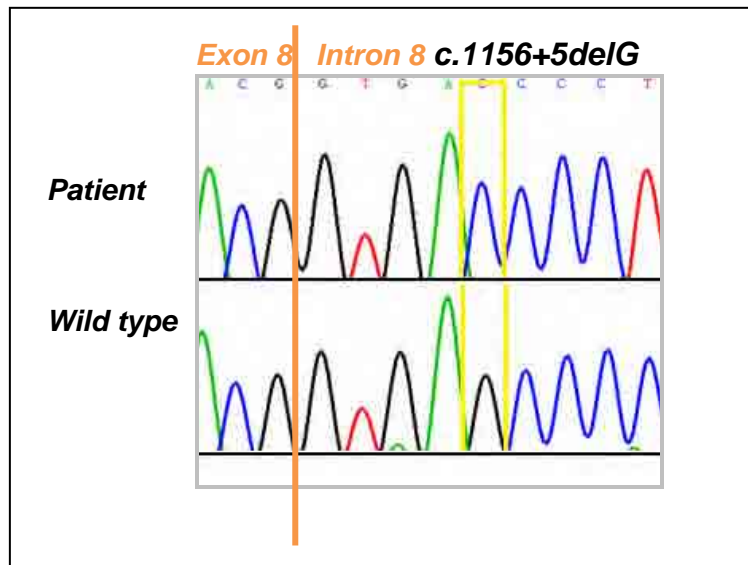
**Figure 5-3**

Novel mutations identified in patient 4, 5, 6, 7, 9, 10 and 11

**Figure 5-3A****Patient 4**

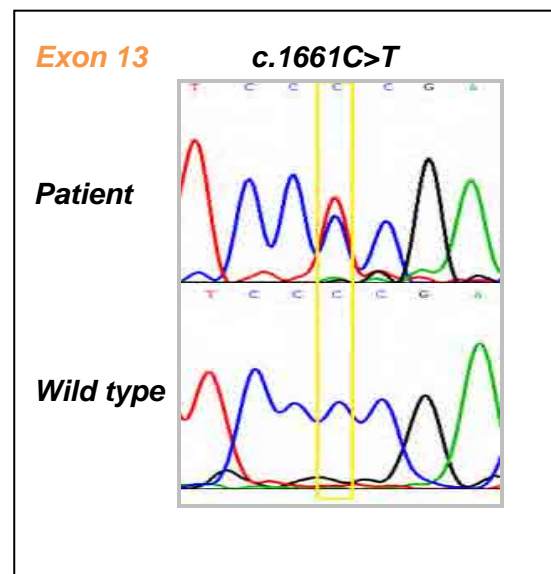
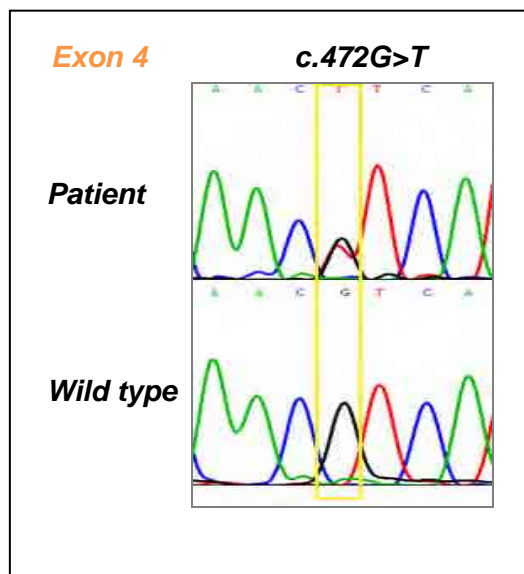
The alignments of SLC6A3 nucleotides c.1153-c.1156 and first 9 nucleotide bases in intron 8 are illustrated

The homozygous splice variant c.1156+5delG is boxed in yellow

**Figure 5-3B****Patient 5**

The alignments of SLC6A3 nucleotides c.469-c.475 and c.1658-c.1664 are illustrated

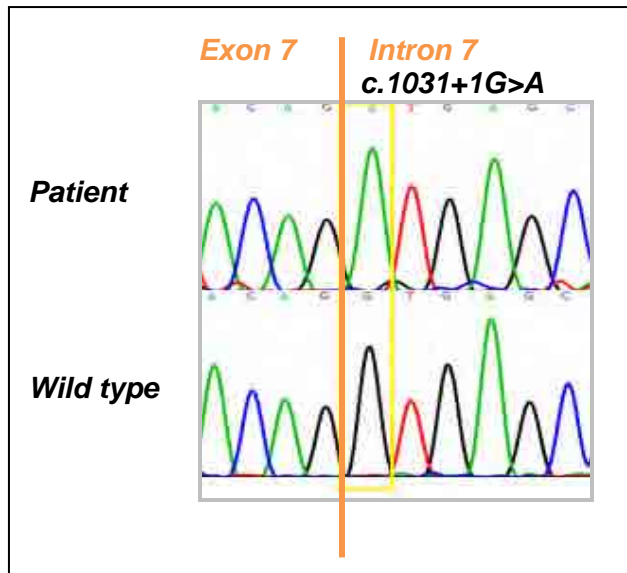
The 2 heterozygous missense mutations identified are boxed in yellow



**Figure 5-3C****Patient 6**

The alignments of SLC6A3 nucleotides c.1028-c.1031 and the first six nucleotide bases of intron 7 are illustrated

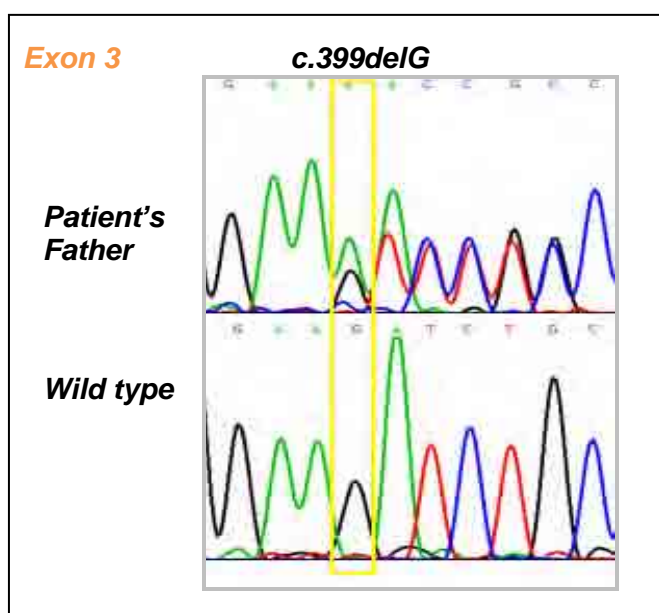
The homozygous splice variant c.1031+1G>A is boxed in yellow

**Figure 5-3D****Patient 7**

The alignments of SLC6A3 nucleotides c.396-c.405 are illustrated

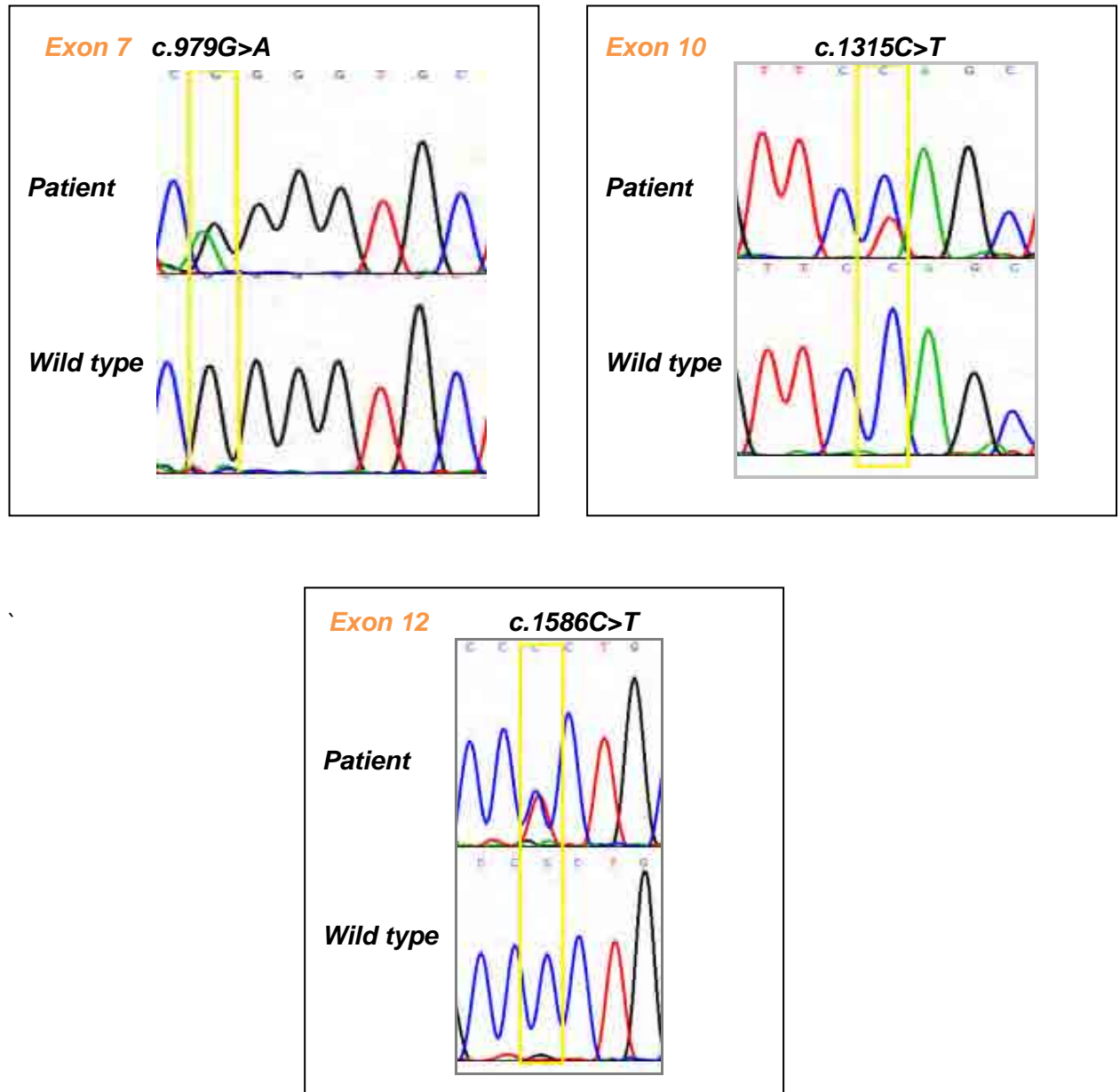
No DNA was available from the child who had died prior to genetic investigation

A heterozygous deletion c.399delG (boxed in yellow) was identified in both parents



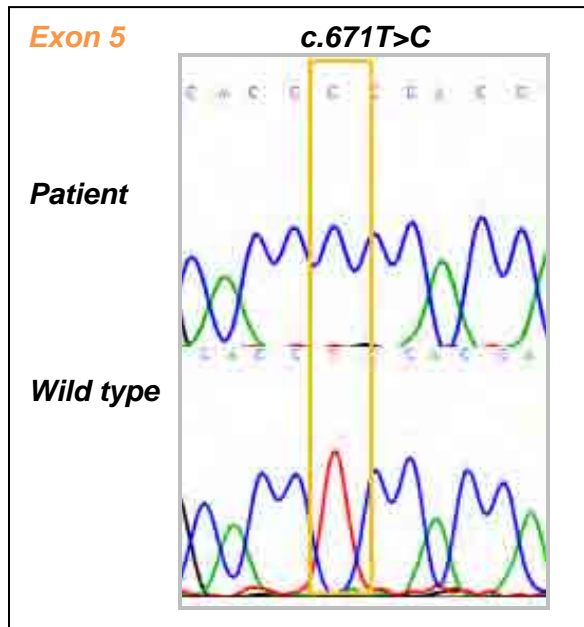
**Figure 5-3E****Patient 9**

The alignments of SLC6A3 nucleotides c.978-c.985, c.1312-c.c1318 and c.1584-c.1589 are illustrated. The 3 heterozygous mutations (2 missense and one nonsense) identified are boxed in yellow

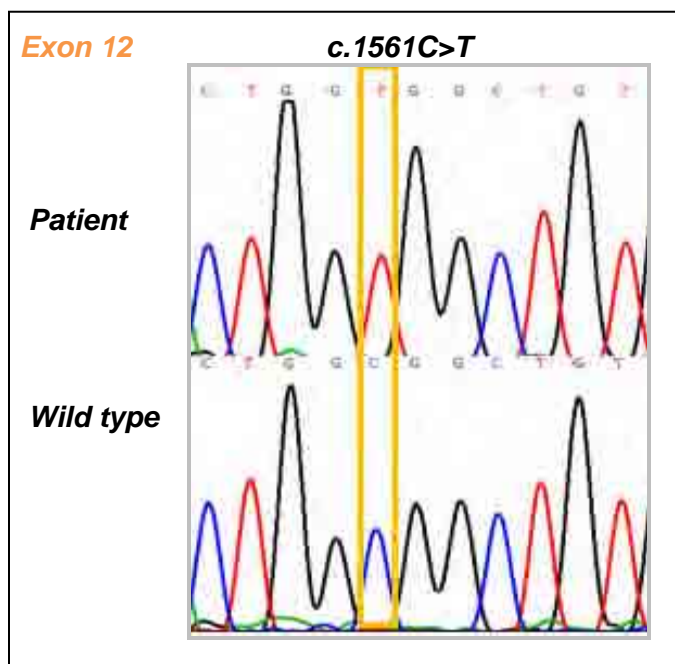


**Figure 5-3F****Patient 10**

The alignments of SLC6A3 nucleotide c.667–c.676 are illustrated  
The homozygous missense change 671T>C is boxed in yellow

**Figure 5-3G****Patient 11**

The alignments of SLC6A3 nucleotides c.1557–c.1567 are illustrated  
The homozygous missense change c.1561C>T is boxed in yellow

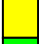



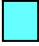



**Figure 5-4**

Conservation of the mutated *SLC6A3* residues Val158, Leu224, Gly327, Arg521, Pro529, Pro554. Six representative vertebrate sequences are aligned.

H. SAPIENS	135	CPILKGVGFTVILISLYVGFFYNV	IIAWALHYLFSSFTTELPWIHCNNSW	184
C.L.FAMILIARIS*	130	CSPALGVGFTVILISLYVGFFYNV	IIAWALHYFFSSFTVELPWVHCNNTW	179
B. TAURUS*	135	CPILRGNGTRPILISLYIGFFYNV	IIAWALHYLLSSFTTELPWTHCNHSW	184
M. MUSCULUS	135	CPVLKGVGFTVILISFYVGFFYNV	IIAWALHYFFSSFTMDLPWIHCNNTW	184
R. NORVEGICUS	135	CPVLKGVGFTVILISFYVGFFYNV	IIAWALHYFFSSFTMDLPWIHCNNTW	184
D. RERIO	151	CPIFKGVGFTVILISLYVGSYYNV	IIAWALFYLFSSFSGELPWIHNCNNTW	200
H. SAPIENS	185	NSPNCSDAHPGDSSGDSGLNDTFGTT	PAAEYFERGVLH	THQSHGIDDLG 234
C.L.FAMILIARIS*	180	NSPNCSDAHSNNS---SSPNDTFR	TTTPATEYFERGVLH	THESRGIDDLG 226
B. TAURUS*	185	NSPRCSDARAPNAS---SGPNGTSR	TTTPAAEYFERGVLH	THESQGIDDLG 231
M. MUSCULUS	185	NSPNCSDAHSNNS-DGLGLNDTFGTT	PAAEYFERGVLH	THQSRGIDDLG 233
R. NORVEGICUS	185	NSPNCSDAHSNNS-DGLGLNDTFGTT	PAAEYFERGVLH	THQSRGIDDLG 233
D. RERIO	201	NSPNCSDPNA-----TLLNDTYKT	TPALEYFERGVLHV	HESSGIDDLG 243
H. SAPIENS	305	LCEA-----SVWIDAATQVCFSLGV	GFVLI	AFSSYNKFTNNCYRDA 346
C.L.FAMILIARIS*	297	LCES-----SVWIDAATQVCFSLGV	GFVLI	AFSSYNKFTNNCYRDA 338
B. TAURUS*	330	PCARRTLPEQGEVWIDAAIQICFSLGV	GLVLI	AFSSYNKFTNNCYRDA 379
M. MUSCULUS	304	LCEA-----SVWIDAATQVCFSLGV	GFVLI	AFSSYNKFTNNCYRDA 345
R. NORVEGICUS	304	LCEA-----SVWIDAATQVCFSLGV	GFVLI	AFSSYNKFTNNCYRDA 345
D. RERIO	314	LYDA-----QVWIEAATQICFSLGV	GFVLI	AFSSYNKFSNNCYRDA 355
H. SAPIENS	497	WFYGVGQFSDDIQQMTGQRPSLY--	WRLCWLKLVSP	CFLLFVVVVSIVTFR 544
C.L.FAMILIARIS*	489	WFYGVVRQFSDDIKQMTGQRPSLY--	WRVCWKVFSPE	CFLLFVVVVSIVTFR 536
B. TAURUS*	523	WFYGVWQFSDDIKQMTGRRPSLY--	WRLCWLKVFSPE	CFLLFVVVVSIVTFR 570
M. MUSCULUS	496	WFYGVQQFSDDIKQMTGQRPNLY--	WRLCWLKLVSP	CFLLYVVVVSIVTFR 543
R. NORVEGICUS	496	WFYGVQQFSDDIKQMTGQRPNLY--	WRLCWLKLVSP	CFLLYVVVVSIVTFR 543
D. RERIO	506	WFYGVDRFSDDIEEMIGQRPGLY--	WRLCWLKVFSPE	CFLLFMVVVSFATFN 553
H. SAPIENS	545	PPHYGAYIFPDW	ANALGWVIATSSMAMVPI	----- 574
C.L.FAMILIARIS*	537	PPHYGAYIFPEW	ANALGWAIATSSMSMVPI	----- 566
B. TAURUS*	571	PPHYGAYVFEW	ATALGWAIAASSMSVVPI	----- 600
M. MUSCULUS	544	PPHYGAYIFPDW	ANALGWIIATSSMAMVPI	----- 573
R. NORVEGICUS	544	PPHYGAYIFPDW	ANALGWIIATSSMAMVPI	----- 573
D. RERIO	554	PPKYGSYYFPTW	ATMVGWCLSISSMIMVPL	----- 583

\* Predicted protein sequence

	Val158
	Leu224
	Gly327
	Arg521
	Pro529
	Pro554

#### 5.3.4.2 Characterisation of the deletion in patient 8

In patient 8, specific PCR primers flanking *SLC6A3* exons 12 and 13 failed to amplify on repeated occasions raising the possibility of a homozygous deletion involving exon 12 and 13.

Long range PCR techniques were subsequently employed to characterise the putative deletion. A forward primer in intron 10 (11F) and a reverse primer in intron 14 (14R) were utilised for long range PCR (Chapter 4, Table 4-4). An amplicon was obtained both in the index case and both parents, but no PCR product was amplifiable in 400 ethnically matched control chromosomes (Figure 5-5A).

Sequencing of this PCR fragment (using serial reverse primers in intron 13, Table 5-1) allowed the genomic deletion to be characterised (Figure 5-5B). The telomeric and centromeric genomic breakpoints were mapped to 1,455,093–1,455,095bp (intron 13) and 1,460,244–1,460,246bp (intron 11) respectively, defining a ~5kb deletion. The precise location of the breakpoint could not be further defined as there was a 3bp sequence (CAG) common to both the intron 11 and intron 13 sequence (Figure 5-5B).

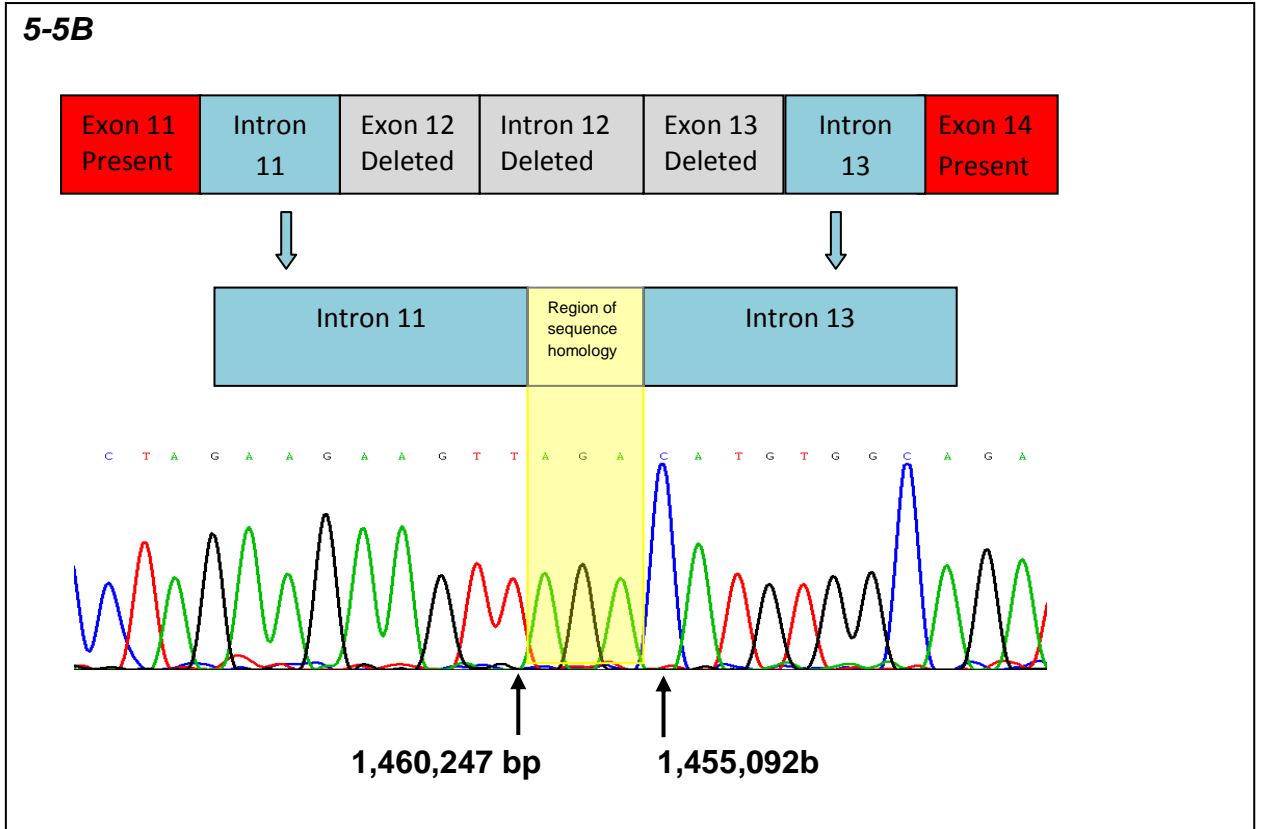
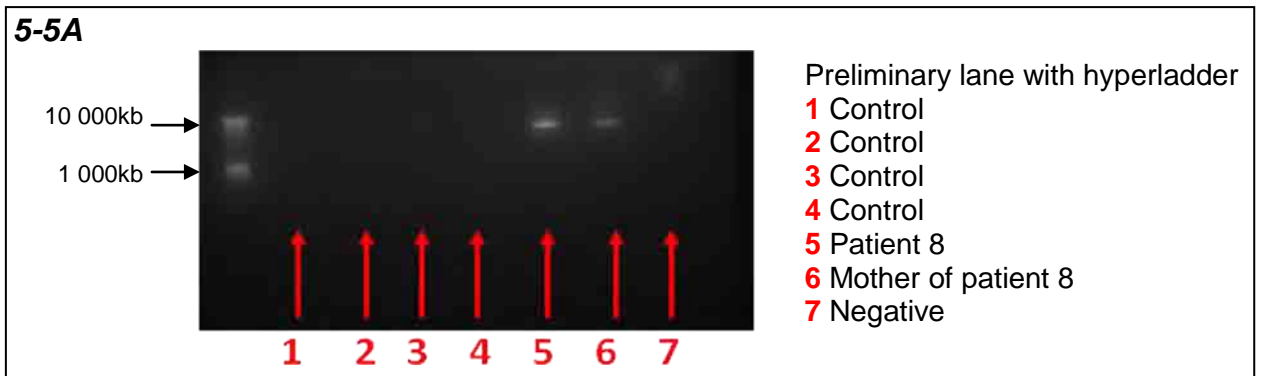


**Figure 5-5**

*Definition of the SLC6A3 deletion in patient 8*

**Figure 5-5A** Agarose gel photograph of PCR amplification of introns 10 to 14 of SLC6A3 showing the presence of bands in patient 8 (Lane 5) and their parent 8 (Lane 6) and the absence of bands in normal controls (Lanes 1-4). Lane 7 is a negative control.

**Figure 5-5B** Determination of the DNA sequence of the genomic breakpoint of the deletion. The exons that are present are indicated in red (exon 11 and 14). The deleted exons/introns are represented in grey (exon 12 and 13). The telomeric and centromeric genomic breakpoints were mapped to 1,455,093–1,455,095bp (intron 13, shaded in blue) and 1,460,244–1,460,246bp (intron 11, shaded in blue). There is a 3 base region of homologous sequence which show 100% homology in both intron 11 and 13 (shaded yellow box).



## **5.4 Discussion**

In this chapter, I have characterised the clinical and molecular genetic features of a precisely diagnosed cohort of children with autosomal recessive DTDS associated with loss-of-function mutations in the *SLC6A3* gene. DTDS is thus a disorder of dopamine homeostasis and the first identified disorder with parkinsonian features due to genetic alterations of the dopamine transporter. In the discussion section of this chapter, I will discuss the physiological and pathological roles of dopamine and its transporter (DAT), and will postulate hypotheses of the underlying disease mechanisms in DTDS.

### **5.4.1 Dopamine: anatomical distribution and physiological role**

Until the mid 1950s, it was believed that dopamine was purely an intermediary substrate in the biosynthesis of norepinephrine and epinephrine. In 1958, Carlsson *et al.*, discovered that dopamine was present in high concentrations in the rat corpus striatum and that administration of the drug reserpine (which blocks the vesicular monoamine transporter, VMAT) resulted in dopamine depletion and a 'parkinsonian' phenotype. Following the reversal of reserpine-induced hypokinesia by L-dopa, Carlsson proposed a biological role for dopamine in neurotransmission, independent of its catecholamine precursor function (Carlsson *et al.*, 1959). This seminal work was, in part, the basis of the Nobel Prize in Medicine awarded to Carlsson in 2000.

Advances in histochemical techniques to visualise cellular localisation of dopamine was the second major breakthrough in understanding the

physiological role of dopamine in the human brain (Anden *et al.*, 1964). The first systematic mapping of dopaminergic pathways was performed by Dahlstrom and Fuxe in 1964, who demonstrated the concentration of dopaminergic cell bodies in the ventral midbrain as well as the widespread distribution of dopamine within the striatum. The finding that the highest concentrations of dopamine were present in the basal ganglia led to the hypothesis that dopamine may be involved in the control of motor function and that decreased striatal dopamine could be the cause of extrapyramidal disorders such as Parkinson's disease. Subsequent mapping studies by in rodents and humans (Hoffman *et al.*, 1976; Sladek *et al.*, 1982; Felten and Sladek, 1983) showed that dopamine has a much wider distribution outside the basal ganglia, which suggested that this neurotransmitter had a complex and more extended role in the brain.

Dopaminergic neurons are thus located prominently in the substantia nigra pars compacta (with projections to the striatum via the nigrostriatal pathway) and in the ventral tegmental area of the midbrain (with mesocorticolimbic projections to the nucleus accumbens, hippocampus, and other corticolimbic structures) (Torres *et al.*, 2003). Consistent with this widespread cerebral distribution, it is now deemed that dopamine has a variety of important physiological functions. It plays a fundamental role in the control of locomotion, cognitive processes, attention, memory and neuroendocrine secretion and is also involved in the control of motivated behaviours such as emotion, affect and reward mechanisms (Carlsson, 1987; Carlsson, 2001; Greengard, 2001).

### 5.4.2 The structure and physiological function of DAT

As briefly discussed in Chapter 4, *SLC6A3* encodes the dopamine transporter DAT, which is a member of the solute carrier family 6 (SLC6) group of Na<sup>+</sup>/Cl<sup>-</sup> dependent transmembrane transport proteins (Torres and Amara, 2007; He *et al.*, 2009). A breakthrough in the structure-function understanding of DAT was made in 2005 by Gouaux and colleagues, who determined a high-resolution crystal structure of LeuT<sub>Aa</sub>. This N<sup>+</sup> dependent 12 TM bacterial leucine transporter from *Aquifex aeolicus* is functionally homologous to the neurotransmitter sodium symporters (Yamashita *et al.*, 2005). DAT consists of 12 transmembrane spanning domains presumed to consist of primarily  $\alpha$ -helical structure. These helices are linked through intracellular loops (IL) and extracellular loops (EL) with the N- and C-termini facing the cytoplasm (Figure 4-9). The DAT possesses numerous post-translational modifications (which are not found in bacterial homologues) that regulate various aspects of its function including glycosylation and disulphide bonding on EL2 and phosphorylation and ubiquitylation on the long N-terminal tail (Parnas and Vaughan, 2008).

DAT is exclusively expressed in dopamine neurons and recaptures released dopamine from the extracellular milieu around the synaptic cleft thereby transporting it back into the presynaptic neuron (Rice and Cragg, 2008). Dopamine is transported inward, against its concentration gradient using the driving force of the sodium gradient across the plasma membrane (see Chapter 4.4). Of note, inherited mutations in the gene for the Na<sup>+</sup>/K<sup>+</sup>-ATPase  $\alpha$ 3 subunit (*ATP1A3*) are associated with the extrapyramidal syndrome autosomal

dominant rapid-onset dystonia-parkinsonism (ROPD) (de Carvalho *et al.*, 2004). It is conceivable that the underlying disease mechanism of ROPD (resulting from loss-of-function *ATP1A3* mutations and disturbance of the electrochemical gradient across the cell membrane) may also thus be indirectly related to disturbance of DAT function.

As briefly discussed in Chapter 4, the transporter thus plays a fundamental role in the deactivation of dopaminergic signalling and is the principle regulator of the amplitude and duration of dopaminergic action (Bannon, 2005). As seen from animal studies, DAT is thus fundamental in the maintenance of dopamine homeostasis since no other physiological mechanisms can sufficiently compensate for its loss of function *in vivo*.

DAT is also a major target for several abused drugs (including amphetamine, cocaine and other psychostimulants) and also for therapeutic agents (such as methylphenidate and bupropion) (Kharkar *et al.*, 2008). Cocaine and other related psychostimulants bind to DAT (thus inhibiting its activity) but are not transported. Amphetamine and other compounds (with structural similarity to dopamine) are carried by the DAT. These exogenous substances thus compete with dopamine for transport, thereby both reducing the rate of dopamine re-uptake and inducing non-exocytotic efflux of dopamine from the neuron into the synapse via reversal of transport. The overall effect of these drugs is thus to increase the concentration and duration of dopamine in the synapse leading to supraphysiological activation of post-synaptic neurons, resulting in euphoria and psychomotor stimulation (Parnas and Vaughan, 2008).

### 5.4.3 The role of dopamine dysregulation in human diseases

Dopamine dysregulation is implicated in a wide variety of human diseases. As discussed in Chapter 4, defects in the dopamine biosynthetic pathway (Chapter 4, Figure 4-1) can cause a dopamine deficient state, resulting in complex neurological neurotransmitter disorders with predominant extrapyramidal features (see Chapter 4.1.2, Table 4-1). Aberrant dopaminergic transmission has also been implicated in other neurological and neuropsychiatric disorders including conditions associated with dopamine deficiency (such as Parkinson's disease) as well as disorders proposed to be associated with states of dopamine excess (such as ADHD, schizophrenia, bipolar disorder and Tourette syndrome) (Mehler-Wex *et al.*, 2006; Mazei-Robinson *et al.*, 2006).

### 5.4.4 The role of variants in *SLC6A3* in human disease

As discussed in 5.4.3, dopamine dysregulation is implicated in a wide variety of neurological and neuropsychiatric conditions and as a consequence, the *SLC6A3* gene (coding exons and gene variants such as the variable number tandem repeat, VNTR at the 3'UTR) has been extensively investigated in a number of disorders including Parkinson's disease (Nutt *et al.*, 2004), ADHD, Tourette syndrome, disorders of addiction (such as alcoholism and smoking) schizophrenia, bipolar disorder and migraine (Vandenbergh, 2008). The interaction of specific drugs (such as cocaine, amphetamines and methylphenidate) with *SLC6A3* has further implicated the role of *SLC6A3* in neuropsychiatric disorders. Despite initial hopes of uncovering new genetic information that would clarify the relationship between DAT and a

disease/disorder/personality, little in the way of consistent reproducible results have been reported. Association studies between *SLC6A3* variants and Parkinson's disease were found by Le Couter *et al.*, (1997) and Leighton *et al.*, (1997) but subsequent work was unable to confirm these findings.

Prior to this current work on DTDS, the strongest convincing genetic relationship between *SLC6A3* and a human disease was with ADHD (Mazei-Robinson and Blakely, 2006; Waldman and Gizer, 2006) with over 170 publications as of 2010. The original work in 1995 demonstrated association and linkage between ADHD and the 10-copy allele of the *SLC6A3* VNTR (Cook *et al.*, 1995). Furthermore, the hyperactive features observed in the DAT knockout mouse model (Giros *et al.*, 1996) also prompted extensive investigation of *SLC6A3* in ADHD. Further evidence has been reported by Mazei-Robinson and colleagues (2008) who reported 2 siblings with an ADHD phenotype harbouring the rare coding missense SNP variant Ala559Val. Analysis of mutant DAT showed increased dopamine efflux (attenuated by amphetamine), via dopamine D<sub>2</sub> autoreceptors (Bowton *et al.*, 2010).

Although from our study it is evident that loss-of-function DAT mutations cause DTDS, other *SLC6A3* variants (such as the one described above in ADHD, Figure 5-6) may affect different facets of the complex functional role of the dopamine transporter (such as the control of behaviour or cognitive processes) thereby resulting in a different clinical phenotype.

### 5.4.5 Clinical features of DTDS

In this chapter I have described novel variants in *SLC6A3* associated with DTDS. This study has enabled detailed clinical delineation of this novel disorder. DTDS is thus an early onset, complex movement disorder (Assmann *et al.*, 2004; Kurian *et al.*, 2009). The onset in early infancy is characterised by an extrapyramidal syndrome, including hypokinetic parkinsonian features (bradykinesia, rigidity and tremor) and/or hyperkinetic symptoms (dystonia, chorea, dyskinesias and oculogyric crises). In DTDS, the variability and relative preponderance of parkinsonian and hyperkinetic features is not dissimilar to that reported in other neurotransmitter syndromes associated with an infantile parkinsonism-dystonia phenotype (Assmann *et al.*, 2003). Over time, children with DTDS become profoundly hypokinetic, with increasingly severe parkinsonism-dystonia (akinesia, profound rigidity, marked tremor, amimia and a generalised fixed postural dystonia), pyramidal tract features and a complex eye movement disorder (saccade initiation failure, ocular flutter).

To date, I have identified 11 cases of DTDS, but it is highly likely that there are more affected patients who remain undiagnosed. Only a limited number of paediatricians have become familiar with the broad clinical spectrum and diagnostic approach to neurotransmitter disorders (Assmann *et al.*, 2003). Although CSF investigations are increasingly performed, in many centres, CSF neurotransmitter analysis is not a routine investigation for children with a complex motor disorder. Clinical features of DTDS can all mimic different forms of cerebral palsy (dyskinetic, spastic, and mixed cerebral palsy). Indeed, based



on the clinical features and early disease evolution, a significant number of children in this cohort were initially labelled as having cerebral palsy prior to neurological and genetic investigation. In patient 8, the evolution of motor features following a complicated labour and delivery was additionally suggestive of possible evolving cerebral palsy. In patient 9, although the white matter abnormalities on MRI brain scan may be an incidental feature, there is nevertheless radiological similarity to the peritrigonal MRI T2-hyperintensity of periventricular leukomalacia apparent in cerebral palsy (Deng *et al.*, 2008). Misdiagnosis and diagnostic delay have also been reported in other neurotransmitter disorders, such as tyrosine hydroxylase deficiency (Willemsen *et al.*, 2010). This work described in this chapter thus emphasises the importance of specific investigations (CSF neurotransmitter analysis and mutational analysis if appropriate) in all children with an undiagnosed complex movement disorder.

#### **5.4.6 Genetic features of DTDS**

All children in the cohort had homozygous or compound heterozygous *SLC6A3* mutations in the gene. A wide variety of variants were identified. 14 missense mutations resulted in amino acid substitutions which were absent in an extensive analysis of ethnically matched control subjects and occurred in highly conserved amino acids of DAT. Other identified mutations included 4 deletions and 1 nonsense mutation, which are likely to result in nonsense-mediated decay or a truncated protein product. In patient 8, a large intragenic out-of-frame homozygous deletion was identified. The mechanism by which the

deletion was generated is unclear as both centromeric and telomeric breakpoints of this intragenic rearrangement did not occur within a repetitive sequence or within regions of sequence homology (<http://www.repeatmasker.org>). Two children (Patient 4 and 6) were homozygous for splice site variants, which are both predicted to cause aberrant splicing ([http://www.fruitfly.org/seq\\_tools/splice.html](http://www.fruitfly.org/seq_tools/splice.html)). In the DTDS cohort, mutations were identified throughout the coding region of the gene and no mutation hotspots were evident (Figure 5-6). Patient 1 and 2 (originating from the same Pakistani kindred) had an identical homozygous missense mutation but otherwise, there was no evidence of any recurrent or common mutations in DTDS. No correlation between the genetic mutation and disease severity was evident in this cohort.

It is possible that variants of the gene may also confer susceptibility to neurological/neuropsychiatric disorders. In our DTDS cohort, none of the parents (obligate carriers) or siblings (with *SLC6A3* mutation carrier status) had a movement disorder or neuropsychiatric condition. However the mother of patient 11 (and heterozygous carrier of the missense mutation p.Arg521Trp) had a history of recurrent severe migraine with aura. Both dopamine and DAT have been implicated in the pathophysiology of migraine (Todt *et al.*, 2009; Charbit *et al.*, 2010) but the precise role of both remain unclear. Although migraine with aura is a common phenomenon, whether heterozygous *SLC6A3* mutation carrier status could increase susceptibility to migraine is yet to be determined.



### 5.4.7 Functional analysis of mutant DAT proteins

To determine the effects of the missense mutations, mutant human DAT (hDAT) proteins were transiently expressed in HEK293 cells and their transport activity compared with that of wild-type. No mutant hDAT was studied for identified splice site variants (patient 4 and 6), with protein product being unknown and deletions (patients 7 and 8), reflecting a frameshift which is likely to lead to nonsense mediated decay and non-DAT expression.

The effect of mutations identified in cases 1-3 have been reported in Chapter 4.4.2. While wild-type showed normal transport activity, other mutants studied (Val158Phe, Leu224Pro, Gly327Arg, Gly327Arg-Gln439X, Leu368Gln, Pro395Leu and Pro554Leu) did not show uptake activity above nonspecific uptake. Pro529Leu (identified in patient 9) displayed 6% of wild-type transport activity and Arg521Trp (identified in patient 11) displayed 27% of wild-type transport activity. Co-expression of Gly327Arg-439X with Pro529Leu (as in patient 9) further lowered activity to nonspecific levels (Table 5-5).

The binding affinity ( $K_d$ ) of the cocaine analogue [ $^3$ H]2 $\beta$ -carbomethoxy-3 $\beta$ -(4-fluorophenyl)-tropane ([ $^3$ H]CFT) was near normal in the mutants (13–44nM), compared with 19nM in wild-type (see Table 5-5) except in Gly327Arg-Gln439X where it was appreciably lower (higher  $K_d$  of 101nM) and in Val158Phe (absent binding). In many mutants, the nonspecific binding of [ $^3$ H]CFT was appreciably higher than in wild-type, contributing to greater than normal variation in the data range.

The potency ( $K_i$ ) of dopamine in inhibiting cocaine analogue binding was near normal in Gly327Arg, Pro395Leu, Arg521Trp, Pro529Leu and Pro554Leu but reduced (higher  $K_i$ ) in Leu368Gln (with same tendency for Gly327Arg-Gln439X and Leu224Pro). Thus, whereas all mutations are loss-of-function mutations with respect to dopamine transport, some also appear to be accompanied by a loss of apparent binding affinity of dopamine.

Maximal binding of [ $^3$ H]CFT to cells, primarily representing surface binding (Chen *et al.*, 2004a) indicated 3- to 5-fold decreases in mutants Leu368Gln, Arg521Trp, Pro529Leu and Pro554Leu and (with similar tendency for Pro395Leu), and 15-fold (or more) decreases in Val158Phe, Leu224Pro and Gly327Arg.

Analysis of whole cell lysates by immunoblotting with anti-C-terminus DAT antibody showed deficiency in mature DAT (85 kDa) in Val158Phe, Leu224Pro, Arg521Trp, Pro529Leu, and Pro554Leu as the previously studied Leu368Gln and Pro395Leu (Figure 5-7). Val158Phe showed particularly low expression. In contrast, Gly327Arg resembled more wild-type with appreciable mature DAT. As expected, Gly327Arg-Gln439X with C-terminus deleted did not show a signal with anti-C-terminus DAT antibody. Some expression of this mutant was detected with anti-N-terminal DAT antibody in the form of lower molecular-weight bands (Figure 5-7 middle panel). Similar patterns were observed for the mutants with both termini intact using both antibodies (compare top and middle panel, and note appreciable mature DAT in Gly327Arg with N-terminal targeting antibody).

**Table 5-5: Dopamine transport and cocaine analogue binding by wild-type and mutant hDAT**

Patient	hDAT Mutant	[ <sup>3</sup> H]dopamine uptake % OF WT	[ <sup>3</sup> H]CFT binding		
			K <sub>d</sub> (nM)	B <sub>max</sub> (pmol/mg)	Inhibition by dopamine, K <sub>i</sub> (μM)
	Wild-type (WT)	Normal	18.8 ± 2.0	2.40 ± 0.51	5.06 ± 0.43
1	Leu368Gln <sup>A</sup>	0 <sup>C</sup>	35.6 ± 8.2	0.384 ± 0.110 *	52.9 ± 1.7 *
2	Leu368Gln <sup>A</sup>	0 <sup>C</sup>	35.6 ± 8.2	0.384 ± 0.110 *	52.9 ± 1.7 *
3	Pro395Leu <sup>A</sup>	0 <sup>C</sup>	30.2 ± 6.5	0.962 ± 0.144	3.35 ± 0.65
4	- <sup>B</sup>				
5	Val158Phe Pro554Leu	0 <sup>C</sup> 0 <sup>C</sup>	N/A <sup>D</sup> 43.8 ± 5.9	N/A <sup>D</sup> 0.48 ± 0.05 *	N/A <sup>D</sup> 4.39 ± 0.71
6	- <sup>B</sup>				
7	Ile134SerfsX5 <sup>B</sup>				
8	Gly500GlufsX13 <sup>B</sup>				
9	Gly327Arg	0 <sup>C</sup>	24.3 ± 12.4	0.18 ± 0.04 *	2.93 ± 1.59
	Gly327Arg-Gln439X	0 <sup>C</sup>	101 ± 6 *	0.85 ± 0.14 *	28.1 ± 21.6
	Pro529Leu	6.22 ± 1.31 <sup>E</sup>	16.5 ± 5.4	0.47 ± 0.07 *	3.54 ± 1.75
	Pro529Leu+Gly327Arg-Gln439X	1.71 ± 1.42 <sup>E</sup>			
10	Leu224Pro	0 <sup>C</sup>	13.0 ± 1.3	0.15 ± 0.04 *	28.8 ± 6.0
11	Arg521Trp	26.9 ± 2.9 <sup>E</sup>	20.5 ± 3.1	0.48 ± 0.09 *	3.82 ± 1.37

<sup>A</sup> Data from Kurian et al., 2009

<sup>B</sup> Protein product unknown or mutation results in a frameshift

<sup>C</sup> No transport activity above nonspecific uptake

<sup>D</sup> No binding detectable above nonspecific binding

<sup>E</sup> P<0.002 compared with wild-type (one-sample t-test with wild-type at 100%). Average uptake in WT was 23 pmol/min/mg protein at 6 nM [<sup>3</sup>H]dopamine in the assay

\* P<0.05 compared with wild-type (1-way ANOVA followed by Dunnett multiple comparisons). Statistics were applied to mutant groups compared with wild-type examined within one and the same experimental set; wild-type values listed are the average of all experiments.

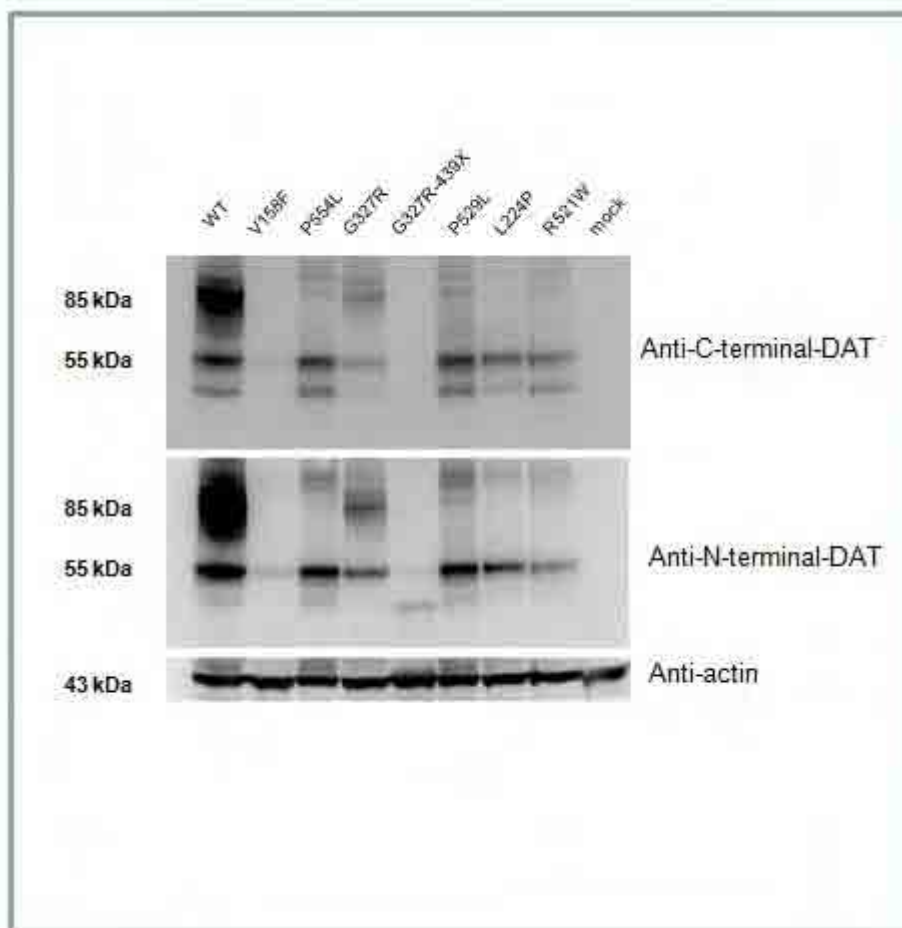
Data are mean ± SEM for 3-5 independent determinations per group

\* P<0.05 compared with wild-type (1-way ANOVA followed by Dunnett multiple comparisons). Data are mean ± SEM for 3-5 independent determinations per group.

Statistics were applied to mutant groups compared with wild-type examined within one and the same experiment; wild-type values listed are the average of all experiments

**Figure 5-7**

*Expression of wild-type (WT) and mutant hDAT in HEK293 cells via immunoblotting analysis. Cells were transiently transfected with WT, mutant hDAT, or reagent only (mock). The same amount of total lysate protein was loaded in all lanes. Protein was probed with antibody against the C-terminal (top panel) or N-terminal (middle panel) of DAT. Anti- $\beta$ -actin antibody showed the relative equivalent loading of total protein (bottom panel)*



Notably, all mutations that are predicted to result in an expressed protein, when studied in hDAT expressing cultured cells, severely incapacitated dopamine transport. Transport was not detectable in any mutant except for an approximate 27% residual activity in Arg521Trp, which interestingly correlates with a degree of dopa-responsiveness in patient 11. In addition, there is 6%

residual activity in Pro529Leu, which is consonant with some dopa responsiveness in Patient 9.

More work is needed to fully characterize the mechanisms underlying the loss of transport function of DAT in each case. First, reduced expression of DAT (see Table 5-5), severe in some cases, is likely to play a role. Second, loss of dopamine recognition by the DAT by reduced affinity is involved for a number of mutants. Third, lack of glycosylation to form mature DAT is known to negatively impact trafficking to the cell surface and transport function of DAT (Li *et al.*, 2004). Glycosylation patterns can vary with the cellular environment, which is dependent upon cell type and physiological state of the cell in which the glycoprotein is made and so analysis of brain DAT glycosylation in IPD cases will be of considerable interest. Finally, homology modelling based on the structure of the bacterial analogue LeuT (Schmitt *et al.*, 2010) of these point mutants compared with wild-type shows subtle structural changes far distal from the mutated residue that could impact conformational changes required during dopamine transport (Reith, personal communication, 2010). The location of mutated residues distal from the dopamine recognition site is consonant with the idea of a general defect in translocation mechanism, i.e. not selective for dopamine. Also in agreement with this is the fact that the point mutations observed in this study occur in amino acids that are present in many other members of the SLC6 transporter family that do not transport dopamine. Thus, for Val224 and Arg521 of DAT there is the same or a similar residue in other monoamine transporters (for norepinephrine and serotonin), whereas for all remaining mutants, the residue in question is even more widespread throughout



the family - also occurring in other transporters (such as in GABA and glycine transporters). Among the residues subject to mutation in the present study, Gly327 is the only one that is actually in the major substrate binding site, so the mutation of small-sized glycine to bulky arginine could be thought to cause a major disruption in the substrate site; however, the normal dopamine affinity measured in the [<sup>3</sup>H]CFT binding assay suggests that this unwound region of TM6 can easily accept the extra bulk from the glycine to arginine substitution.

#### 5.4.8 Proposed disease mechanisms in DTDS

In this chapter, imaging modalities for DAT using SPECT (Nikolaus *et al.*, 2007a; Nikolaus *et al.*, 2007b) has provided a crucial link between the clinical phenotype, molecular genetic investigation and *in vitro* functional analysis of mutant DAT proteins. Such functional imaging of DAT has been a useful clinical tool in aiding the diagnosis and differentiation of movement disorders such as Parkinson's disease, other disorders of nigrostriatal dysfunction and ADHD (Spencer *et al.*, 2005; Scherfler *et al.*, 2007). The DaTSCAN imaging undertaken in patient 3 shows almost complete loss of dopamine transporter activity in the basal nuclei (Figure 5-2C). DaTSCAN imaging is not performed routinely in children and there is thus limited paediatric data for comparative analysis. The high background counts seen on this DaTSCAN image are also reported in adult patients with poor uptake in the basal nuclei. It is due to unbound DaTSCAN in the blood pool, occurring because there are little or no transporter sites with which to bind. DaTSCAN imaging in DTDS is markedly different to that of an age-matched control (Figure 5-2A). Loss of dopamine

transporter activity also appears to be much more extensive in DTDS than in a patient (of similar age) with juvenile parkinsonism, in whom DaTSCAN imaging showed symmetrical reduction (but not absence) of dopamine transporter activity from basal nuclei (Figure 5-2B). These in-vivo DaTSCAN SPECT imaging findings are consistent with the in-vitro assessment of mutant DAT function, and provide further evidence that loss of dopamine transporter function has a causative role in DTDS pathogenesis.

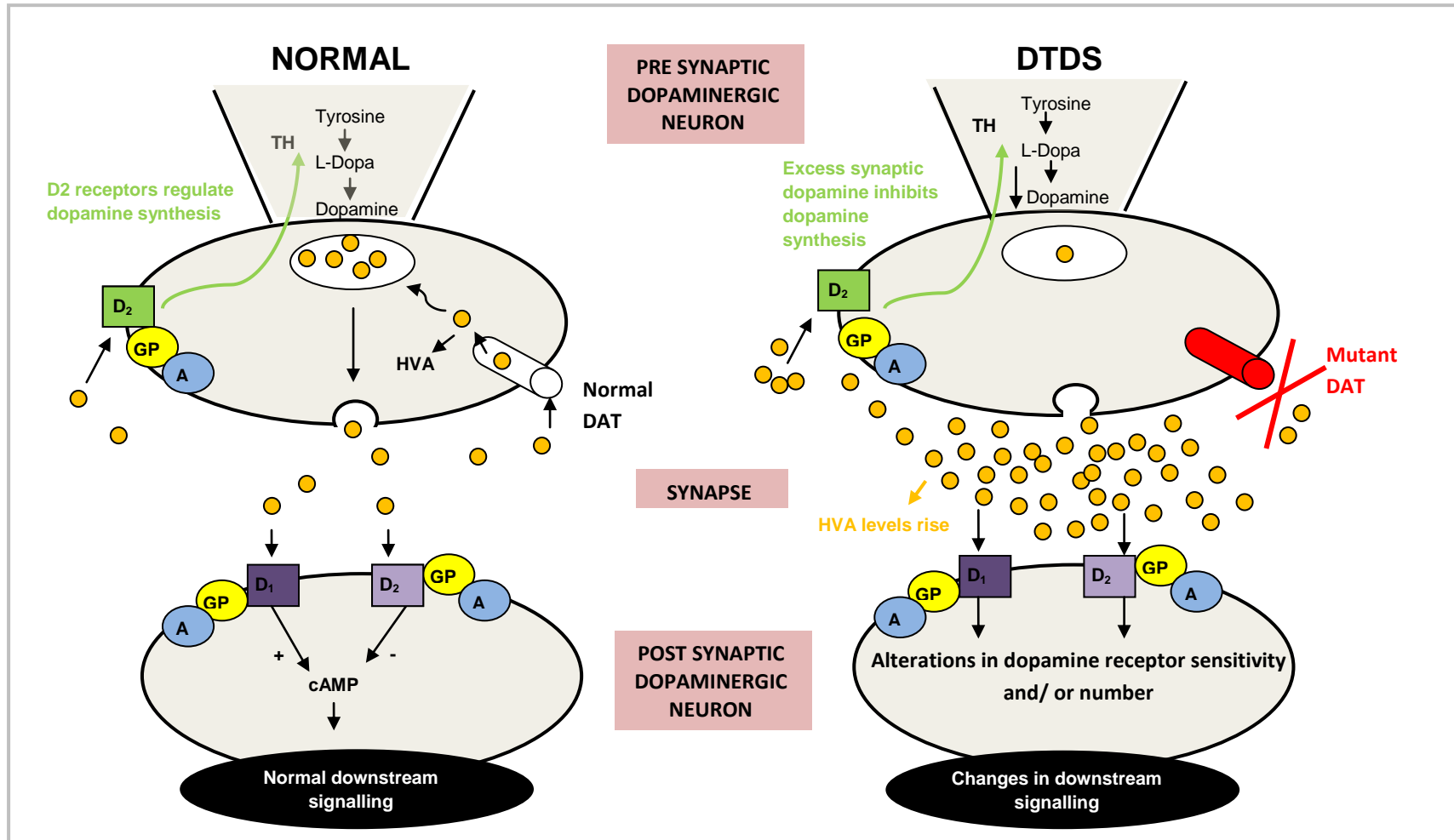
The symptoms of DTDS thus appear to result from loss of DAT function. From this work it may be postulated that inhibition of dopamine re-uptake into the pre-synaptic neuron causes accumulation of extraneuronal dopamine producing increased dopamine degradation by catechol O-methyltransferase (COMT) to HVA (Blackstone, 2009, Figure 5-8). Elevated HVA levels are thus detectable in lumbar CSF neurotransmitter analysis. Dopamine transporter defects are not expected to affect the serotonin biosynthetic pathway so CSF 5-HIAA levels are normal in DTDS (and the ratio of CSF HVA: 5-HIAA ratio is thus increased). It is postulated that lack of dopamine re-uptake subsequently results in depleted pre-synaptic dopamine stores of intracellular dopamine to be packaged into synaptic vesicles for release into the synaptic cleft (Blackstone, 2009, Figure 5-8) and subsequent diffusion perisynaptically (Rice and Cragg, 2008). It is also postulated that excess synaptic dopamine may have effects on pre- and postsynaptic dopamine receptors. Overstimulation of presynaptic D<sub>2</sub> autoreceptors (D<sub>3</sub> receptors) may result in inhibition of phosphorylation dependent activation of tyrosine hydroxylase (the rate-limiting step in dopamine production) thus decreasing dopamine production (Blackstone, 2009, Figure 5-

8). Mutant mice lacking DAT and other monoamine transporters also show similar consequences of transporter dysfunction (reduced extracellular monoamine clearance rate, decreased amplitude of stimulated monoamine release, elevated basal extracellular monoamine levels, decreased monoamine storage, increased monoamine synthesis rate and disrupted autoreceptor function) (Gainetdinov and Caron, 2003). Excess extraneuronal dopamine may additionally have postsynaptic effects, such as downregulation or desensitisation of postsynaptic dopamine receptors, with alterations in downstream signalling (Figure 5-8). Knockout mouse models also show such evidence of postsynaptic receptor downregulation (Gainetdinov and Caron, 2003). D<sub>2</sub> receptor dysfunction may also be evident in children with DTDS. The reduced IBZM binding found on SPECT studies in patient 4 may be indicative of dopamine overflow (with enhanced dopamine levels competing for IBZM binding to D<sub>2</sub> receptors) but could also be secondary to reduced dopamine receptor density.

**Figure 5-8 (overleaf)**

*Diagram of a dopaminergic synapse postulating disease mechanisms in DTDS (adapted from Blackstone 2009). The presynaptic neuron, postsynaptic neuron and synaptic cleft are illustrated in the normal and DTDS disease state. Dopamine (indicated by orange circles) may bind presynaptically to D<sub>2</sub> autoreceptors, perisynaptically to DAT and postsynaptically to D<sub>1</sub> and D<sub>2</sub> receptors. D<sub>1</sub> and D<sub>2</sub> receptors are coupled to adenylyl cyclase (A) via G proteins (GP). Dopamine may also be metabolised to HVA by COMT and MAO-B. In DTDS, there is reduced DAT-mediated re-uptake of dopamine into the presynaptic cleft. This results in excess synaptic dopamine, which is converted by COMT to HVA. Excess synaptic dopamine may also overstimulate D<sub>2</sub> autoreceptors which will inhibit the activation of tyrosine hydroxylase, thereby reducing endogenous dopamine production. Prolonged dopamine in the synaptic cleft may also cause some downregulation/desensitisation of postsynaptic D<sub>1</sub> and D<sub>2</sub> receptors thereby altering downstream signalling.*

**Figure 5-8**  
Proposed disease mechanisms in DTDS (Adapted from Blackstone, 2009)



### 5.4.9 DTDS is a dopamine ‘transportopathy’

The majority of the monoamine neurotransmitter disorders (see Chapter 4.1.2) are due to inherited recessive inborn errors of metabolism of the pterin or monoamine biosynthetic pathway and neurotransmitter analysis reveals a reduction in CSF dopamine metabolites. In this chapter, the CSF neurotransmitter profile and pathophysiology of dopamine deficiency in DTDS is different to the other monoamine neurotransmitter disorders and thus allows us to add ‘transportopathy’ as a novel disease mechanism in this group of diseases (Blackstone, 2009). Indeed an increasing number of neurological diseases are attributed to inherited loss-of-function mutations in genes which encode other transporters, such as GLUT1 deficiency syndrome MIM #606777 (due to mutations in the gene encoding the glucose transporter, *SLC2A1*) (Brockmann, 2009) and hyperekplexia MIM #149400 (due to mutations in the gene encoding the presynaptic glycine transporter-2, *SLC6A5*) (Rees *et al.*, 2006)

### 5.4.10 Differences between DTDS and other related disorders

Although DTDS and other monoamine neurotransmitter disorders share some common features of dopamine deficiency (Chapter 4.1.2), clinical differences are evident. In some dopamine deficiency syndromes, the replenishment of dopamine stores during motor inactivity can lead to improvement of motor symptoms after a night’s sleep, and conversely, deterioration of symptoms over the afternoon and evening (Hoffmann *et al.*, 1998; Pearl *et al.*, 2007). Such diurnal variation of dystonic symptoms is not evident in this cohort of DTDS.

This is as predicted, as given the postulated pathogenic disease mechanism, dopamine transporter function is not expected to improve when neuronal dopamine stores are restored during a period of inactivity or rest. The extent of ocular features reported in this cohort appear specific to DTDS and have not been described in other disorders associated with dopamine deficiency (Assmann *et al.*, 2004, Kurian *et al.*, 2009). The exact pathogenic mechanism of the eye movement disorder remains unclear but may be caused by secondary brainstem involvement. The role of dopamine (and dopamine regulation) in aspects of early infantile brain development may also account for phenotypic differences between DTDS (and other infantile monoamine disorders) and adult-onset Parkinson's disease, in which pyramidal tract signs, prominent dystonia and such eye movement disorders are less commonly reported.

#### **5.4.11 DTDS and the *SLC6A3* knockout mouse model**

Despite the fundamental phenotypic differences between DTDS and DAT homozygous null mice, several of the early clinical findings are recapitulated in the mouse phenotype, which is characterised by hyperlocomotion/ hyperkinesis (Giros *et al.*, 1996) restlessness, irritability, feeding difficulties, growth retardation, sleep disturbance and cognitive delay (Gainetdinov *et al.*, 2003). The relative cognitive sparing seen in human DTDS may indicate that although DAT dysfunction may impact on some aspects of learning, it may not completely prevent some intellectual progress. Although the mouse model does not accurately recapitulate all aspects of the human DTDS movement disorder, choreiform and dystonic components are often observed in such mice during the first few months of life. This is accompanied by a loss of medium spiny

neurons of in the striatum. However, the hypokinetic features evident in older children with DTDS (secondary to progression of parkinsonism-dystonia) is not evident in the established knockout mouse model. Interestingly, if these mice are treated acutely with an inhibitor of the synthesis of dopamine (which does not behaviourally affect wild type mice) they display one of the best pharmacologically inducible and reversible parkinsonian symptoms ever seen in an animal model. It is possible that the observed differences in mice and humans may reflect a more highly developed extrapyramidal system in humans as is evident in other mouse models of human infantile onset movement disorders (Koeller *et al.*, 2002). However, this study may prompt further evaluation of disease semiology and evolution in DAT homozygous null mice as well as investigation of *SLC6A3/DAT1 knock-in* mice harbouring corresponding DTDS pathogenic mutations to understand their effects in a physiological context.

#### **5.4.12 Therapeutic strategies in DTDS**

Data from this DTDS cohort confirms that the vast majority of current medical and surgical therapeutic strategies do not correct the intraneuronal dopamine deficiency and have either little (and often temporary) or no impact on clinical symptomatology. In some neurotransmitter disorders, supplementation of L-dopa can result in clinical improvement and in some cases, even symptom reversal (see Chapter 4.1.4). However in DTDS, for the majority of patients, there was no clinical improvement with L-dopa and in fact, some patients had deterioration of motor symptoms. Only patient 9 and 11 showed a clear clinical

response to L-dopa (with improvement in motor symptoms) and interestingly both these patients' mutations displayed a degree of residual DAT activity. Analysis of more cases of DTDS will allow further investigation into whether the level of residual DAT activity in DTDS may actually be predict a patient's response to medication. Identification and analysis of further cases of DTDS will allow these outstanding issues to be addressed. The recent use of the dopamine receptor agonist ropinirole (utilised in adult onset Parkinson's disease, Matheson and Spencer, 2000) has resulted in short term benefits for two patients, but the wider impact of these agents in other children with DTDS and their impact on long term outcome remain yet to be determined. It is possible that optimum clinical benefit from treatment with dopamine agonists may require the instigation of therapy early in the disease course, before the hypothesised postsynaptic downregulation of downstream signalling. If there were to be neurodegenerative loss of dopamine terminals in DTDS, which is currently not known, early treatment with neuroprotective agents such as pramipexole or ropinirole could thus be beneficial. Although deep brain stimulation (DBS) targeting the GPi was of minimal benefit in one patient, it is conceivable that early DBS (which is increasingly used to treat paediatric movement disorders, Marks *et al.*, 2009) may have a future neuromodulatory role in DTDS.



## **5.5 Conclusion**

In Chapters 4 and 5, I have characterised the features of a novel and emerging neurotransmitter disorder. DTDS is a severe complex motor disorder and dopamine 'transportopathy' which is predicted to cause cerebral dopamine deficiency. Future identification of DTDS cases will expand the phenotypic spectrum, allow accurate diagnosis and genetic counselling, prevent unnecessary neurological investigations, provide further insight into genotype-phenotype correlations and facilitate molecular investigation of the consequences of DAT dysfunction. This multifaceted approach to understanding DAT-related disease mechanisms may then facilitate the development of novel therapeutic strategies to ameliorate the severe clinical symptoms in DTDS and other related/ parkinsonian phenotypes.

## **Chapter 6**

### ***PLA2G6-associated Neurodegeneration (PLAN)***

## 6.1 Introduction

Neurodegeneration with brain iron accumulation (NBIA) comprises a heterogeneous group of progressive complex motor disorders characterised by the presence of high brain iron, particularly within the basal ganglia. A number of autosomal recessive NBIA syndromes can present in childhood, including phospholipase A2 group 6 associated neurodegeneration (*PLA2G6-associated neurodegeneration*, PLAN). In this chapter, I have investigated a cohort of patients with *PLA2G6* mutations in order to define the clinical, radiological and genetic features of infantile PLAN.

### 6.1.1 Spectrum of NBIA disorders

Neurodegenerative disorders with brain iron accumulation encompass a wide spectrum of adult and paediatric neurological diseases. Although, the accumulation of iron within the basal ganglia and dentate nuclei is part of the normal ageing process (Gelman *et al.*, 2007), brain iron deposition is implicated in the pathogenesis of both common multifactorial neurodegenerative diseases and rarer inherited disorders.

Iron deposits have been demonstrated in the substantia nigra in Parkinson disease and within structures affected by  $\beta$  amyloid plaques in Alzheimer disease (Gerlach *et al.*, 2006; House *et al.*, 2007). Inherited monogenic NBIA disorders are also described and can be due to specific defects in iron metabolism. Autosomal dominant mutations in the ferritin light chain gene (*FTL1*) cause adult-onset neuroferritinopathy (Curtis *et al.*, 2001), a progressive movement disorder with features of chorea, dystonia and

parkinsonism (Burn and Chinnery, 2006). Aceruloplasminaemia is another adult-onset NBIA disorder of autosomal recessive inheritance, caused by mutations in the gene encoding ceruloplasmin, *CP* (Yoshida *et al.*, 1995). It is clinically characterised by a progressive extrapyramidal disorder, cerebellar ataxia, dementia, retinal degeneration and diabetes mellitus (McNeill *et al.*, 2008a). Recently NBIA has also been described in patients with a Kufoor-Rakeb phenotype associated with mutations in the *ATP13A2* gene (Schneider *et al.*, 2010).

NBIA may also present in childhood. Childhood NBIA comprises a clinically and genetically heterogeneous group of disorders, characterised predominantly by a progressive extrapyramidal phenotype, associated with excess deposition of brain iron (Gregory *et al.*, 2009). The two major NBIA phenotypes that present in childhood are classified as the autosomal recessive neuroaxonal dystrophies, and include pantothenate kinase associated degeneration (PKAN, caused by mutations in the *PANK2* gene) and PLA2G6-associated neurodegeneration (PLAN, caused by mutations in the *PLA2G6* gene). Mutations in these genes are thought to disrupt the normal cellular functions of phospholipid remodelling and fatty acid metabolism. Childhood NBIA is genetically heterogeneous and indeed a significant group of children with NBIA currently have no genetic diagnosis ('idiopathic NBIA'). It is likely that more, currently undetermined NBIA genes account for a number of these patients.

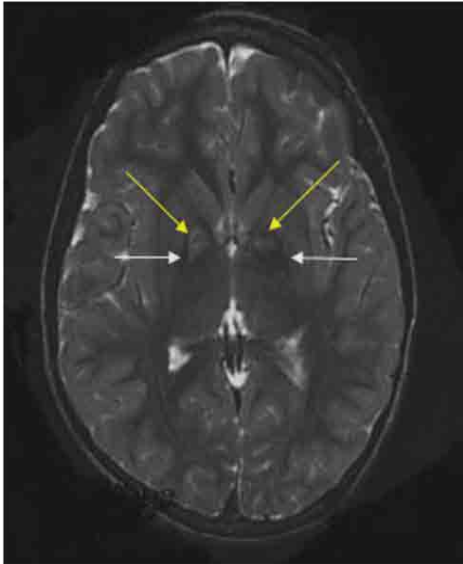
### 6.1.2 Radiological diagnosis of NBIA disorders

Brain iron accumulation is radiologically discernible and thus brain MRI is an important diagnostic tool and a major key to the diagnosis of NBIA disorders. Iron deposition characteristically appears as a pattern of reduced signal intensity (hypointensity) on T2, FLAIR (Fluid-attenuated inversion recovery), T2\* gradient, fast spin ECHO (FSE) and diffusion-weighted MRI (compared to age matched norms) in the globus pallidi and substantia nigra pars reticulata (Gregory *et al.*, 2009). Examples of MR images showing these features are illustrated in figure 6-1. T1 isointensity distinguishes the lesions from other changes (such as calcium deposition). Brain iron also appears as reduced density on CT neuroimaging (Kurian *et al.*, 2008). The specific pattern of iron accumulation helps to distinguish the various forms of NBIA (McNeill *et al.*, 2008b). In most cases of PKAN, abnormalities are restricted to the globus pallidus and substantia nigra and the majority of cases display the eye-of-the-tiger sign. In PLAN, globus pallidus and substantia nigra are involved on T2\* and FSE scans with dentate involvement seen only on T2\*. By contrast, the dentate nuclei, globus pallidus and putamen appear to be consistently involved in neuroferritopathy, with confluent areas of hyperintensity (due to probable cavitation) involving the pallida and putamen in approximately half of cases. Some patients with neuroferritinopathy also have changes in the caudate nuclei and thalami. More uniform involvement of the basal ganglia and the thalami (without cavitation) is typical in aceruloplasminaemia.

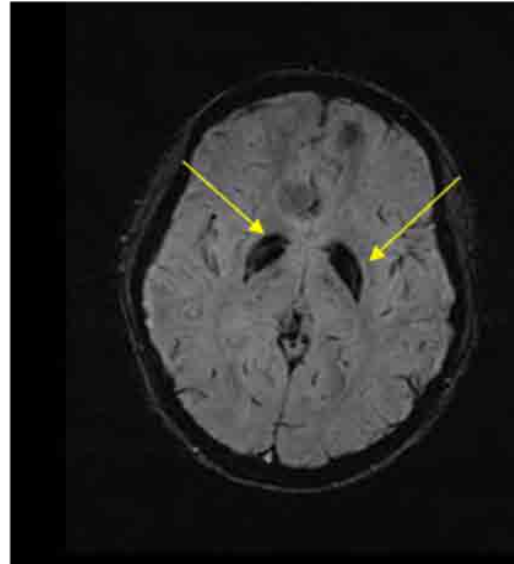
**Figure 6-1****Examples of MR Images of NBIA disorders**

- 6-1A Patient age 5.9 years, classical PKAN. Axial T2-weighted FSE (fast spin echo) sequences showing bilateral eye-of-the-tiger sign with a medial central hyperintense region (yellow arrow) surrounding a region of hypointensity (white arrow) in the globus pallidi
- 6-1B Patient, age 12 years, childhood PLAN. Axial susceptibility-weighted image showing abnormal low signal in the globus pallidi
- 6-1C Patient, age 9 years, idiopathic NBIA. Axial T2-weighted gradient echo image showing abnormal low signal in the globus pallidi
- 6-1D Patient age 12 years, idiopathic NBIA. Axial T2-weighted image (contrast enhanced fast field echo, FFE) showing reduction in T2 signal in the substantia nigra

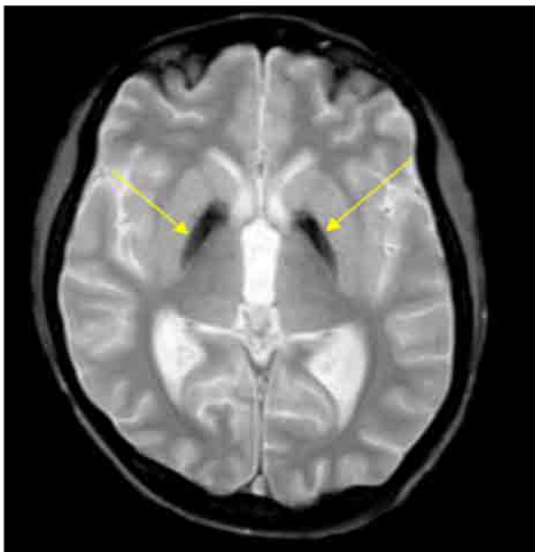
6-1A



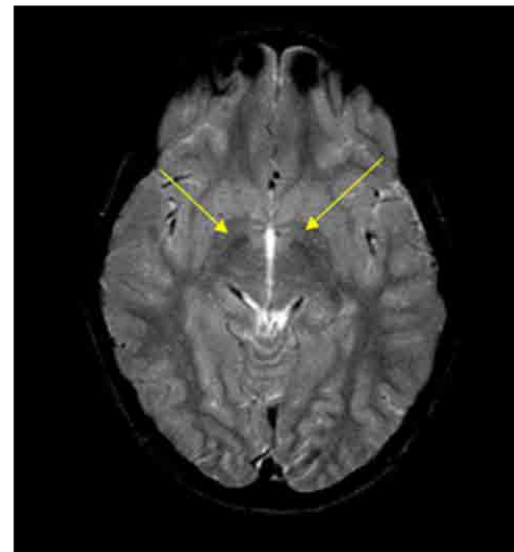
6-1B



6-1C



6-1D



## 6.2 PKAN

PKAN is one of the two major NBIA disorders of childhood and shows phenotypic overlap with PLAN. The clinical features of this related disorder will thus be discussed in detail below. PKAN (MIM #606157) accounts for approximately 50% of childhood NBIA disorders. It has a proposed prevalence rate of between 1 and 3 per million population (Gregory *et al.*, 2009).

### 6.2.1 Clinical syndromes

#### 6.2.1.1 Typical PKAN

The clinical features of PKAN have been delineated by large cohort studies of patients from North America (Hayflick *et al.*, 2003) and Western Europe (Hartig *et al.*, 2006). Two thirds of PKAN cases have a classical phenotype, with a relatively homogenous presentation. The majority (88%) of cases clinically present before 6 years of age but there is great variability in age of presentation (range 0.5-12 years). Affected children are often thought to be dyspraxic or clumsy prior to neurological presentation and the majority of patients present initially with gait or postural problems secondary to dystonia (Gregory *et al.*, 2009). Extrapyrimal features predominate in the disease course (dystonia in 87%). The almost universal presence of oromandibular dystonia and dysarthria in PKAN patients was highlighted by Hartig *et al.*, (2006). Corticospinal tract signs are also common, resulting in hypertonicity, hyperreflexia, spasticity and upgoing plantar responses. Though a movement disorder is the most prominent manifestation of PKAN, both visual impairment

and cognitive dysfunction contribute to the burden of disability. The majority also have retinitis pigmentosa which can lead to significant visual impairment (Hayflick *et al.*, 2003) and cataracts can also develop. Patients with PKAN have a wide range of cognitive abilities, but tests of both IQ and adaptive behaviour indicate that cognition declines with disease progression (Freeman *et al.*, 2007). The natural history of classical PKAN is for stepwise regression, with periods of clinical stability interspersed with periods of neurological deterioration. There is no correlation of neurological deterioration with periods of catabolic stress such as intercurrent infection. The majority of patients (85%) become non-ambulant within 15 years after diagnosis (Hartig *et al.*, 2006). Later complications include dysphagia (resulting in feeding difficulties), gastroesophageal reflux and constipation. Death is usually secondary to cardiorespiratory complications (chest infections, aspiration pneumonia), the secondary deleterious effects of malnutrition and rarely status dystonicus.

#### **6.2.1.2 Atypical PKAN**

Patients with atypical PKAN are on average significantly older at presentation with a mean age of 14 years (range 1–28, Hayflick *et al.*, 2003; Hartig *et al.*, 2006). Atypical PKAN shows significant phenotypic overlap with atypical PLAN and idiopathic NBIA disorders. In such patients, speech difficulties (such as palilalia or dysarthria) are common presenting features although mild gait disturbance and neuropsychiatric presentation (with emotional lability, personality change, aggression, impulsivity, obsessive-compulsive disorder and depression) are also described. Motor and vocal tics and obsessions suggestive of Tourette syndrome have also been described



(Pellecchia *et al.*, 2005). Almost a third of patients with atypical disease manifest psychiatric problems, behavioural difficulties or a frontotemporal like dementia early in their disease. Most atypical PKAN patients, over time, develop an extrapyramidal phenotype, although the dystonia is thought to be less severe than that seen in classical disease (Hayflick *et al.*, 2003). Rarely movement phenotypes may be evident on initial presentation. An adult onset pure akinesia (Molinuevo *et al.*, 2003), early onset-parkinsonism, focal hand dystonia and intermittent severe dystonia have been reported (Zhou *et al.*, 2005). Corticospinal tract signs and freezing of gait are also prevalent. Retinitis pigmentosa is also described in atypical disease although it is less prevalent than in classical disease. Atypical PKAN is less aggressive than classical disease, and most patients remain ambulant into adulthood.

#### **6.2.1.3 HARP syndrome**

The HARP (hypoprebetalipoproteinaemia, acanthocytosis, retinitis pigmentosa and pallidal degeneration) syndrome is caused by *PANK2* mutations and is part of the PKAN spectrum (Ching *et al.*, 2002).

#### **6.2.2 Radiological features of PKAN**

The characteristic imaging feature is the ‘eye-of-the-tiger’ sign (Figure 6-1A), defined as a medial area of hyperintensity within a hypointense globus pallidus (Hayflick *et al.*, 2003). Cases of PKAN may also have hypointensity of the substantia nigra (Gregory *et al.*, 2009). There are however reports of patients with *PANK2* mutations without this classical radiological sign (Zolkipli *et al.*, 2006). Although the majority of patients with *PANK2* mutations have

this radiological sign, patients with an NBIA phenotype and an ‘eye-of-the-tiger’ sign who are *PANK2* mutation negative are also described (Kumar *et al.*, 2006). The ‘eye-of-the-tiger’ is also observed in conditions other than PKAN, including multiple system atrophy (Strecker *et al.*, 2007), neuroferritinopathy (McNeill *et al.*, 2008b) and progressive supranuclear palsy (Kumar *et al.*, 2006). The sign, whilst diagnostically useful, must be interpreted correctly in clinical context.

### 6.2.3 Neurological Investigations in PKAN

Full blood count will reveal acanthocytosis in 8% of patients (Hayflick *et al.*, 2003). ERG can demonstrate subclinical retinopathy in a significant proportion of patients (Egan *et al.*, 2005). Ocular motility studies show hypometric slowed saccadic eye movements. Ophthalmological examination also reveals sluggish papillary reactions with sectoral iris paralysis and partial loss of the papillary ruff (Gregory *et al.*, 2009).

### 6.2.4 Molecular genetics of PKAN

PKAN is caused by mutations in the Pantothenate Kinase 2 (*PANK2*) gene (Zhou *et al.*, 2001). The *PANK2* gene codes for the enzyme pantothenate kinase 2, which phosphorylates pantothenate, the initial rate limiting step in Co-enzyme A biosynthesis. Co-enzyme A has a vital role in ATP synthesis, fatty acid and neurotransmitter metabolism. The *PANK2* enzyme has a mitochondrial targeting sequence and is localised to mitochondria in human brain. Mitochondrial dysfunction is proposed to result from *PANK2* mutations, leading to neurodegeneration. The neurotoxic metabolites cysteine and

pantetheine are substrates for *PANK2*, and abnormal *PANK2* function will lead to their accumulation. Cysteine is a potent iron chelator, and it is proposed that high local cysteine levels lead to secondary iron accumulation. Iron accumulation will exacerbate neuronal injury by inducing oxidative stress. There is no animal model of PKAN which satisfactorily recapitulates the human phenotype. A *Drosophila melanogaster* with deficient *PANK2* has defects in cell division leading to sterility and is also described as uncoordinated with impaired ability to climb (Yang *et al.*, 2005). A knockout mouse model of PKAN develops retinal degeneration and azoospermia (Kuo *et al.*, 2005). However, the mice do not develop a movement disorder despite being followed up to 12 months of age, and neither MRI nor brain histology demonstrated iron accumulation. It is possible that the other PANK isoforms (1, 3 and 4) compensate for *PANK2* loss in knockout mice. Deprivation of dietary pantothenate causes a movement disorder proposed to be dystonia in wild type mice (Kuo *et al.*, 2007).

Mutations have been identified in all 7 exons of the *PANK2* gene. The majority of *PANK2* variants are missense mutations, evenly distributed across the conserved domains of *PANK2*. Deletions and splice site variants are also described (Hayflick *et al.*, 2003). The amount of residual enzyme activity in the mutated *PANK2* enzyme influences disease severity, with earlier disease onset in patients with homozygous null mutations and later disease onset in patients with mutations which allow residual enzyme activity (Pellecchia *et al.*, 2005). Globally the 1561G>A missense mutation is the most common cause of PKAN, and homozygotes have classical PKAN (Hartig *et al.*, 2006). This

mutation has been described on a background of a shared haplotype, suggestive of a founder effect. The other most common identified mutations are 1583C>T and 1351C>T. In about 10 % of cases only 1 mutated allele can be detected, and it is believed that intragenic deletions, duplications and possibly mutations in the promoter or regulatory regions may account for a proportion of these cases.

## **6.3 PLAN**

### **6.3.1 Discovery of a second NBIA locus**

In 2006, Morgan and colleagues undertook autozygosity mapping studies in a UK-based extended consanguineous Pakistani kindred with multiple affected members with NBIA. In this family, microsatellite marker analysis of the PKAN locus excluded linkage to the *PANK2* gene. Subsequent genome-wide linkage analysis using microsatellite markers identified a minimal region of linkage of 4.9Mb on chromosome, 22q12-q13 between D22S426 and D22S276 containing the disease locus (LOD score 4.65). During the same time period, Hayflick and colleagues also undertook parallel genome-wide linkage studies (using microsatellite markers) in 12 families with INAD (infantile neuroaxonal dystrophy), and mapped a novel disease-locus to a 6.0Mb region of chromosome 22q12.3-q13.2 (LOD score 4.78). In view of the common region of linkage, it was hypothesised that both the NBIA variant and INAD would be allelic, thus defining a new disease locus on chromosome 22.

### 6.3.2 Identification of *PLA2G6* mutations in NBIA and INAD

Screening of candidate genes from this region on chromosome 22 was subsequently undertaken, initially in 3 families with INAD and in the extended kindred with NBIA. After sequencing 70 of the 100 genes in the region, germline mutations in *PLA2G6* were identified in all 4 kindreds. *PLA2G6* mutations were identified in 28 additional probands with INAD, and in individuals with Karak syndrome (Morgan *et al.*, 2006). A total of 44 unique mutations were identified, suggesting that *PLA2G6* was the causative gene in the majority of cases of infantile neuroaxonal dystrophy and also in some cases of 'idiopathic' NBIA (Morgan *et al.*, 2006).

### 6.3.3 PLAN is clinically heterogeneous

It is now evident that PLAN comprises a phenotypically diverse group of autosomal recessive neurodegenerative disorders associated with genetic defects in the *PLA2G6* gene. Following gene identification in 2006 the phenotypic spectrum of *PLA2G6*-related disorders has expanded and is becoming increasingly defined. There are currently 3 distinct phenotypes which may be classified according to the average age of disease presentation

- **Infantile PLAN**

*Classical infantile neuroaxonal dystrophy, INAD, MIM #256600*

- **Childhood PLAN**

*Atypical neuroaxonal dystrophy and Karak syndrome, MIM #610217*

- **Adult PLAN**

*Early-onset dystonia-parkinsonism, MIM #612953*

In order to better define the clinical phenotype of infantile PLAN, a cohort of children with *PLA2G6* mutations was investigated. All clinical phenotypes of PLAN are subsequently discussed in detail in the Discussion section (Chapter 6.6)

## **6.4 Materials and methods**

### **6.4.1 Clinical assessment**

#### **6.4.1.1 Case acquisition**

14 children with mutations in the *PLA2G6* gene consistent with a phenotype of infantile onset PLAN were identified from the National *PLA2G6* Diagnostic Screening Service (West Midlands Regional Genetic Laboratory). Informed consent was obtained from all participants and the study was approved by local ethics research committees.

#### **6.4.1.2 Clinical phenotyping**

All children with PLAN were clinically assessed by myself (8 children) or another paediatric neurologist. The patient's medical case notes were analysed in order to delineate the clinical features on history and examination. Where available, video footage of the children was also examined. CT and brain MRI of 17 patients were examined independently by me and two consultant paediatric radiologists to determine the radiological features seen in this disorder (with consensus agreement on disparities). Neurological investigations including electroencephalogram (EEG), nerve conduction studies (NCS), electromyogram (EMG), visual evoked potentials

(VEP) and skin/sural nerve biopsy were also undertaken in some patients and the results of these were also ascertained from the medical notes.

#### **6.4.2 Molecular genetic investigation**

*PLA2G6* mutation analysis was kindly undertaken by the West Midlands Regional Genetic Laboratory as part of the routine diagnostic service. DNA was extracted from peripheral lymphocytes using standard techniques. PureGene (Gentra) chemistry was used to extract DNA from those samples received as blood. DNA samples were quantified using the NanoDrop-1000 Spectrophotometer (LabTech, Sussex UK). The complete coding region of the *PLA2G6* gene, including all splice junctions, was amplified and sequenced from genomic DNA using primers for exons 1-6, 8, 11 and 13-15 designed by Dr Neil Morgan, Department of Medical & Molecular Genetics, University of Birmingham. Primers for exons 7, 9, 10, 12, 16 and 17 were designed using Primer3 software. Primers were analysed using the National Genetics Reference laboratory Manchester Diagnostic SNP Check software (<http://ngrl.man.ac.uk/SNPCheck/>) in order to identify any single nucleotide polymorphisms (SNPs) lying under the primer binding site. Previously unreported putative mutations were evaluated by demonstrating appropriate segregation within families, absence in more than 200 ethnically matched control patients and conservation of normal amino acid throughout lower species.

## **6.5 Results**

### **6.5.1 Clinical phenotype of PLAN**

#### **6.5.1.1 Family history**

14 children (5 boys and 9 girls) from nine families were studied. The majority of children in this cohort (11 children) were of Pakistani origin, 2 were British Caucasian, and 1 child was of Arabic origin. 8 children from 4 families were born to consanguineous parents. 8/14 children were found to have a similarly affected relative. There was a history of an unexplained death in childhood within the extended family in 6/14 cases.

#### **6.5.1.2 Presenting clinical symptoms and signs**

All children in this cohort presented with psychomotor regression following a normal infancy. They were born following an uneventful pregnancy, had a normal perinatal history and normal early developmental milestones. The median age at symptom presentation was 14 months (range 12–22 months). Initial symptom presentation followed a respiratory illness in 4 children. Of these, two had further profound neurologic regression and motor skill loss after subsequent intercurrent infections. All children presented with motor and cognitive skill regression and global developmental delay. All patients developed bulbar dysfunction within 7 years of presentation. Axial hypotonia was evident in all children by age 8 years. Spasticity was evident in all children within 15 months of presentation. Thirteen children developed contractures by 6 years of age. Spinal deformities such as kyphoscoliosis developed in 10/14 children. Dystonia developed in all patients. All children



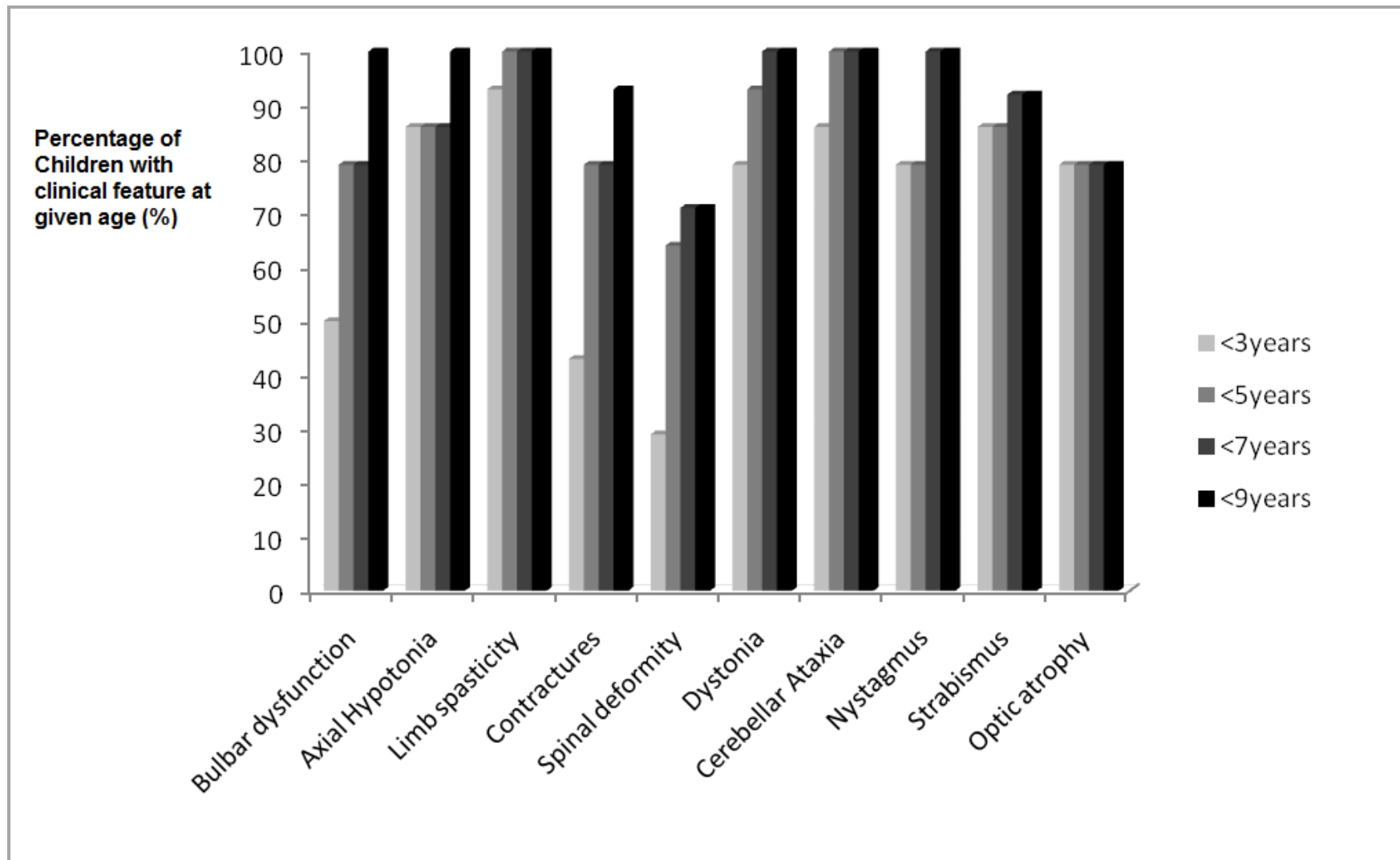
had cerebellar features within 5 years of clinical presentation. Acquired strabismus was found in 13 children. Clinical ophthalmology examination revealed optic atrophy in 11 patients. None of the children were dysmorphic and epilepsy was not reported in this cohort. Microcephaly (occipitofrontal circumference below third percentile) was found in only two children. The age at onset of each clinical feature is summarized in Table 6-1. The development of neurological features in this cohort is illustrated in Figure 6-2.

#### **6.5.1.3 Disease progression**

After presentation, all children demonstrated rapid symptom progression, with further evidence of neurologic regression and increasing motor disability. The described clinical features became increasingly severe in all patients. To date, five children have died; mean age at death was 9.1 years (range 6.5–14 years).

**Figure 6-2**

*Development of neurological features in the PLAN cohort*



**Table 6-1**  
**Age of onset of clinical features for patients in the PLAN cohort**

Patient	Cognitive and motor regression	Bulbar dysfunction	Axial hypotonia	Limb spasticity	Contractures	Spinal deformity	Dystonia	Cerebellar Ataxia	Nystagmus	Strabismus	Optic Atrophy
1	15m	7y	18m	18m	4y	4y	18m	18m	18m	18m	18m
2	22m	3y2m	2y	3y2m	3y2m	3y2m	3y10m	3y2m	3y10m	2y	2y
3	12m	12m	15m	15m	15m	15m	15m	15m	15m	15m	15m
4	12m	3y10m	15m	15m	4y2m	4y2m	15m	15m	2y	15m	15m
5	15m	15m	18m	18m	6y	6y	18m	4y	4y	18m	18m
6	15m	4y	18m	18m	18m	4y	18m	18m	18m	18m	18m
7	12m	8y	8y	2y6m	4y	A	7y	12m	2y6m	3y	A
8	12m	8y	8y	2y	A	A	36m	15m	15m	A	A
9	18m	18m	21m	21m	21m	A	2y	21m	21m	21m	21m
10	12m	12m	15m	15m	6y	A	15m	15m	15m	15m	15m
11	18m	18m	20m	20m	20m	20m	20m	20m	20m	20m	20m
12	12m	12m	15m	15m	15m	15m	15m	5y6m	5y6m	15m	15m
13	18m	4y5m	22m	22m	4y	4y	22m	22m	22m	22m	22m
14	13m	13m	16m	16m	16m	16m	18m	16m	16m	16m	A

m months  
y years  
A clinical feature absent

### 6.5.2 Radiological findings

Patients 1–13 in the cohort had brain imaging. Patient 14 did not have brain imaging studies. All available brain scans were reviewed and the findings summarised in Table 6-2. Initial imaging (some including diffusion and T2\* gradient MR sequences) was undertaken during active neuroregression, at a median time of 1.8 years after first clinical presentation. Cerebellar cortical atrophy was universally present (mean age 4.2 years) as illustrated by Figure 6-3. Imaging of all patients showed either high signal on T2-weighted or FLAIR MR sequences or reduced density on CT imaging, indicative of cerebellar cortical gliosis (Figure 6-3). The extent of this gliosis was variable and most marked in Patient 6 (the oldest child in the cohort). Patient 13 showed borderline changes of cerebellar cortical gliosis, but the patient was only 3.8 years when imaging was performed and no subsequent imaging was available for comparison.

#### **Figure 6-3**

*MR Imaging of patient 4, age 5.8 years: axial FLAIR (6-3A) and coronal T2-weighted (6-3B) sequences showing cerebellar cortical atrophy and gliosis, with increased CSF spaces around the cerebellum and increased signal on T2 and FLAIR sequences in the residual cortex of the cerebellum*

Figure 6-3A

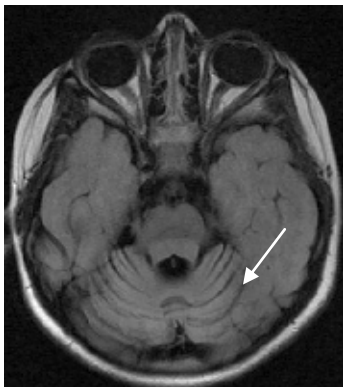
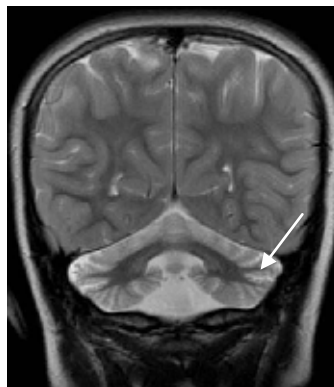


Figure 6-3B

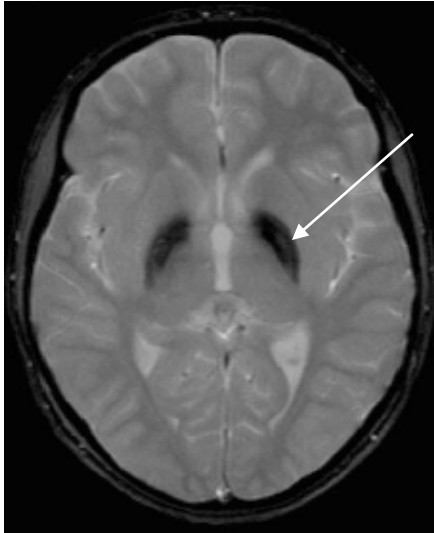
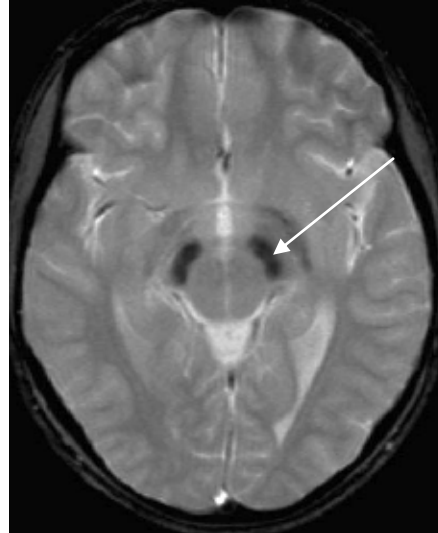
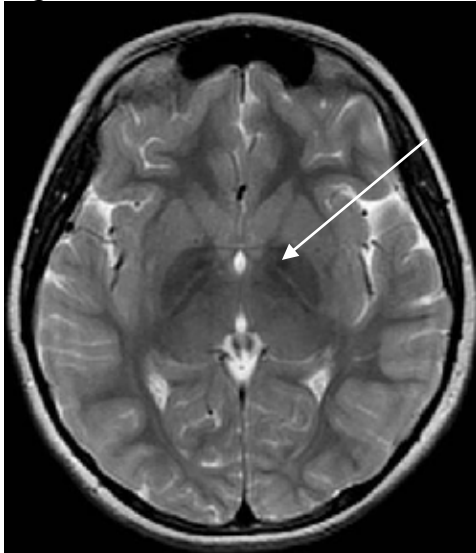
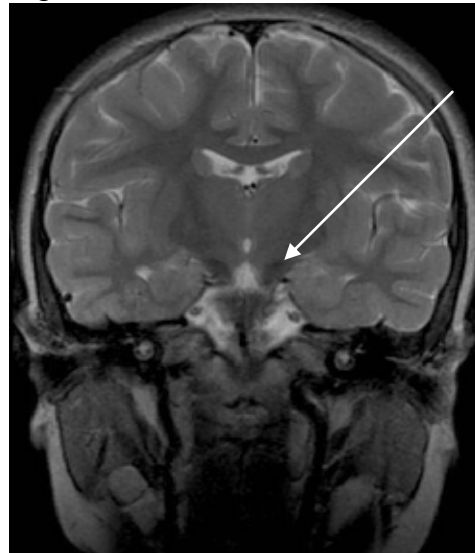


10/13 children had evidence of increased iron deposition in the globus pallidi seen as reduced signal on T2, FLAIR, and T2\* gradient and diffusion weighted MR sequences (Figure 6-4) or as reduced density on CT imaging compared to age-matched norms. This hypointensity was most apparent in the medial aspect of the globus pallidus in 5/10 children, the others showing more diffuse globus pallidal changes. 6/10 children showed globus pallidal changes on the initial scan (performed at a mean age of 5.9 years). 4/10 children did not have, or showed borderline changes in the globus pallidi on initial MR imaging (performed at a mean age of 2.4 years). However, definite changes were detected on subsequent scans performed 1-3 years later. From our cohort, it appears that the globus pallidal changes are more severe with increasing age (Figure 6-5). Increased iron deposition in the globus pallidus was not evident in 3 children; these children had brain imaging at a mean age of 2.8 years with no subsequent scans to date.

10/13 patients had MR scans of sufficient quality to assess imaging changes of increased iron in the substantia nigra (Figure 6-4). 4 of these patients showed such changes on imaging performed at a mean age of 7.2 years. 3/10 showed borderline changes on imaging performed at a mean age of 3 years 5 months. 3/10 patients had early scans with normal signal in the substantia nigra, developing abnormal signal on later imaging performed over 5 years of age.

**Figure 6-4**

MR imaging of patient 6, age 13.9 years (6-4A and 6-4B) and patient 4, age 5.9 years (6-4C and 6-4D). Axial T2\* gradient sequences (6-4A, 6-4B, 6-4C) and coronal T2-weighted sequence (6-4D) showing marked reduction in T2 signal in the globus pallidi (6-4A,6-4C) and more medially on 6-4C and substantia nigra (6-4B,6-4D). The degree of iron deposition is much more marked in patient 6 (the older child) compared to patient 4

**Figure 6-4A****Figure 6-4B****Figure 6-4C****Figure 6-4D**

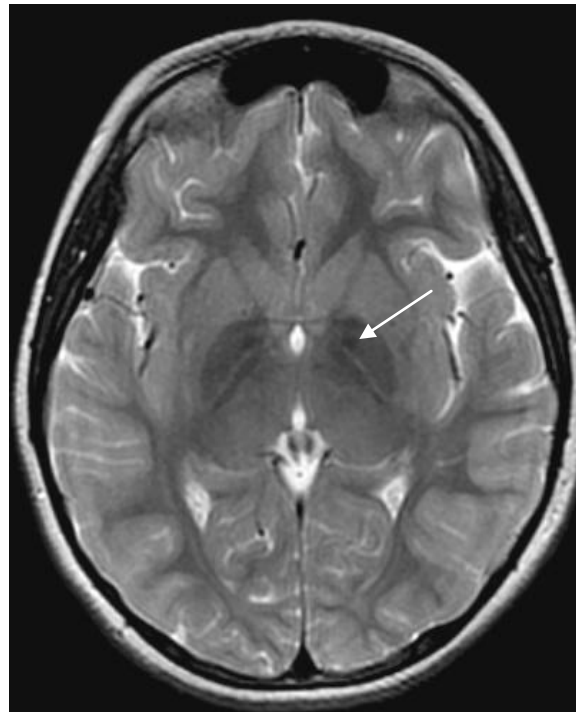
**Figure 6-5**

*MR imaging: Axial T2-weighted sequences in 3 children within the cohort. The abnormal reduced signal in the globus pallidi increases in severity with increasing age*

6-5A  
Age 3.8 years



6-5B  
Age 5.9 years



6-5C  
Age 13.8 years



Three additional features were identified. 8 children showed reduced volume in the optic chiasm and optic nerves, suggesting optic pathway atrophy. Borderline optic atrophy was evident in three further children. Cerebral white matter changes were present in 7 of the 12 patients with imaging affording adequate assessment (Table 6-2). The posterior corpus callosum was almost universally abnormal, with a simple appearance to the splenium, which was thin, elongated, and slightly vertically orientated (Figure 6-6).

**Figure 6-6**

*MR imaging: Sagittal T1-weighted sequence showing thin, elongated and vertical orientation of the splenium (posterior) corpus callosum (long arrow). Note marked atrophy of the vermis of the cerebellum (short arrow)*  
*Patient 4, age 2.3 years*





**Table 6-2**  
**Radiological findings in the cohort**

Patient	Scan Type	Age (years)	Cerebellar Atrophy	Cerebellar gliosis	Low signal/density globus pallidus	Low signal/density substantia nigra/subthalamic nuclei	Cerebral white matter	Optic pathway atrophy	Corpus callosum
1	CT	4.9	+	+	+	I	-	I	I
	MR	7.4	+	+	+	I	I	I	I
2	MR	4.0	+	+	+	+	H	B	B
3	CT	1.9	+	+	-	I	-	I	I
	MR	2.5	+	+	B	-	H	B	S
	MR	5.3	+	+	+	+	H	B	S
4	MR	2.3	+	+	-	-	-	+	S
	MR	5.8	+	+	+	+	-	+	S
5	MR	2.3	+	+	B	-	-	-	S
	MR	3.3	+	+	+	-	H	+	S
	MR	5.2	+	+	+	B	H A	+	S A
6	MR	13.7	+	+	++	++	H A	+	S A
7	MR	3.3	+	+	-	B	-	+	S
8	MR	2.3	+	+	-	B	-	+	S
9	MR	3.3	+	+	+	I	H A	+	S
10	MR	6.0	+	+	+	I	A	+	S A
11	MR	2.8	+	+	-	-	-	-	S
12	MR	3.4	+	+	(-)	-	-	B	B
	CT	6.1	+	+	+	I	A	I	I
13	MR	3.8	+	B	+	-	-	+	S

**KEY**

+ Changes present  
B Borderline changes  
- Changes absent

I Imaging quality or type not suitable to assess feature  
H High (mild) T2 MR signal in cerebral white matter  
A Atrophy  
S Simple splenium (posterior) corpus callosum

### **6.5.3 Results of other investigations**

#### **6.5.3.1 Neurophysiology and histology**

On EEG, widespread high amplitude fast activity (at 16 to 22 Hz) was seen in 71.4% (5/7) of patients who had this investigation. EMG signs of denervation were seen in all seven children who had this investigation. Of these seven children, a distal axonal-type sensorimotor neuropathy was evident in 43% (3/7) of patients who had NCS. Absent or delayed VEP were seen in 7/8 children examined. Histological examination of sural nerve and skin tissue was undertaken in 4 patients. 3 children showed features of axonal swelling and spheroid body formation on skin biopsy. One patient had negative findings on both skin and sural nerve examination.

#### **6.5.3.2 Other investigations**

As all patients presented with neuroregression (associated with intercurrent illness in some cases), detailed investigation was undertaken (prior to diagnosis) to rule out an inborn error of metabolism. Children in this cohort had the following tests: blood glucose, lactate, amino acids, acid/base status, ammonia, CK, carnitine, acylcarnitine profile, very long chain fatty acids, uric acid, B12, folate, cholesterol, isoelectric focusing of transferrin, biotinidase, lysosomal enzymes; urine amino acids, organic acids, oligosaccharides, and mucopolysaccharide screen; CSF glucose, lactate, amino acids, and neurotransmitters. Neurometabolic investigations did not indicate the presence of a metabolic disorder.

### 6.5.4 Results of molecular genetic investigation

Details of the genetic findings are reported in Table 6-3. 13 patients had missense mutations (9 of whom were homozygous for p.Lys545Thr). No clinical or radiological differences were apparent between p.Lys545Thr mutation cases and the rest.

**Table 6-3**  
**Mutations identified in the cohort**

Patient	Ethnicity	Parents Related	Mutation(s)	State	Effect on protein product	Mutation(s) reported
1	Pakistani	Yes	c.1634A>C	Homozygous	p.Lys545Thr	Morgan <i>et al.</i> , 2006
2	Pakistani	Yes	c.1634A>C	Homozygous	p.Lys545Thr	Morgan <i>et al.</i> , 2006
3	Pakistani	No	c.1634A>C	Homozygous	p.Lys545Thr	Morgan <i>et al.</i> , 2006
4	Pakistani	No	c.1634A>C	Homozygous	p.Lys545Thr	Morgan <i>et al.</i> , 2006
5	British Caucasian	No	c.2221C>T	Heterozygous	p.Arg741Trp	Morgan <i>et al.</i> , 2006
6	Pakistani	Yes	c.1634A>C	Homozygous	p.Lys545Thr	Morgan <i>et al.</i> , 2006
7	Pakistani	Yes	c.1634A>C	Homozygous	p.Lys545Thr	Morgan <i>et al.</i> , 2006
8	Pakistani	Yes	c.1634A>C	Homozygous	p.Lys545Thr	Morgan <i>et al.</i> , 2006
9	Arabic	No	c.719T>C c.1978C>A	Compound heterozygote	p.Leu240Pro p.Pro660Thr	Kurian <i>et al.</i> , 2008
10*	Pakistani	No	c.109C>T	Heterozygous	p.Arg37X	Morgan <i>et al.</i> , 2006
11	British Caucasian	No	c.1103C>A c.1417G>T	Compound heterozygote	p.Ala368Asp p.Glu473X	Kurian <i>et al.</i> , 2008
12	Pakistani	Yes	c.1634A>C	Homozygous	p.Lys545Thr	Morgan <i>et al.</i> , 2006
13	Pakistani	Yes	c.1634A>C	Homozygous	p.Lys545Thr	Morgan <i>et al.</i> , 2006
14	Pakistani	Yes	c.905T>G	Homozygous	p.Met302Arg	Kurian <i>et al.</i> , 2008

(\*) Maternal DNA – one mutation detected. DNA on affected patient and father was not available

## 6.6 Discussion

Infantile neuroaxonal dystrophy (INAD) was reported as a clinical entity almost 50 years ago (Cowen & Olmstead, 1963) and cohorts of patients have been frequently reported (Aicardi and Castelein, 1979; Nardocci *et al.*, 1999). Since gene identification, the term *PLA2G6*-associated neurodegeneration (PLAN) has been adopted to account for this subgroup of patients as well as the other different phenotypes associated with this gene.

### 6.6.1 Clinical features of infantile PLAN

In this chapter, detailed review of the clinical and radiologic features of 14 cases has allowed delineation of this homogeneous infantile PLAN phenotype. Infantile PLAN is thus characterised by the onset of rapidly progressive psychomotor regression in children, with disease onset under 2 years of age (Gregory *et al.*, 2008; Kurian *et al.*, 2008). In this cohort, intercurrent illness triggered symptom presentation in some cases, thus mimicking the clinical presentation of a metabolic disorder. This finding suggests that it is important to include infantile PLAN in the differential diagnosis of inborn errors of metabolism. Gait disturbance and axial hypotonia as well as visual features (nystagmus, new-onset strabismus and optic atrophy) were also frequently reported in the early stages of disease. During the first decade, children develop a spastic tetraparesis with symmetrical pyramidal tract signs (initially with hyperreflexia and later with areflexia), spinal deformities and limb contractures. Bulbar dysfunction was evident in the majority of this cohort by 5 years of age. Extrapyr

features such as dystonia were also prominent with increasing age. Although not evident in this cohort, generalised seizures have also been frequently reported and in certain populations, may be an early disease feature (Wu *et al.*, 2009). Over time, children demonstrated progressive neurological regression, worsening spasticity, ongoing cognitive decline and worsening visual impairment, resulting in a vegetative state. Death occurred around the end of the first decade and is usually secondary to cardiorespiratory complications, infection, malnutrition and rarely status dystonicus (Gregory *et al.*, 2009).

### **6.6.2 Radiological features of infantile PLAN**

This study also confirmed that features on MRI brain can aid diagnosis of infantile PLAN (Tanabe *et al.*, 1993; Farina *et al.*, 1999). Cerebellar atrophy is a universal feature and often the earliest sign on MRI (Gregory *et al.*, 2008). In this cohort, cerebellar gliosis was also commonly present (increasing in severity with age, Kurian *et al.*, 2008) but not all patients have this feature (Biancheri *et al.*, 2007). Atrophy of the cerebellum is associated with secondary posterior corpus callosum abnormalities with evidence of a simple vertically orientated, thin elongated splenium. Many children (40-50%) also have evidence of brain iron accumulation with increased iron deposition in the globus pallidi (particularly in the medial aspect of the globus pallidus), dentate nuclei and substantia nigra (Gregory *et al.*, 2009). In the described cohort of children, the iron accumulation also appeared to become increasingly severe with age (Kurian *et al.*, 2008). There were also features of optic pathway

atrophy (reduced volume of the optic chiasm and optic nerves) and evidence of cerebral white matter changes.

### 6.6.3 Features on neurological investigation of infantile PLAN

Other investigations also aided diagnosis (Carrilho *et al.*, 2008), such as characteristic high amplitude fast activity on EEG, denervation on EMG, distal axonal-type sensorimotor neuropathy on NCS and absent/delayed, reduced amplitude VEP. Histological features of axonal swelling and spheroid body formation are evident on skin, sural nerve, conjunctiva, rectal or muscle biopsy (Gregory *et al.*, 2009). Dystrophic axons viewed by electron microscopy exhibit membranotubular profiles, mitochondrial aggregates and axons with increased diameter and a thinned membrane. As in one case in this cohort, negative biopsy results are commonly reported (Ramaekers *et al.*, 1987). Biopsy at an age prior to the development of pathologic changes or biopsy from a site where changes are not evident may both account for the absence of dystrophic axons in such patients (Morgan *et al.*, 2006). Less than a third of in this cohort had histological tissue analysis as, in recent years, the availability of molecular genetic testing has eliminated the need for invasive biopsy in the majority of cases.

### 6.6.4 Other PLAN phenotypes

Since gene identification, *PLA2G6* has been investigated in a number of neurological conditions and *PLA2G6* mutations have been described in a further two 'PLAN' phenotypes.

#### 6.6.4.1 Childhood onset PLAN

A subgroup of patients with childhood onset PLAN has been described (Gregory *et al.*, 2008). This is much rarer than infantile PLAN and includes the condition previously described as Karak syndrome (Mubaidin *et al.*, 2003). To date, 8 cases have been reported (Morgan *et al.*, 2006; Gregory *et al.*, 2008). The clinical phenotype appears more heterogeneous than infantile PLAN but will be increasingly characterised as more atypical cases are recognised and diagnosed. Childhood onset PLAN has a later disease onset (1.5-6.5 years, mean age 4.4 years) and tends to present more insidiously with slower disease progression than that observed in infantile PLAN. Subtle gait abnormalities (instability and ataxia), dyspraxia and speech regression are common presenting features. Diminished social communication and peer interaction is particularly evident in this phenotype, with the result that some affected children have been misdiagnosed with autism prior to the onset of detectable neurological symptoms and signs (L. Cif, personal communication, 2009). Over time, children develop optic atrophy, nystagmus, tetraparesis (with joint contractures) and seizures similar to children with infantile PLAN. However, other features of infantile PLAN (such as early truncal hypotonia and strabismus) have not been described in childhood PLAN. This phenotype shows considerable phenotypic overlap with adolescent/adult NBIA phenotypes. Extrapyrarnidal features (of dystonia and dysarthria) and neuropsychiatric disturbances (emotional lability, compulsivity, hyperactivity, reduced attention span, neurobehavioural disturbances) become major features later in the disease course, reminiscent of the clinical phenotype of

idiopathic NBIA and PKAN (Chapter 6.2). The lifespan of atypical PLAN is not currently determined. Cerebellar atrophy and gliosis may be evident in this group of patients. Brain iron accumulation is a consistent universal feature of childhood PLAN, involving both globus pallidus and substantia nigra. Fast rhythms of EEG have not been reported in childhood PLAN although some children may develop EEG changes consistent with an epileptic process. VEPs may be delayed with reduced amplitude. EMG/NCS and ERG are normal. Histopathological findings are identical to that described for classical PLAN.



#### **6.6.4.2 Adult onset PLAN**

*PLA2G6* mutations have also recently been described in a third subgroup of patients with a phenotype of autosomal recessive dystonia-parkinsonism (Paisan-Ruiz *et al.*, 2009; Sina *et al.*, 2009). Such affected individuals with adult PLAN are from consanguineous kindreds and all have homozygous missense *PLA2G6* mutations. To date, patients from 4 consanguineous kindreds with this adult PLAN phenotype have been described. Affected individuals are born following a normal pregnancy and had normal milestones. Symptom presentation occurs in late adolescence/early adulthood (age 18–26 years) with features of subacute dystonia-parkinsonism (facial hypomimia, generalised rigidity, cogwheeling, pill rolling resting tremor, bradykinesia and dystonia) associated with the evolution of pyramidal signs. Patients also develop eye movement abnormalities, including eye lid opening apraxia, blepharoclonus, square wave jerks in the primary position, jerky saccadic pursuit, supranuclear vertical gaze palsy and hypometric vertical



saccades. Rapid cognitive decline results in impaired intellectual function, visual memory and executive function. Personality changes are also reported. Cerebellar symptoms and signs are absent. All patients are initially responsive to dopaminergic therapy (L-dopa or dopamine agonists), although early development of dyskinesia has been reported. On radiological investigation, unlike infantile/ childhood PLAN, no cerebellar or basal ganglia abnormalities are noted. MRI brain scans are initially either normal, or show features of non-specific mild generalised volume loss or increased white matter signal intensity on T2 FLAIR around the frontal horns. A DaTSCAN showed markedly reduced uptake in both striata.

The above discussion highlights the number of clinical similarities between the various forms of PKAN and PLAN. The different subgroups of PKAN and PLAN are compared and contrasted in Table 6-4 and 6-5. The key for Table 6-4 and 6-5 is as follows:-

	<b>PLAN</b>
	<b>PKAN</b>
<b>++</b>	<b>Clinical feature commonly described in this phenotype</b>
<b>+</b>	<b>Clinical feature sometimes described</b>
<b>(+)</b>	<b>Clinical feature only rarely described</b>
<b>-</b>	<b>Clinical feature more commonly absent in this phenotype</b>
<b>L</b>	<b>May be a late feature of disease</b>
<b>N</b>	<b>Normal in majority of cases</b>

**Table 6-4 Comparison of the clinical features of PKAN and PLAN**

Clinical Feature	Infantile PLAN	Childhood PLAN	Adult PLAN	Classical PKAN	Atypical PKAN
Average age Presentation	0.5–2 years Mean age 1.3 years	1.5–6.5 years Mean age 4.4 years	18-26 years	0.5-12 years Mean age 3.4 years	1-28 years Mean age 13.7 years
Common Presenting Features	Gait disturbance Psychomotor regression	Gait disturbance Speech delay ↓ social interaction	Dystonia- parkinsonsim Spasticity	Gait/postural disturbance Dyspraxia	Gait disturbance Speech disturbance Psychiatric symptoms
Axial Hypotonia	++	-	-	-	-
Limb spasticity	++	++	++	+	+
Contractures/ Spinal deformity	++	++	-	+	+
Dystonia	++	++	++	++	++
Parkinsonism	-	-	++	(+)	(+)
Bulbar Dysfunction	++	++	++	++	+
Cerebellar signs (ataxia, nystagmus)	++	++	-	-	-
Squint	++	-	-	-	-
Optic Atrophy	++	++	-	(+)	-
Retinitis pigmentosa	-	-	-	++	+
Neuropsychiatric Features	-	++	++	(+)	++
Seizures	+ L	+ L	-	-	-
Expected rate of disease progression	Rapid - Ambulation loss <5 years after presentation	Slower	Variable	Rapid - Ambulation loss <15 years after presentation	Slower. Ambulation loss 15-40 years after presentation
Estimated life expectancy	End of 1st decade Mean age of death 9.1 yrs	Undetermined	Undetermined	Variable	Variable

**Table 6-5 Comparison of the features of PKAN and PLAN on investigation**

	Infantile PLAN	Childhood PLAN	Adult PLAN	Classical PKAN	Atypical PKAN
<b>RADIOLOGICAL FEATURES</b>					
Cerebellar Atrophy	++	+	-	-	-
Cerebellar Gliosis	++	(+)	-	-	-
Brain iron in globus pallidus	+	++	-	++ 'Eye-of-the-tiger' sign	++ 'Eye-of-the-tiger' sign
Brain iron in substantia nigra/ subthalamic nuclei	+	++	-	++	++
Cerebral White matter changes	+ (Atrophy)	-	+ (Atrophy)	-	-
Optic pathway atrophy	++	+	-	-	-
Corpus callosum abnormal	++	(+)	-	-	-
<b>NEUROLOGICAL INVESTIGATION</b>					
EEG	Fast rhythm Epileptiform changes	No fast rhythm Epileptiform changes	N	N	N
EMG	Denervation	Denervation L	N	N	N
NCS	Distal axonal sensory motor neuropathy L	Distal axonal sensory motor neuropathy L	N	N	N
VEP	Delayed Reduced amplitude	Delayed Reduced amplitude L	N	N	N
ERG	N	N	N	++ Retinopathy	+ Retinopathy
Skin/ Sural/ Rectal Nerve Biopsy	Axonal swelling and spheroid bodies	Axonal swelling and spheroid bodies	N	N	N
<b>GENETIC INVESTIGATION</b>					
Appropriate Genetic Investigation	<i>PLA2G6</i>	<i>PLA2G6</i>	<i>PLA2G6</i>	<i>PANK2</i>	<i>PANK2</i>

### 6.6.5 Postulated function of *PLA2G6*

*PLA2G6* encodes a calcium-independent phospholipase enzyme iPLA2-VIA which catalyzes the hydrolysis of glycerophospholipids at the sn-2 position generating a free fatty acid, usually arachidonic acid and a lysophospholipid (Balsinde and Balboa, 2005). The iPLA2-VIA protein is active as a tetramer with proposed roles in phospholipids metabolism, arachidonic acid release, and leukotriene and prostaglandin synthesis. Levels of phosphoditylcholine, abundant in mammalian cell membranes and essential in maintaining cell membrane integrity, are regulated by the opposing actions of CTP:cytidylphosphocholine transferase and iPLA2-VIA (Tanaka *et al.*, 2004). Defects in iPLA2-VIA could lead to a relative abundance of membrane phosphoditylcholine and secondary structural abnormalities. Current evidence also suggests that iPLA2-VIA-derived lysophosphatidylcholine may play a prominent role in mediating the chemoattractant and recognition/engulfment signals that accompany the process of apoptotic cell death. iPLA2-VIA may also be involved in the control of arachidonic acid levels within cells, which may provide important signals for the onset of apoptosis. It may also contribute to the effective clearance of dying cells by circulating phagocytes (Balsinde *et al.*, 2006). Defects in iPLA2-VIA thus cause abnormalities in cell membrane structure and affect apoptosis, which may underlie the axonal pathology and high brain iron seen in this disorder. Recently, *PLA2G6* knock-out mouse models have been developed which display several phenotypic features that are evident in the human phenotype (Shinzawa *et al.*, 2008; Malik *et al.*, 2008; Wada *et al.*, 2009). Impaired phospholipid metabolism has

also been implicated in the pathogenesis of the other major NBIA disorder of childhood, PKAN (Gregory *et al.*, 2005, Hayflick *et al.*, 2006). It is thus possible that the phenotypic overlap seen in these conditions may be reflective of similarities in their underlying aetiologies.

### 6.6.6 Genetic features of PLAN

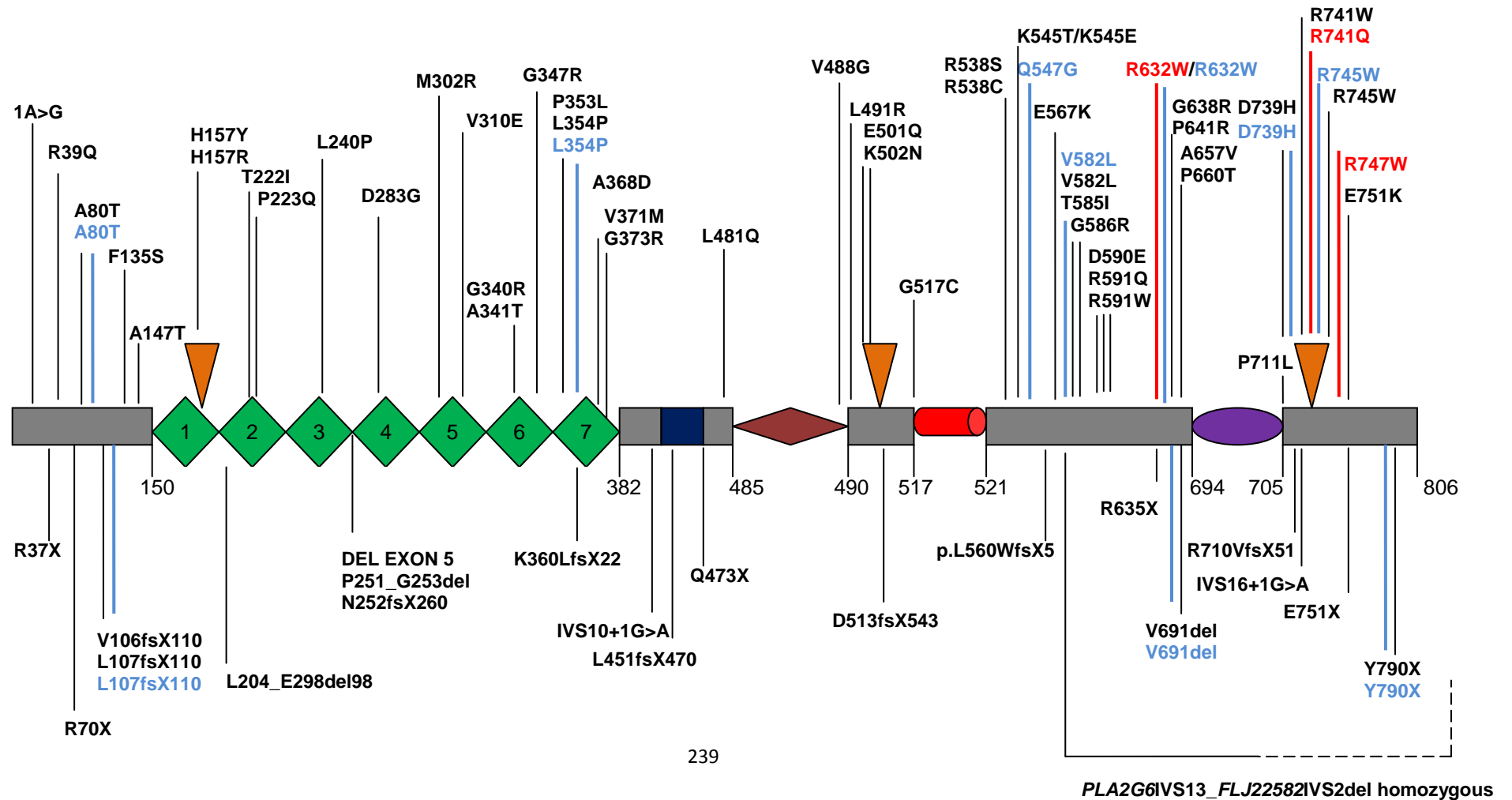
As illustrated by the findings in this cohort, the majority of *PLA2G6* variants detected in PLAN are missense mutations but insertions, deletions, nonsense mutations and splice site mutations are also described (Gregory *et al.*, 2008). The mutations reported in the literature to date are illustrated in Figure 6-7. In our cohort, despite extensive investigation only one mutation was identified (p.Arg741Trp) in patient 5. It is possible that the other mutation may be in a promoter region, embedded deep within an intronic sequence or a heterozygous deletion which would be undetected by standard direct sequencing methodology. Indeed recent local collaborative work I have undertaken has identified pathogenic copy number variants (detected by MLPA, multiplex ligation-dependent probe amplification) in infantile PLAN (Crompton *et al.*, 2010). It is estimated that copy number variants account for up to 12.5% *PLA2G6* mutations in PLAN. MLPA may thus be a useful technique (and adjunct to direct sequencing) to detect copy number variants in patients who show clinical features of PLAN but in whom both disease-causing mutations are not identified on routine sequencing.

Analysis of this cohort is further confirmation of the current observation that genotype is a relatively weak predictor of phenotype. Although no definitive

genotype-phenotype correlations are evident, it been proposed that patients with two null mutations are more likely to have infantile PLAN, while compound heterozygotes (for two missense mutations) are more likely to have childhood PLAN (Gregory *et al.*, 2009). There also appears to be an increased proportion of missense *PLA2G6* mutations (located towards the 3' end of the coding sequence) in atypical and adult onset PLAN. The variable phenotypic presentation of PLAN may depend on a combination of 'allelic heterogeneity' (i.e. type of mutation and effect on protein function) as well as genetic and environmental modifier effects (Hayflick, 2009).

### Figure 6-7

Schematic representation of PLA2G6 protein structure (adapted from Balsinde & Balboa 2005, Morgan et al., 2006) and reported PLA2G6 mutations (Morgan et al., 2006, Kurian et al 2008, Gregory et al 2008, Carrilho et al 2008, Paisan Ruiz et al 2009, Sina et al 2009, Wu et al 2009, Crompton et al 2010). The protein consists of 7 ankyrin repeats (green), a proline-rich motif (dark blue), a glycine rich nucleotide binding site (brown), a lipase motif (red), a putative C-terminus calcium-dependent calmodulin binding site (purple) and three proposed caspase cleavage sites (orange). Numbers indicate amino acids. Missense mutations are indicated above the protein and deletions, duplications, nonsense, and splice site mutations are indicated below the protein. Mutations described in infantile PLAN (black), childhood PLAN (light blue) and adult PLAN (red) are illustrated



## 6.7 Conclusion

Advances in molecular genetics have contributed to increased understanding and definition of NBIA disorders. In this chapter, analysis of this infantile PLAN cohort should facilitate the future identification of patients who are most likely to have a *PLA2G6* mutation. Careful assessment of the natural history and radiologic features has allowed the proposal of clinical and radiologic criteria, which in conjunction with molecular genetic analysis can provide early definitive diagnosis of this neurodegenerative disorder.

It is thus evident that the childhood NBIA disorders PKAN and PLAN are becoming increasingly well defined clinical syndromes with genetic aetiologies. However, there are a number of patients and families with NBIA syndromes (who are negative for *PANK2* and *PLA2G6* mutations) in whom a genetic aetiology has not been determined. Recently at the American Society of Human Genetics Annual Meeting (2009) Hartig *et al.*, presented an abstract describing a cohort of Polish patients with mutations in a novel NBIA gene on chromosome 19 (*MIN*) which is postulated also to have a role in phospholipid metabolism. Hayflick *et al.*, have also recently identified mutations in a novel gene for patients with radiological features of NBIA and pontocerebellar atrophy (Hayflick, personal communication, 2010). Childhood NBIA is thus clinically and genetically heterogeneous and it is extremely likely that in the future, more genes accounting for a number of these NBIA syndromes will be identified.



There are currently no curative treatments for NBIA disorders and therapeutic strategies focus on supportive measures (such as the medical and surgical management of spasticity, dystonia, seizures and nutrition) to improve patient quality of life. In the future, a detailed knowledge of the natural history of PLAN may help evaluate potential therapeutic interventions. Understanding the mechanisms of pathogenesis may additionally contribute to our understanding of more common neurodegenerative disorders with iron dyshomeostasis (such as Parkinson and Alzheimer disease, Zecca *et al.*, 2004) as well as providing targets for neuroprotection strategies in this group of neurodegenerative disorders.

## **Chapter 7**

### **References**

- Aicardi, J. and Goutieres, F. (1978) Encéphalopathie myoclonique néonatale. **Rev. EEG Neurophysiol.** 8 (1): 99-101
- Aicardi, J. and Castelein, P. (1979) Infantile neuroaxonal dystrophy. **Brain.** 102 (4): 727-748
- Aicardi, J. (1992) "Early myoclonic encephalopathy". In: Roger, J., Bureau, M., Dravet, C., Dreifuss, F.E., Perret, A. and Wolf, P. (eds.) **Epileptic syndromes in infancy, childhood and adolescence.** 2<sup>nd</sup> ed. London: John Libbey. pp. 13-23
- Aicardi, J. and Ohtahara, S. (2002) "Severe neonatal epilepsies with suppression-burst pattern". In: Roger, J., Bureau, M., Dravet, C., Genton, P., Tassinari, C. and Wolf, P. (eds.) **Epileptic Syndromes in Infancy, Childhood and Adolescence.** 3<sup>rd</sup> ed. Eastleigh: John Libbey. pp. 33-44
- Aird, R.B. (1994) **Foundations of Modern Neurology: A Century of Progress.** New York: Raven Press
- Alexander, G.E. and Crutcher, M.D. (1990) Functional architecture of basal ganglia circuits: neural substrates of parallel processing. **Trends Neurosci.** 13 (7): 266-271
- Aligianis, I.A., Johnson, C.A., Gissen, P. *et al.* (2005) Mutations of the catalytic subunit of RAB3GAP cause Warburg Micro syndrome. **Nat Genet.** 37 (3): 221-223
- Aligianis, I.A., Morgan, N.V., Mione, M. *et al.* (2006) Mutation in Rab3 GTPase-activating protein (RAB3GAP) noncatalytic subunit in a kindred with Martolf syndrome. **Am J Hum Genet.** 78 (4): 702-707
- Amir, R.E., Van den Veyver, I.B., Wan, M. *et al.* (1999) Rett syndrome is caused by mutations in X-linked MECP2, encoding methyl-CpG-binding protein 2. **Nat Genet.** 23 (2): 185-188
- Anden, N.E., Carlsson, A., Dahlstroem, A. *et al.* (1964) Demonstration and mapping out of nigro-neostriatal dopamine neurons. **Life Sci.** 3: 523-530
- Ashwal, S. (1990) **The Founders of Child Neurology.** San Francisco: Norman Publishing
- Assmann, B., Köhler, M., Hoffmann, G.F. *et al.* (2002) Selective decrease in central nervous system serotonin turnover in children with dopa-nonresponsive dystonia. **Pediatr Res.** 52 (1): 91-94
- Assmann, B., Surtees, R. and Hoffmann, G.F. (2003) Approach to the diagnosis of neurotransmitter diseases exemplified by the differential diagnosis of childhood-onset dystonia. **Ann Neurol.** 54 Suppl 6: S18-S24

- Assmann, B.E., Robinson, R.O., Surtees, R.A. *et al.* (2004) Infantile Parkinsonism-dystonia and elevated dopamine metabolites in CSF. **Neurology**. 62 (10): 1872-1874
- Avallone, J., Gashi, E., Magrys, B. *et al.* (2006) Distinct regulation of metabotropic glutamate receptor (mGluR1 $\alpha$ ) in the developing limbic system following multiple early-life seizures. **Exp Neurol**. 202 (1): 100-111
- Balsinde, J. and Balboa, M.A. (2005) Cellular regulation and proposed biological functions of group VIA calcium-independent phospholipase A2 in activated cells. **Cell Signal**. 17 (9): 1052-1062
- Balsinde, J., Perez, R. and Balboa, M.A. (2006) Calcium-independent phospholipase A2 and apoptosis. **Biochim Biophys Acta**. 1761 (11): 1344-1350
- Bandmann, O., Goertz, M., Zschocke, J. *et al.* (2003) The phenylalanine loading test in the differential diagnosis of dystonia. **Neurology**. 60 (4): 700-702
- Banerjee, P.N., Filippi, D. and Allen Hauser, W. (2009) The descriptive epidemiology of epilepsy - a review. **Epilepsy Res**. 85 (1): 31-45
- Bannon, M.J. (2005) The dopamine transporter: role in neurotoxicity and human disease. **Toxicol Appl Pharmacol**. 204 (3): 355-360
- Baulac, S., Huberfeld, G., Gourfinkel-An, I. *et al.* (2001) First genetic evidence of GABA(A) receptor dysfunction in epilepsy: a mutation in the gamma2-subunit gene. **Nat Genet**. 28 (1): 46-48
- Ben-Ari, Y., Khazipov, R., Leinekugel, X. *et al.* (1997) GABAA, NMDA and AMPA receptors: a developmentally regulated ménage à trois. **Trends Neurosci**. 20 (11): 523-529
- Berg, A.T., Berkovic, S.F., Brodie, M.J. *et al.* (2010) Revised terminology and concepts for organization of seizures and epilepsies: report of the ILAE Commission on Classification and Terminology, 2005-2009. **Epilepsia**. 51 (4): 676-685
- Bergeron, L. and Yuan, J. (1998) Sealing one's fate: control of cell death in neurons. **Curr Opin Neurobiol**. 8 (1): 55-63
- Bergman, H., Feingold, A., Nini, A. *et al.* (1998) Physiological aspects of information processing in the basal ganglia of normal and parkinsonian primates. **Trends Neurosci**. 21 (1): 32-38
- Berkovic, S.F., Harkin, L., McMahon, J.M. *et al.* (2006) De-novo mutations of the sodium channel gene SCN1A in alleged vaccine encephalopathy: a retrospective study. **Lancet Neurol**. 5 (6): 488-492

- Bertani, I., Rusconi, L., Bolognese, F. *et al.* (2006) Functional consequences of mutations in CDKL5, an X-linked gene involved in infantile spasms and mental retardation. **J Biol Chem.** 281 (42): 32048-32056
- Beuming, T., Shi, L., Javitch, J.A. *et al.* (2006) A comprehensive structure-based alignment of prokaryotic and eukaryotic neurotransmitter/Na<sup>+</sup> symporters (NSS) aids in the use of the LeuT structure to probe NSS structure and function. **Mol Pharmacol.** 70 (5): 1630-1642
- Biancheri, R., Rossi, A., Alpigiani, G. *et al.* (2007) Cerebellar atrophy without cerebellar cortex hyperintensity in infantile neuroaxonal dystrophy (INAD) due to PLA2G6 mutation. **Eur J Paediatr Neurol.** 11 (3): 175-177
- Bienvenu, T., Poirier, K., Friocourt, G. *et al.* (2002) ARX, a novel Prd-class-homeobox gene highly expressed in the telencephalon, is mutated in X-linked mental retardation. **Hum Mol Genet.** 11 (8): 981-991
- Biervert, C., Schroeder, B.C., Kubisch, C. *et al.* (1998) A potassium channel mutation in neonatal human epilepsy. **Science.** 279 (5349): 403-406
- Bittles, A.H., and Neel J.V. (1994) The costs of human inbreeding and their implications for variations at the DNA level. **Nat Genet.** 8 (2): 117-121
- Bittles, A. (2001) Consanguinity and its relevance to clinical genetics. **Clin Genet.** 60 (2): 89-98
- Blackstone, C. (2009) Infantile parkinsonism-dystonia: a dopamine "transportopathy". **J Clin Invest.** 119 (6): 1455-1458
- Blennow, M., Zeman, J., Dahlin, I. *et al.* (1995) Monoamine neurotransmitters and metabolites in the cerebrospinal fluid following perinatal asphyxia. **Biol Neonate.** 67 (6): 407-413
- Bockenbauer, D., Feather, S., Stanescu, H.C. *et al.* (2009) Epilepsy, ataxia, sensorineural deafness, tubulopathy, and KCNJ10 mutations. **N Engl J Med.** 360 (19): 1960-1970
- Böhm, D., Schwegler, H., Kotthaus, L. *et al.* (2002) Disruption of PLC-beta 1-mediated signal transduction in mutant mice causes age-dependent hippocampal mossy fiber sprouting and neurodegeneration. **Mol Cell Neurosci.** 21 (4): 584-601
- Botstein, D., White, R.L., Skolnick, M. *et al.* (1980) Construction of a genetic linkage map in man using restriction fragment length polymorphisms. **Am J Hum Genet.** 32 (3): 314-331
- Bowton, E., Saunders, C., Erreger, K. *et al.* (2010) Dysregulation of dopamine transporters via dopamine D2 autoreceptors triggers anomalous

- dopamine efflux associated with attention-deficit hyperactivity disorder. **J Neurosci.** 30 (17): 6048-6057
- Bräutigam, C., Wevers, R.A., Jansen, R.J. *et al.* (1998) Biochemical hallmarks of tyrosine hydroxylase deficiency. **Clin Chem.** 44 (9): 1897-1904.
- Bräutigam, C., Weykamp, C., Hoffmann, G.F. *et al.* (2002) Neurotransmitter metabolites in CSF: an external quality control scheme. **J Inherit Metab Dis.** 25 (4): 287-298
- Brenner, M., Johnson, A.B., Boespflug-Tanguy, O. *et al.* (2001) Mutations in GFAP, encoding glial fibrillary acidic protein, are associated with Alexander disease. **Nat Genet.** 27 (1): 117-120
- Brockmann, K. (2009) The expanding phenotype of GLUT1-deficiency syndrome. **Brain Dev.** 31 (7): 545-552
- Broman, K.W., Murray, J.C., Sheffield, V.C. *et al.* (1998) Comprehensive human genetic maps: individual and sex-specific variation in recombination. **Am J Hum Genet.** 63 (3): 861-869
- Brown, P. (2007) Abnormal oscillatory synchronisation in the motor system leads to impaired movement. **Curr Opin Neurobiol.** 17 (6): 656-664
- Brunelli, S., Faiella, A., Capra, V. *et al.* (1996) Germline mutation in the homeobox gene EMX2 in patients with severe schizencephaly. **Nat Genet.** 12 (1): 94-96
- Brunner, H.G., Nelen, M., Breakefield, X.O. *et al.* (1993) Abnormal behavior associated with a point mutation in the structural gene for monoamine oxidase A. **Science.** 262 (5133): 578-580
- Bugiani, M., Al Shahwan, S., Lamantea, E. *et al.* (2006) GJA12 mutations in children with recessive hypomyelinating leukoencephalopathy. **Neurology.** 67 (2): 273-279
- Bundey, S. and Alam, H. (1993) A five-year prospective study of the health of children in different ethnic groups, with particular reference to the effect of inbreeding. **Eur J Hum Genet.** 1 (3): 206-219
- Burn, J., and Chinnery, P.F. (2006) Neuroferritinopathy. **Semin Pediatr Neurol.** 13 (3): 176-181
- Carlsson, A., Lindqvist, M., Magnusson, T. *et al.* (1958) On the presence of 3-hydroxytyramine in the brain. **Science.** 127 (3296): 471
- Carlsson, A. (1959) The occurrence, distribution and physiological role of catecholamines in the nervous system. **Pharmacol Rev.** 11 (2, Part 2): 490-493

- Carlsson, A. (1987) Perspectives on the discovery of central monoaminergic neurotransmission. **Annu Rev Neurosci.** 10: 19-40
- Carlsson, A. (2001) A paradigm shift in brain research. **Science.** 294 (5544): 1021-1024
- Carrilho, I., Santos, M., Guimarães, A. *et al.* (2008) Infantile neuroaxonal dystrophy: what's most important for the diagnosis? **Eur J Paediatr Neurol.** 12 (6): 491-500
- Castaldo, P., del Giudice, E.M., Coppola, G. *et al.* (2002) Benign familial neonatal convulsions caused by altered gating of KCNQ2/KCNQ3 potassium channels. **J Neurosci.** 22 (2): RC199
- Charbit, A.R., Akerman, S. and Goadsby, P.J. (2010) Dopamine: what's new in migraine? **Curr Opin Neurol.** 23 (3): 275-281
- Charlier, C., Singh, N.A., Ryan, S.G. *et al.* (1998) A pore mutation in a novel KQT-like potassium channel gene in an idiopathic epilepsy family. **Nat Genet.** 18 (1): 53-55
- Chechlac, M. and Gleeson, J.G. (2003) Is mental retardation a defect of synapse structure and function? **Pediatr Neurol.** 29 (1): 11-17
- Chen, N., Zhen, J. and Reith, M.E. (2004a) Mutation of Trp84 and Asp313 of the dopamine transporter reveals similar mode of binding interaction for GBR12909 and benztropine as opposed to cocaine. **J Neurochem.** 89 (4): 853-864
- Chen, N., Rickey, J., Berfield, J.L. *et al.* (2004b) Aspartate 345 of the dopamine transporter is critical for conformational changes in substrate translocation and cocaine binding. **J Biol Chem.** 279 (7): 5508-5519
- Chen, N. and Reith, M.E.A. (2007) Substrates and inhibitors display different sensitivity to expression level of the dopamine transporter in heterologously expressing cells. **J Neurochem.** 101 (2): 377-388
- Chen, N. and Reith, M.E. (2008) Substrates dissociate dopamine transporter oligomers. **J Neurochem.** 105 (3): 910-920
- Chenn, A. and Walsh, C.A. (2002) Regulation of cerebral cortical size by control of cell cycle exit in neural precursors. **Science.** 297 (5580): 365-369
- Chiken, S., Shashidharan, P. and Nambu, A. (2008) Cortically evoked long-lasting inhibition of pallidal neurons in a transgenic mouse model of dystonia. **J Neurosci.** 28 (51): 13967-13977
- Ching, K.H., Westaway, S.K., Gitschier, J. *et al.* (2002) HARP syndrome is allelic with pantothenate kinase associated neurodegeneration. **Neurology.** 58 (11): 1673-1674

- Choi, S.Y., Chang, J., Jiang, B. *et al.* (2005) Multiple receptors coupled to phospholipase C gate long-term depression in visual cortex. **J Neurosci.** 25 (49): 11433-11443
- Claes, L., Del-Favero, J., Ceulemans, B. *et al.* (2001) De novo mutations in the sodium-channel gene *SCN1A* cause severe myoclonic epilepsy of infancy. **Am J Hum Genet.** 68 (6): 1327-1332
- Claes, L., Ceulemans, B., Audenaert, D. *et al.* (2003) De novo *SCN1A* mutations are a major cause of severe myoclonic epilepsy of infancy. **Hum Mutat.** 21 (6): 615-621
- Commission on Classification and Terminology of the International League Against Epilepsy (ILAE) (1993) Guidelines for epidemiologic studies on epilepsy Commission on Epidemiology and Prognosis. **Epilepsia.** 34 (4): 592-596
- Cook, E.H. Jr, Stein, M.A., Krasowski, M.D. *et al.* (1995) Association of attention-deficit disorder and the dopamine transporter gene. **Am J Hum Genet.** 56 (4): 993-998
- Coppola, G., Plouin, P., Chiron, C. *et al.* (1995) Migrating partial seizures in infancy: a malignant disorder with developmental arrest. **Epilepsia.** 36 (10): 1017-1024
- Coppola, G., Veggiotti, P., Del Giudice, E.M. *et al.* (2006) Mutational scanning of potassium, sodium and chloride ion channels in malignant migrating partial seizures in infancy. **Brain Dev.** 28 (2): 76-79
- Coppola, G. (2009) Malignant migrating partial seizures in infancy: an epilepsy syndrome of unknown etiology. **Epilepsia.** 50 Suppl 5: 49-51
- Cossette, P., Liu, L., Brisebois, K. *et al.* (2002) Mutation of *GABRA1* in an autosomal dominant form of juvenile myoclonic epilepsy. **Nat Genet.** 31 (2): 184-189
- Cowen, D. and Olmstead, E.V. (1963) Infantile neuroaxonal dystrophy. **J Neuropathol Exp Neurol.** 22: 175-236
- Crompton, D., Rehal, P.K., MacPherson, L. *et al.* (2010) Multiplex ligation-dependent probe amplification (MLPA) analysis is an effective tool for the detection of novel intragenic *PLA2G6* mutations: implications for molecular diagnosis. **Mol Genet Metab.** 100 (2): 207-212
- Crow, Y.J. and Livingston, J.H. (2008) Aicardi-Goutieres syndrome: an important Mendelian mimic of congenital infection. **Dev Med Child Neurol.** 50 (6): 410-416



- Crow, Y.J. and Rehwinkel, J. (2009) Aicardi-Goutieres syndrome and related phenotypes: linking nucleic acid metabolism with autoimmunity. **Hum Mol Genet.** 18 (R2): R130-R136
- Curtis, A.R., Fey, C., Morris, C.M. *et al.* (2001) Mutation in the gene encoding ferritin light polypeptide causes dominant adult-onset basal ganglia disease. **Nat Genet.** 28 (4): 350-354
- Dahlstroem, A. and Fuxe, K. (1964) Evidence for the existence of monoamine-containing neurons in the central nervous system: I. Demonstration of monoamines in the cell bodies of brain stem neurons. **Acta Physiol Scand Suppl.** 232 (62): 1-55
- Dalla Bernardina, B., Dulac, O., Fejerman, J. *et al.* (1983) Early myoclonic epileptic encephalopathy. **Eur J Pediatr.** 140 (3): 248-252
- Darr, A. and Modell, B. (1988) The frequency of consanguineous marriage among British Pakistanis. **J Med Genet.** 25 (3): 186-190
- De Camilli, P., Emr, S.D., McPherson, P.S. *et al.* (1996) Phosphoinositides as regulators in membrane traffic. **Science.** 271 (5255): 1533-1539
- De Carvalho Aguiar, P., Sweadner, K.J., Penniston, J.T. *et al.* (2004) Mutations in the Na<sup>+</sup>/K<sup>+</sup> -ATPase alpha3 gene ATP1A3 are associated with rapid-onset dystonia parkinsonism. **Neuron.** 43 (2): 169-175
- De Fusco, M., Becchetti, A., Patrignani, A. *et al.* (2000) The nicotinic receptor beta 2 subunit is mutant in nocturnal frontal lobe epilepsy. **Nat Genet.** 26 (3): 275-276
- De Long, M.R. (1990) Primate models of movement disorders of basal ganglia origin. **Trends Neurosci.** 13 (7): 281-285
- Dedek, K., Kunath, B., Kananura, C. *et al.* (2001) Myokymia and neonatal epilepsy caused by a mutation in the voltage sensor of the KCNQ2 K<sup>+</sup> channel. **Proc Natl Acad Sci U S A.** 98 (21): 12272-12277
- Deloukas, P., Schuler, G.D., Gyapay, G. *et al.* (1998) A physical map of 30,000 human genes. **Science.** 282 (5389): 744-746
- Delous, M., Baala, L., Salomon, R. *et al.* (2007) The ciliary gene RPGRIP1L is mutated in cerebello-oculo-renal syndrome (Joubert syndrome type B) and Meckel syndrome. **Nat Genet.** 39 (7): 875-881
- Deng, F., Price, M.G., Davis, C.F. *et al.* (2006) Stargazin and other transmembrane AMPA receptor regulating proteins interact with synaptic scaffolding protein MAGI-2 in brain. **J Neurosci.** 26 (30): 7875-7884

- Deng, W., Pleasure, J. and Pleasure, D. (2008) Progress in periventricular leukomalacia. **Arch Neurol.** 65 (10): 1291-1295
- Depienne, C., Bouteiller, D., Keren, B. *et al.* (2009) Sporadic infantile epileptic encephalopathy caused by mutations in PCDH19 resembles Dravet syndrome but mainly affects females. **PLoS Genet.** 5(2):e1000381.
- Devinsky, O., Emoto, S., Goldstein, D.S. *et al.* (1992) Cerebrospinal fluid and serum levels of dopa, catechols, and monoamine metabolites in patients with epilepsy. **Epilepsia.** 33 (2): 263-270
- Dib, C., Faure, S., Fizames, C. *et al.* (1996) A comprehensive genetic map of the human genome based on 5,264 microsatellites. **Nature.** 380 (6570): 152-154
- Dibbens, L.M., Tarpey, P.S., Hynes, K. *et al.* (2008) X-linked protocadherin 19 mutations cause female-limited epilepsy and cognitive impairment. **Nat Genet.** 40(6): 776-81
- Dravet, C. (1978) Les epilepsies graves de l'enfant. **La Vie Médicale.** 8: 543-548
- Dravet, C., Bureau, M., Oguni, H.Y. *et al.* (2005) "Severe myoclonic epilepsy in infancy (Dravet syndrome)". In: Roger, J., Bureau, M., Dravet, C., Genton, P., Tassinari, C.A. and Wolf, P. (eds.) **Epileptic syndromes in infancy, childhood and adolescence.** 4<sup>th</sup> ed. Mountrouge: John Libbey Eurotext Ltd. pp. 89-113
- Dulac, O.J. and Chiron, C. (1996) Malignant epileptic encephalopathies in children. **Baillieres Clin Neurol.** 5 (4): 765-781
- Dulubova, I., Khvotchev, M., Liu, S. *et al.* (2007) Munc18-1 binds directly to the neuronal SNARE complex. **Proc Natl Acad Sci U S A.** 104 (8): 2697-2702
- Dzhala, V.I., Talos, D.M., Sdrulla, D.A. *et al.* (2005) NKCC1 transporter facilitates seizures in the developing brain. **Nat Med.** 11 (11): 1205-1213
- Egan, R.A., Weleber, R.G., Hogarth, P. *et al.* (2005) Neuro-ophthalmologic and electroretinographic findings in pantothenate kinase-associated neurodegeneration (formerly Hallervorden-Spatz syndrome). **Am J Ophthalmol.** 140 (2): 267-274
- El Shakankiry, H.M. (2010) Epileptiform discharges augmented during sleep: is it a trait with diverse clinical presentation according to age of expression? **Epilepsy Res.** 89 (1): 113-120
- Engel, J. (2006) Report of the ILAE Classification Core Group. **Epilepsia.** 47 (9): 1558-1568

- Escayg, A., MacDonald, B.T., Meisler, M.H. *et al.* (2000) Mutations of SCN1A, encoding a neuronal sodium channel, in two families with GEFS+2. **Nat Genet.** 24 (4): 343-345
- Escayg, A. and Goldin, A.L. (2010) Sodium channel SCN1A and epilepsy: Mutations and mechanisms. **Epilepsia.** May 28 [Epub ahead of print]
- Ever, L. and Gaiano, N. (2005) Radial 'glial' progenitors: neurogenesis and signaling. **Curr Opin Neurobiol.** 15 (1): 29-33
- Fabbri, M., Bannykh, S. and Balch, W.E. (1994) Export of protein from the endoplasmic reticulum is regulated by a diacylglycerol/phorbol ester binding protein. **J Biol Chem.** 269 (43): 26848-26857
- Faraone, S.V. and Mick, E. (2010) Molecular genetics of attention deficit hyperactivity disorder. **Psychiatr Clin North Am.** 33 (1): 159-180
- Farina, L., Nardocci, N., Bruzzone, M.G. *et al.* (1999) Infantile neuroaxonal dystrophy: neuroradiological studies in 11 patients. **Neuroradiology.** 41 (5): 376-380
- Felten, D.L. and Sladek, J.R. Jr. (1983) Monoamine distribution in primate brain V. Monoaminergic nuclei: anatomy, pathways and local organization. **Brain Res Bull.** 10 (2): 171-284
- Fisher, R.S., Boas, W.V.E., Blume, W. *et al.* (2005) Epileptic seizures and epilepsy: definitions proposed by the International League Against Epilepsy (ILAE) and the International Bureau for Epilepsy (IBE). **Epilepsia.** 46 (4): 470-472
- Fisher, S.K., Heacock, A.M. and Agranoff, B.W. (1992) Inositol lipids and signal transduction in the nervous system: an update. **J Neurochem.** 58 (1): 18-38
- Freeman, K., Gregory, A., Turner, A. *et al.* (2007) Intellectual and adaptive behaviour functioning in pantothenate kinase-associated neurodegeneration. **J Intellect Disabil Res.** 51(Pt. 6): 417-426
- Friocourt, G. and Parnavelas, J.G. (2010) Mutations in ARX result in several defects involving GABAergic neurons. **Front Cell Neurosci.** 4: 4
- Frost, J.D. Jr. and Hrachovy, R.A. (2003) **Infantile spasms.** Boston: Kluwer Academic Publishers
- Gainetdinov, R.R. and Caron, M.G. (2003) Monoamine transporters: from genes to behavior. **Annu Rev Pharmacol Toxicol.** 43: 261-284
- Gambardella, A. and Marini, C. (2009) Clinical spectrum of SCN1A mutations. **Epilepsia.** 50 Suppl 5: 20-23

- García-Cazorla, A., Serrano, M., Pérez-Dueñas, B. *et al.* (2007) Secondary abnormalities of neurotransmitters in infants with neurological disorders. **Dev Med Child Neurol.** 49 (10): 740-744
- Garcia-Cazorla, A., Duarte, S., Serrano, M. *et al.* (2008) Mitochondrial diseases mimicking neurotransmitter defects. **Mitochondrion.** 8 (3): 273-278
- Garelis, E., Young, S.N., Lal, S. *et al.* (1974) Monoamine metabolites in lumbar CSF: the question of their origin in relation to clinical studies. **Brain Res.** 79 (1): 1-8
- Gelman, N., Gorell, J.M., Barker, P.B. *et al.* (1999) MR imaging of human brain at 3.0 T: preliminary report on transverse relaxation rates and relation to estimated iron content. **Radiology.** 210 (3): 759-767
- Gerlach, M., Double, K.L., Youdim, M.B. *et al.* (2006) Potential sources of increased iron in the substantia nigra of parkinsonian patients. **J Neural Transm Suppl.** (70): 133-142
- Gillberg, C. and Svennerholm, L. (1987) CSF monoamines in autistic syndromes and other pervasive developmental disorders of early childhood. **Br J Psychiatry.** 151: 89-94
- Giros, B. and Caron, M.G. (1993) Molecular characterization of the dopamine transporter. **Trends Pharmacol Sci.** 14 (2): 43-49
- Giros, B., Jaber, M., Jones, S.R. *et al.* (1996) Hyperlocomotion and indifference to cocaine and amphetamine in mice lacking the dopamine transporter. **Nature.** 379 (6566): 606-612
- Gissen, P., Johnson, C.A., Morgan, N.V. *et al.* (2004) Mutations in VPS33B, encoding a regulator of SNARE-dependent membrane fusion, cause arthrogryposis-renal dysfunction-cholestasis (ARC) syndrome. **Nat Genet.** 36(4): 400-4
- Gopal, S.C., Pandey, A., Das, I. *et al.* (2008) Comparative evaluation of 5-HIAA (5-hydroxy indoleacetic acid) and HVA (homovanillic acid) in infantile hydrocephalus. **Childs Nerv Syst.** 24 (6): 713-716
- Gordon, A., McManus, A., Anderson, J. *et al.* (2003) Chromosomal imbalances in pleomorphic rhabdomyosarcomas and identification of the alveolar rhabdomyosarcoma-associated PAX3-FOXO1A fusion gene in one case. **Cancer Genet Cytogenet.** 140 (1): 73-77
- Gordon, N. (2008) Segawa's disease: dopa-responsive dystonia. **Int J Clin Pract.** 62 (6): 943-946
- Grattan-Smith, P.J., Wevers, R.A., Steenbergen-Spanjers, G.C. *et al.* (2002) Tyrosine hydroxylase deficiency: clinical manifestations of catecholamine insufficiency in infancy. **Mov Disord.** 17 (2): 354-359

- Greene, N.D., Stanier, P. and Copp, A.J. (2009) Genetics of human neural tube defects. **Hum Mol Genet.** 18 (R2): R113-R129
- Greengard, P. (2001) The neurobiology of slow synaptic transmission. **Science.** 294 (5544): 1024-1030
- Gregory, A. and Hayflick, S.J. (2005) Neurodegeneration with brain iron accumulation. **Folia Neuropathol.** 43 (4): 286-296
- Gregory, A., Westaway, S.K., Holm, I.E. *et al.* (2008) Neurodegeneration associated with genetic defects in phospholipase A(2). **Neurology.** 71 (18): 1402-1409
- Gregory, A., Polster, B.J. and Hayflick, S.J. (2009) Clinical and genetic delineation of neurodegeneration with brain iron accumulation. **J Med Genet.** 46 (2): 73-80
- Grinberg, I., Northrup, H., Ardinger, H. *et al.* (2004) Heterozygous deletion of the linked genes ZIC1 and ZIC4 is involved in Dandy-Walker malformation. **Nat Genet.** 36 (10): 1053-1055
- Guerrini, R., Dravet, C., Genton, P. *et al.* (1998) Lamotrigine and seizure aggravation in severe myoclonic epilepsy. **Epilepsia.** 39 (5): 508-512
- Guerrini, R., Sicca, F. and Parmeggiani, L. (2003) Epilepsy and malformations of the cerebral cortex. **Epileptic Disord.** Suppl 2 5: S9-S26
- Hagenah, J., Saunders-Pullman, R., Hedrich, K. *et al.* (2005) High mutation rate in dopa-responsive dystonia: detection with comprehensive GCHI screening. **Neurology.** 64 (5): 908-911
- Hamdan, F.F., Piton, A., Gauthier, J. *et al.* (2009) De novo STXBP1 mutations in mental retardation and nonsyndromic epilepsy. **Ann Neurol.** 65 (6): 748-753
- Hannan, A.J., Blakemore, C., Katsnelson, A. *et al.* (2001) PLC-beta1, activated via mGluRs, mediates activity-dependent differentiation in cerebral cortex. **Nat Neurosci.** 4 (3): 282-288
- Hartig, M.B., Hörtnagel, K., Garavaglia, B. *et al.* (2006) Genotypic and phenotypic spectrum of PANK2 mutations in patients with neurodegeneration with brain iron accumulation. **Ann Neurol.** 59 (2): 248-256
- Hayflick, S.J., Westaway, S.K., Levinson, B. *et al.* (2003) Genetic, clinical, and radiographic delineation of Hallervorden-Spatz syndrome. **N Engl J Med.** 348 (1): 33-40

- Hayflick, S.J. (2006) Neurodegeneration with brain iron accumulation: from genes to pathogenesis. **Semin Pediatr Neurol.** 13 (3): 182-185
- Hayflick, S.J. (2009) Dystonia-parkinsonism disease gene discovery: expect surprises. **Ann Neurol.** 65 (1): 2-3
- He, L., Vasiliou, K. and Nebert, D.W. (2009) Analysis and update of the human solute carrier (SLC) gene superfamily. **Hum Genomics.** 3 (2): 195-206
- Helbig, I., Scheffer, I.E., Mulley, J.C. *et al.* (2008) Navigating the channels and beyond: unravelling the genetics of the epilepsies. **Lancet Neurol.** 7 (3): 231-245
- Herdegen, T. and Leah, J.D. (1998) Inducible and constitutive transcription factors in the mammalian nervous system: control of gene expression by Jun, Fos and Krox, and CREB/ATF proteins. **Brain Res Brain Res Rev.** 28 (3): 370-490
- Heron, S.E., Crossland, K.M., Andermann, E. *et al.* (2002) Sodium-channel defects in benign familial neonatal-infantile seizures. **Lancet.** 360 (9336): 851-852
- Hodes, M.E., Pratt, V.M. and Dlouhy, S.R. (1993) Genetics of Pelizaeus-Merzbacher disease. **Dev. Neurosci.** 15 (6): 383-394
- Hoffman, G.E., Felten, D.L. and Sladek, J.R. Jr. (1976) Monoamine distribution in primate brain. III. Catecholamine-containing varicosities in the hypothalamus of *Macaca mulatta*. **Am J Anat.** 147 (4): 501-513
- Hoffmann, G.F., Surtees, R.A. and Wevers R.A. (1998) Cerebrospinal fluid investigations for neurometabolic disorders. **Neuropediatrics.** 29 (2): 59-71
- House, M.J., St Pierre, T.G., Kowdley, K.V. *et al.* (2007) Correlation of proton transverse relaxation rates (R2) with iron concentrations in postmortem brain tissue from alzheimer's disease patients. **Magn Reson Med.** 57 (1): 172-180
- Hrachovy, R.A. and Frost, J.D. Jr. (2003) Infantile epileptic encephalopathy with hypsarrhythmia (infantile spasms/West syndrome). **J Clin Neurophysiol.** 20 (6): 408-425
- Hu, J., Jiang, C.C., Ng, H.K. *et al.* (2003) An allelotype study of primary and corresponding recurrent glioblastoma multiforme. **Zhonghua Yi Xue Yi Chuan Xue Za Zhi.** 20 (1): 56-58
- Hyland, K., Surtees, R.A., Heales, S.J. *et al.* (1993) Cerebrospinal fluid concentrations of pterins and metabolites of serotonin and dopamine in a pediatric reference population. **Pediatr Res.** 34 (1): 10-14

- Ilja Boor, P.K., de Groot, K., Mejaski-Bosnjak, V. *et al.* (2006) Megalencephalic leukoencephalopathy with subcortical cysts: an update and extended mutation analysis of MLC1. **Hum Mutat.** 27 (6): 505-512
- International HapMap Consortium, Frazer, K.A., Ballinger, D.G. *et al.* (2007) A second generation human haplotype map of over 3.1 million SNPs. **Nature.** 449 (7164): 851-861
- Isom, L.L. (2002) The role of sodium channels in cell adhesion. **Front Biosci.** 7: 12-23
- Ito, M., Okuno, T., Mikawa, H. *et al.* (1980) Elevated homovanillic acid in cerebrospinal fluid of children with infantile spasms. **Epilepsia.** 21 (4): 387-392
- Jansen, F.E., Sadleir, L.G., Harkin, L.A. *et al.* (2006). Severe myoclonic epilepsy of infancy (Dravet syndrome): recognition and diagnosis in adults. **Neurology.** 67 (12): 2224-2226
- Kalachikov, S., Evgrafov O., Ross, B. *et al.* (2002) Mutations in LGI1 cause autosomal-dominant partial epilepsy with auditory features. **Nat Genet.** 30 (3): 335-341
- Kalinichenko, S.G. and Matveeva, N.Y. (2008) Morphological characteristics of apoptosis and its significance in neurogenesis. **Neurosci Behav Physiol.** 38 (4): 333-344
- Kalscheuer, V.M., Tao, J., Donnelly, A. *et al.* (2003) Disruption of the serine/threonine kinase 9 gene causes severe X-linked infantile spasms and mental retardation. **Am J Hum Genet.** 72 (6): 1401-1411
- Kandel, E.R., Schwarz, J.H. and Jessell, T.M. (eds.) (2000a) **Principles of Neuroscience.** 4<sup>th</sup> ed. New York: McGraw Hill
- Kandel, E.R. (2000b) "The Basal Ganglia". *In*: Kandel E.R., Schwarz, J.H. and Jessell, T.M. (eds.) **Principles of Neuroscience.** 4<sup>th</sup> ed. New York: McGraw Hill. pp. 853-873
- Kanold, P.O. and Luhmann, H.J. (2010) The subplate and early cortical circuits. **Annu Rev Neurosci.** 33: 23-48
- Kaul, R., Gao, G.P., Balamurugan, K. *et al.* (1993) Cloning of the human aspartoacylase cDNA and a common missense mutation in Canavan disease. **Nature Genet.** 5 (2): 118-123
- Kharkar, P.S., Dutta A.K. and Reith, M.E.A. (2008) "Structure-activity relationship study of piperidine derivatives for dopamine transporters". *In*: Trudell, M.L. and Izenwasser, S. (eds.) **Dopamine Transporters:**

- Chemistry Biology and Pharmacology.** New Jersey: John Wiley & Sons Inc. (Drug Discovery and Development series). pp. 233-265
- Kibar, Z., Torban, E., McDearmid, J.R. *et al.* (2007) Mutations in VANGL1 associated with neural-tube defects. **New Eng J Med.** 356 (14): 1432-1437
- Kibar, Z., Bosoi, C.M., Kooistra, M. *et al.* (2009) Novel mutations in VANGL1 in neural tube defects. **Hum Mutat.** 30 (7): E706-E715
- Kim, D., Jun, K.S., Lee, S.B. *et al.* (1997) Phospholipase C isozymes selectively couple to specific neurotransmitter receptors. **Nature.** 389 (6648): 290-293
- Kinali, M., Arechavala-Gomeza, V., Feng, L. *et al.* (2009) Local restoration of dystrophin expression with the morpholino oligomer AVI-4658 in Duchenne muscular dystrophy: a single-blind, placebo-controlled, dose-escalation, proof-of-concept study. **Lancet Neurol.** 8 (10): 918-928
- Kishino, T., Lalande, M. and Wagstaff, J. (1997) UBE3A/E6-AP mutations cause Angelman syndrome. **Nat Genet.** 15 (1): 70-73
- Klintsova, A.Y. and Greenough, W.T. (1999) Synaptic plasticity in cortical systems. **Curr Opin Neurobiol.** 9 (2): 203-208
- Koeller, D.M., Woontner, M., Crnic, L.S. *et al.* (2002) Biochemical, pathologic and behavioral analysis of a mouse model of glutaric acidemia type I. **Hum Mol Genet.** 11 (4): 347-357
- Koh, H.Y., Kim, D., Lee, J. *et al.* (2008) Deficits in social behavior and sensorimotor gating in mice lacking phospholipase C $\beta$ 1. **Genes Brain Behav.** 7 (1): 120-128
- Kong, A., Gudbjartsson, D.F., Sainz, J. *et al.* (2002) A high-resolution recombination map of the human genome. **Nat Genet.** 31 (3): 241-247
- Kumar, N., Boes, C.J., Babovic-Vuksanovic, D. *et al.* (2006) The "eye-of-the-tiger" sign is not pathognomonic of the PANK2 mutation. **Arch Neurol.** 63 (2): 292-293
- Kumar, S.S., Bacci, A., Kharazia, V. *et al.* (2002) A developmental switch of AMPA receptor subunits in neocortical pyramidal neurons. **J Neurosci.** 22 (8): 3005-3015
- Kuo, Y.M., Duncan, J.L. and Westaway, S.K. (2005) Deficiency of pantothenate kinase 2 (Pank2) in mice leads to retinal degeneration and azoospermia. **Human Mol Genet.** 14 (1): 49-57



- Kuo, Y.M., Hayflick, S.J. and Gitshier, J. (2007) Deprivation of pantothenic acid elicits a movement disorder and azoospermia in a mouse model of pantothenate kinase-associated neurodegeneration. **J Inherit Metab Dis.** 30 (3): 310-317
- Kurian, M.A., Morgan, N.V., MacPherson, L. *et al.* (2008) Phenotypic spectrum of neurodegeneration associated with mutations in the PLA2G6 gene (PLAN). **Neurology.** 70 (18): 1623-1629
- Kurian, M.A., Zhen, J., Cheng, S.Y. *et al.* (2009) Homozygous loss-of-function mutations in the gene encoding the dopamine transporter are associated with infantile parkinsonism-dystonia. **J Clin Invest.** 119 (6): 1595-1603
- Kurian M.A., Meyer E., Vassallo, G. *et al.* (2010a) Phospholipase C Beta 1 (PLCB1) Deficiency is associated with Early Onset Epileptic Encephalopathy. **Brain.** 133(10): 2964-2970
- Kurian, M.A., Li, Y., Zhen, J. *et al.* (2010b) Clinical and Molecular Characterisation of Dopamine Transporter Deficiency Syndrome. **Lancet Neurol.** *In press*
- Kyttala, M., Tallila, J., Salonen, R. *et al.* (2006) MKS1, encoding a component of the flagellar apparatus basal body proteome, is mutated in Meckel syndrome. 38 (2): 155-157
- Lander, E.S. and Botstein, D. (1987) Homozygosity mapping: a way to map human recessive traits with the DNA of inbred children. **Science.** 236 (4808): 1567-1570
- Lau, C.G. and Zukin, R.S. (2007) NMDA receptor trafficking in synaptic plasticity and neuropsychiatric disorders. **Nat Rev Neurosci.** 8 (6): 413-426
- Le Couteur, D.G., Leighton, P.W., McCann, S.J. *et al.* (1997) Association of a polymorphism in the dopamine-transporter gene with Parkinson's disease. **Mov Disord.** 12 (5): 760-763
- Leblois, A., Meissner, W., Bioulac, B. *et al.* (2007) Late emergence of synchronized oscillatory activity in the pallidum during progressive parkinsonism. **Eur J Neurosci.** 26 (6): 1701-1713
- Lees, A.J., Hardy, J. and Revesz, T. (2009) Parkinson's disease. **Lancet.** 373 (9680): 2055-2066
- Lei, Y.-P., Zhang, T., Li, H. *et al.* (2010) VANGL2 mutations in human cranial neural-tube defects. **New Eng J Med.** 362 (23): 2232-2235

- Leighton, P.W., Le Couteur, D.G., Pang, C.C. *et al.* (1997) The dopamine transporter gene and Parkinson's disease in a Chinese population. **Neurology**. 49 (6): 1577-1579
- Li, L.B., Chen, N., Ramamoorthy, S. *et al.* (2004) The role of N-glycosylation in function and surface trafficking of the human dopamine transporter. **J Biol Chem**. 279 (20): 21012-21020
- Lin, C., Franco, B., Rosner, M.R. (2005) CDKL5/Stk9 kinase inactivation is associated with neuronal developmental disorders. **Hum Mol Genet**. 14 (24): 3775-3786
- Little, W.J. (1862) On the influence of abnormal parturition, difficult labors, premature birth, and asphyxia neonatorum, on the mental and physical condition of the child, especially in relation to deformities. **Trans Obstet Soc (Lond)**. 2: 293-344
- Lo Vasco, V.R., Calabrese, G., Manzoli, L. *et al.* (2004) Leukemia Inositide-specific phospholipase c beta1 gene deletion in the progression of myelodysplastic syndrome to acute myeloid leukemia. **Leukaemia**. 18 (6): 1122-1126
- Lombroso, C.T. (1990) Early myoclonic encephalopathy, early infantile epileptic encephalopathy, and benign and severe infantile myoclonic epilepsies: a critical review and personal contributions. **J Clin Neurophysiol**. 7 (3): 380-408
- Longo, N. (2009) Disorders of bipterin metabolism. **J Inherit Metab Dis**. 32 (3): 333-342
- Lossin, C., Wang, D.W., Rhodes, T.H. *et al.* (2002) Molecular basis of an inherited epilepsy. **Neuron**. 34 (6): 877-884
- Loturco, J.J., Owens, D.F., Heath, M.J. *et al.* (1995) GABA and glutamate depolarize cortical progenitor cells and inhibit DNA synthesis. **Neuron**. 15 (6): 1287-1298
- Lux, A.L. and Osborne, J.P. (2004a) A proposal for case definitions and outcome measures in studies of infantile spasms and West syndrome: consensus statement of the West Delphi group. **Epilepsia**. 45 (11): 1416-1428
- Lux, A.L., Edwards, S.W., Hancock, E. *et al.* (2004b) The United Kingdom Infantile Spasms Study comparing vigabatrin with prednisolone or tetracosactide at 14 days: a multicentre, randomised controlled trial. **Lancet**. 364 (9447): 1773-1778
- Malik, I., Turk, J., Mancuso, D.J. *et al.* (2008) Disrupted membrane homeostasis and accumulation of ubiquitinated proteins in a mouse model of

- infantile neuroaxonal dystrophy caused by PLA2G6 mutations. **Am J Pathol.** 172 (2): 406-416
- Mari, F., Azimonti, S., Bertani, I. *et al.* (2005) CDKL5 belongs to the same molecular pathway of MeCP2 and it is responsible for the early-onset seizure variant of Rett syndrome. **Hum Mol Genet.** 14 (14): 1935-1946
- Marín-Valencia, I., Serrano, M., Ormazabal, A. *et al.* (2008) Biochemical diagnosis of dopaminergic disturbances in paediatric patients: analysis of cerebrospinal fluid homovanillic acid and other biogenic amines. **Clin Biochem.** 41 (16-17): 1306-1315
- Marini, C., Mei, D., Parmeggiani, L. *et al.* (2010) Protocadherin 19 mutations in girls with infantile-onset epilepsy. **Neurology.** 75(7): 646-53
- Marks, W.A., Honeycutt, J., Acosta, F. *et al.* (2009) Deep brain stimulation for pediatric movement disorders. **Semin Pediatr Neurol.** 16 (2): 90-98
- Marsh, E., Fulp, C., Gomez, E. *et al.* (2009) Targeted loss of Arx results in a developmental epilepsy mouse model and recapitulates the human phenotype in heterozygous females. **Brain.** 132 (Pt 6): 1563-1576
- Marshall, C.R., Young, E.J., Pani, A.M. *et al.* (2008) Infantile spasms is associated with deletion of the MAG12 gene on chromosome 7q11.23-q21.11. **Am J Hum Genet.** 83 (1): 106-111
- Matheson, A.J. and Spencer, C.M. (2000) Ropinirole: a review of its use in the management of Parkinson's disease. **Drugs.** 60 (1): 115-137
- Mazei-Robinson, M.S. and Blakely, R.D. (2006) ADHD and the dopamine transporter: are there reasons to pay attention? **Handb Exp Pharmacol.** (175): 373-415
- Mazei-Robison, M.S., Bowton, E., Holy, M. *et al.* (2008) Anomalous dopamine release associated with a human dopamine transporter coding variant. **J Neurosci.** 28 (28): 7040-7046
- McConnell, H. and Bianchine, J. (eds.) (1994) "CSF as a reflection of cerebral metabolism." In: McConnell, H. and Bianchine, J. (eds.) **Cerebrospinal fluid in Neurology and Psychiatry.** London: Chapman & Hall Medical. pp. 35-42
- McElvain, J.S. and Schenk, J.O. (1992) A multisubstrate mechanism of striatal dopamine uptake and its inhibition by cocaine. **Biochem Pharmacol.** 43 (10): 2189-2199
- McIntyre, C.C., Savasta, M., Walter, B.L. *et al.* (2004) How does deep brain stimulation work? Present understanding and future questions. **J Clin Neurophysiol.** 21 (1): 40-50

- McNeill, A., Pandolfo, M., Kuhn, J. *et al.* (2008a) The neurological presentation of ceruloplasmin gene mutations. **Eur Neurol.** 60 (4): 200-205
- McNeill, A., Birchall, D., Hayflick, S.J. *et al.* (2008b) T2\* and FSE MRI distinguishes four subtypes of neurodegeneration with brain iron accumulation. **Neurology.** 70 (18): 1614-1619
- McOmish, C.E., Burrows, E.L., Howard, M. *et al.* (2008) PLC-beta1 knockout mice as a model of disrupted cortical development and plasticity: behavioral endophenotypes and dysregulation of RGS4 gene expression. **Hippocampus.** 18 (8): 824-834
- Mehler-Wex, C., Riederer, P. and Gerlach, M. (2006) Dopaminergic dysbalance in distinct basal ganglia neurocircuits: implications for the pathophysiology of Parkinson's disease, schizophrenia and attention deficit hyperactivity disorder. **Neurotox Res.** 10 (3-4): 167-179
- Mena, M.A., Aguado, E.G. and de Yebenes, J.G. (1984) Monoamine metabolites in human cerebrospinal fluid: HPLC/ED method. **Acta Neurol Scand.** 69 (4): 218-225
- Miano, M.G., Jacobson, S.G., Carothers, A. *et al.* (2000) Pitfalls in homozygosity mapping. **Am J Hum Genet.** 67 (5): 1348-1351
- Millichap, J.J. and Millichap, J.G. (2009) Child neurology: Past, present, and future: part 1: history. **Neurology.** 73 (7): e31-e33
- Modell, B. and Darr, A. (2002) Science and society: genetic counselling and customary consanguineous marriage. **Nat Rev Genet.** 3 (3): 225-229
- Molinari, F., Raas-Rothschild, A., Rio, M. *et al.* (2005) Impaired mitochondrial glutamate transport in autosomal recessive neonatal myoclonic epilepsy. **Am J Hum Genet.** 76 (2): 334-339
- Molinuevo, J.L., Martí, M.J., Blesa, R. *et al.* (2003) Pure akinesia: an unusual phenotype of Hallervorden-Spatz syndrome. **Mov Disord.** 18 (11): 1351-1353
- Morgan, N.V., Westaway, S.K., Morton, J.E. *et al.* (2006) PLA2G6, encoding a phospholipase A2, is mutated in neurodegenerative disorders with high brain iron. **Nat Genet.** 38 (7): 752-754
- Morgan T.H. (1911) Random segregation versus coupling in Mendelian inheritance. **Science.** 34: 384
- Morton, N.E. (1955) Sequential tests for the detection of linkage. **Am J Hum Genet.** 7 (3): 277-318

- Mubaidin, A., Roberts, E., Hampshire, D. *et al.* (2003) Karak syndrome: a novel degenerative disorder of the basal ganglia and cerebellum. **J Med Genet.** 40 (7): 543-546
- Mueller, R.F. and Bishop, D.T. (1993) Autozygosity mapping, complex consanguinity, and autosomal recessive disorders. **J Med Genet.** 30 (9): 798-799
- Mulley, J.C., Scheffer, I.E., Petrou, S. *et al.* (2003) Channelopathies as a genetic cause of epilepsy. **Curr Opin Neurol.** 16 (2): 171-176
- Nakanishi, S. (1994) Metabotropic glutamate receptors: synaptic transmission, modulation, and plasticity. **Neuron.** 13(5): 1031-1037
- Nambu, A. (2008) Seven problems on the basal ganglia. **Curr Opin Neurobiol.** 18 (6): 595-604
- Nardocci, N., Zorzi, G., Farina, L. *et al.* (1999) Infantile neuroaxonal dystrophy: clinical spectrum and diagnostic criteria. **Neurology.** 52 (7): 1472-1478
- Nielsen, J.B., Bertelsen, A. and Lou, H.C. (1992) Low CSF HVA levels in the Rett syndrome: a reflection of restricted synapse formation? **Brain Dev.** 14 Suppl: S63-S65
- Nikolaus, S., Antke, C., Kley, K. *et al.* (2007a) Investigating the dopaminergic synapse in vivo. I. Molecular imaging studies in humans. **Rev Neurosci.** 18 (6): 439-472
- Nikolaus, S., Larisch, R., Beu, M. *et al.* (2007b) Investigating the dopaminergic synapse in vivo. II. Molecular imaging studies in small laboratory animals. **Rev Neurosci.** 18 (6): 473-504
- Norregaard, L., Loland, C.J. and Gether, U. (2003) Evidence for distinct sodium-, dopamine-, and cocaine-dependent conformational changes in transmembrane segments 7 and 8 of the dopamine transporter. **J Biol Chem.** 278 (33): 30587-30596
- Nutt, J.G., Carter, J.H. and Sexton, G.J. (2004) The dopamine transporter: importance in Parkinson's disease. **Ann Neurol.** 55 (6): 766-773
- Obeso, J.A., Marin, C., Rodriguez-Oroz, C. *et al.* (2008) The basal ganglia in Parkinson's disease: current concepts and unexplained observations. **Ann Neurol.** 64 Suppl 2: S30-S46
- Ohtahara, S., Ishida, T., Oka, E. *et al.* (1976) On the specific age dependent epileptic syndrome: the early-infantile epileptic encephalopathy with suppression bursts. **No To Hattatsu.** 8: 270-280

- Ohtahara, S., Ohtsuka, Y., Yamatogi, Y. *et al.* (1987) The early infantile epileptic encephalopathy with suppression-burst: developmental aspects. **Brain Dev.** 9 (4): 371-376
- Ohtahara, S. and Yamatogi, Y. (1990) "Evolution of seizures and EEG abnormalities in childhood onset epilepsy". In: Wada, J.A. and Ellingson, R.J. (eds.) **Clinical Neurophysiology of Epilepsy; Handbook of Electroencephalography and Clinical Neurophysiology**. Amsterdam: Elsevier (Revised Series, vol. 4.). pp. 457-477
- Ohtahara, S., Ohtsuka, Y., Yamatogi, Y. *et al.* (1992) "Early-infantile epileptic encephalopathy with suppression bursts". In: Roger, J., Bureau, M., Dravet, C., Dreifuss, F.E., Perret, A. and Wolf, P. (eds.) **Epileptic Syndromes in Infancy, Childhood and Adolescence**. 2<sup>nd</sup> ed. London: John Libbey. pp. 25-34
- Ohtahara, S. and Yamatogi, Y. (2003) Epileptic encephalopathies in early infancy with suppression-burst. **J Clin Neurophysiol.** 20 (6): 398-407
- Ott, J. (1991) "Principles of human genetic linkage analysis." In: Brosius, J. and Freneau, R.T. (eds.) **Molecular Genetic Approaches to Neuropsychiatric Diseases**. New York: Academic Press. pp. 35-53
- Ott, J. (1999) **Analysis of Human Genetic Linkage**. 3<sup>rd</sup> ed. Baltimore: The Johns Hopkins University Press
- Paisan-Ruiz, C., Bhatia, K.P., Li, A. *et al.* (2009) Characterization of PLA2G6 as a locus for dystonia-parkinsonism. **Ann Neurol.** 65 (1): 19-23
- Parisi, M. and Glass, I. (2007) **Joubert Syndrome**. [online] In: Pagon, R.A., Bird, T.C., Dolan, C.R. and Stephens, K. (eds.) GeneReviews University of Washington, Seattle. Available from <http://www.ncbi.nlm.nih.gov.ezproxyd.bham.ac.uk/bookshelf/br.fcgi?book=gene&part=joubert> [Accessed June 15<sup>th</sup> 2010]
- Parnas, M.L. and Vaughan, R.A. (2008) "Molecular Structure and Composition of Dopamine Transporters". In: Trudell, M.L. and Izenwasser, S. (eds.) **Dopamine Transporters: Chemistry Biology and Pharmacology**. New Jersey: John Wiley & Sons Inc. (Drug Discovery and Development series). pp. 73-95
- Paul, L.K., Brown, W.S., Adolphs, R. *et al.* (2007) Agenesis of the corpus callosum: genetic, developmental and functional aspects of connectivity. **Nat Rev Neurosci.** 8 (4): 287-299
- Pearl, P.L., Capp, P.K., Novotny, E.J. *et al.* (2005) Inherited disorders of neurotransmitters in children and adults. **Clin Biochem.** 38 (12): 1051-1058

- Pearl, P.L., Hartka, T.R. and Taylor, J. (2006) Diagnosis and Treatment of Neurotransmitter Disorders. **Curr Treat Options Neurol.** 8 (6): 441-450
- Pearl, P.L., Taylor, J.L., Trzcinski, S. *et al.* (2007) The pediatric neurotransmitter disorders. **J Child Neurol.** 22 (5): 606-616
- Pellecchia, M.T., Valente, E.M., Cif, L. *et al.* (2005) The diverse phenotype and genotype of pantothenate kinase-associated neurodegeneration. **Neurology.** 64 (10): 1810-1812
- Peng, Z., Zhou, C., Zhang, F. *et al.* (2002) Loss of heterozygosity of chromosome 20 in sporadic colorectal cancer. **Chin Med J (Engl).** 115 (10): 1529-1532
- Peruzzi, D., Calabrese, G., Faenza, I. *et al.* (2000) Identification and chromosomal localisation by fluorescence in situ hybridisation of human gene of phosphoinositide-specific phospholipase C beta(1). **Biochim Biophys Acta.** 1484 (2-3): 175-182
- Peruzzi, D., Aluigi, M., Manzoli, L. *et al.* (2002) Molecular characterization of the human PLC beta1 gene. **Biochim Biophys Acta.** 1584 (1): 46-54
- Poirier, K., Keays, D.A., Francis, F. *et al.* (2007) Large spectrum of lissencephaly and pachygyria phenotypes resulting from de novo missense mutations in tubulin alpha 1A (TUBA1A). **Hum Mutat.** 28 (11): 1055-1064
- Pollak, M.R., Chou, Y.H., Cerda, J.J. *et al.* (1993) Homozygosity mapping of the gene for alkaptonuria to chromosome 3q2. **Nat Genet.** 5 (2): 201-214
- Polten, A., Fluharty, A.L., Fluharty, C.B. *et al.* (1991) Molecular basis of different forms of metachromatic leukodystrophy. **New Eng J Med.** 324 (1): 18-22
- Pranzatelli, M.R., Huang, Y., Tate, E. *et al.* (1995) Cerebrospinal fluid 5-hydroxyindoleacetic acid and homovanillic acid in the pediatric opsoclonus-myoclonus syndrome. **Ann Neurol.** 37 (2): 189-197
- Rakhade, S.N. and Jensen, F.E. (2009) Epileptogenesis in the immature brain: emerging mechanisms. **Nat Rev Neurol.** 5 (7): 380-391
- Ramaekers, V.T., Lake, B.D., Harding, B. *et al.* (1987) Diagnostic difficulties in infantile neuroaxonal dystrophy. A clinicopathological study of eight cases. **Neuropediatrics.** 18 (3): 170-175
- Rees, M.I., Harvey, K., Pearce, B.R. *et al.* (2006) Mutations in the gene encoding GlyT2 (SLC6A5) define a presynaptic component of human startle disease. **Nat Genet.** 38 (7): 801-806

- Rice, D. and Barone, S. Jr. (2000) Critical periods of vulnerability for the developing nervous system: evidence from humans and animal models. **Environ Health Perspect.** 108 Suppl 3: 511-533
- Rice, M.E. and Cragg, S.J. (2008) Dopamine spillover after quantal release: rethinking dopamine transmission in the nigrostriatal pathway. **Brain Res Rev.** 58 (2): 303-313
- Robertson, D., Haile, V., Perry, S.E. *et al.* (1991) Dopamine beta hydroxylase deficiency. A genetic disorder of cardiovascular regulation. **Hypertension.** 18 (1): 1-8
- Saitsu, H., Kato, M., Mizuguchi, T. *et al.* (2008) De novo mutations in the gene encoding STXBP1 (MUNC18-1) cause early infantile epileptic encephalopathy. **Nat Genet.** 40 (6): 782-788
- Saitsu, H., Tohyama, J., Kumada, T. *et al.* (2010) Dominant-negative mutations in alpha-II spectrin cause West syndrome with severe cerebral hypomyelination, spastic quadriplegia, and developmental delay. **Am J Hum Genet.** 86 (6): 881-891
- Sakai, N., Inui, K., Fujii, N. *et al.* (1994) Krabbe disease: isolation and characterization of a full-length cDNA for human galactocerebrosidase. **Biochem Biophys Res Commun.** 198 (2): 485-491
- Salinas, E., Opris, I., Zainos, A. *et al.* (2000) "Motor and non motor roles of the corticobasal ganglia circuitry". In: Miller, R. and Wickens, J. (eds.) **Brain dynamics and the striatal complex. Conceptual advances in brain research** (vol 1) Singapore: Harwood Academic. pp. 237-255
- Sanchez, R.M. and Jensen, F.E. (2001) Maturational aspects of epilepsy mechanisms and consequences for the immature brain. **Epilepsia.** 42 (5): 577-585
- Scherfler, C., Schwarz, J., Antonini, A. *et al.* (2007) Role of DAT-SPECT in the diagnostic work up of parkinsonism. **Mov Disord.** 22 (9): 1229-1238
- Schmitt, K.C., Mamidyala, S., Biswas, S. *et al.* (2010) Bivalent phenethylamines as novel dopamine transporter inhibitors: evidence for multiple substrate-binding sites in a single transporter. **J Neurochem.** 112 (6): 1605-1618
- Schneider, S.A., Paisan-Ruiz, C., Quinn, N.P. *et al.* (2010) ATP13A2 mutations (PARK9) cause neurodegeneration with brain iron accumulation. **Mov Disord.** 25 (8): 979-984



- Segawa, M. (2009) Autosomal dominant GTP cyclohydrolase I (AD GCH 1) deficiency (Segawa disease, dystonia 5; DYT 5). **Chang Gung Med J.** 32 (1): 1-11
- Serrano, M., Ormazábal, A., Pérez-Dueñas, B. *et al.* (2007) Perinatal asphyxia may cause reduction in CSF dopamine metabolite concentrations. **Neurology.** 69 (3): 311-313
- Sertie, A.L., Sossi, V., Camargo, A.A. *et al.* (2000) Collagen XVIII, containing an endogenous inhibitor of angiogenesis and tumor growth, plays a critical role in the maintenance of retinal structure and in neural tube closure (Knobloch syndrome). **Hum Mol Genet.** 9 (13): 2051-2058
- Shaywitz, B.A., Cohen, D.J. and Bowers, M.B. (1975) Reduced cerebrospinal fluid 5-hydroxyindoleacetic acid and homovanillic acid in children with epilepsy. **Neurology.** 25 (1): 72-79
- Shen, J., Gilmore, E.C., Marshall, C.A. *et al.* (2010) Mutations in PNKP cause microcephaly, seizures and defects in DNA repair. **Nat Genet.** 42 (3): 245-249
- Shi, L., Quick, M., Zhao, Y. *et al.* (2008) The mechanism of a neurotransmitter:sodium symporter--inward release of Na<sup>+</sup> and substrate is triggered by substrate in a second binding site. **Mol Cell.** 30 (6): 667-677
- Shinzawa, K., Sumi, H., Ikawa, M. *et al.* (2008) Neuroaxonal dystrophy caused by group VIA phospholipase A2 deficiency in mice: a model of human neurodegenerative disease. **J Neurosci.** 28 (9): 2212-2220
- Shoubridge, C., Cloosterman, D., Parkinson-Lawrence, E. *et al.* (2007) Molecular pathology of expanded polyalanine tract mutations in the Aristaless-related homeobox gene. **Genomics.** 90 (1): 59-71
- Shoubridge, C., Fullston, T. and Gécz, J. (2010) 'ARX spectrum disorders'; making inroads in to the molecular pathology. **Hum Mutat.** [Epub ahead of print]
- Silverstein, F.S. and Jensen, F.E. (2007) Neonatal seizures. **Ann Neurol.** 62 (2): 112-120
- Simeone, T.A., Sanchez, R.M. and Rho, J.M. (2004) Molecular biology and ontogeny of glutamate receptors in the mammalian central nervous system. **J Child Neurol.** 19 (5): 343-360
- Sina, F., Shojaee, S., Elahi, E. *et al.* (2009) R632W mutation in PLA2G6 segregates with dystonia-parkinsonism in a consanguineous Iranian family. **Eur J Neurol.** 16 (1): 101-104

- Singh, N.A., Charlier, C., Stauffer, D. *et al.* (1998) A novel potassium channel gene, KCNQ2, is mutated in an inherited epilepsy of newborns. **Nat Genet.** 18 (1): 25-29
- Singh, S.K., Yamashita, A. and Gouaux, E. (2007) Antidepressant binding site in a bacterial homologue of neurotransmitter transporters. **Nature.** 448 (7156): 952-956
- Sladek, J.R. Jr., Garver, D.L. and Cummings, J.P. (1982) Monoamine distribution in primate brain IV. Indoleamine –containing perikarya in the brainstem of *Macaca arctoides*. **Neuroscience.** 7 (2): 477-493
- Smith, C. (1953) The detection of linkage in human genetics; **J R Stat Soc Brit.** 15: 135-184
- Smith, I., Hyland, K. and Kendall, B. (1985) Clinical role of pteridine therapy in tetrahydrobiopterin deficiency. **J Inherit Metab Dis.** 8 Suppl 1: 39-45
- Spalice, A., Parisi, P., Nicita, F. *et al.* (2009) Neuronal migration disorders: clinical, neuroradiologic and genetics aspects. **Acta Paediatr.** 98 (3): 421-433
- Spencer, T.J., Biederman, J., Madras, B.K. *et al.* (2005) In vivo neuroreceptor imaging in attention-deficit/hyperactivity disorder: a focus on the dopamine transporter. **Biol Psychiatry.** 57 (11): 1293-1300
- Spires, T.L., Molnár, Z., Kind, P.C. *et al.* (2005) Activity-dependent regulation of synapse and dendritic spine morphology in developing barrel cortex requires phospholipase C-beta1 signalling. **Cereb Cortex.** 15 (4): 385-393
- Stallings, R.L., Ford, A.F., Nelson, D. *et al.* (1991) Evolution and distribution of (GT)<sub>n</sub> repetitive sequences in mammalian genomes. **Genomics.** 10 (3): 807-815
- Steinlein, O.K., Mulley, J.C., Propping, P. *et al.* (1995) A missense mutation in the neuronal nicotinic acetylcholine receptor alpha 4 subunit is associated with autosomal dominant nocturnal frontal lobe epilepsy. **Nat Genet.** 11 (2): 201-203
- Storch, A., Ludolph, A.C. and Schwarz, J. (2004) Dopamine transporter: involvement in selective dopaminergic neurotoxicity and degeneration. **J Neural Transm.** 111 (10-11): 1267-1286
- Strecker, K., Hesse, S., Wegner, F. *et al.* (2007) Eye of the tiger sign in multiple system atrophy. **Eur J Neurol.** 14 (11): e1-e2
- Stromme, P., Mangelsdorf, M.E., Shaw, M.A. *et al.* (2002) Mutations in the human ortholog of *aristaless* cause X-linked mental retardation and epilepsy. **Nat Genet.** 30 (4): 441-445

- Sugawara, T., Tsurubuchi, Y., Agarwala, K.L. *et al.* (2001) A missense mutation of the Na<sup>+</sup> channel alpha II subunit gene Na(v)1.2 in a patient with febrile and afebrile seizures causes channel dysfunction. **Proc Natl Acad Sci U S A.** 98 (11): 6384-6389
- Swaiman, K.F. (1999) "Movement disorders and disorders of the basal ganglia". In: Swaiman, K.F., Ashwal, S. and Ferriero, D.M. (eds.) **Paediatric Neurology: Principles and Practice.** (Volume 2) 3<sup>rd</sup> ed. Philadelphia: Mosby Elsevier. pp. 801-831
- Tanabe, Y., Iai, M., Ishii, M. *et al.* (1993) The use of magnetic resonance imaging in diagnosing infantile neuroaxonal dystrophy. **Neurology.** 43 (1): 110-113
- Tanaka, H., Minakami, R., Kayana, H. *et al.* (2004) Catalytic residues of group VIB calcium-independent phospholipase A2 (iPLA2gamma). **Biochem Biophys Res Commun.** 320 (4): 1284-1290
- Tassin, J., Dürr, A., Bonnet, A.M. *et al.* (2000) Levodopa-responsive dystonia. GTP cyclohydrolase I or parkin mutations? **Brain.** 123 (Pt 6): 1112-1121
- Ten Donkelaar, H.J. and Lammens, M. (2009) Development of the human cerebellum and its disorders. **Clin Perinatol.** 36 (3): 513-530
- Thaxton, C. and Bhat, M.A. (2009) Myelination and regional domain differentiation of the axon. **Results Probl Cell Differ.** 48: 1-28
- Thomas, P.Q., Dattani, M.T., Brickman, J.M. *et al.* (2001) Heterozygous HESX1 mutations associated with isolated congenital pituitary hypoplasia and septo-optic dysplasia. **Hum Mol Genet.** 10 (1): 39-45
- Thornton, G.K. and Woods, C.G. (2009) Primary microcephaly: do all roads lead to Rome? **Trends Genet.** 25 (11): 501-510
- Todt, U., Netzer, C., Tolia, M. *et al.* (2009) New genetic evidence for involvement of the dopamine system in migraine with aura. **Hum Genet.** 125 (3): 265-279
- Toonen, R.F. and Verhage, M. (2007) Munc18-1 in secretion: lonely Munc joins SNARE team and takes control. **Trends Neurosci.** 30 (11): 564-572
- Torres, G.E., Gainetdinov, R.R. and Caron, M.G. (2003) Plasma membrane monoamine transporters: structure, regulation and function. **Nat Rev Neurosci.** 4 (1): 13-25
- Torres, G.E. and Amara, S.G. (2007) Glutamate and monoamine transporters: new visions of form and function. **Curr Opin Neurobiol.** 17 (3): 304-312

- Vajsar, J. and Schachter, H. (2006) Walker-Warburg syndrome. **Orphanet J Rare Dis.** 1: 29
- Valiente, M. and Marín, O. (2010) Neuronal migration mechanisms in development and disease. **Curr Opin Neurobiol.** 20 (1): 68-78
- Vallano, M.L. (1998) Developmental aspects of NMDA receptor function. **Crit Rev Neurobiol.** 12 (3): 177-204
- van der Knaap, M.S., Leegwater, P.A.J., Konst, A.A.M. *et al.* (2002) Mutations in each of the five subunits of translation initiation factor eIF2B can cause leukoencephalopathy with vanishing white matter. **Ann Neurol.** 51 (2): 264-270
- Vandenbergh, D.J. (2008) "Cloning and genetic analysis of dopamine transporters". *In*: Trudell, M.L. and Izenwasser, S. (eds.) **Dopamine Transporters: Chemistry Biology and Pharmacology.** New Jersey: John Wiley & Sons Inc. (Drug Discovery and Development series). pp. 47-71
- Velisek, L. and Moshe, S. (2001) "Pathophysiology of seizures and epilepsy in the immature brain: cells, synapses and circuits". *In*: Pellock, J.M., Dodson, W.E. and Bourgeois, B.F.D. (eds.) **Paediatric Epilepsy: Diagnosis and Therapy.** 2<sup>nd</sup> ed. New York: Demos Medical Publishing Inc. pp. 1-23
- Volpe, J.J. (2008a) "Neural Tube Formation and Prosencephalic Development". *In*: **Neurology of the Newborn.** 5<sup>th</sup> ed. Philadelphia: Saunders (Elsevier). pp. 3-50
- Volpe, J.J. (2008b) "Neuronal Proliferation, Migration, Organization and Myelination". *In*: **Neurology of the Newborn.** 5<sup>th</sup> ed. Philadelphia: Saunders (Elsevier). pp. 51-118
- Wada, H., Yasuda, T., Miura, I. *et al.* (2009) Establishment of an improved mouse model for infantile neuroaxonal dystrophy that shows early disease onset and bears a point mutation in *Pla2g6*. **Am J Pathol.** 175 (6): 2257-2263
- Waldman, I.D. and Gizer, I.R. (2006) The genetics of attention deficit hyperactivity disorder. **Clin Psychol Rev.** 26 (4): 396-432
- Wallace, R.H., Wang, D.W., Singh, R. *et al.* (1998) Febrile seizures and generalized epilepsy associated with a mutation in the Na<sup>+</sup>-channel beta1 subunit gene *SCN1B*. **Nat Genet.** 19 (4): 366-370
- Wallace, R.H., Marini, C., Petrou, S. *et al.* (2001) Mutant GABA(A) receptor gamma2-subunit in childhood absence epilepsy and febrile seizures. **Nat Genet.** 28 (1): 49-52

- Wallis, D. and Muenke, M. (2000) Mutations in holoprosencephaly. **Hum Mutat.** 16 (2): 99-108
- Wallis, D.E., Roessler, E., Hehr, U. *et al.* (1999) Mutations in the homeodomain of the human SIX3 gene cause holoprosencephaly. **Nat Genet.** 22 (2): 196-198
- Waterston, R.H., Lindblad-Toh, K., Birney, E. *et al.* (2002) Initial sequencing and comparative analysis of the mouse genome. **Nature.** 420 (6915): 520-562
- Weber, J.L. and May, P.E. (1989) Abundant class of human DNA polymorphisms which can be typed using the polymerase chain reaction. **Am J Hum Genet.** 44 (3): 388-396
- Weissenbach, J., Gyapay, G., Dib, C. *et al.* (1992) A second-generation linkage map of the human genome. **Nature.** 359 (6398): 794-801
- West, W.J. (1841) On a peculiar form of infantile convulsions. **Lancet:** 724-725
- WHO (2001). World Health Organization: epilepsy: epidemiology, aetiology and prognosis. **WHO factsheet**
- Wichmann, T., Bergman, H., Starr, P.A. *et al.* (1999) Comparison of MPTP-induced changes in spontaneous neuronal discharge in the internal pallidal segment and in the substantia nigra pars reticulata in primates. **Exp Brain Res.** 125 (4): 397-409
- Wicking, C. and Williamson, B. (1991) From linked marker to gene. **Trends Genet.** 7 (9): 288-293
- Willemsen, M.A., Verbeek, M.M., Kamsteeg, E.J. *et al.* (2010) Tyrosine hydroxylase deficiency: a treatable disorder of brain catecholamine biosynthesis. **Brain.** 133 (Pt 6): 1810-1822
- Williams, C.A., Dagli, A. and Battaglia, A. (2008) Genetic disorders associated with macrocephaly. **Am J Med Genet A.** 146A (15): 2023-2037
- Woods, C.G., Bond, J. and Enard, W. (2005) Autosomal recessive primary microcephaly (MCPH): a review of clinical, molecular, and evolutionary findings. **Am J Hum Genet.** 76 (5): 717-728
- Wu, Y., Jiang, Y., Gao, Z. *et al.* (2009) Clinical study and PLA2G6 mutation screening analysis in Chinese patients with infantile neuroaxonal dystrophy. **Eur J Neurol.** 16 (2): 240-245
- Yamashita, A., Singh, S.K., Kawate, T. *et al.* (2005) Crystal structure of a bacterial homologue of Na<sup>+</sup>/Cl<sup>-</sup>-dependent neurotransmitter transporters. **Nature.** 437 (7056): 215-223

- Yamatogi, Y. and Ohtahara, S. (1981) Age-dependent epileptic encephalopathy: a longitudinal study. **Folia Psychiatr Neurol Jpn.** 35 (3): 321–332
- Yamatogi, Y. and Ohtahara, S. (2002) Early-infantile epileptic encephalopathy with suppression-bursts, Ohtahara syndrome; its overview referring to our 16 cases. **Brain Dev.** 24 (1): 13-23
- Yan, H.D., Villalobos, C. and Andrade, R. (2009) TRPC Channels Mediate a Muscarinic Receptor-Induced Afterdepolarization in Cerebral Cortex. **J Neurosci.** 29 (32): 10038-10046
- Yang, Y., Wu, Z., Kuo, Y.M. *et al.* (2005) Dietary rescue of fumble--a *Drosophila* model for pantothenate-kinase-associated neurodegeneration. **J Inherit Metab Dis.** 28 (6): 1055-1064
- Yeung, W.L., Lam, C.W., Hui, J. *et al.* (2006) Galactorrhea-a strong clinical clue towards the diagnosis of neurotransmitter disease. **Brain Dev.** 28 (6): 389-391
- Yoshida, K., Furihata, K., Takeda, S. *et al.* (1995) A mutation in the ceruloplasmin gene is associated with systemic hemosiderosis in humans. **Nat Genet.** 9 (3): 267-272
- Young, I. (1999) **Risk calculation in genetic counselling.** 2<sup>nd</sup> ed. New York: Oxford University Press
- Yu, F.H., Mantegazza, M., Westenbroek, R.E. *et al.* (2006) Reduced sodium current in GABAergic interneurons in a mouse model of severe myoclonic epilepsy in infancy. **Nat Neurosci.** 9 (9): 1142-1149
- Zecca, L., Youdim, M.B., Riederer, P. *et al.* (2004) Iron, brain ageing and neurodegenerative disorders. **Nat Rev Neurosci.** 5 (11): 863-873
- Zeng, L.H., Xu, L., Gutmann, D.H. *et al.* (2008) Rapamycin prevents epilepsy in a mouse model of tuberous sclerosis complex. **Ann Neurol.** 63 (4): 444–453
- Zhou, B., Westaway, S.K., Levinson, B. *et al.* (2001) A novel pantothenate kinase gene (PANK2) is defective in Hallervorden-Spatz syndrome. **Nat Genet.** 28 (4): 345-349
- Zhou, Z., Zhen, J., Karpowich, N.K. *et al.* (2007) LeuT-desipramine structure reveals how antidepressants block neurotransmitter reuptake. **Science.** 317 (5843): 1390-1393
- Zolkipli, Z., Dahmouh, H., Saunders, D.E. *et al.* (2006) Pantothenate kinase 2 mutation with classic pantothenate-kinase-associated neurodegeneration without 'eye-of-the-tiger' sign on MRI in a pair of siblings. **Pediatr Radiol.** 36 (8): 884-886

Zupanc, M.L. (2009) Clinical evaluation and diagnosis of severe epilepsy syndromes of early childhood. **J Child Neurol.** 24 8 Suppl: 6S-14S

## **Chapter 8**

## **Appendix**



**Appendix 1:****See Chapter 4.2.2.4****Pedigree file for multipoint linkage analysis****Pedigree: A**

1	0	0	2	1	0	0	0	0	0	0	0	0
2	0	0	1	1	0	0	0	0	0	0	0	0
3	2	1	1	1	0	0	0	0	0	0	0	0
4	0	0	2	1	0	0	0	0	0	0	0	0
5	2	1	2	1	0	0	0	0	0	0	0	0
6	0	0	1	1	0	0	0	0	0	0	0	0
7	0	0	2	1	0	0	0	0	0	0	0	0
8	3	4	1	1	0	0	0	0	0	0	0	0
9	3	4	1	1	0	0	0	0	0	0	0	0
10	3	4	2	1	0	0	0	0	0	0	0	0
11	0	0	1	1	0	0	0	0	0	0	0	0
12	0	0	2	1	0	0	0	0	0	0	0	0
13	6	5	1	1	0	0	0	0	0	0	0	0
14	8	7	2	1	0	0	0	0	0	0	0	0
15	11	10	1	1	0	0	0	0	0	0	0	0
16	0	0	2	1	0	0	0	0	0	0	0	0
17	13	12	1	1	3	3	1	3	1	2	2	3
18	13	12	2	1	0	0	0	0	0	0	0	0
19	13	12	1	1	0	0	0	0	0	0	0	0
20	13	12	1	1	0	0	0	0	0	0	0	0
21	15	16	1	1	0	0	0	0	0	0	0	0
22	15	16	1	1	0	0	0	0	0	0	0	0
23	15	16	1	1	0	0	0	0	0	0	0	0
24	0	0	2	1	0	0	0	0	0	0	0	0
25	15	16	2	1	0	0	0	0	0	0	0	0
26	22	14	1	1	0	0	0	0	0	0	0	0
27	22	14	1	1	0	0	0	0	0	0	0	0
28	22	14	2	1	2	3	1	4	1	1	2	3
29	23	24	1	1	1	3	1	3	1	2	2	4
30	23	24	2	1	0	0	0	0	0	0	0	0
31	23	24	1	1	0	0	0	0	0	0	0	0
32	23	24	1	1	0	0	0	0	0	0	0	0
33	22	14	2	1	2	3	1	4	1	1	2	3
34	29	28	1	2	3	3	1	1	1	1	2	2
35	29	28	1	1	1	3	1	3	1	2	2	4
36	17	33	2	2	3	3	1	1	1	1	2	2

**Pedigree: B**

37	0	0	2	1	0	0	0	0	0	0	0	0
38	0	0	1	1	0	0	0	0	0	0	0	0
39	0	0	1	1	0	0	0	0	0	0	0	0
40	38	37	2	1	0	0	0	0	0	0	0	0
41	0	0	2	1	0	0	0	0	0	0	0	0
42	38	37	1	1	0	0	0	0	0	0	0	0
43	39	40	2	1	0	0	0	0	0	0	0	0
44	39	40	1	1	0	0	0	0	0	0	0	0
45	39	40	1	1	0	0	0	0	0	0	0	0
46	39	40	2	1	0	0	0	0	0	0	0	0
47	0	0	1	1	0	0	0	0	0	0	0	0
48	0	0	2	1	0	0	0	0	0	0	0	0
49	42	41	1	1	0	0	0	0	0	0	0	0
50	42	41	1	1	0	0	0	0	0	0	0	0

51	42	41	1	1	0	0	0	0	0	0	0	0
52	42	41	2	1	0	0	0	0	0	0	0	0
53	42	41	2	1	0	0	0	0	0	0	0	0
54	42	41	1	1	0	0	0	0	0	0	0	0
55	42	41	2	1	0	0	0	0	0	0	0	0
56	42	41	2	1	0	0	0	0	0	0	0	0
57	42	41	1	1	0	0	0	0	0	0	0	0
58	47	46	1	1	0	0	0	0	0	0	0	0
59	47	46	2	1	2	4	3	4	1	2	1	4
60	49	48	1	1	3	4	3	4	1	2	1	4
61	60	59	1	1	2	4	3	4	1	2	1	4
62	60	59	2	2	4	4	4	4	2	2	4	4
63	60	59	1	1	3	4	3	4	1	2	1	4

**Appendix 2:  
See Chapter 4.2.3 and 5.2.3****Functional investigation of mutant hDAT proteins**

Functional investigation of all *SLC6A3* mutations that were predicted to result in an expressed protein was undertaken. Mutant constructs of hDAT were prepared from wild-type pCIN4-hDAT (gift from Dr. Jonathan A. Javitch, Columbia University, NY, USA) as the template for polymerase chain reaction (PCR) using the QuikChange® site-directed mutagenesis kit (Stratagene, La Jolla, CA, USA) with some modifications. 50ng of DNA template (pCIN4-hDAT) was mixed with a primer and its complementary primer (100ng each), 1µl dNTP mix, 2.5µl of 10X reaction buffer, and 1.25 units of PfuTurbo DNA polymerase in a final volume of 25µl. The PCR conditions were an initial denaturation cycle (1 min, 95°C); 18 cycles of denaturation (30 sec, 95°C), annealing (1 min, 55°C), and extension (16 min, 68°C); a final extension cycle (10 min, 68°C); and termination at 4°C. PCR products were digested with 10 units of DpnI at 37°C for 1 hr to remove the parental strands. The digested DNA mixture was transformed into E. coli XL-1 blue supercompetent cells by heat shock. Mutagenesis was verified by DNA sequence analysis (New York University, Skirball Institute of Biomolecular Medicine, DNA sequencing facility). The following primers and their complementary primers (IDT, Inc., Coralville, IA, USA) were used:

Mutant	Primers (5' to 3')
Val158Phe	TC TTT TAC AAC TTC ATC ATT GCC TG
Leu224Pro	CGG GGC GTG CTG CAC CCC CAT CAG AGC CAC GGC
Gly327Arg	GGC GTG GGA TTC AGG GTC CTG ATC GCC TTC
Leu368Gln	GTCGTGTTTCAGCTTTTCAGGGATACATGGCCCAG
Pro395Leu	GATCTTCATTATCTACCTTGAGGCCATCGCTACCC
Arg521Trp	CCA GCC TGT ACT GGT GGCTGT GCT GGA AGC
Pro529Leu	TGG AAG CTC GTC TCC CTC TGC TTC CTC CTG TTC
Pro554Leu	GGC GCC TAC ATC TTC CTC GAC TGG GCC AAT GCA
Gln439X - Gly327Arg	CTG ATC GAC GAA TTC TAG CTC CTG CAC CGG CAT

Culturing and transient transfection of HEK-293 cells with Lipofectamine 2000, was carried out (Zhou *et al.*, 2007). Uptake of [ $^3$ H]dopamine into hDAT expressing cells was measured for 5 min at 21°C (Zhou *et al.*, 2007) with high sodium, low potassium, glucose and tropolone containing buffer (Chen *et al.*, 2004b). Nonspecific uptake was defined by 1 $\mu$ M CFT. For measurement of cocaine analogue binding, cells were incubated with 4nM [ $^3$ H]CFT (Perkin Elmer) for 20 min at 21°C in 200 $\mu$ l of the same buffer used for the uptake assay. For saturation analysis, increasing concentrations of nonradioactive CFT (0.1-100nM) were included in assay. The procedures were as described by Chen and Reith (2007). Non-specific binding was defined with 1 $\mu$ M CFT. The dopamine concentration producing half-maximal transport velocity ( $K_m$ ), the maximal velocity ( $V_{max}$ ), the equilibrium dissociation constant ( $K_d$ ) for [ $^3$ H]CFT binding, and maximal binding ( $B_{max}$ ), were estimated with nonlinear regression fitting by Radlig software (KELL program, Biosoft, Cambridge, UK). The equilibrium dissociation constant ( $K_i$ ) for inhibition of [ $^3$ H]CFT binding was computed with the Cheng-Prusoff equation (Chen and Reith, 2007) from the concentration inhibiting binding by 50% as estimated with logistic fitting of data by the ORIGIN software

(OriginLab Co., Northampton, MA). Comparisons of the mutants with wild-type DAT were performed by one-way ANOVA followed by the Dunnett multiple comparisons test. Statistical significance was considered at  $P < 0.05$ .

### **DAT surface protein preparation by biotinylation and western blotting**

Cells transiently expressing wild-type and mutant hDAT and mock cells were processed as described previously (Chen and Reith, 2008) with minor changes. Briefly, the cells were washed with cold PBS and incubated with Sulfo-NHS-SS-Biotin (1 mg/mL PBS) for 60 min at 4°C, followed by incubation with 50 mM glycine in PBS for 20 min and extensive wash. The washed cells were lysed in Mammalian Protein Extraction Reagents supplemented with protein inhibitor cocktail for 10 min at 21°C followed by 60 min at 4°C with vortexing at 5 min intervals. The lysate samples were centrifuged at 14 000 g for 15 min to remove cell debris. The biotinylated proteins were separated with immobilized monomeric NeutrAvidin and eluted with sodium dodecyl sulfate-polyacryl amide gel electrophoresis (SDS-PAGE) sample buffer. The total lysates and biotinylated proteins were resolved on 4%–12% Bis-tris NuPAGE gels (Invitrogen, Carlsbad, CA). DAT was probed with polyclonal anti-DAT antibody (0.3 µg/mL) against the C-terminus of DAT (Millipore, Billerica, MA) followed by HRP-conjugated goat anti-rabbit antibody. Polyclonal anti-β-actin antibody (Sigma, St. Louis, MO) was used as an internal control for loading. The transporter signal was visualized with SuperSignal West Dura Extended Duration chemiluminescence substrate solution (Thermo Scientific, Rockford, IL).

### Appendix 3:

#### See Chapter 4.3.2.2

#### Microsatellite marker analysis and exclusion of potential IPD loci on chromosome 7, 9 and 14 in family A

Chromosome Region on SNP(bp)	Marker	Start physical Position (bp)	End physical Position (bp)	VI:3	VI:5	VII:1	VII:2	VI:4	IV:4	VII:3
<b>Chromosome 7</b> <b>32 000929 –</b> <b>34 201718</b>	D7S817	32 102921	32 403079	172 172	164 172	164 172	172 172	172 172	172 172	172 172
	D7S2211	33 602237	33 602615	371 385	379 385	379 385	385 385	370 384	370 370	370 370
	D7S2758	33 611477	33 611617	138 138	138 138	138 138	138 138	138 138	138 138	138 138
<b>Chromosome 7</b> <b>42 521005-</b> <b>48 537723</b>	D7S678	43 247692	43 247865	163 173	163 173	163 173	163 163	163 171	163 171	163 163
	D7S2436	44 686503	44 686764	262 262	262 262	262 262	262 262	262 262	262 262	262 262
	D7S519	46 082558	46 082813	265 276	265 267	265 267	265 265	265 276	265 276	265 265
	D7S2561	47 359975	47 360192	214 214	214 214	214 214	214 214	210 214	214 214	214 214
<b>Chromosome 9</b> <b>(Spans centromere)</b> <b>32 229114 –</b> <b>73 854511</b>	D9S1817	33 849625	33 849887	283 285	283 297	283 297	283 297	285 294	283 285	285 285
	D9S1791	36 383383	36 383557	168 180	168 180	168 180	168 180	168 168	168 177	168 168
	D9S1874	37 212295	37 212493	192 196	192 196	192 196	192 196	192 192	192 194	192 192
	D9S2148	38 285718	38 285887	149 166	149 166	149 166	149 166	149 153	153 166	153 153
	D9S273	71 729255	71 729401	216 220	210 216	210 216	210 216	212 216	210 212	212 212
	D9S301	72 992540	72 992774	206 231	206 206	206 206	206 206	219 231	227 231	231 231
<b>Chromosome 14</b> <b>25 377656 –</b> <b>36 301274</b>	D14S1280	25 725631	25 725926	289 295	291 295	291 295	295 295	287 294	287 298	287 287
	D14S275	25 766620	25 766814	155 157	151 157	151 157	157 157	149 155	151 155	155 155
	D14S608	27 919195	27 919400	200 200	200 200	200 200	200 200	200 229	200 229	229 229
	D14S70	33 528945	33 529156	104 104	104 110	104 110	104 104	104 106	104 106	106 106
	D14S599	33 723548	33 723631	112 112	112 112	112 112	112 112	109 112	109 112	109 109